Catalytic Enantioselective Methods for Challenging Polar Addition Reactions

A thesis submitted in partial fulfilment of the requirement for the degree of Doctor of Philosophy (DPhil)

Connor J. Thomson

Oriel College

University of Oxford

Michaelmas Term 2021

Declaration

The work described in this thesis was carried out in the Chemistry Research Laboratory, University of Oxford, from October 2017 to June 2021, under the supervision of Prof. Darren J. Dixon. I declare that this thesis has been written in its entirety by me, that it is the record of work carried out by me and that it has not been submitted previously for any other higher degree at this or any other university.

Connor J. Thomson

September 2021

Abstract

Chapter 1 serves as an introduction to the fundamental principles of organocatalysis and enantioselective synthesis. Seminal contributions to the evolution of modern superbase catalysis are discussed.

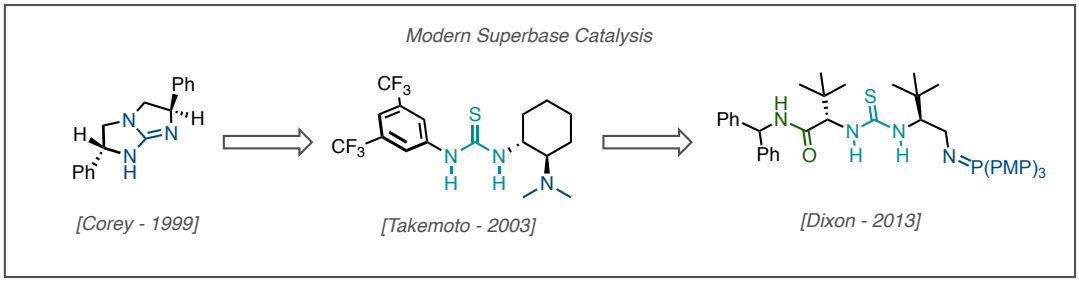

Chapter 2 describes the development of a novel enantioselective direct aldol reaction catalysed by a bifunctional iminophosphorane. The ability of a BIMP catalyst to activate high-pK_a aryl methyl ketone pro-nucleophiles is emphasised against the backdrop of traditional *Cinchona* and thiourea organocatalysis. The broad downstream utility of the β-hydroxy ketone products is demonstrated, along with an efficient scale-up protocol showcasing catalyst recyclability. Finally, mechanistic considerations are discussed based on NMR studies and reaction observations.

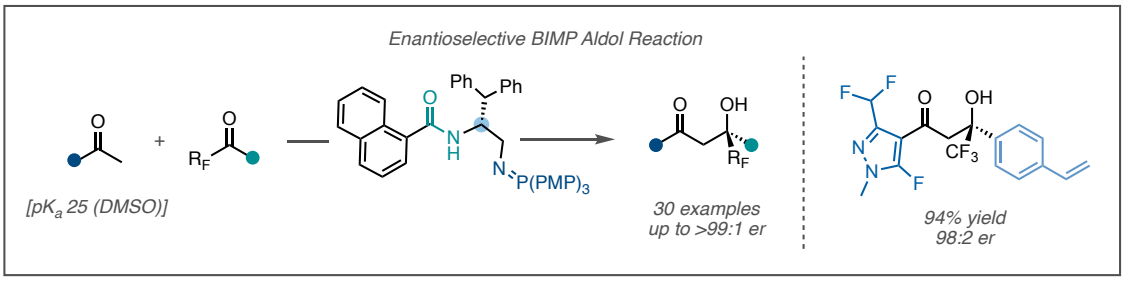

Chapter 3 outlines the development of an efficient aza-Michael addition/condensation strategy for the preparation of enantioenriched 2-pyrazolines. A simple one-pot protocol affords useful heterocycles from readily accessible enones. Highly reactive hydrazines are made amenable to enantioselective catalysis by *in situ* conversion to the corresponding hydrazone, which subsequently engages in an enantio-determining aza-Michael addition. The *Cinchona* alkaloid-derived catalyst is recyclable, and the large-scale utility of the method was demonstrated with the preparation of over 80 grams of a product in a single reaction.

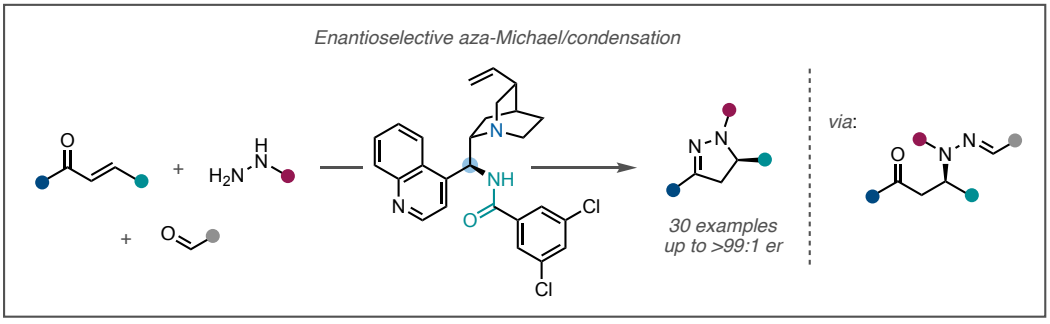

Acknowledgements

Firstly, I would like to thank Darren for his endless encouragement and unique wisdom. His passion for chemistry is truly infectious, and our conversations always left me with a new idea to contemplate. Through the best and worst of times his support for the group is unwavering. Thank you for taking an almost-pilot under your wing.

I am also extremely grateful to Bayer for their generous support. In particular, my deep gratitude goes to David Barber and his colleagues for their valuable insights and continued interest in both my primary research and often-questionable side projects.

To the labmates who were basically roommates through the long days and nights: Thomas, Mix Mix, Jonny, Yao, Pablo, Jimbo, Sam, Big Dan, Little Dan, Ben, Tao, Andrew, GL, Pete, Julia, Tats, Lucia, Roman, Ken, Yaseen, Elliot, Bran, Shinya, Samiha, and many more who passed through over the years. Thank you for not only making this thesis possible, but also making my time in the group such a rewarding experience through the ups and downs.

List of Abbreviations

(+)	Dextrorotary
(−)	Levorotatory
δ	NMR chemical shift
Ac	Acetyl
aq.	Aqueous
Ar	Aryl
BEMP	2-*tert*-Butylimino-2-diethylamino-1,3-dimethylperhydro-1,3,2-diazaphosphorine
BIMP	Bifunctional Iminophosphorane
BINOL	1,1'-Bi-2-naphthol
Bn	Benzyl
Boc	*tert*-Butoxycarbonyl
BOX	Bisoxazoline
br	Broad
BTMG	2-*tert*-Butyl-1,1,3,3-tetramethylguanidine
Bu	Butyl
Bz	Benzoyl
Cat.	Catalyst
Cbz	Carboxybenzyl

conc.	Concentrated
conv.	Conversion
COSY	Correlation Spectroscopy
CPME	Cyclopentyl Methyl Ether
Cy	Cyclohexyl
d	Doublet
DBU	1,8-Diazabicyclo-[5.4.0]-undec-7-ene
dd	Doublet of doublets
ddd	Doublet of doublet of doublets
ddt	Doublet of doublet of triplets
DIAD	Diisopropyl azodicarboxylate
DFT	Density functional theory
DIPEA	*N,N*-Diisopropylethylamine
DMF	*N,N*-Dimethylformamide
DMSO	Dimethylsulfoxide
DPP	Diphenylphosphinyl
DPPA	Diphenylphosphorylazide
dq	Doublet of quartets
dr	Diastereomeric ratio
dt	Doublet of triplets
E	Entgegen
ee	Enantiomeric excess

ent	Enantiomer
er	Enantiomeric ratio
et al.	et alia
Et	Ethyl
eq.	Equivalents
FCC	Flash Column Chromatography
g	Grams
HMDS	Hexamethyldisilazane
HPLC	High Performance Liquid Chromatography
HRMS	High Resolution Mass Spectrometry
HSQC	Heteronuclear Single Quantum Coupling
IMDAF	Intramolecular Diels−Alder Addition of Furan
FT-IR	Fourier Transform Infrared
J	Coupling constant
LDA	Lithium Diisopropylamide
LRMS	Low Resolution Mass Spectrometry
m	Multiplet
m	Meta
M	Molar
Me	Methyl
m/z	Mass to charge ratio
m.p.	Melting Point

MS	Molecular Sieves
n.d.	not determined
NMR	Nuclear Magnetic Resonance
NOESY	Nuclear Overhauser Effect Spectroscopy
Nu	Nucleophile
o	Ortho
p	Para
Ph	Phenyl
PMP	Para-methoxy phenyl
ppm	Parts per million
Pr	Propyl
q	Quartet
qd	Quartet of doublets
quant.	Quantitative
R	Rectus
R	Unspecified organic group
rr	Regioisomeric ratio
rt/RT	Room temperature
s	Singlet
S	Sinister
SCXRD	Single Crystal X-Ray Diffraction
SMA	Sulfa-Michael Addition

T	Temperature
t	Triplet
$t_{1/2}$	Half-life
TBME	*tert*-Butyl methyl ether
td	Triplet of doublets
TEA	Triethylamine
TFA	Trifluoroacetic acid
THF	Tetrahydrofuran
TLC	Thin Layer Chromatography
TMS	Trimethylsilyl
t_R	Retention time
Ts	*para*-Toluenesulfonyl
TS	Transition State
tt	Triplet of triplets
UV	Ultraviolet
ν_{max}	Infrared absorption maximum
w	Weight
Z	Zusammen

Table of Contents

Chapter 2: Catalytic Direct Aldol Additions of Aryl Ketones

Chapter 3: Catalytic Enantioselective Synthesis of 2-Pyrazolines

Chapter 1

Introduction

1.1 Chirality in Everyday Life

The last century of scientific endeavour has seen wide-reaching impacts on the everyday lives of people across the globe. Significant advancements in pharmaceutical science coupled with the development of cheap agrochemicals has enabled huge improvements to quality of life as well as rapid economic expansions. At the heart of this growth has been the invention of synthetic methods for the increasingly efficient preparation of complex molecules. More specifically, an explosion of research into the synthesis of enantiopure materials has been fuelled by the growing relevance of optically active chemicals. The stereo-dependant potency and physiological effects of chiral molecules have been known for decades and continue to dictate the necessity for new stereoselective methods.

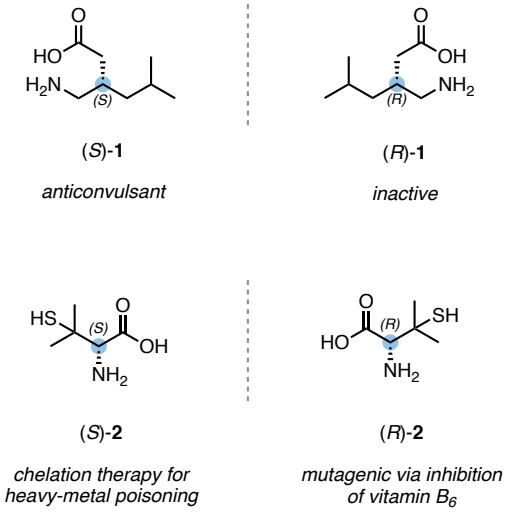

Figure 1. Structures of pregabalin and penicillamine enantiomers and their contrasting biological roles.

The relationship between stereochemical configuration and biological activity is exemplified by pregabalin (**1**) and penicillamine (**2**). While the (*S*) enantiomer of pregabalin is a blockbuster anticonvulsant for the treatment of epilepsy and related disorders, its mirror image (*R*) enantiomer is inactive in humans (**Figure 1**).[1] Penicillamine further illustrates this phenomenon; the use of (*S*)-penicillamine as a safe treatment for heavy-metal poisoning is juxtaposed by the mutagenic toxicity of its (*R*) counterpart, which acts as an inhibitor of the essential vitamin B_6.[2] Since the thalidomide disaster in the 1960's, scientists and drug regulators alike have been acutely aware of the role played by stereochemical configuration in drug design and the resulting safety profile of a therapeutic.[3]

1.2 Strategies for Stereoselective Synthesis

The umbrella of stereoselective synthesis features four prominent strategies for the installation of enantioenriched stereocentres, including: (1) chiral resolution or separation, (2) synthesis from the chiral pool, (3) auxiliary-directed diastereoselective synthesis, and (4) enantioselective synthesis.[4]

1.2.1 Chiral resolution or separation

Chiral resolution by crystallisation was historically prominent prior to the development of sophisticated methods for the selective synthesis of single enantiomers.[5] Similarly, chromatographic separation of enantiomers obviates the need for an effective synthetic method but requires expensive chiral media and typically vast quantities of solvent compared to the mass of isolated material. Although these options are inherently wasteful due to the maximum 50% recovery of the desired compound from a racemic mixture, they remain popular in certain industrial settings, such as early-stage drug research programs where high cost is traded for faster development progress.

1.2.2 Synthesis from the chiral pool

Early preparations of enantioenriched compounds featured the use of naturally occurring chiral molecules as convenient sources of enantiopure scaffolds for further manipulation.[6] Small modifications to natural products – for example terpenes and amino acids – can rapidly give rise to desirable enantiopure intermediates. Hence, the so-called 'chiral pool' has long been a valuable resource for synthetic chemists. On the downside, the collection of natural compounds that are cheap and abundantly available beholds relatively limited

structural diversity, which can restrict the efficiency of the 'chiral pool' as a starting point towards a target compound.[7] This limitation has led chemists to explore alternative avenues that allow selective introduction of chiral centres.

1.2.3 Diastereoselective synthesis

Amongst the most popular of the aforementioned strategies is diastereoselective synthesis. Covalently linking a chiral auxiliary to a substrate is typically highly effective as a method for the introduction of chirality, while allowing the reliable prediction of stereochemical outcomes.[8] However, the use of stoichiometric auxiliaries is seen as intrinsically wasteful in terms of extended synthetic effort and reduced overall atom-economy. Yet chiral auxiliaries remain essential to the industrial preparation of many drug molecules because of the robustness of this strategy. In many cases there is simply a lack of available enantioselective alternatives, which further encourages the use of this wasteful strategy.

1.2.4 Enantioselective synthesis

Considering the limitations described above, catalytic enantioselective synthesis is usually the theoretically preferable method for stereoselective synthesis. Such a strategy obviates the inefficiencies inherent to chiral auxiliaries, resolutions and separations, and allows chirality to be imparted by sub-stoichiometric amounts of a chiral catalyst. For these reasons, enantioselective synthesis has become the most desirable method for the favoured formation of a stereocentre in any given synthetic route. Enantioselective reactions can be so pivotal that synthetic routes are often guided around a single key enantioselective reaction in a long sequence of structural transformations.[9-10] The initial time investment required to

optimise an enantioselective strategy for a specific substrate is rewarded for by the potential cost-savings on large scale. The remainder of this Chapter will focus on enantioselective catalysis.

1.3 Catalytic Enantioselective Synthesis

1.3.1 Organometallic and biocatalytic approaches

Enantioselective catalysis encompasses the broad use of substoichiometric quantities of chemical or biological tools for the preparation of compounds enriched with a single enantiomer. Organometallic catalysts arguably account for the most prominent form of enantioselective chemistry in the large-scale manufacturing of fine chemicals.[11–13] Typically, organometallic catalysts feature a transition metal ligated by a chiral organic structure. Advantages often include extremely high catalytic activity and robustness culminating in exceptionally low catalyst loadings. In the most optimised industrial processes for the preparation of feedstock reagents and pharmaceutical intermediates it is not uncommon for low ppm catalyst loadings to be sufficient for effective production. On the other hand, the high cost and rarity of precious transition metals (ie. Pt, Pd, Rh, Ir) and bespoke chiral ligands characterise the main drawbacks of these catalytic systems. Furthermore, the challenges of scavenging trace quantities of toxic metal residues (including Ni, Ru, Ti) and, sometimes, the need for rigorously inert conditions result in stringent requirements for the use of homogeneous and heterogeneous organometallic catalysts.

An emerging alternative technology is biocatalysis. The use of natural or synthetic enzymes as catalysts can offer a more environmentally friendly option for catalytic synthesis and

avoids the cost and toxicity concerns associated with transition metals.[14] The inherently high substrate specificity of enzymes oftentimes affords extremely high levels of regio-, chemo- and enantioselectivity. Directed evolution of the genes encoding for the active site of a protein can lead to the production of new catalysts with novel substrate scopes. Hence the power of directed evolution is likely to lead to a rapid expansion of biocatalysis in the future. This fact was recognised in 2018 when the Nobel Prize for Chemistry was partly awarded to Francis Arnold for her work on directed evolution strategies.[15]

The limitations of organometallic catalysis and the relative infancy of enzymatic methodologies have driven a flood of research into metal-free small-molecule enantioselective catalysis, otherwise known as organocatalysis, during the last two decades. The remainder of this Chapter will focus on organocatalysis.

1.3.2 Enantioselective organocatalysis

The ability to mimic the active site of an enzyme by using a small organic molecule to affect the synthesis of chemicals with high selectivity and efficiency is the ultimate desire of organocatalysis. The use of simple compounds that can be rapidly synthesised in the laboratory overcomes some of the compatibility issues of enzymatic catalysis and the costs and safety concerns associated with organometallics.

The popularisation of enantioselective organocatalysis is largely credited to David MacMillan and co-workers following seminal reports of iminium enantioselective catalysis in 2000.[16,17] MacMillan's influence in the field was recently acknowledged with receipt of the 2021 Nobel

Prize for Chemistry, alongside Benjamin List. The explosion of research into organocatalysis triggered by the early reports of MacMillan has continued to flourish in the decades since, and hundreds of significant organocatalytic systems have been developed as a result. Organocatalysts are designed with ease-of-use in mind, and reaction conditions are typically quite mild and more tolerant of moisture and air than organometallic catalysts, which often requires glove-box conditions to protect the sensitive metal-centred structures. It is these favourable characteristics that have led to a diverse range of catalysts, include enamine, phase-transfer, iminium, and Brønsted-base and Brønsted-acid catalysis. **Figure 2** illustrates a selection of common organocatalyst motifs (**3**-**8**).

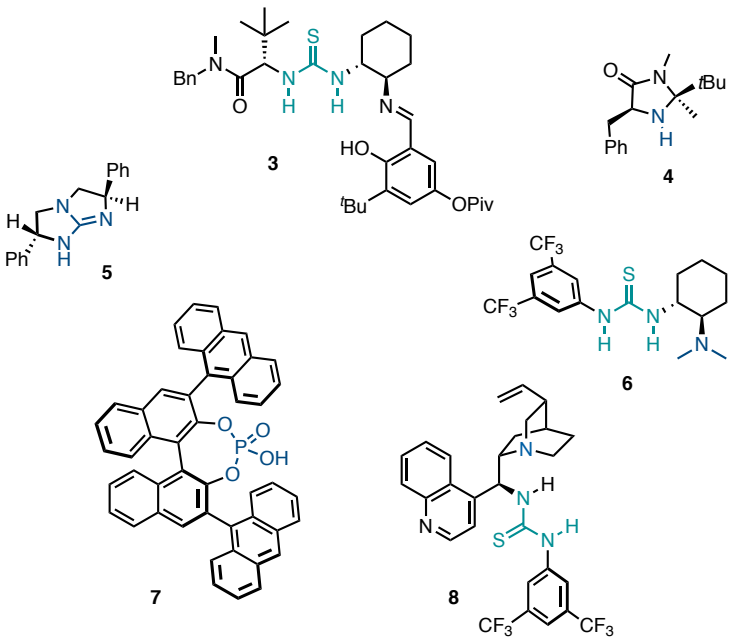

Figure 2. Common motifs seen in organocatalysis, including H-bond donors, Brønsted-acids and Brønsted-bases.

Reports of organocatalysis were rare prior to the new millennium. Perhaps the most well-known examples nowadays come from the work of Hajos and Parrish, and Eder, Sauer and

Weichert on proline catalysed enantioselective intramolecular aldol reactions in the early 1970s.[18,19] These examples are discussed in more detail in Chapter 2.2.2. Following on from those inspiring reports of enantioselective aldol chemistry, Inoue demonstrated in 1981 an elegant solution for the enantioselective metal-free hydrocyanation of aldehydes (**Scheme 1**).[20] This represents one of the earliest examples of non-covalent organocatalysis whereby stereochemical information is transferred through transition state organisation controlled by hydrogen-bonding interactions. Using the diketopiperazine organocatalyst **9** – which is easily prepared from *L*-phenylalanine and *L*-histidine – cyanohydrin **11** was derived from benzaldehyde (**10**) and hydrogen cyanide in 97% yield and 97% ee. The proposed stereochemical model suggests that hydrogen-bonding places the more sterically demanding group of the aldehyde pointing up and away from the concave face of the diketopiperazine. Attack of cyanide on the aldehyde then occurs preferentially on the least hindered *si* face; the *re* face is blocked by the benzyl substituent of catalyst **9**.[21]

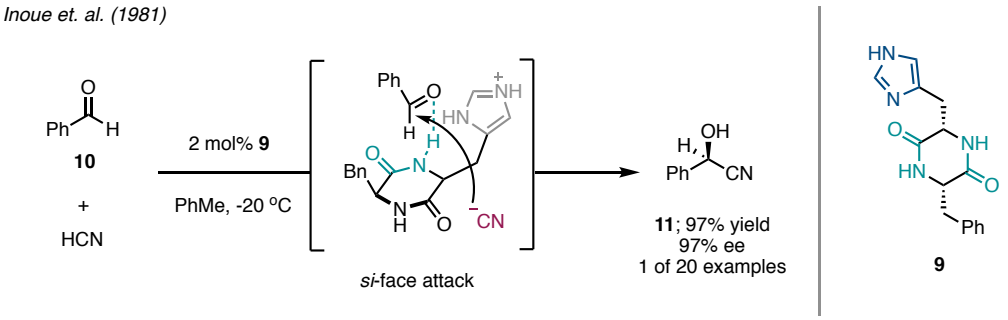

Scheme 1. Inoue's elegant enantioselective hydrocyanation of aryl aldehydes.

MacMillan's seminal report of organocatalytic iminium chemistry in 2000 proved to be a pivotal moment in the timeline of contemporary organocatalytic research. The publication specifically outlined an efficient enantioselective Diels-Alder cycloaddition between enals

and dienes catalysed by the imidazolidinone salt **12** (**Scheme 2**).[17] Under extremely mild conditions (room temperature in aqueous methanol) the reaction between enal **13** and cyclohexadiene (**14**) afforded an 82% yield of adduct **15** with an impressive 94% ee and high endo:exo selectivity of 14:1. Mechanistically, following condensation of the rigid imidazolidinone catalyst with enal **13** MacMillan suggests a stereochemical model featuring a preference to place the vinyl iminium in the *s*-trans-(*E*) configuration to avoid unfavourable allylic 1,3 interactions with the gem-dimethyl group, and steric clash with the adjacent benzyl group. Hence the 'upper' face of the transition state is sterically blocked by the benzyl group, and cycloaddition occurs favourably on the lower, *re* face of the activated alkene.

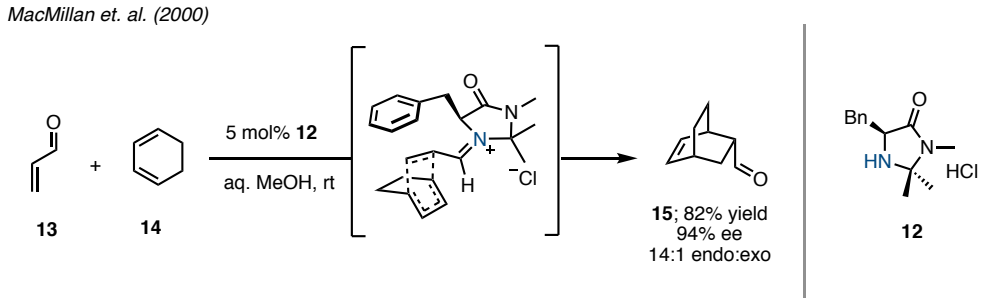

Scheme 2. MacMillan's seminal demonstration of enantioselective iminium catalysis.

1.4 Bifunctional Organocatalysis

Many of the earliest examples of organocatalysis typically featured only one explicit mode of activation (enamine or iminium activation for example). These are known as monofunctional catalysts, and they often fail to activate high-pK_a nucleophiles and/or low-

electrophilicity acceptors.[22–24] Furthermore, a common criticism of organocatalysis is the problem of slow reaction rates regularly seen in literature reports across the field of monofunctional metal-free catalysis.[25] This has led to the advent of bifunctional organocatalysis, wherein two explicit activating groups are combined into a single catalyst to increase catalytic power.[26–28] Towards this end, a range of new bifunctional designs have enabled enhanced catalytic behaviour. Among the most successful are the Brønsted base/H-bond donor catalysts, chiral phosphoric acids, and phase-transfer ammonium salts. The remainder of this Chapter will focus in more detail on the applications and development of bifunctional Brønsted base organocatalysts.

1.4.1 Founding examples of Brønsted base organocatalysis

The union of a Brønsted base with one or more H-bond donors can a be powerful strategy for the creation of effective organocatalysts, whereby the former activates a pro-nucleophile through acid/base equilibria and the latter activates and organises the electrophilic acceptor through non-covalent interactions. A seminal example from Takemoto and co-workers in 2003 elegantly illustrates this concept.[29] To fill a synthetic gap, Takemoto recognised the need for a powerful catalyst able to promote the Michael addition of malonates to nitro-olefins through simultaneous activation of both reaction components (**Scheme 3**). Hence, bifunctional catalyst **6** was developed to bear both a highly activated thiourea and a tertiary amine assembled around a chiral *trans*-diamine backbone. Principal studies found that both activating groups are required in a single molecule for efficient catalysis to be achieved. The conjugate addition of malonate **16** to nitro-olefin **17** proceeded efficiently to allow isolation

of adduct **18** in high yield and excellent enantioselectivity (86% yield, 93% ee) after 24 hours and under mild conditions. The authors hypothesise a transition state that features organisation and activation of the electrophilic nitro-olefin through H-bond interactions between the thiourea protons and the oxygen atoms of the nitro group. The dimethylamino moiety simultaneously deprotonates the malonate, followed by attack of the resulting enolate on the sterically preferred face of the activated electrophile, as directed by the chiral backbone of **6**. Hence, the desired conjugate addition products are afforded with high levels of enantioselectivity.

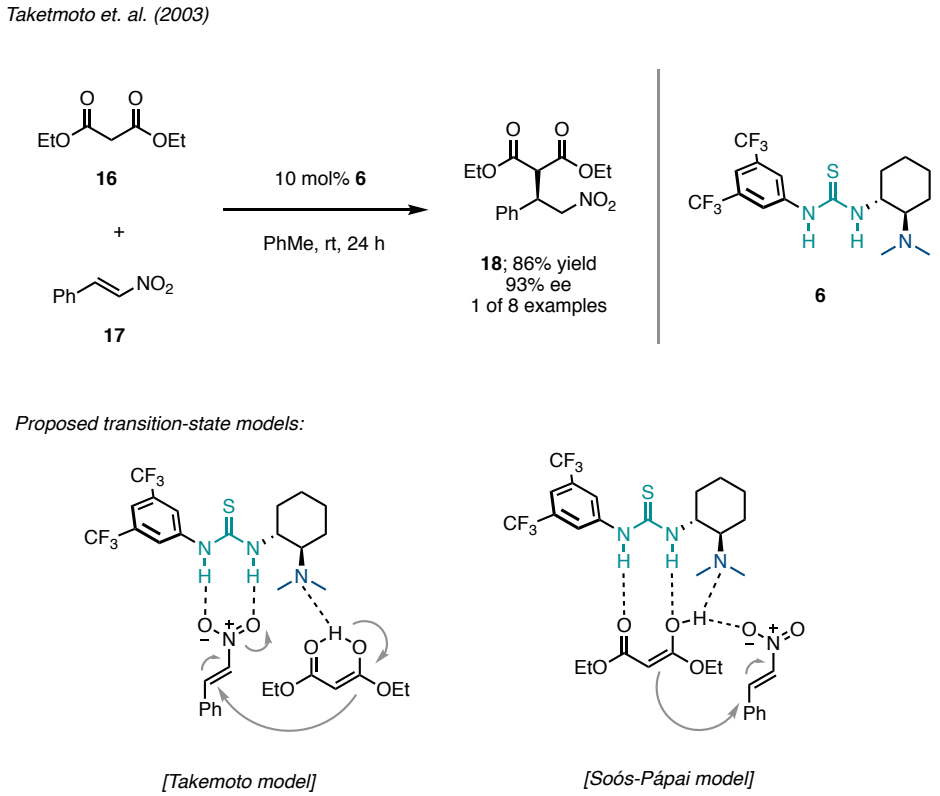

Scheme 3. Enantioselective Michael addition of malonates to nitro-olefins as reported by Takemoto.

Later, an alternative stereochemical model supported by computational calculations was proposed by the groups of Pápai and Soós. Their findings suggest binding of nitrostyrene **17** to the ammonium salt, and simultaneous H-bonding between the thiourea and enol moieties.[30] Overall, this model is calculated to be 2.7 kcal/mol more energetically preferred to the Takemoto model. However, both models predict the correct enantiomeric outcome of the reaction, and it is possible that the actual transition state is more complex than has been calculated thus far. Furthermore, Takemoto confirmed a strong qualitative relationship between the pK_a of pro-nucleophilic donors and their reaction rate with electrophiles in conjugate additions reactions. Pro-nucleophiles of higher acidity exist as the deprotonated form in higher levels under acid/base equilibria with the tertiary amine, and therefore react at higher rates under otherwise identical reaction conditions.

Following the influential discovery of catalyst **6** by Takemoto, an abundance of creative catalyst designs have been revealed by dozens of research groups worldwide. In the early-2000s, a particular group of catalysts came to the forefront of the field when the *Cinchona* alkaloids were recognised as useful chiral scaffolds. The alkaloids quinine and quinidine, along with their pseudoenantiomeric pairs cinchonidine and cinchonine, are naturally abundant, commercially available, and inexpensive. The quinuclidine motif offers a relatively strong tertiary amine Brønsted base, while the remaining molecular architecture provides several points of variation for derivatisation. Modification of the quinoline, methoxy, alkene, quinuclidine and alcohol groups of the parent alkaloids have all been reported to give rise to catalysts with unique structure-activity relationships. Partly for these reasons, catalysts derived from *Cinchona* alkaloids have become extremely prominent in synthetic chemistry

and remain one of the most important tools in the platform of Brønsted base organocatalysis.[31–34]

Deng was one of the earliest adopters of the *Cinchona* alkaloid scaffold for bifunctional organocatalysis. In 2004, his group revealed the use of *O*-Desmethyl-quinidine (**19**) as an affordable catalyst for the addition of malonates to nitro-olefins.[35] Shortly thereafter the groups of Chen, Connon, Dixon and Soós independently researched the *Cinchona* alkaloids as skeletons for thiourea/Brønsted base catalyst design. Consequently, a flurry of reports came in 2005. Soós found quinine-derived catalyst **20** to be effective in the addition of nitroalkanes to chalcones in high yield and enantioselectivity (up to 98% ee).[36] Chen then reported the 1,4-addition of aromatic thiols to unsaturated imides and enones catalysed by **21**, albeit with low levels of enantioselectivity.[37] Slightly later Connon and Dixon simultaneously noted that **20** and **21**, respectively, could affect the conjugate addition of malonates to nitro-olefins.[38,39] **Figure 3** show representative structures of the original thiourea *Cinchona* catalysts.

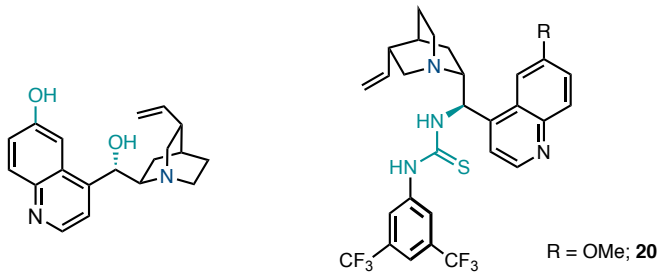

19

Deng

Chen, Connon, Dixon, Soós

Figure 3. Typical structures of bifunctional *Cinchona* alkaloid derived organocatalysts.

Inspired by the work of Chen, Connon, Dixon and Soos, further variations to the *Cinchona* alkaloid backbone from Hiemstra and Rawal gave rise to new reactivities. Hiemstra's work illustrated modifications to the quinoline heterocycle such that the native methoxy substituent is replaced with a thiourea H-bond donor group to afford catalyst **22** (**Scheme 4**).[40] This relocation of the H-bond donor massively improved enantioselectivity in the Henry reaction of nitromethane with aromatic aldehydes. For example, 1,2-nitroalcohol **23** derived from benzaldehyde (**10**) and nitromethane was obtained with only 6% ee using catalyst **24** but with 92% ee using thiourea **22**. Hiemstra's report represented a large step for the field of organocatalysis and explicitly highlights the role of intelligent catalyst design in organic synthesis.

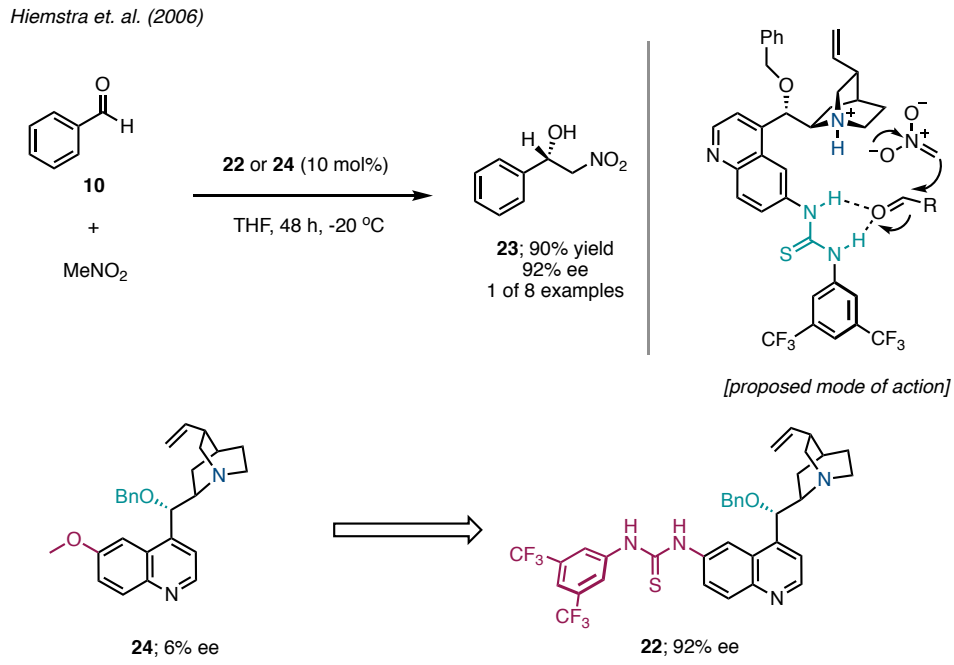

Scheme 4. Enantioselective nitro-Henry reaction as reported by Hiemstra.

By this point, the thiourea had become a privileged motif in H-bond donor organocatalysis. In 2008, Rawal and co-workers illustrated an innovative example of catalyst design by using a squaramide to create a new catalophore and thereby breaking through the dominance of the thiourea motif in the field of organocatalysis. The group found cinchonine-derived squaramide **25** to be a competent organocatalyst for the conjugate addition of 2,4-pentanedione (**26**) to nitrostyrene **17** (**Scheme 5**).[41] Impressively, the reaction was found to proceed at room temperature with only 0.5 mol% of catalyst to afford nitroalkanes such as **27** with extremely high levels of enantiocontrol (>99% ee) and high yields (94%) in only 8 hours. In this context, squaramides act similarly to thioureas and ureas by providing two adjacent Hydrogen-bonds to act as dual activators of the incoming electrophile. The presence of two H-bonds additionally serves to reduce the degree of free rotation of the substrate. Specifically, the authors suggest that the greater distance between the two squaramide N-H bonds (~2.8Å vs ~2.1Å for thiourea) may provide more selective catalyst-substrate binding with 1,3-diketones. Squaramides have since become popular motifs in bifunctional organocatalysis.[41–45]

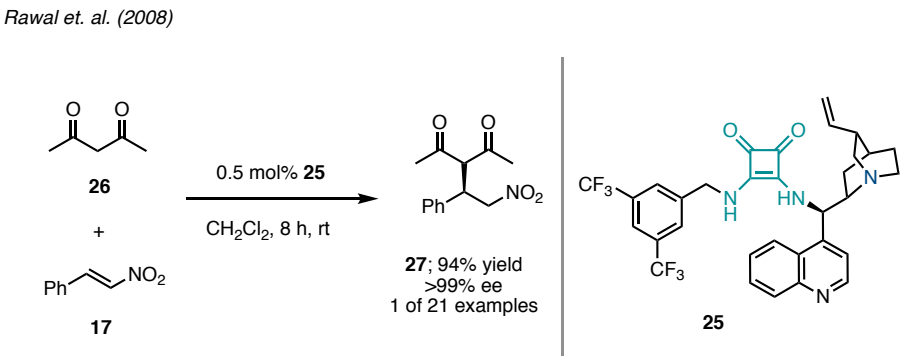

Scheme 5. Highly enantioselective conjugated addition to nitrostyrene as reported by Rawal.

1.4.2 Limitations of early organocatalysis designs

Testament to the general utility and convenience of tertiary-amine bifunctional catalysts is the plethora of enantioselective catalytic methods that have been designed to exploit the potential of these chiral Brønsted bases. Applications to Michael and Mannich reactions have featured prominently, along with Strecker reactions, and α-functionalisations of ketones. Creative solutions to challenging Diels-Alder and *aza*-Henry transformations have also been widely disseminated.[46–54]

Although tertiary-amine bifunctional organocatalysts have been responsible for significant innovations in the field of synthetic organic chemistry, several limitations are apparent. Primarily, tertiary amine catalysts only offer high-performance for the aforementioned reactions in a narrow pK_a range (**Figure 4**).[24] Typically, these molecular tools fail to activate high pK_a pro-nucleophiles above approximately pK_a 15 (in DMSO) and are severely limited to only the most activated electrophiles approaching pro-nucleophiles of pK_a 17 and higher. The use of low pK_a substrates is well established; for example, thiophenol (pK_a 10.3 in DMSO) is well studied and performs efficiently as a pro-nucleophile under tertiary-amine Brønsted base catalysis.[28,55] Divergence in performance is seen with increasingly higher pK_a pro-nucleophiles including *n*-propane thiol (pK_a 17.0 in DMSO) and nitromethane (pK_a 17.2 in DMSO), which often require unsatisfactory reaction times (5-10 days) to perform conjugate additions to unactivated substrates.[56,57]

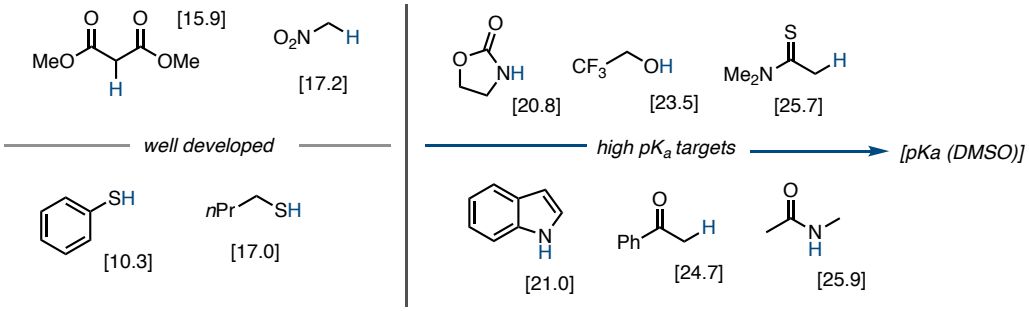

Figure 4. pKa scale of common and challenging pro-nucleophiles.

As a result of these restrictions, most reports of tertiary-amine bifunctional organocatalysis feature varying combinations of the same relatively acidic pro-nucleophiles with (typically) highly reactive electrophilic acceptors. Hence the subset of pronucleophiles and electrophilic partners amenable to enantioselective coupling with tertiary amine organocatalysts is relatively limited. These wide-spread issues are exemplified by the conjugate addition of nitromethane (pK_a 17.2 in DMSO) to chalcones (e.g., **28**) to afford nitro-Michael adducts (**29**), as reported by Soós and co-workers (**Scheme 6**). This transformation required a 122-hour reaction time and 10 mol% of catalyst **30** to achieve high conversion at room temperature.[36]

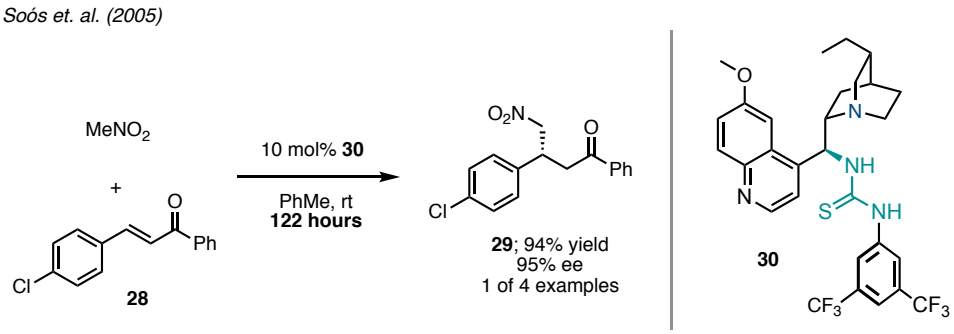

Scheme 6. Long reaction times highlighted by Soós's Michael addition of high pK_a nitromethane.

1.5 Superbasic Bifunctional Organocatalysts

Addressing the concerns of low reactions rates, high catalyst loadings and limited substrate compatibility is necessary to support Brønsted base organocatalysis as a wide-spread synthetic tool. Reports of high-pK$_a$ substrates amenable to tertiary-amine organocatalysis are rare and extremely challenging such that cooperative-catalysis systems are often required.[58] One approach allowing access to higher pK$_a$ pro-nucleophiles and/or lower electrophilicity coupling partners is the use of activating groups, for example aryl esters, *N*-heterocycle amides, and N-DPP ketimines.[59–62] Like the use of chiral auxiliaries, this approach suffers from the reduced atom economy and increased step-count dictated by the need to add and remove these activating partners.

Rather than relying on activating groups, improved catalyst design is a more elegant, though challenging, approach towards improving reactivity and unlocking major advancements in organocatalysis. One hallmark of next-generation Brønsted base bifunctional organocatalysts is the introduction of superbasic moieties. Substitutes for tertiary-amines as the Brønsted base component can greatly extend the potential pK$_a$ range of pro-nucleophiles amenable to organocatalysis, thereby allowing the activation of previously inaccessible substrates.[63–65]

1.5.1 Definition of a superbase

Several authors have attempted to ascribe a specific definition to the term '*superbase*'. Ishikawa and co-workers assign the term to any compound bearing a pK_{BH+} greater than that of Proton-sponge® (18.6 in MeCN, 7.5 in DMSO).[63,66] pK_{BH+} is defined as the negative logarithm of the equilibrium constant represented by eq. 1, such that a higher pK_{BH+} value denotes higher basicity:

$$BH^+ \rightleftharpoons B + H^+ \qquad \text{(eq. 1)}$$

Meanwhile, Caubere defines a superbase as a basic compound resulting from the combination of multiple basic compounds/moieties to afford new inherent properties.[67] Ishikawa's interpretation is generally considered more useful in practical chemistry for its ease of quantitatively comparing bases. Following this, the general rule of thumb can be followed that a superbase is any compound with a basicity greater than that of Proton-sponge® or triethylamine (both pK_{BH+} approx. 18. in MeCN). **Figure 5** illustrates some of the most popular achiral superbase types ranked on a relative scale of basicity. The higher acidity (lower pK_{BH+} values) for bases when measured in DMSO vs MeCN is due to the greater ability of DMSO to efficiently stabilise anions of Brønsted acids upon their deprotonation.[68]

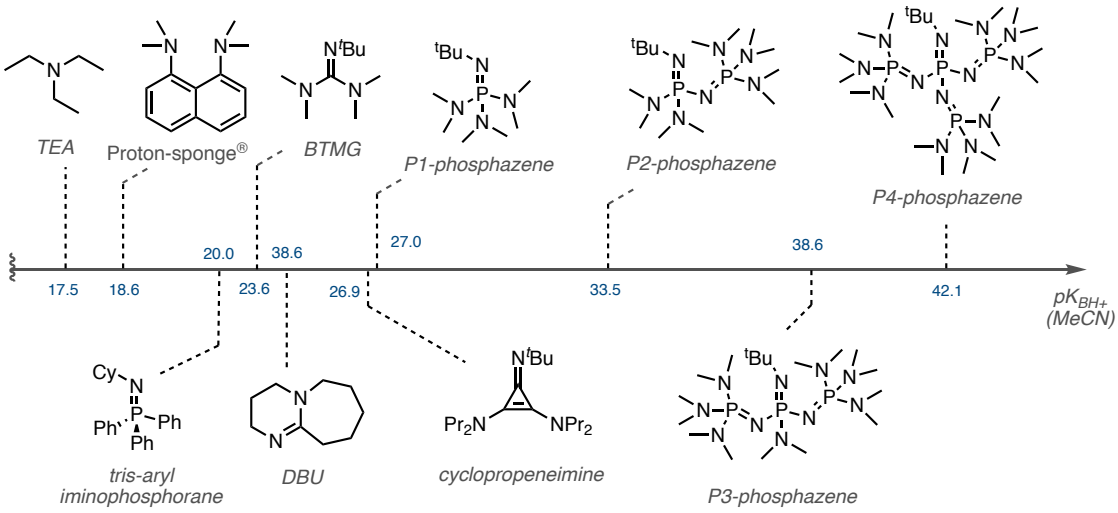

Figure 5. Basicity scale featuring some of the most common organosuperbases, according to Ishikawa's definition.

1.5.2 Guanidines

Many of the 1st-generation superbase organocatalysts developed in the 90's and early 2000's featured a superbasic guanidine core.[69,70] Relative to tertiary amines, these catalysts have enhanced basicity resulting from additional nitrogen atoms with lone pairs available for stabilisation of the resulting positive charge upon protonation. Basicity can be tuned somewhat by steric and electronic alteration of the flanking groups. Corey's seminal 1999 report on the enantioselective addition of hydrogen cyanide to achiral aldimines such as **31** employed a bifunctional C_2-symmetric guanidine catalyst **5** to efficiently afford valuable Strecker products.[71] For example, **32** was obtained in 96% yield and 86% ee after 20 hours at -40 °C (**Scheme 7**). Tan later suggested a stereochemical model dependant on a combination of interactions; Hydrogen-bonding between the protonated form of **5** and the aldimine, as well as pi-pi stacking between the benzhydryl group of **31** and catalyst **5** both

position the aldimine for biased attack by the incoming cyanide.[72] The *tert*-butyl analogue of Corey's catalyst (**33**) was reported by Tan to affect the addition of secondary phosphine oxides to nitrostyrenes with high yield and enantioselectivities.[73]

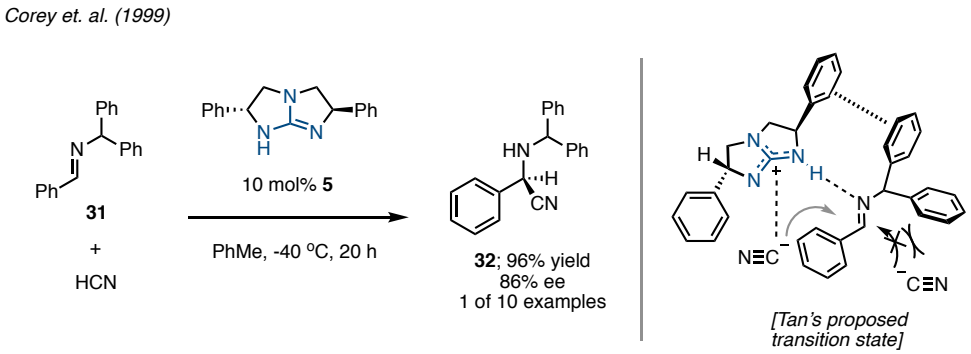

Scheme 7. Enantioselective Strecker reaction catalysed by a chiral C_2-symmetric guanidine as reported by Corey. Stereochemical model shown was later proposed by Tan.

Figure 6 illustrates catalysts designs arising from the valuable contributions of Tan (**33**), Ishikawa (**34**-**35**) and Teradas (**36**) since Corey's influential report. The synthetic utility of these catalysts has been partly offset by their often-challenging syntheses and limited modularity. As a result, guanidine-based designs have largely been ignored by chemists seeking cost-effective catalysts for scalable commercial synthesis. Moreover, guanidines rank relatively low on the basicity scale compared to other superbasic iterations disclosed more recently. Hence, chemists seeking higher-order superbasicity have sought to develop new systems incorporating motifs such as cyclopropeneimines and phosphazenes.[65,74–76]

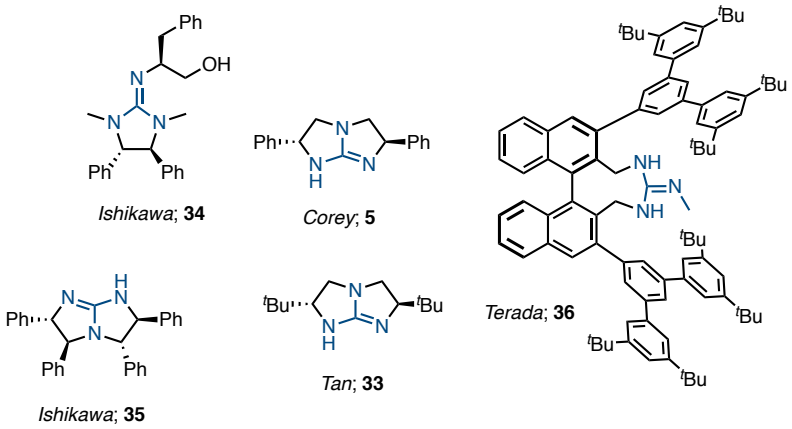

Figure 6. Chiral guanidine superbase catalysts reported by Terada, Corey, Tan and Ishikawa.

1.5.3 Cyclopropeneimines

The attractiveness of cyclopropeneimines as catalysts for enantioselective synthesis was recognised by Lambert and co-workers in their influential 2012 publication. Cyclopropenium/H-bond donor catalyst **37** was designed for the alkylation of glycine imine esters with Michael acceptors (**Scheme 8**). Alkylation of **38** efficiently proceeds with generally high yields and enantioselectivity for a range of Michael acceptors to afford alkylated derivatives, including from acrylate esters (**39**-**40**), a vinyl ketone (**41**), acrylonitrile (**42**) and phenyl vinyl sulfone (**43**).[77] Interestingly, the authors also highlighted the greatly enhanced efficacy of the cyclopropenium scaffold compared to the analogous guanidine-based catalyst disclosed by Ishikawa much earlier in 2001. With 20 mol% of Ishikawa's guanidine catalyst **34** the same transformation required a 7-day reaction time to achieve full conversion to **39**. Meanwhile, when performed under neat conditions, 10 mol% of Lambert's cyclopropeneimine **37** achieved full conversion and quantitative yield of **39** in only 5 minutes, thus demonstrating a true innovation in the field of superbase catalysis.

Although cyclopropeneimines were previously known, Lambert was the first to experimentally verify the basicity of this family; catalyst **37** boasts basicity comparable to P_1-phosphazenes at approximately pK_{BH+} 27 (in MeCN).[78,79] However, the instability of cyclopropeneimine **37** highlights another recurring theme in superbase catalysis. Like many nitrogen-rich organosuperbases, this catalyst cannot be stored for extended periods of time and has an experimental half-life of 15 days in its neat state and only 7 hours in solution.

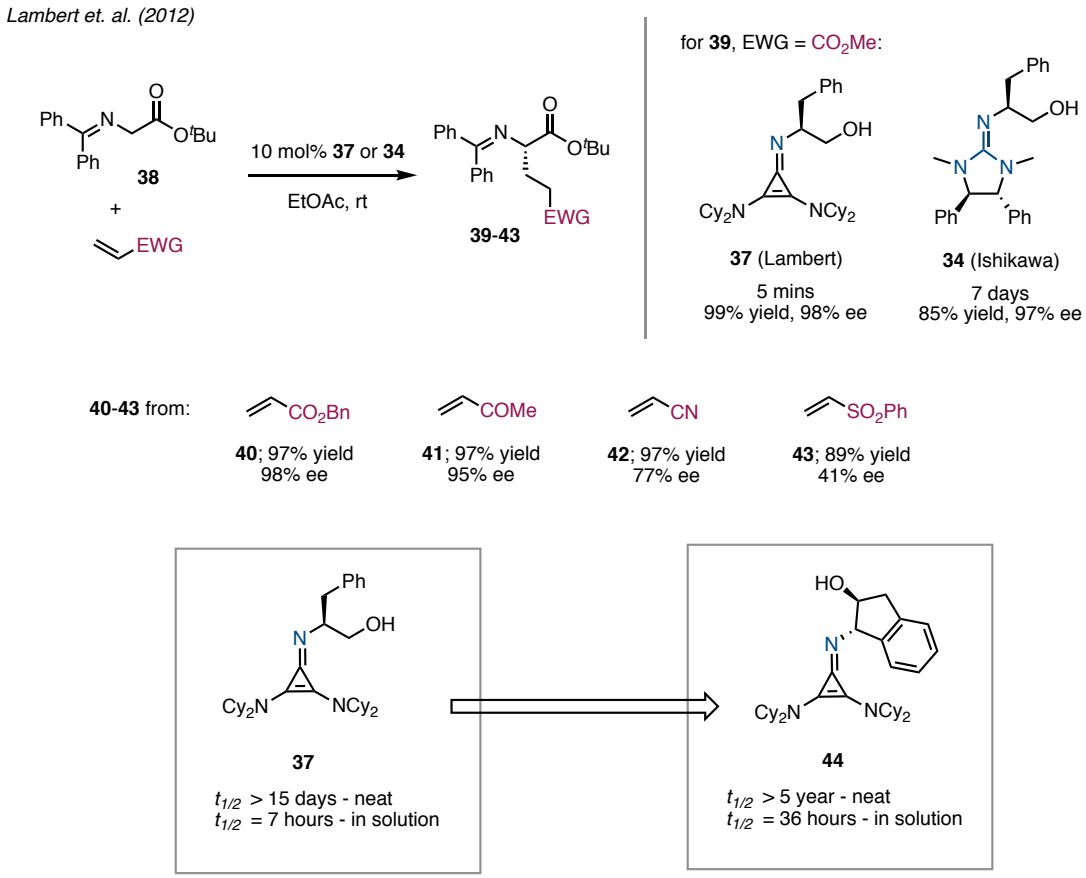

Scheme 8. Superbasic chiral cyclopropeneimine catalysts developed by Lambert, their applications and stability.

Lambert addressed the issue of catalyst stability in a later publication through iterative optimisation of the chiral 1,3-amino alcohol component to afford catalyst **44**, which boasts improved solution and solid-state stability of 36 hours and greater than 5 years, respectively.[78] Importantly, the 2nd-generation cyclopropeneimine maintains the levels of catalytic efficiency and enantioselectivity achieved with the original, less stable **37** in similar transformations. Lambert has also disclosed next generation cyclopropeneimines with far superior basicity up to pK_{BH+} 42 (in MeCN), however these impressive structures have yet to be applied to enantioselective catalysis.[80] Jørgensen and co-workers have also demonstrated the ability of **37** to catalyse enantioselective [3+2] cycloadditions of cycloheptatrienes to azomethine ylides.[80]

1.5.4 Phosphazenes

A further class of useful organosuperbase catalysts with superior basicity are phosphazenes.[81] Featuring a central phosphorus atom flanked by three amines and one imine, these compounds are remarkably strong non-nucleophilic bases and represent some of the strongest known non-ionic bases.[82] The basicity scale shown in **Figure 5** illustrates a series of increasingly basic commercially available phosphazenes primarily developed by Schwesigner in the 1980s.[83] The addition of further phosphazene units around the central iminophosphorane results in astounding increases in basicity. The most hindered of these bases also display surprisingly high resistance to hydrolysis and the action of alkylating reagents. The fully substituted *t*Bu-P$_4$-phosphazene (with four phosphazene units) achieves a staggering pK_{BH+} of 42.1 in MeCN, compared with P$_1$-phosphazene with a pK_{BH+} of 27.0

in MeCN. The extremely high basicity of these structures makes them attractive tools for enantioselective catalysis targeting high-pK_a substrates. However, chiral non-racemic examples of phosphazenes are rare and mostly restricted to the P_1 type.

Terada and Ooi pioneered niche applications of nitrogen-rich phosphazenes as catalysts. Ooi first disclosed a chiral phosphazene superbase catalyst in 2007 in the form novel spirocyclic salt **45** (**Scheme 9**).[84] To aid with catalyst handling, **45** was prepared as its HCl salt from an *L*-valine derived diamine scaffold, and liberated as the active superbasic phosphazene *in situ* using KO*t*Bu. Application of this catalyst to the Henry reaction of nitroethane and various benzaldehydes (e.g., **10**) produced benzyl alcohols with high enantio- and diastereoselectivity, for example **46** (97% ee, 19:1 dr). Tight ion-pair hydrogen-bonding between the nucleophile and phosphonium catalyst is suggested by the authors to be responsible for the high stereoselective outcome; Paton later provided computational evidence for H-bonding in this type of catalytic system.[85]

Terada subsequently used Ooi's work as a stepping-stone to design the much enhanced superbase **49** for efficient enantioselective amination of ketones with azidocarboxylates (**Scheme 9**).[86] Featuring two guanidine units anchored onto the P-centre, the active form of this catalyst is also produced *in situ* by deprotonation of its HBr salt with NaHMDS. Hence, the **49**-catalysed alpha-keto amination of tetralones (e.g., **47**) with azenes such as **48** affords aminated products **50** (95% ee). The enhanced basicity resulting from the addition of electron-rich guanidine groups is noticeable in a comparison of Terada's phosphazene **49** and Ooi's **45** in this reaction; >99% yield vs. only 18% yield, respectively.

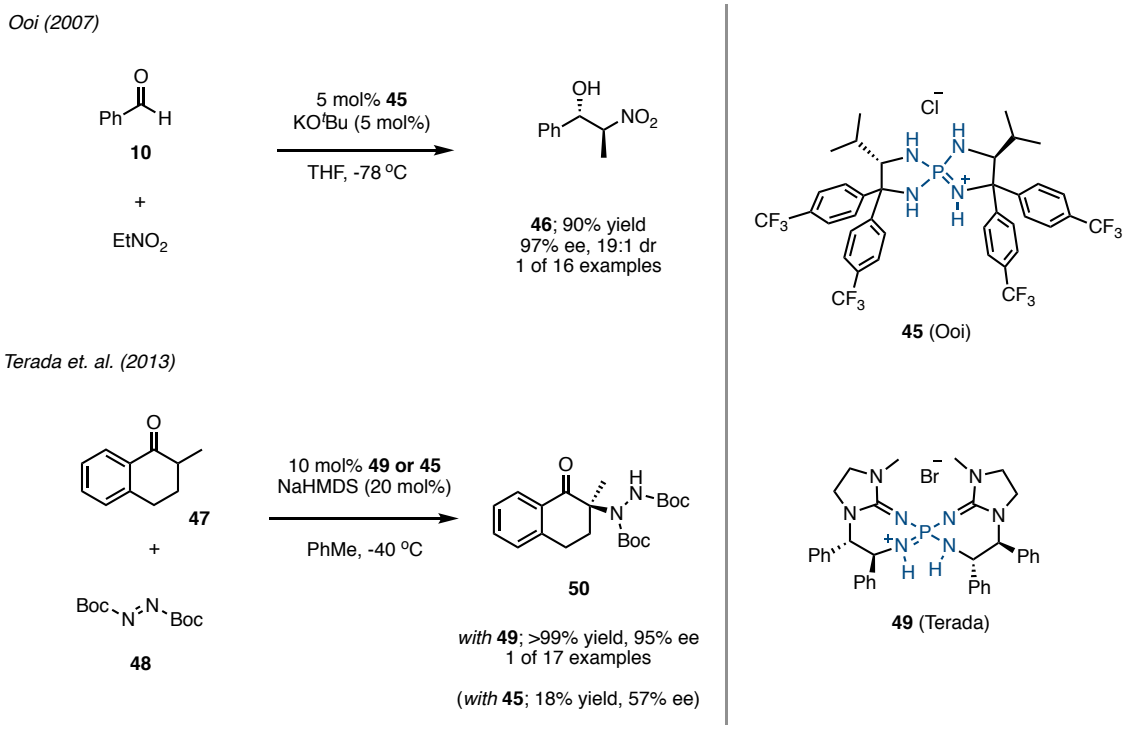

Scheme 9. Applications of novel chiral P-spirocyclic phosphazene superbases reported by Ooi and Terada.

Most recently, Terada revealed a pioneering structural design incorporating two common superbasic functionalities. This new construction unites a guanidine with a P_2-phosphazene residue through a chiral linker to deliver superbase **53** (**Scheme 10**).[86] The authors hypothesised that, in its active state, this catalyst would form a 7-membered intramolecular ring *via* H-bonding between the two basic residues. The resulting rigid conformation places the nucleophile in a tight chiral space, assuming H-bonding interactions to the guanidinium group. Application of **53** to the Mannich-type addition of thioacetates such as **51** to activated aldimines (**52**) demonstrated effectiveness to deliver Mannich products (**54**) with high enantioselectivity and moderate to high diastereoselectivity (95% yield, 88:12 dr, 95%/-3% ee for **54**). Furthermore, the authors were able to confirm their intramolecular H-bonding

theory by preparing *N*-methylated catalyst **55**, which, while demonstrating similar levels of diastereoselectivity, afforded Mannich products with very low levels of enantioselectivity (<5% *ee*).

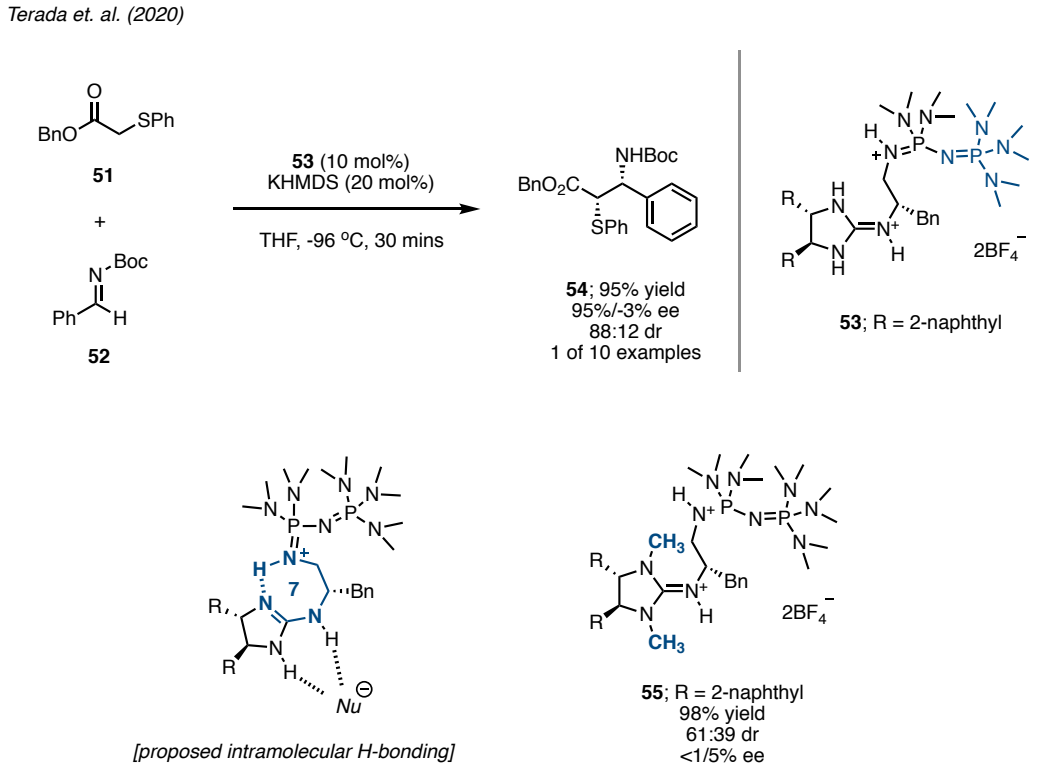

Scheme 10. Mannich reaction of thioethers with activated aldimines using **53**, and conformational analysis.

1.5.5 Iminophosphoranes

The portfolio of chiral superbase catalysts mentioned thus far has given rise to an abundance of new synthetic methodologies. Many developments have allowed chemists to overcome the imposition of low-basicity, which is characterised by the tertiary-amine organocatalysts

discussed earlier. Yet, the most effective chiral superbases - guanidines, phosphazenes and cyclopropeneimines - still suffer from high synthetic cost and difficulties with respect to their handling, as well as poor modularity. Widespread access to such catalysts in commercial and academic settings has been muted as a result.

Considering that further innovations are necessary in the field of chiral superbase catalysis, Dixon and co-workers recognised the need for a fundamentally different concept.[64] Hence, bifunctional iminophosphoranes (BIMPs) were envisaged and realised as a possible solution to both insufficient activation of pro-nucleophiles and the widespread problem of unsatisfactory enantiocontrol arising from challenging catalyst synthesis and optimisation. BIMPs have come to the forefront of superbase innovation since their inception in the early 2010's.

1.5.5.1 Design and synthesis of BIMPs

The design of the BIMP platform mirrors that of other bifunctional organocatalyst scaffolds with respect to the combination of a superbasic moiety and a H-bond donor group linked through a chiral backbone. However, the favourable properties of iminophosphoranes allow for a higher degree of modularity in their construction compared to previous superbase iterations. Such benefits lend simplicity to the task of structure-activity optimisation, and catalyst library generation with BIMPs.

The foundation of BIMP synthesis lies in preparation of a chiral amino azide; typically, these enantiopure building blocks are easily derived from cheap amino acids. Variation of the H-

bond donor is conveniently achieved by reaction of the amino azide with a desired carboxylic acid or iso(thio)cyanate to provide an amide or thio(urea). Crucially, the superbasic iminophosphorane is readily generated in a final-stage Staudinger reaction performed *in situ* and with no need to isolate the active catalyst. Judicious choice of the trivalent phosphine expedites catalyst optimisation and allows for late stage fine-tuning of the BIMP basicity. Furthermore, the requisite phosphines are usually commercially available, easy to handle and inexpensive.

Iminophosphoranes are often viewed as hydrolytically and/or thermally unstable, and indeed, synthetically, iminophosphoranes find most relevance as intermediates towards primary amines in the Staudinger reduction of azides to amines.[87,88] In this transformation, an azide is typically reacted with trimethylphosphine, and the resulting iminophosphorane hydrolysed with excess water. However, research from Dixon and co-workers has shown BIMPs to be highly air- and moisture-stable when isolated and stored in their active forms for many years under ambient conditions.[89] This provides a suitable alternative to *in situ* catalyst formation when larger amounts of catalyst are desired, for example during well-plate screening studies. Hence, iminophosphoranes are comparatively easy to prepare and handle relative to many guanidines, amidines and phosphazenes, and this simplicity is key to the inherent modularity and tunability of BIMPs.

1.5.5.2 Applications of 1st-generation BIMPs

The seminal report of the BIMP platform demonstrated efficacy in the enantioselective 1,2-addition of nitromethane to low-electrophilicity ketimines such as **56** (**Scheme 11**). This unsolved synthetic challenge was not catalysed at all by *Cinchona* alkaloid bifunctional catalyst **21** after 32 hours due to its low basicity, whereas thiourea BIMP **57** provided the addition product **58** in about 3 hours with 95% yield and 96:4 er.[90] The modularity of the BIMP design allowed for efficient optimisation of the reaction through rapid synthesis of a catalyst library by variation of the phosphine, chiral backbone, and H-bond donor. Key to the exceptional efficacy of **57** in this transformation is its high basicity; **57** has a pK_{BH+} of approximately 22.5 in MeCN. The reaction was scaled-up at 1 mol% catalyst loading to afford over 8 grams of product.

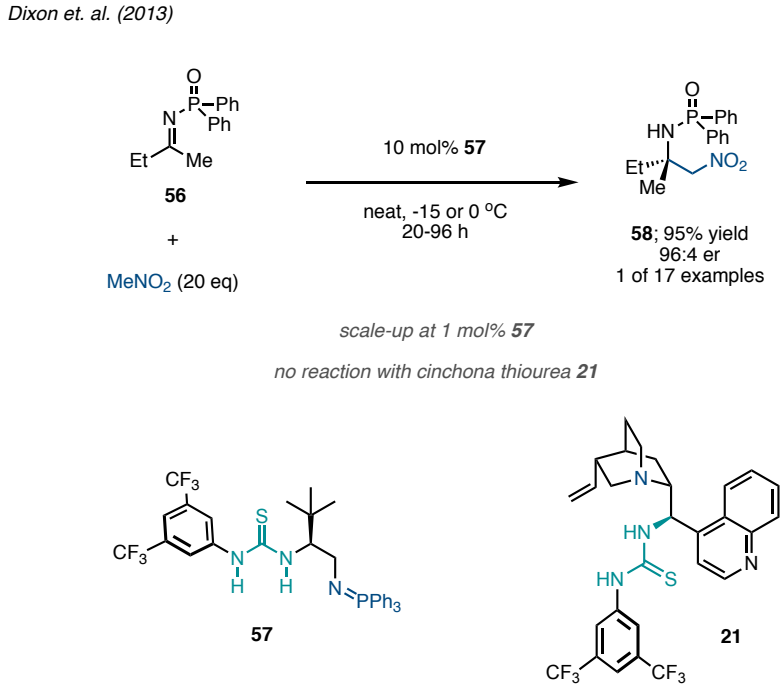

Scheme 11. Enantioselective nitro-Mannich reaction catalysed by BIMP **58** under mild conditions.

Johnson and co-workers have also been major contributors to the field of bifunctional iminophosphorane catalysis. As in the nitro-Mannich example described above, Johnson found that standard *Cinchona* derived organocatalysts where insufficient to catalyse a multicomponent cascade Pudovik addition-phospha-Brooke rearrangement reaction (**Scheme 12**).[91] BIMP **57** was found to be a superior alternative, capable of deprotonating dialkylphosphites such as **59** under cryogenic conditions to promote a 1,2-addition into benzylidene pyruvates (**60**), and control enantioselectivity in the subsequent phospha-Brooke rearrangement with benzaldehydes (**61**). The reaction affords synthetically useful and functional-group-rich products with good yield and enantio- and diastereoselectivity; the highly functionalised product **62** was obtained in 55% yield, with 96:4 er and 10:1 dr. Johnson has also reported on the conjugate additions of nitroalkanes and alkyl thiols to enone diesters catalysed by 1st-generation BIMP catalysts and demonstrated elegant downstream derivatisation of the resulting conjugate adducts.[92,93]

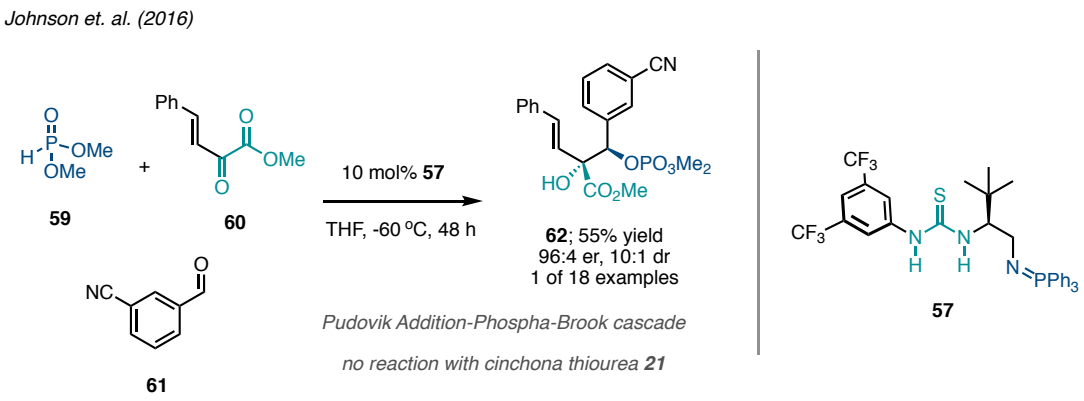

Scheme 12. Johnson's BIMP catalyzed enantioselective rearrangement cascade reaction.

Interestingly, the hindered benzhydryl-substituted catalyst **65** was employed in the total synthesis of (-)-himalensine A, a chiral alkaloid natural product.[94] BIMP **65** played an essential role in the key step, namely involving a novel cascade enantioselective prototropic shift/intramolecular Diels-Alder cycloaddition of the achiral cycloheptanone **63** (**Scheme 13**). Initially, low-basicity *Cinchona* alkaloid derived tertiary-amine catalysts were investigated as chiral bases for this reaction and were found to be largely unreactive. For example, amide **64** required an unacceptable reaction time of 7 days to afford satisfactory yields, albeit with good levels of enantioselectivity (86.5:16.5 er). The authors turned to BIMP superbases to address the issue of slow reactivity and were able to quickly optimise the method to obtain the tricycle **66** in 86% yield, 95:5 er and 92:8 dr after a reaction time of only 24 hours using only 5 mol% catalyst loading. Surprisingly, **65** could be formed *in situ* by addition of triphenylphosphine to a mixture of substrate and the azide precursor of the intended iminophosphorane catalyst.

Further research by Dixon and others has yielded 1st-generation BIMP-catalysed methods including phospha-Mannich additions to *N*-DPP-ketimines, the Michael addition of high-pK_a malonate esters to nitroalkenes, and several ring-opening polymerisation reactions of lactone and lactides.[95–100]

Dixon et. al. (2017)

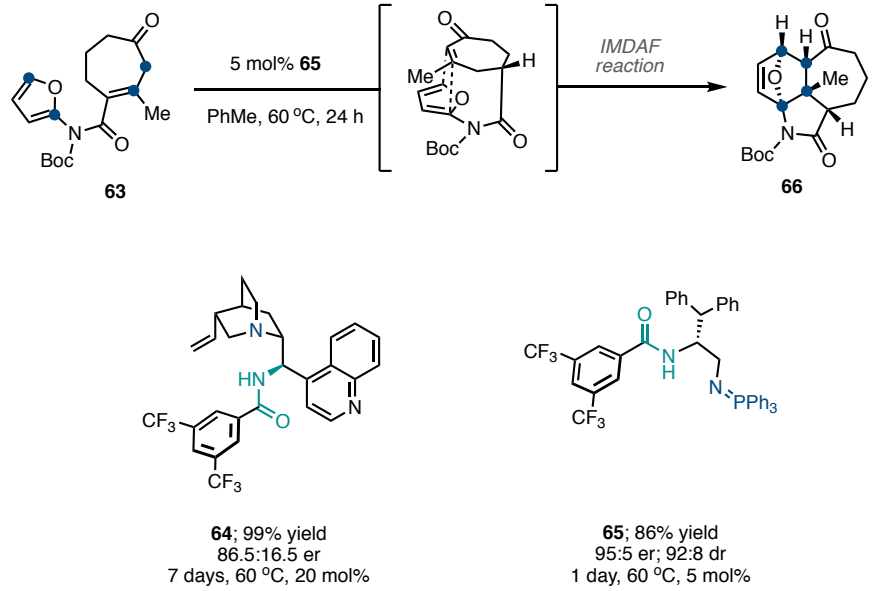

Scheme 13. Dixon's application of BIMP catalysis in the IMDAF reaction towards a key intermediate in the total synthesis of (-)-himalensine A.

1.5.5.3 Applications of 2nd-generation BIMPs

Elaboration of the 1st-generation design – which feature a single stereocentre – has afforded improved reactivity and stereoselectivity in particularly challenging transformations through the generation of a 2nd-generation family of BIMP catalysts bearing two or more stereocentres. These structures are partly inspired by the catalyst designs of Jacobsen (for example, **3**, **Figure 2**).

A representative example is BIMP **69**, illustrated in **Scheme 14**, which was developed in response to a challenging enantioselective sulfa-Michael addition (SMA) of alkyl thiols to alpha-substituted acrylate esters.[101] The combination of the low acidity of alkyl thiols (pK_a 17 in DMSO) with the low electrophilicity of alpha-substituted acrylate esters characterise the

particularly challenging aspects of this chemistry. Hence, this transformation was not possible using existing organocatalysts at the time. As seen in many other demanding reactions, *Cinchona* derived organocatalyst **21** was not capable of affording any product in the addition of propane thiol (**67**) to methyl methacrylate (**68**), even after 12 days at room temperature. 1st-generation BIMP **71**, however, afforded the SMA product **70** in quantitative yield and 72% ee after only 3 hours. Exhaustive attempts to optimise this result with other 1st-generation catalysts failed to improve selectivity, and as a result the 2nd-generation BIMPs were envisaged.

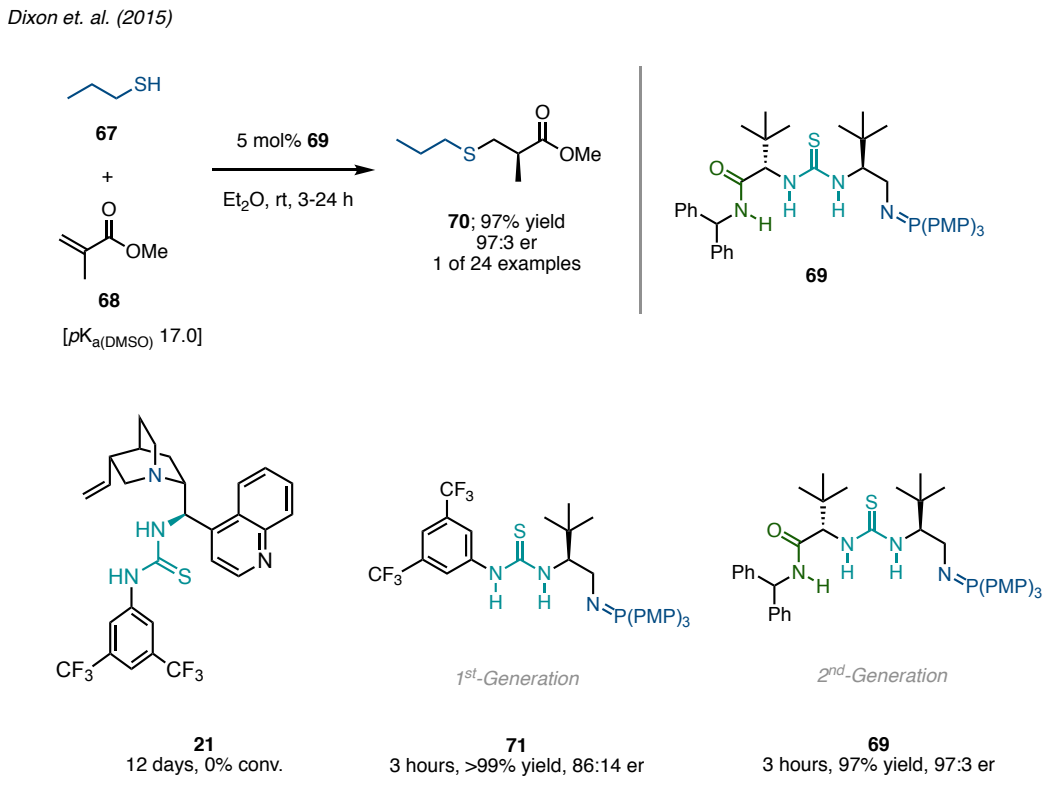

Scheme 14. Enantioselective sulfa-Michael addition catalysed by a 2nd-generation BIMP catalyts.

The addition of a distal, secondary stereocentre derived from *tert*-leucine – affording BIMP **69** - improved performance of the model reaction, allowing **70** to be isolated in 97% yield and with 97:3 er. The developed method exhibited an extremely broad scope with consistently high enantioselectivity, and a scale-up experiment that required only 48 mg of **69** (0.05 mol%) to catalyse the reaction on a 20 g scale.

Since the original dissemination of 2nd-generation of BIMPs, further applications have demonstrated the benefit of added tunability that come with an additional stereocentre. Among the achievements are the enantioselective nucleophilic desymmetrisation of phosphonate esters, enantioselective prototropic shifts applied to cyclohexanones, and the sulfa-Michael addition alkyl thiols to alkenyl benzimidazoles.[102–104]

1.5.5.4 Applications of 3rd-generation BIMPs

The most recent developments in BIMP catalyst design feature the introduction of the squaramide as an alternative H-bond donor group to amides and (thio)ureas. This strategy was first employed in the intramolecular aza-Michael addition of ureas to afford hydroquinazoline products (for example, **74**) with high enantioselectivity from the easily prepared β-aryl acrylates such as **72** (**Scheme 15**).[I] Replacing the thiourea component of catalyst **75** with a squaramide to provide 3rd-generation BIMP **73** resulted in an upside change

[I] I contributed to this work, but further details of the project will not be discussed in the context of this thesis.

in both yield (>99% vs. 71%) and enantioselectivity (94.5:5.5 er vs 80.5:19.5 er) for the isolation of **74**.[105] DFT calculations found the squaramide to be responsible for reducing destabilising Pauli repulsions between the reactants, and thereby increasing reactivity and yields. Specifically, this reduction is purported to arise from polarisation of the occupied pi-orbital of the Michael acceptor away from the electrophilic β-carbon that forms a new bond. Such polarisation reduces unfavourable orbital overlap with the incoming nucleophile. Computational studies also suggested that squaramide H-bonding, relative to a urea or thiourea, is most capable of creating an optimal chiral pocket for highly selective enantiofacial discrimination. The presence of a third stereocentre adjacent to the distal amide group had a minor positive effect on enantioselectivity.

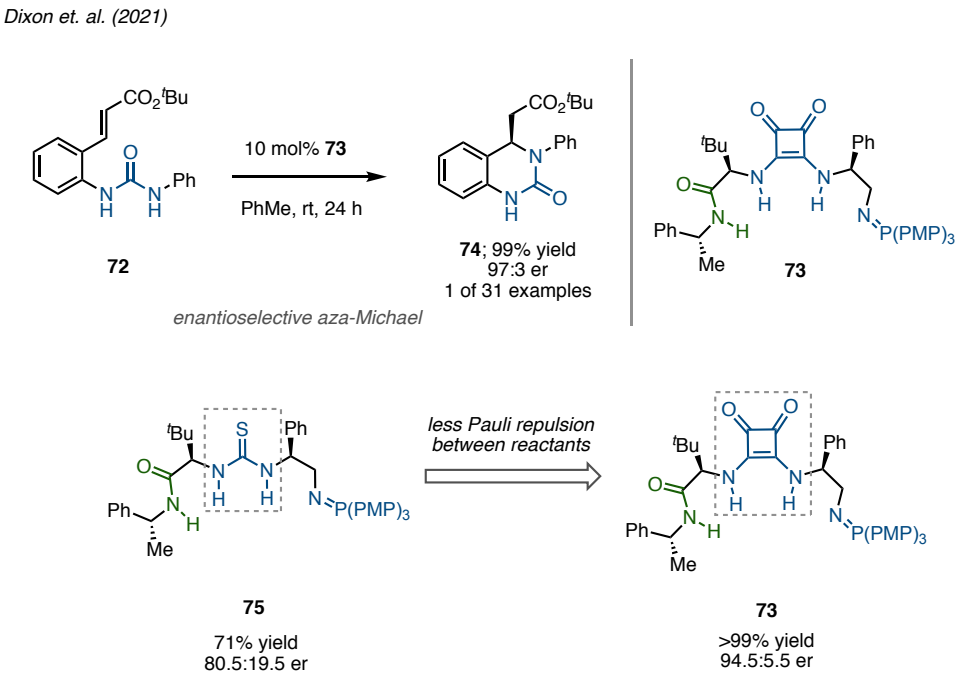

Scheme 15. Enantioselective intramolecular aza-Michael reaction catalysed by 3rd-generation BIMP **73**.

Lastly, and most recently, a highly hindered squaramide-derived BIMP (**77**) was developed as a catalyst for the extremely challenging sulfa-Michael addition of alkyl thiols to β-substituted, *N*,*N*-disubstituted acrylamides (**Scheme 16**).[106] These acceptors have previously been resistant to metal-free catalytic enantioselective Michael additions due to their low electrophilicity. Once again, the squaramide H-bond donor group was found to be essential for high reactivity and selectivity; model product **78** from the reaction between dibenzyl amide **76** and propane thiol (**67**) was isolated in 88% yield and 95% ee. Following DFT studies on the model system, calculations revealed that a crucial H-bond between the squaramide and amide groups act to rigidify the catalyst-binding site during the C-S bond formation event, thus ensuring high selectivity.

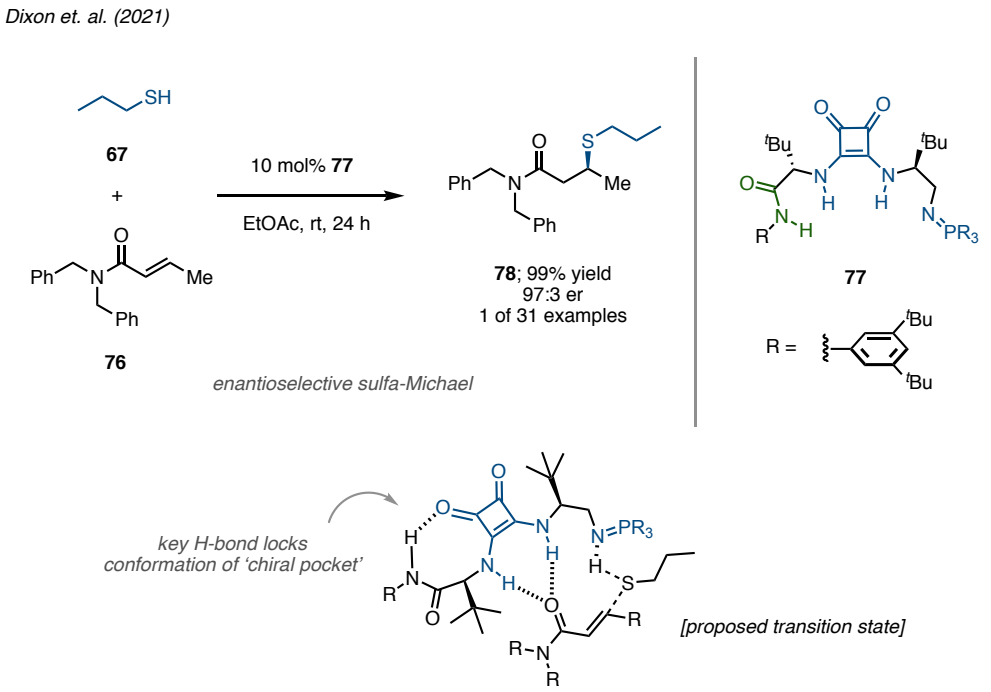

Scheme 16. Application of novel squaramide BIMP **77** to challenging SMA reactions of acrylamides.

The BIMP catalysis platform has been widely demonstrated as a sophisticated technology for highly enantioselective organocatalysis. Further to several reports of Michael additions, the range of BIMP-catalysed reactions broadly covers some of the most fundamental reactions in organic synthesis. Challenging Mannich, prototropic shift, and Diels-Alder reactions, using some of the least activated pro-nucleophiles and electrophiles currently accessible to organocatalysis, have been studied. Furthermore, BIMPs have proven utility in large-scale synthesis and shown to be amenable to immobilisation and flow-chemistry.

1.6 DPhil Aims

By 2017, the BIMP catalyst platform was well recognised as a leading technology in the field of Brønsted-base organocatalysis. Considering the existing developments, we envisaged the use of BIMP catalysts to prepare yet more challenging products and investigate underexplored pro-nucleophiles and/or electrophiles. In this context, the DPhil project aimed to explore new methodologies with the hope that challenges along the way may present opportunities for new catalyst design or reactivity. Specifically, this thesis outlines two of the most complete projects.

Initially, we identified the potential for BIMPs to act as catalysts in challenging direct aldol additions. It was hypothesised that superbasic iminophosphoranes could sufficiently deprotonate high-pK$_a$ aryl methyl ketones to act as pro-nucleophiles in the direct aldol addition reaction. These investigations are reported in Chapter 2.

Next, we recognised the importance and prevalence of pyrazolines in pharmaceuticals and agrochemicals. A lacking toolkit of synthetic strategies to access these motifs in a single enantiomeric form prompted us to explore the use of BIMPs in their preparation. Ultimately, however, it was found that BIMPs were not optimal for this purpose by way of their ability to catalyse the retro-Michael addition of a key intermediate. Subsequent investigations into alternative organocatalysts proved more successful; the findings of this study are presented in Chapter 3.

Chapter 2

Catalytic Direct Aldol Additions of Aryl Ketones

2.1 Chapter Overview

This chapter outlines the fundamental principles of the aldol reaction and its implications in both modern and historical enantioselective synthesis. Building on these concepts, the development of a bifunctional organocatalyst and its application in the catalytic enantioselective direct aldol reaction of aryl ketones is described. Specifically, chiral β-hydroxy ketones were prepared with high enantioselectivity (up to >99:1 er) from (hetero)aryl methyl ketones and (hetero)aryl α-fluorinated ketones. The strong Brønsted basicity required for efficient activation of (hetero)aryl methyl ketones is provided by a

bifunctional iminophosphorane (BIMP) superbase. The developed method is convenient and offers high tolerance of functional groups and pharmaceutically relevant heterocycles. Several mechanistic considerations are discussed, and the efficiency of the new method is compared to existing catalytic systems.

2.2 Introduction

The aldol reaction is amongst the most powerful and well-known tools in synthetic organic chemistry. This class of reaction has thus found widespread use in the fine chemical industry for the development of molecular complexity.[107] The keto-alcohol products serve as rich synthetic handles for downstream functionalisation.[108,109] Furthermore, the potential for perfect atom-economy in direct addition reactions has strengthened the aldol platform as a central area of study while the role of sustainability becomes ever more pertinent to chemists.[110,111] Although offering fundamental reactivity for the synthesis of carbon-carbon bonds, aldol reactions often suffer from several drawbacks. Disadvantages include undesired side-reactions such as dehydration, cross-condensation, and over-addition resulting from low chemoselectivity.

2.2.1 Preformation of enolate equivalents

Oftentimes pre-activation of the nucleophilic ketone component in any given aldol reaction is required to minimise serious side-reactions and ensure high yields of the desired product. The two most common strategies involve either: (1) metal enolates, derived from strong sodium, potassium or lithium bases, which are highly reactive even in the absence of

activating agents or catalysts, or (2) less reactive silicon enolates typically requiring additional catalysts to promote reactivity with an electrophilic carbonyl.[112–115] Under kinetic control, these metal/metalloid species allow for cleaner reaction profiles and greater reaction control to afford aldol products in a chemo- and regioselective manner.

Applications of preformed enolate equivalents to catalytic stereoselective aldol chemistry is generally limited to the less reactive silicon enolate species. Such reactions are known as Mukaiyama aldol additions, and the explicit need for an activating agent in combination with silyl enol ether derivatives presents an opportunity for the introduction of chiral non-racemic additives that function sub-stoichiometrically as activators. Hundreds of examples have been reported, covering the use of chiral complexes of boron, lithium, palladium, silver, copper and zinc, amongst others.[116–122] Meanwhile, the metal enolates, for example lithium, are often too reactive for satisfactory reaction control to be achieved in a stereoselective context.

The Mukaiyama aldol reaction remains as one of the most fundamental applications of metal-free Lewis acid chemistry.[123] Classically, a Lewis acid activates a carbonyl acceptor by increasing its electrophilicity towards addition of the silicon enolate. For example, List and co-workers have demonstrated the use of chiral Brønsted acid catalysts for the enantioselective Mukaiyama aldol reaction of simple enolsilanes and aldehydes, such as the reaction of TBS enol ether **82** with pivaldehyde (**83**) (**Scheme 17**).[124] The hindered imidodiphosphoramidate catalyst **84** was found to be essential for extremely efficient reactivity; product **85** was obtained in 86% yield and 95:5 er. The authors suggest that the confined nature of the catalyst creates a buried binding pocket too small for the reaction

products to dock into, therefore preventing further reaction of the products (specifically over-additions). While List's example of rational catalyst design resulted in an elegant method, similar examples of high-efficiency catalysis are rare in the primary literature, and the preparations of effective catalysts such as **84** are typically synthetically cumbersome.

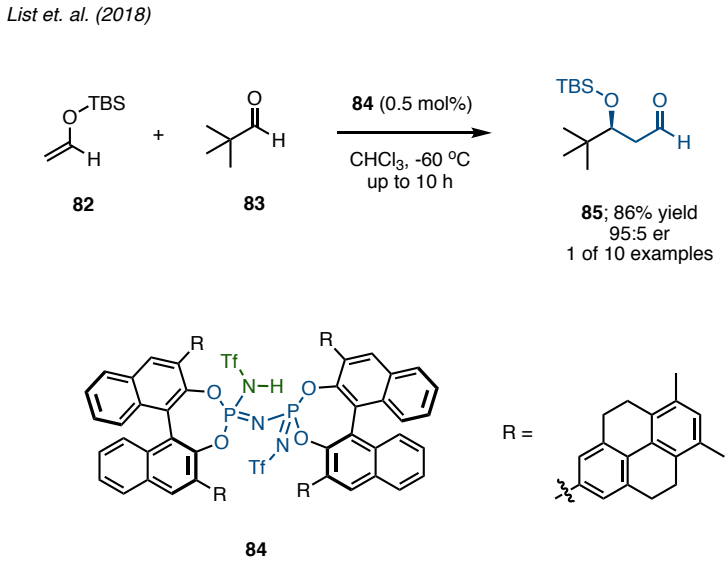

Scheme 17. List's chiral Brønsted-acid catalysed aldol addition of silyl enol ethers to aldehydes.

2.2.2 Direct aldol additions

The use of pre-activated species in enantioselective chemistry remains largely unappealing due to the poor atom economy associated with the preparation and isolation of activated enolate equivalents such as enol silanes. A more attractive approach is the direct aldol addition reaction; the need for pre-activation of the nucleophile is obviated by the use of a catalyst capable of *in situ* activation of a pro-nucleophile. Chemistry of this type allows access to fundamental synthetic intermediates with theoretically perfect atom-economy.

In the early 1970s, Hajos and Parrish, and Eder, Sauer and Weichert independently reported the first known enantioselective direct aldol addition reaction.[18,19] Their seminal reports use *L*-proline (**87**) to catalyse the highly enantioselective enol-*endo* aldolization of ketone **86** to afford the attractive bicycle **88** in 93% ee (**Scheme 18**). The reaction likely proceeds through an organised chair-like transition state. Attack of the intermediate enamine on one of the cyclic ketones is controlled by intramolecular H-bonding interactions that allow discrimination between the enantiotopic and prochiral electrophilic ketones.

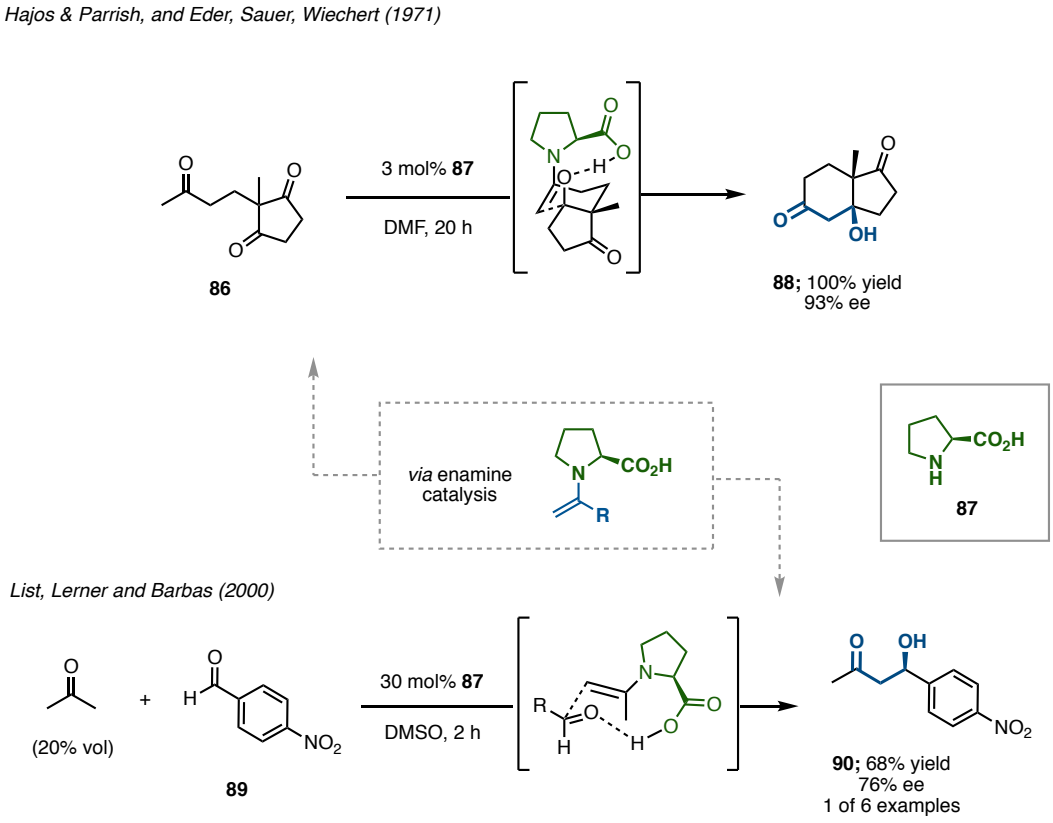

Scheme 18. First examples of the intramolecular (top) and intermolecular (bottom) enantioselective direct aldol additions.

Several decades later, Barbas, Lerner and List realised the intermolecular counterpart to the Hajos–Parrish–Eder–Sauer–Wiechert reaction by performing an aldol reaction between acetone and 4-nitrobenzeladehyde (**89**) (**Scheme 18**).[125] Again, relying on *L*-proline as a cheap and widely available organocatalyst, their method likely involves an enamine mechanism wherein the condensation product of acetone and proline attacks the non-enolisable aldehyde **89** to afford the desired β-hydroxy ketone **90**. Hydrogen-bonding is key to the high enantiocontrol of the reaction. Specifically, a H-bond between the proline carboxylic acid and the incoming electrophilic aldehyde arranges the reaction partners according to the Zimmerman-Traxler model through an organised chair-like transition-state organisation. Hence, the most sterically demanding substituent of the aldehyde is located favourably at the pseudo-equatorial position, to afford the (*R*)-enantiomer of product **90** with 76% ee and 69% yield.

These formative discoveries have inspired numerous enantioselective variations of the direct aldol addition, collectively allowing the construction of optically active natural products, macromolecules, and modern small-molecule drugs.[107,114,126–130] Significant developments in this field have since come from the groups of MacMillan,[131–133] Shibasaki,[134–136] Maruoka,[137–140] and many others,[141–148] and have fuelled the growing utility of this familiar reaction. The wide breadth of publications on this matter highlights the enormous substrate scope of enantioselective direct aldol additions. With respect to electrophilic acceptors, a variety of compounds are able to react efficiently with ketone donors under mild conditions, including but not limited to ketones, aldehydes, keto-esters,[149,150] keto-phosphonate,[151,152]

glyoxal derivatives,[153,154] isatins,[155–157] and keto-acids (**Figure 7**).[158,159] However, the scope of this platform is still somewhat limited with respect to the range of compatible nucleophilic donor synthons.

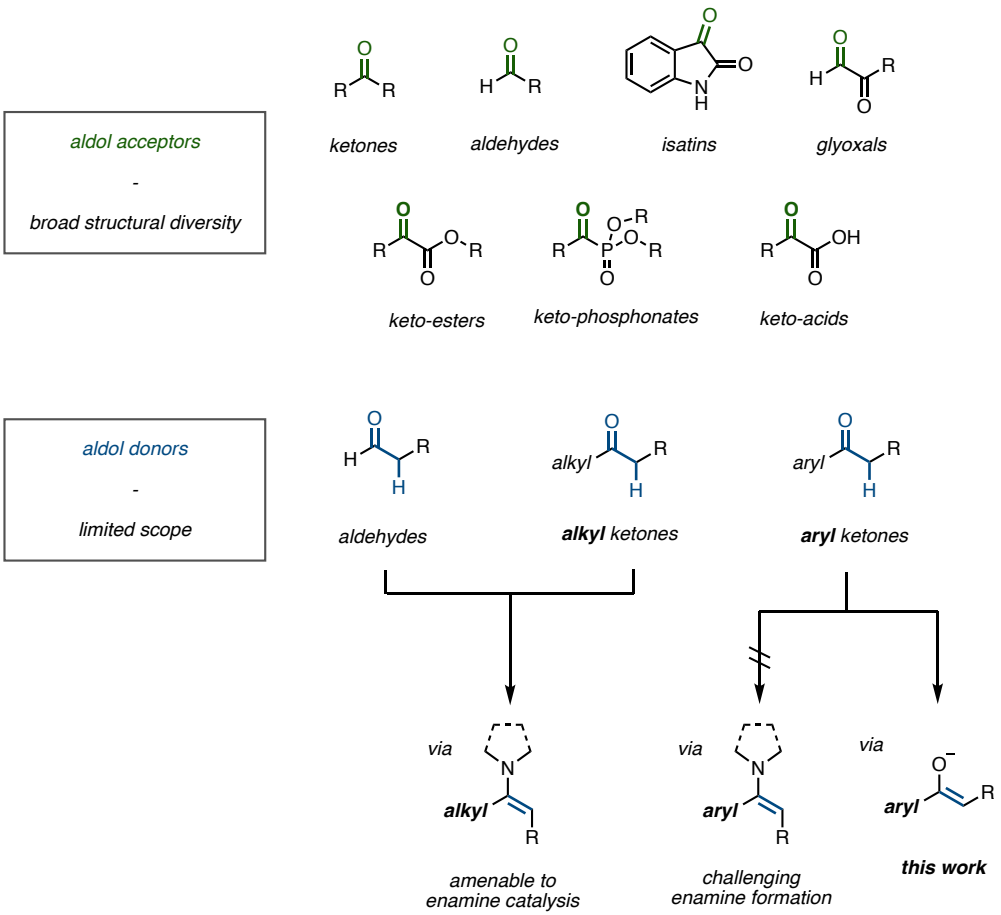

Figure 7. Overview of typical donor and acceptors synthons in enantioselective direct aldol addition reactions.

Primary or secondary amine catalysis is commonly employed in the direct aldol reaction of ketones.[160] The efficiency of these strategies is highly dependent on the ability of the ketone donor and amine catalyst to form a transient reactive enamine. Aliphatic ketones are generally amenable to this strategy due to their facile activation *via* enamines and have been

extensively utilised in enantioselective aldol reactions.[161–166] Meanwhile, the use of (hetero)aryl ketones as pro-nucleophilic synthons is mostly an outstanding challenge due to their low electrophilicity and reluctance for enamine formation. Hence, aryl ketones are generally precluded from being synthetically useful in the context of enantioselective enamine catalysis towards 1,2-additions.

An alternative to enamine activation for (hetero)aryl ketones is enolate formation. However, the high pK_a of these substrates (pK_a ~25 in DMSO) generally limits catalytic access to aryl enolate intermediates.[24] Stoichiometric amounts of strong organometallic bases, such as LDA, can overcome this challenge but with the drawback of simultaneously limiting substrate tolerance and the potential for catalytic enantioselective methods. To date, examples of enantioselective ketone-ketone aldol reactions are relatively rare for high pK_a donors such as feedstock aryl methyl ketones (e.g., acetophenone).

2.2.3 α-Fluorinated ketones as aldol substrates

Of the many reported aldol acceptors, some of the most competent are α-fluorinated ketones.[167–169] Being intrinsically activated by the electron-withdrawing fluorine atom(s), α-fluorinated ketones act as convenient sources for the incorporation of C-F bonds, which are privileged in medicinal chemistry.[170–172] In the primary literature, over 20 reports describe the enantioselective direct aldol addition of *aliphatic* ketones to trifluoromethyl ketones. Many reports demonstrate the use of chiral primary or secondary amine catalysis, principally favouring proline-derived catalysts.[173–177] For example, two reports from the groups of Nakamura and Kokotos in 2011 demonstrate the efficacy of enamine catalysis when applied

to the aldol reaction of simple aliphatic ketones such as acetone (**Scheme 19**). Nakamura described the 8-quinolinesulfonamide proline derivative **92** as a competent catalyst for the direct addition of acetone to (trifluoromethyl)acetophenone (**91**).[174] The authors proposed a transition state involving a chair-like conformation centred around H-bonding to the sulfonamide proton. Steric repulsion from the quinoline places the bulky trifluoromethyl group in the pseudo-equatorial position resulting in high enantiofacial discrimination during subsequent attack by the nucleophilic enamine. Meanwhile, Kokotos reported prolinamide **93** bearing a thiourea as the H-bond donor for efficient catalysis of the identical reaction.[177] In both reports, β-hydroxy ketone **94** was obtained with high yield and good to high enantioselectivity.

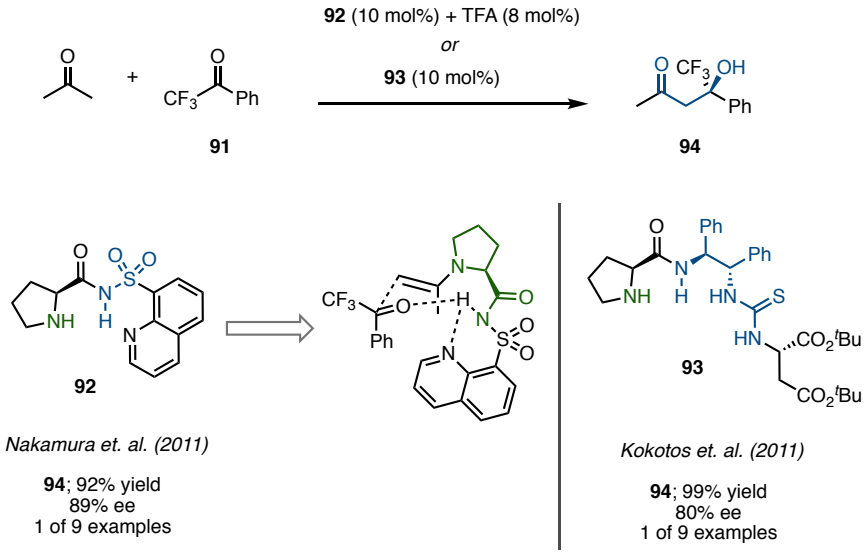

Scheme 19. Examples of alkyl ketones engaging in aldol chemistry *via* enamine catalysis as reported by Nakamura and Kokotos in separate 2011 publications.

Comprehensive research surrounding *aliphatic* ketone additions has enabled facile access to a broad scope of aliphatic β-hydroxy ketone products derived from α-fluorinated ketones.

On the other hand, only two examples utilising *aryl* ketones as the donor component have been reported to the best of our knowledge (**Scheme 20**).[178,179] Owing to the difficulty of forming aryl enamines, both examples instead use Takemoto's bifunctional tertiary amine catalyst (**6**) as a weak Brønsted base to promote enolate formation.[29]

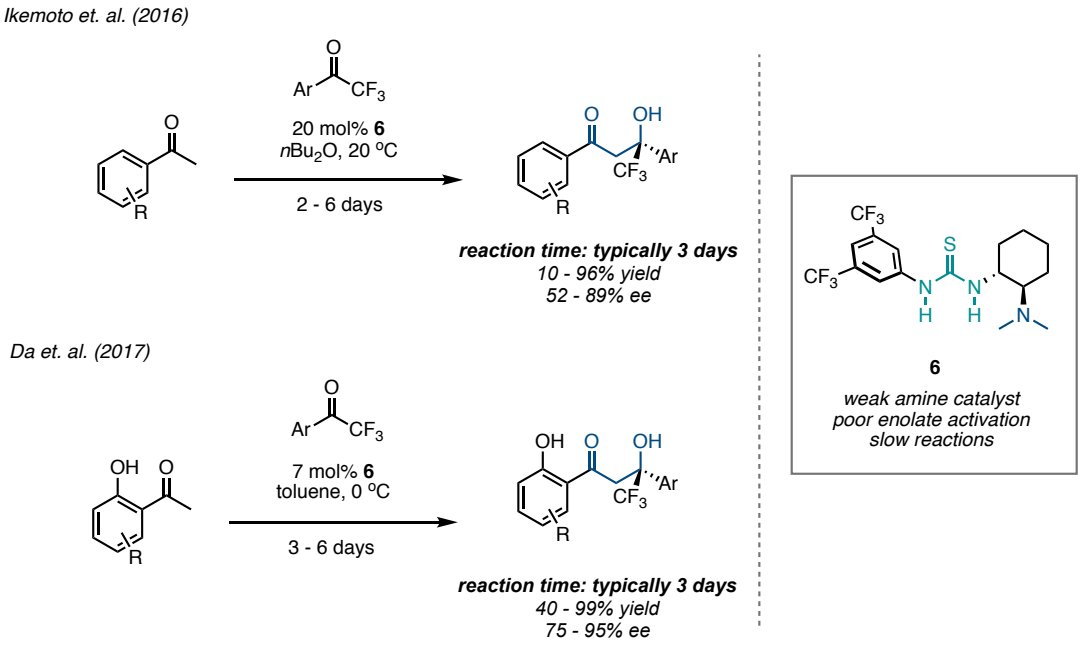

Scheme 20. Literature precedent for the direct aldol reaction of ketones to trifluoromethyl ketones.

Both reports, from the groups of Ikemoto and Da, are constrained by the low basicity of catalyst **6**. Reaction times of up to 6 days for unactivated substrates, and typically 3 days for activated substrates, are required to achieve acceptable yields. Da's report is further limited to exclusively *ortho*-hydroxyacetophenones. The presence of the hydroxy group is thought to lend an additional H-bond to the adjacent ketone to increase acidity of the alpha-proton and aid in enolisation. Although they demonstrate synthetic utility, both reports embody a limitation in the synthetic toolbox for constructing simple β-hydroxy ketones in an

enantioselective manner. Specifically, these limitations arise from the low Brønsted basicity of Takemoto's tertiary-amine catalyst, which results in limited activation of the high-pK_a pro-nucleophilic aryl ketone as an ammonium enolate.

More revealing to the challenging nature of this chemistry is the absence of metal-catalysed enantioselective methods, or any diastereoselective methods, in the primary literature for the stereoselective direct aldol reaction of aryl methyl ketones and trifluoromethyl aryl ketones. Consequently, given the clear challenges and lack of precedent, the identification of new catalyst systems capable of efficiently activating aryl ketones towards aldol chemistry would significantly advance the field. The opportunity for new catalyst design, and the attractiveness of enantioenriched β-hydroxy ketones as building blocks made this challenge particularly appealing to us. Towards this end, we directly targeted the design of high-basicity catalysts, which could rapidly form aryl enolate intermediates to be stereoselectively trapped by α-fluorinated ketones. We specifically envisaged the use of a bifunctional iminophosphorane (BIMP) superbase of the type developed by Dixon and co-workers, such as those described in Chapter 1.5.5.

2.3 Proof of Concept and Optimisation

As a representative model system, we began assessing organocatalysts for efficacy in the reaction of acetophenone (**95**) with 2,2,2-trifluoroacetophenone (**91**). It is worth noting that prior to development of the herein reported method, the best previously reported process to enantioselectively access aldol adduct **96** required a reaction time of 144 hours (6 days),

as reported by Ikemoto with Takemoto's catalyst (**6**).[179] As expected from its low basicity, the *Cinchona* alkaloid **20** was not competent in the studied aldol reaction, affording only traces of aldol adduct **96** after 24 hours, as determined by ^{1}H NMR (**Table 1**; entry 1). Pleasingly, treating equimolar amounts of **95** and **91** with 10 mol% of 1st-generation BIMP **97** at room temperature in diethyl ether afforded product with 64% conversion and 62:38 er after 24 hours (**Table 1**; entry 2).

Having established proof of concept, we turned our attention to modification of the catalyst structure. As described in Chapter 1.5.5, the synthesis of BIMPs is highly modular in nature, allowing for rapid optimisation. The 2nd-generation BIMP **98** bearing a *cis-tert*-butyl chiral backbone did not afford an improvement of enantioselectivity (**Table 1**; entries 3). Further screening of 2nd-generation BIMPs was not fruitful (see Chapter 4. for more details). Returning to the simpler 1st-generation BIMP scaffold, catalyst **99** bearing a sterically demanding benzhydryl-substituted backbone and a secondary amide gave a pleasing uplift in enantioselectivity and yield to 75:25 er and >95%, respectively (**Table 1**; entry 4). Generation and testing of less-basic analogues of **99** by variation of the iminophosphorane substituents highlighted the need for high-basicity in this challenging aldol reaction. For example, use of the less electron-rich, and therefore less basic, *tris*(phenyl) iminophosphorane **65** lowered conversion to only 63% yield after 24 hours (**Table 1**; entry 5). Likewise, use of the more electron deficient iminophosphorane derived from *tris*(4-chlorophenyl)phosphine eliminated almost all reactivity - only 8% conversion to **100** was observed (**Table 1**; entry 6). Further fine-tuning of the catalyst found the strongly basic and sterically demanding 1-naphthyl amide catalyst **102** to be optimal, which, in combination

with a solvent change to CPME and cooling to -15 °C, afforded **96** in 97:3 er and 96% isolated yield (**Table 1**; entry 10).

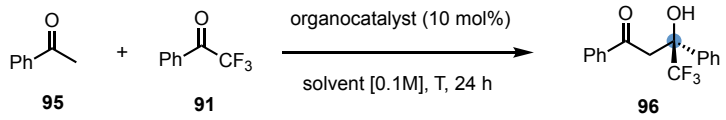

entry	catalyst	solvent	T	conversion (%)[a]	er[b]
1	**20**	Et_2O	rt	trace	N.D.
2	**97**	Et_2O	rt	64	62:38
3	**98**	Et_2O	rt	52	61:39
4	**99**	Et_2O	rt	>95	75:25
5	**65**	Et_2O	rt	63	74.5:25.5
6	**100**	Et_2O	rt	8	N.D
7	**99**	CPME	rt	>95	82:18
8	**99**	CPME	-15 °C	>95	90:10
9	**101**	CPME	-15 °C	>95	94:6
10[c]	**102**	CPME	-15 °C	96[d]	97:3

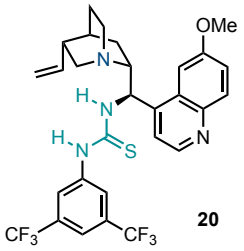

20

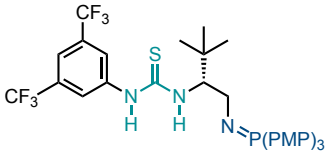

97

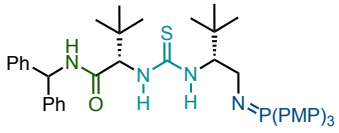

98

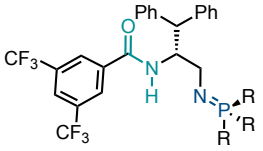

99: R = PMP
65: R = Ph
100: R = 4-ClC$_6$H$_4$

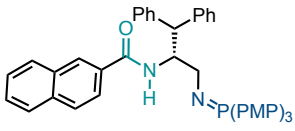

101

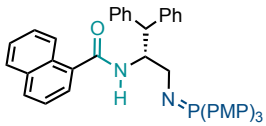

102

Table 1. Optimization of the direct aldol addition of acetophenone (**95**) to 2,2,2-trifluoroacetophenone (**91**). [a] determined by ^{1}H NMR analysis of crude reaction mixture. [b] determined by HPLC analysis on chiral stationary phase. [c] 18 hour reaction time. [d] isolated yield. N.D. = not determined. CPME = cyclopentyl methyl ether. PMP = *para*-methoxy phenyl.

2.4 Evaluation of Reaction Scope

With an efficient protocol in hand, the efficacy and limitations of our new catalytic system were probed across a wide range of donor and acceptor (hetero)aryl ketones.

2.4.1 Scope of the reaction with respect to aryl ketones

Simple halogen substituents at the *para*- or *meta*-positions of either the donor or acceptor ketone were well tolerated; 4-fluoro (**103**), 4-bromo (**104**) and 3-iodo (**105**) derivatives were obtained with consistently high enantioselectivity of 95:5 er or higher (**Scheme 21**). Synthetic handles were also incorporated at the *para*-position with minimal fluctuation of selectivity and yield: 4-nitro (**106**), 4-vinyl (**107**), 4-cyano (**108**), and 4-thiomethyl (**109**) functionalised products were isolated with generally high yield and enantioselectivity. Aldol derivative **110** was obtained in 96:4 er and 60% yield from the reaction of 4-phenylacetophenone. Aryl methyl ketones bearing 3-methyl and 3-methoxy substituents were also well tolerated and afforded products **111** and **112** with 95:5 er.

Unfortunately, variation at the *ortho*-position was not tolerated on the α-fluorinated ketone, and only *ortho*-fluoro was accommodated on the methyl ketone to afford 2-fluoro aldol adduct **113** in 88% yield and 96:4 er. It is most likely that tight catalyst-substrate binding is interrupted by the steric bulk associated with *ortho*-substitution, thereby preventing activation and organisation of one or both ketone substrates.

Introduction of multiple substituents was well tolerated by BIMP **102**, allowing the preparation of products decorated with 3-methyl-4-benzoate and 3-trifluoromethyl-4-methyl substitution patterns (**114** and **115**). Finally, variations to the benzene core provided

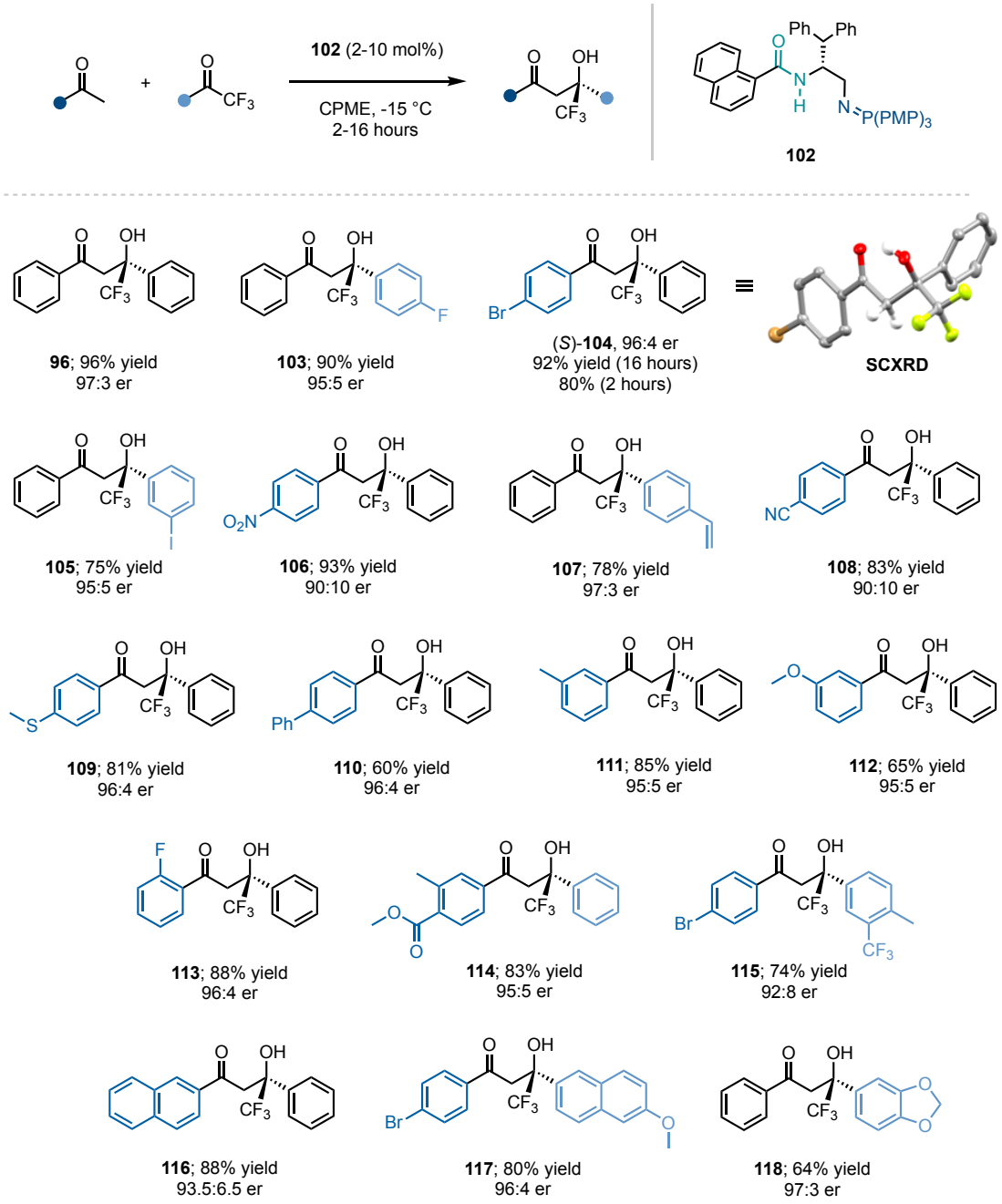

Scheme 21. Scope of the BIMP catalyzed direct aldol addition with aryl ketones. Stereochemical configuration was assigned by analogy with (*S*)-**104** (determined by single crystal X-ray diffraction studies).

2-naphthyl and methylenedioxyaryl derivatives **116**-**118**. Absolute configuration was determined on the crystalline 4-bromo derivative **104**; single crystal X-ray diffraction studies confirmed (*S*) stereochemical configuration at the benzylic tertiary alcohol. All other products were assigned by analogy. Interestingly, subjecting 1,4-acetylbenzene (**119**) to the standard reaction conditions, but with 3 equivalents of **91** instead of 1 equivalent, the *para*-bis-aldol product **120** was furnished (**Scheme 22**). The diastereoselectivity was high (20:1 dr determined by ^{1}H NMR of the crude reaction mixture) and the major diastereomer was isolated in 80% yield with 95:5 er.

Scheme 22. Double aldol addition between 1,4-diacetylbenzene (**119**) and trifluoromethyl ketone **91**.

2.4.2 Scope of the reaction with respect to heteroaryl and alkenyl ketones

Following the successful evaluation of reaction scope with respect to substituted aryl groups, we proceeded to investigate the use of heteroaryl ketones as an avenue to generate enantioenriched aldol product bearing heterocycles commonly found in pharmaceutical drug candidates. We were pleased to find that the new BIMP-catalysed transformation was amenable to a wide variety of heterocyclic methyl ketones and trifluoromethyl ketones (**Scheme 23**). Attractive products bearing nitrogen heterocycles such as quinoline (**121**),

pyrazine (**122**), pyridine (**123**), 2-thiazole (**124**), 4-thiazole (**125**) and pyrazole (**126**) were furnished under standard conditions with generally high enantioselectivity (92:8 to >99:1 er) and good to excellent yield (72–98%). Notably, 2-thiophene adduct **127** was isolated as a single enantiomer (>99:1 er). When the reaction was performed with an α,β-unsaturated methyl ketone we were pleased to find that catalytic efficiency was maintained; alkenyl β-hydroxy ketone **128** was obtained with 98:2 er and 91% yield.

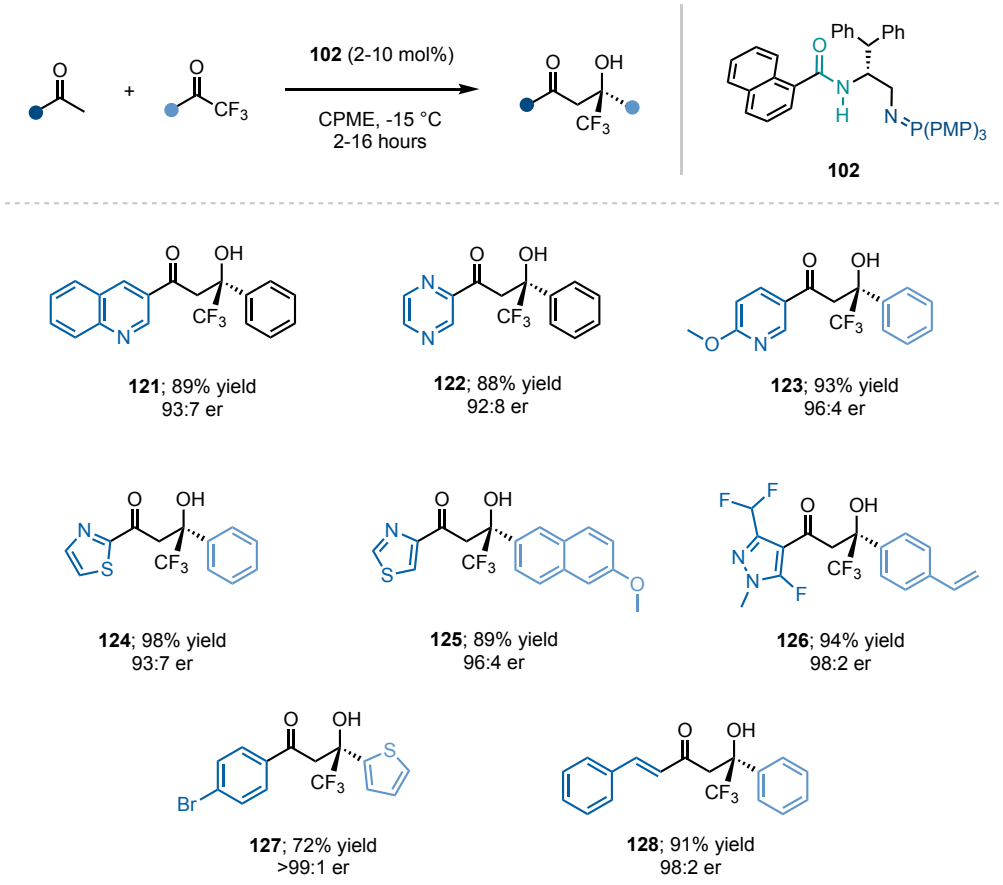

Scheme 23. Scope of the BIMP catalyzed direct aldol addition with respect to heteroaryl ketone donors and acceptors. Stereochemical configuration was assigned by analogy with (*S*)-**104** (determined by single crystal X-ray diffraction studies).

2.4.3 Variation of the fluorinated group

Having demonstrated a wide scope with respect to heterocycles and functional group tolerance, attention turned to variation of the fluorinated group positioned at the acceptor ketone. Extension of the trifluoromethyl group to higher-order fluorinated alkyl chains proved successful. Perfluoro-*ethyl* and perfluoro-*heptyl* ketones efficiently performed in the aldol addition with acetophenone and 4-(bromo)acetophenone to respectively afford **129** and **130** with high yield and enantioselectivity (**Scheme 24**). Furthermore, reaction of a chlorodifluoromethyl ketone smoothly furnished **131** with 85% yield and 96.5:3.5 er.

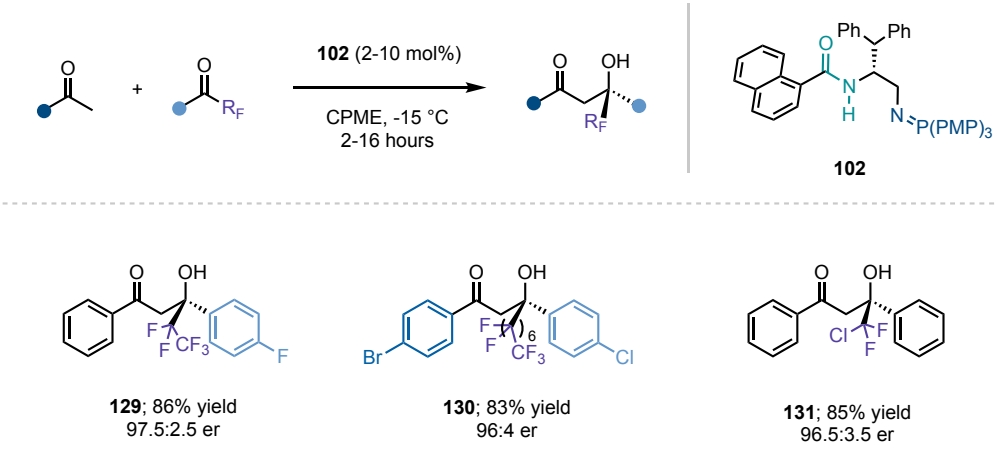

Scheme 24. Scope of the BIMP catalyzed direct aldol addition with respect to non-CF_3 alpha-fluorinated ketone acceptors. Stereochemical configuration was assigned by analogy with (*S*)-**104** (determined by single crystal X-ray diffraction studies).

2.4.4 Limitations of the reaction scope

Generally, the reaction profile was clean, with only unreacted starting materials, catalyst and products observed in the crude reaction mixture (along with catalyst decomposition

products, which will be discussed later in this chapter). However, the method has several limitations (**Figure 8**). For example, (trichloromethyl)acetophenone **132** failed to afford any product, possibly due to insufficient electrophilicity or higher steric hinderance compared to its trifluoromethyl analogue. Similarly, 2,4,6-trimethylacetophenone (**133**) also failed to participate in the aldol addition, very likely due to steric hinderance from the *ortho* positions blocking catalyst association. The failure of electron-deficient *bis*(3,5-trifluoromethyl) ketone **134** to afford any product probably relates to its ability to deactivate catalyst **102** – the origins of this observation are discussed further in Chapter 2.7.5. Furthermore, highly electron-rich aryl methyl ketones do not engage in this method, for example 3,5-(dimethoxy)acetophenone (**135**). It is most likely that the pK_a of this substrate is beyond the activating power of catalyst **102**.

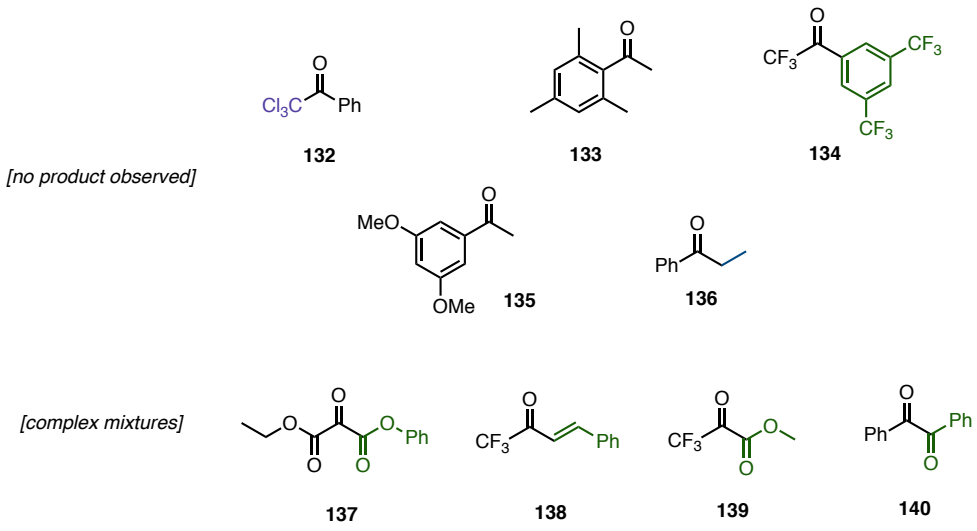

Figure 8. Ketone donors and acceptors that failed in the BIMP catalysed aldol reaction.

Disappointingly, enolisable aryl ketones other than methyl ketones, such as propiophenone (**136**), failed to afford the expected aldol adduct. We believe that rapid reversibility of the reaction with substrates of this type (*via* a retro-aldol reaction) most likely arises from the steric strain in the desired product, which would place hindered tertiary and quaternary centres adjacent to each other. Higashiyama reported observing this retro-aldol process in the diethylzinc catalysed preparation of the identical reaction product of **136** and **91**.[180] Lastly, a range of highly activated ketone acceptors failed to cleanly afford the corresponding aldol addition products. Complex mixtures of products were observed with ketones **137**-**140**.

2.5 Preparative Scale Synthesis and Catalyst Recycling

With a desire to substantiate the scalability of the new method, and elaborate possible downstream applications, the reaction of (4-bromo)acetophenone (**141**) with **91** was performed on an 8-gram scale. To limit financial and environmental costs, catalyst loading was reduced to 2 mol%, the solvent was switched to TBME (a cheaper alternative to CPME), and the reaction concentration increased ten-fold to reduce the solvent volume (1.0 M reaction concentration, instead of the standard 0.1 M). Upon lowering the catalyst loading, a longer reaction time of 36 hours was required to achieve full conversion and provide crude product with 94.5:5.5 er (**Scheme 25**). Following a single recrystallisation, and without the need for chromatographic purification, 13 grams of enantiopure (>99.5:0.5 er) aldol adduct **104** was obtained in 87% yield.

Recovery of the catalyst was facile. Upon reaction completion, the mixture was poured into water to precipitate BIMP **102**. Filtration and drying of the solids allowed 96% recovery of catalyst. Hydrolysis of the potentially water-sensitive iminophosphorane was not observed. The recovered catalyst was sufficiently pure to be resubjected, under the standard reaction conditions, to the model reaction of **95** with **91**. No erosion of activity was observed and enantioselectivity was maintained to afford **96** in 96% yield and 97:3 er (identical to using fresh catalyst).

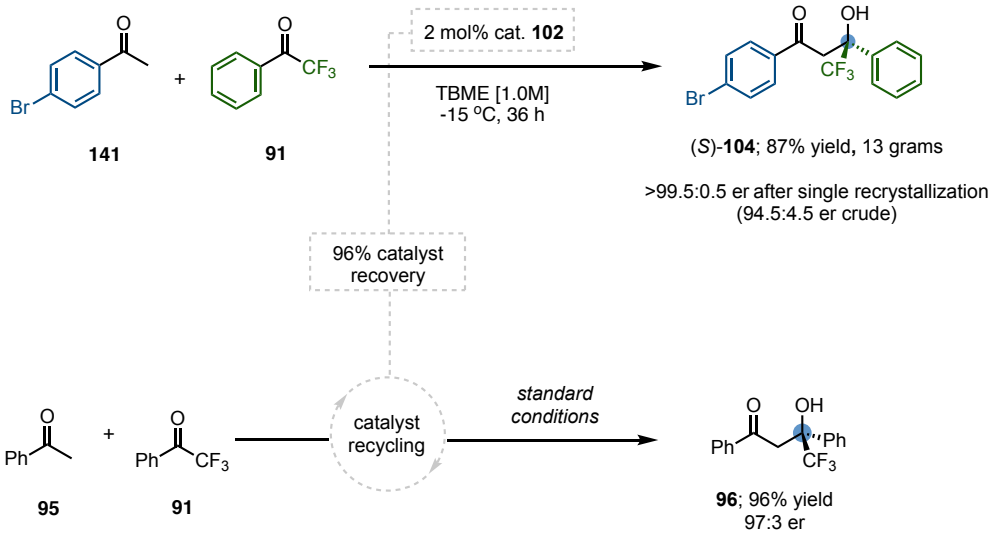

Scheme 25. Preparative scale synthesis of **104**, with demonstration of catalyst recovery and recycling.

2.6 Synthetic Utility of Aldol Adducts

β-Hydroxy ketones are commonly encountered in natural products, drug candidates, and as synthetic intermediates. Hence, we wished to explore the potential for functionalisation of

the trifluoromethyl alcohol products generated using the BIMP-catalysed aldol platform. Enantiopure 4-bromo derivative **104** – obtained from the scale-up reaction described above – was selected as a model scaffold for late-stage derivatisation (**Scheme 26**).

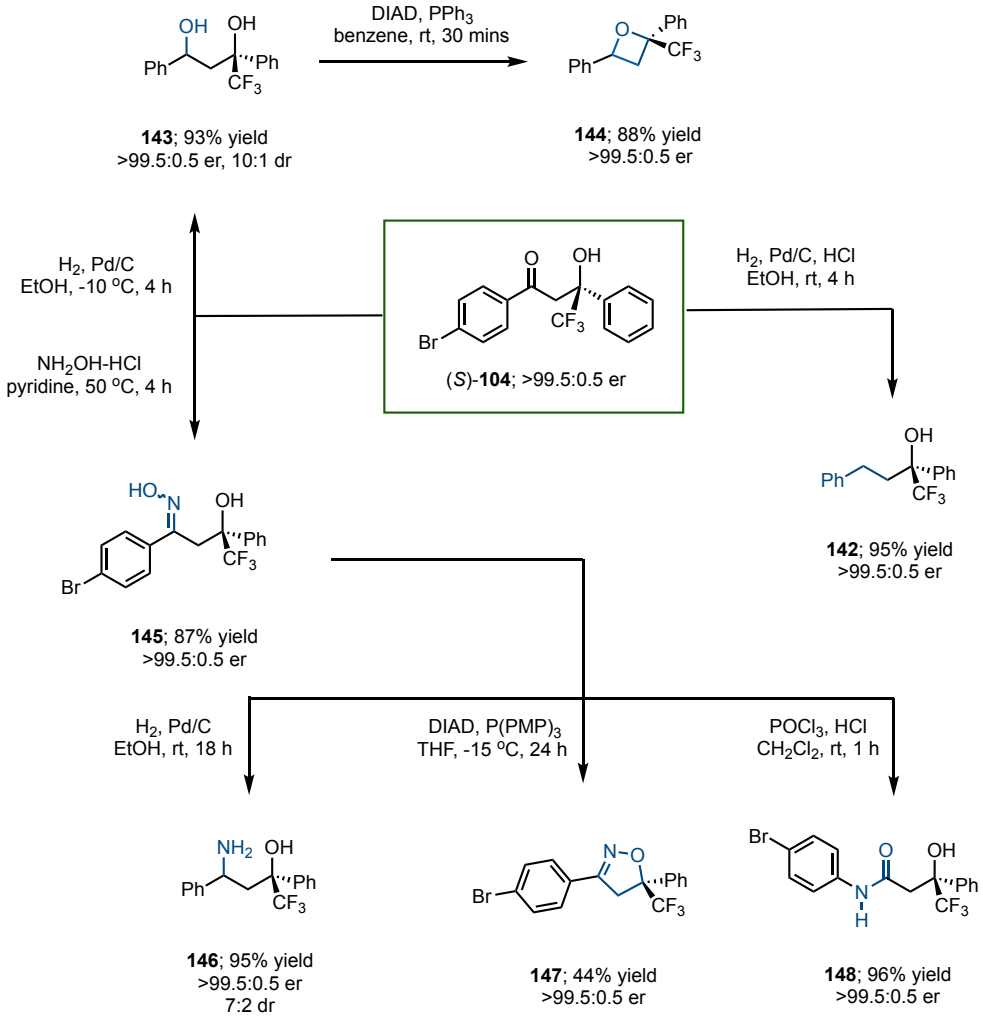

Scheme 26. Late-stage derivatisation of aldol product (*S*)-**104**.

Firstly, under acidic conditions with palladium on carbon, the hydrogenation of **104** at atmospheric pressure afforded γ-benzylic tertiary alcohol **142** in 95% yield. Presumably, this is formed *via* hydrogenation of the intermediary styrene arising from acid-catalysed elimination of the resulting benzylic alcohol. Meanwhile with the omission of acid, **104** was converted to the corresponding diol using a similar hydrogenation protocol, producing **143** with 10:1 dr. Attempts to assign the relative configuration of **143** were not fruitful; NOESY NMR experiments did not provide data which gave confidence to either stereochemical configuration at the benzylic position. Furthermore, attempts to analyse the Mosher's esters of **143** failed due to significant overlap of all relevant resonances in several NMR solvents. Possibly, the structure of **143** could be assigned by NMR analysis after conversion to its cyclic acetal.

Subjecting **143** to standard Mitsunobu reaction conditions efficiently promoted intramolecular cyclisation of the diol to oxetane **144**. Absolute configuration was not determined since the mechanism of cyclisation is unknown with confidence and reliable NOESY NMR analysis is precluded by the presence of an adjacent quaternary fluorine atom.

It was recognised that oxime **145** could be a particularly versatile intermediate for functionalisation of the β-hydroxy ketone motif; thus, **104** was condensed with hydroxylamine to cleanly afford **145**. Hydrogenation of this oxime furnished the valuable 1,3-amino alcohol **146** in 7:2 dr and 95% yield. It was identified that intramolecular cyclisation of this amino alcohol would be an attractive method for expedient preparation of enantioenriched isoxazoline **147**. Hence, treatment of **145** with DIAD and *tris*(*para*-

methoxybenzene)phosphine afforded **147** in 44% yield; such heterocycles are prominent motifs in agrochemicals.[181,182] Finally, in the presence of $POCl_3$ and HCl oxime **145** underwent a Beckmann rearrangement to furnish secondary amide **148**. Importantly, in all derivatisation reactions, no degradation of enantiopurity was observed.

2.7 Mechanistic Considerations

2.7.1 Comparison of reaction rates

With the aim of visualising and quantifying the exceptionally enhanced reactivity of the new BIMP catalysed aldol reaction, the **102**-catalysed reaction of acetophenone and trifluoromethyl ketone **91** was monitored by ^{1}H NMR. To compare the new catalyst system to the existing state-of-the-art reported method, tertiary-amine catalyst **6** was also investigated using the conditions reported by Ikemoto and co-workers. Finally, the *Cinchona* alkaloid **20** was chosen as a reference point for comparison against a low basicity organocatalyst (studied under the optimal conditions for BIMP **102** for comparison).

Initially, direct analysis of the reaction mixture in real-time was attempted by performing the standard reaction of **95** and **91** in an NMR tube in d_8-THF. However, poor reactivity was observed, possibly due to the solvent change or lack of stirring. An alternative protocol was devised to allow the reaction to be performed in a flask using CPME as solvent. Hence, the under the standard reaction set-up, aliquots were taken periodically and quenched immediately with glacial acetic acid then evaporated quickly under a stream of nitrogen gas. The resulting residues were redissolved for immediate analysis by ^{1}H NMR, and the conversion was tracked over time.

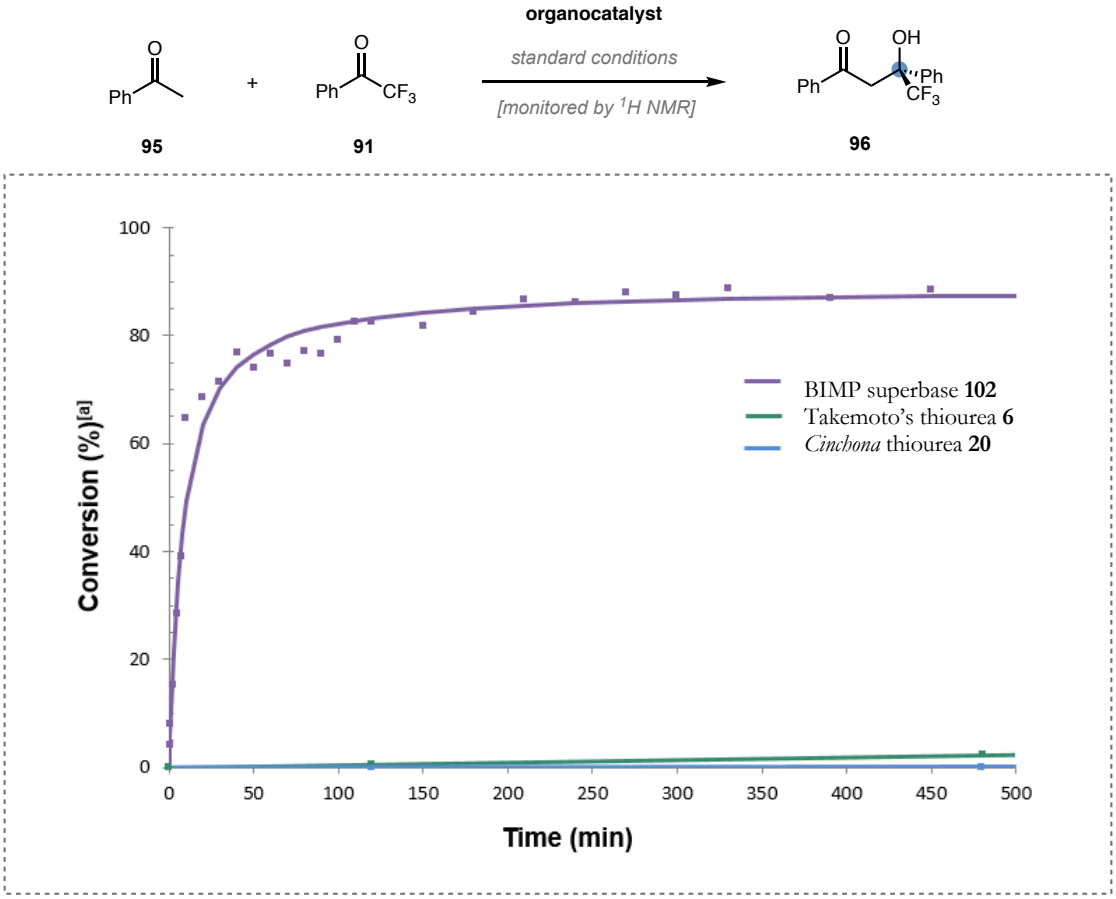

Relative rates of chosen organocatalysts

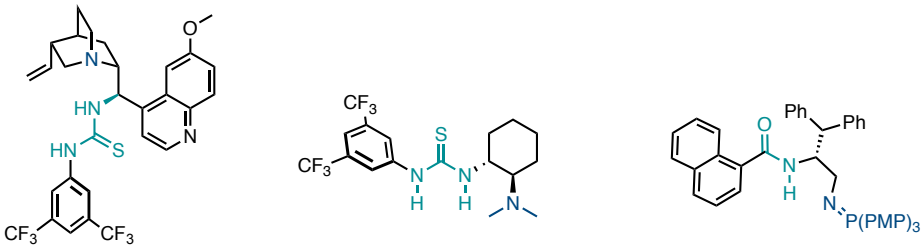

***Cinchona* (20)**

Takemoto's catalyst (6)

prior state of the art

BIMP (102)

pK_{BH+} 25.5 [MeCN]

$[k_{rel}]$ — *0.03* — *1* — *1414*

Figure 9. Rates determined from the relative intial slope of conversion *vs.* time for each catalyst. Relative rates for *Cinchona* **20** and BIMP **102** were measured under standard conditions for the herein reported method; relative rate for thiourea **6** was measured using the best known conditions (reported by Iketmoto).

Figure 9 illustrates a >1400-fold initial-rate enhancement with BIMP **102**, relative to the prior state-of-the-art catalytic system, namely Takemoto's catalyst **6** (analysed under the conditions reported by Ikemoto). As expected, *Cinchona* alkaloid **20** struggled to afford trace amounts of product over the analysis period. Most notably, synthetically useful yields of **96** were observed in minutes under BIMP catalysed conditions; approximately 75% conversion after 45 minutes, and 83% isolated yield after 2 hours. Takemoto's thiourea catalyst **6** afforded <1% conversion in the same timeframe, as determined by ^{1}H NMR.

2.7.2 Determination of BIMP pK_{BH+}

To quantify the origins of the observed enhanced reactivity, we endeavoured to approximate the pK_{BH+} of BIMP **102**. For this purpose, NMR spectroscopy can be conveniently used as an appropriate analytical method due to the fact that the protonated and free-base forms of a superbase have substantially different NMR chemical shifts for selected resonances.[183–185] The pK_{BH+} determination can be performed rapidly by comparing the chemical shifts of chosen resonances of the protonated superbase with and without an equimolar amount of an additional base of known pK_{BH+}.

The AcOH salt of BIMP catalyst **102** was prepared by addition of excess AcOH to **102** in CPME, followed by evaporation and trituration (**Scheme 27**). The ^{1}H, ^{31}P and ^{13}C NMR spectra of the salt (**102-AcOH**) and freebase forms of **102** were obtained in d_3-MeCN and compared. Clear differences in the chemicals shift of the <u>*P*</u> atom, and the <u>*C*</u>H$_2$NP(PMP)$_3$ atoms were noted upon protonation, however no well-defined separation of any resonance

was observed by ^{1}H NMR. Hence, only ^{31}P and ^{13}C data were used in the necessary calculations for pK_{BH+} determination.

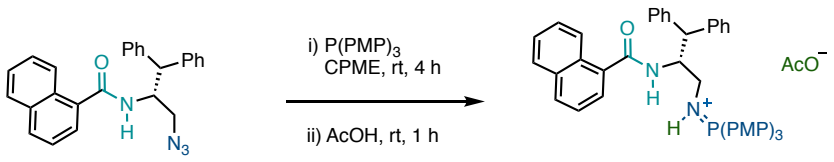

149 **102-AcOH**; 97% yield

Scheme 27. Preparation of BIMP salt **102-AcOH**

Upon protonation, the ^{31}P resonance of the iminophosphorane shifts downfield from +9.2 ppm to +36.8 ppm, as expected considering the new positive charge located on the adjacent nitrogen atom. Meanwhile, the ^{13}C shift of the methylene carbon atom adjacent to the iminophosphorane shifts downfield by 2.1 ppm. The NMR experiments were performed again using salt **102-AcOH** in the presence of 1 equivalent of TMG, which has a known pK_{BH+} of 23.3 in MeCN.[186]

Based on an average of triplicate runs for both ^{13}C and ^{31}P NMR experiments, the pK_{BH+} of BIMP **102** was estimated to be 25.5 in MeCN (see Chapter 4.2.8.4 for calculations). This is superior to the common organosuperbase DBU (pK_{BH+} of 24.3) and approaching the basicity of the commercially available achiral phosphazene superbases, such as P$_1$-*t*Bu phosphazene **102** (pK_{BH+} of 26.9).[187] The result confirms that **102** is highly basic, but it's ability to deprotonate acetophenone is likely due to one or more further activating effects beyond the role of the superbasic iminophosphorane (for example, H-bonding interactions).

2.7.3 Verification of hydrogen-bonding

To support the theory that iminophosphorane catalyst **102** is indeed operating through bifunctional activation, *N*-methylation of the BIMP was hypothesised as a test for the role of H-bonding by the amide moiety. Hence, BIMP precursor **149** was reacted with NaH followed by MeI to afford the *N*-methylated azide **150** (**Scheme 28**). The Staudinger reaction between **150** and *tris*(4-methoxyphenyl)phosphine was performed subsequently performed *in situ*, and confirmed to quantitatively form the corresponding iminophosphorane **151** by ^{31}P NMR. The crude solution of *N*-methyl **151** was used under standard conditions in the model reaction of acetophenone (**95**) and trifluoroacetophenone **91**.

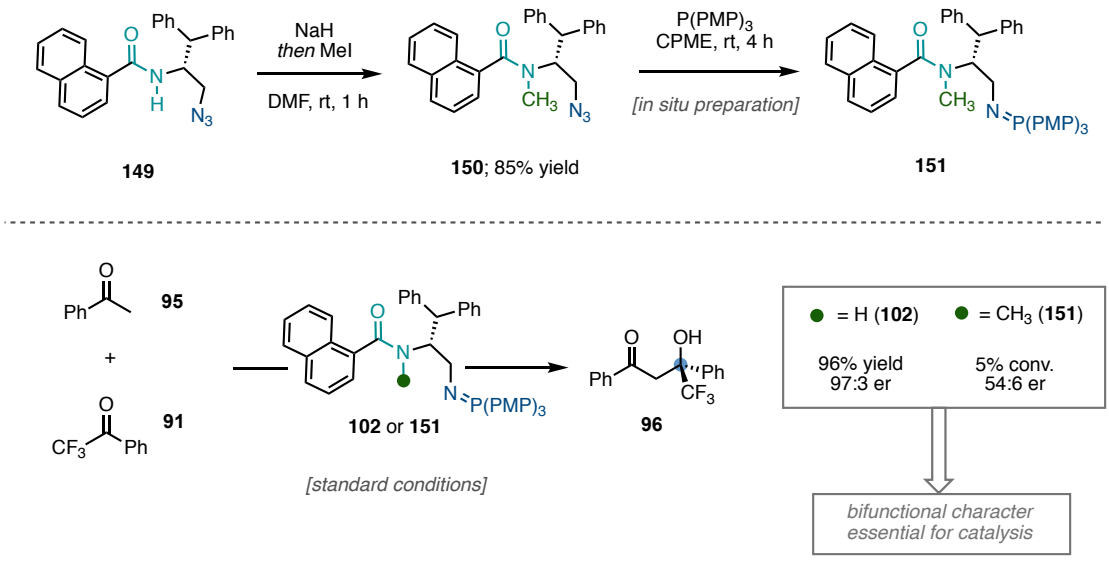

Scheme 28. *N*-methylation of catalyst **102** removes essential bifunctional character.

After 18 hours, only 5% conversion to aldol adduct **96** was observed (determined by ^{1}H NMR) and this product was found to be only slightly enantioenriched (54:46 er). Hence, it

is most likely that the significant rate enhancement and stereoselectivity of the aldol reaction with BIMP is due to a synergy of competent H-bonding and high basicity provided by the amide and iminophosphorane groups of **102**; thus, lending support to the general theory that iminophosphorane superbase catalysts such as those described here do operate by dual activation/organisation of substrates.

2.7.4 Product-catalyst inhibition

The rapid decrease of reaction rate over the course of the reaction suggests that product inhibition may be hindering the reaction. To investigate if a product-catalyst complex exists, two methods were used to obtain evidence for the hypothesised binding. Firstly, the method of continuous variation was used to construct a Job's plot, followed by product-doping studies to observe changes in reaction rate.[188–191]

Job's method of continuous variation – used to construct of Job plot – relies on the assumption that, in solution, two or more chemical entities may bind to each other to form one dominant transient complex. By continuous variation of the mole fraction of each component, while maintaining constant overall concentration, the complexation event can be indirectly observed by monitoring any physical property that varies proportionally with the binding event. A job plot is produced by plotting the mole fraction of one component against the product of the mole fraction of the other component with the observed change in the chosen physical property. In this case, NMR was selected as an appropriate tool for observation of physical changes. If the binding complex is comprised of one molecule of each component, a Job plot featuring a maxima inflection point at 0.5 on the x-axis is

expected – indicating that maximum binding occurs when each component is present in equal concentration. Likewise, a maxima at 0.75 mole fraction would be expected for a complex involving one and three molecules each of the two components present, for example.

It is important to note that plots obtained from Job's method of continuous variation should be analysed with caution. Many examples of incorrect or misleading Job plots have been found in the primary literature.[192,193] Usually, these are due to the use of inappropriate analysis methods for particular chemical systems, or because of abnormal binding coefficients. However, these mistakes typically occur when dealing with supramolecular structures, enzyme-enzyme interactions, and systems containing heavy metals, rather than systems dealing with organic small molecules.

The Job plot shown in **Figure 10** was obtained by continuous variation of the catalyst:product ratio (**102**:**96**) with monitoring of the methoxy chemical shift of **102** in the ^{1}H NMR spectra of the obtained mixture (see Chapter 4.2.8.3 for details). The plot shows a maximum at 0.474, suggesting an approximate 1:1 ratio for catalyst:product binding under Job's standard method of continuous variation.

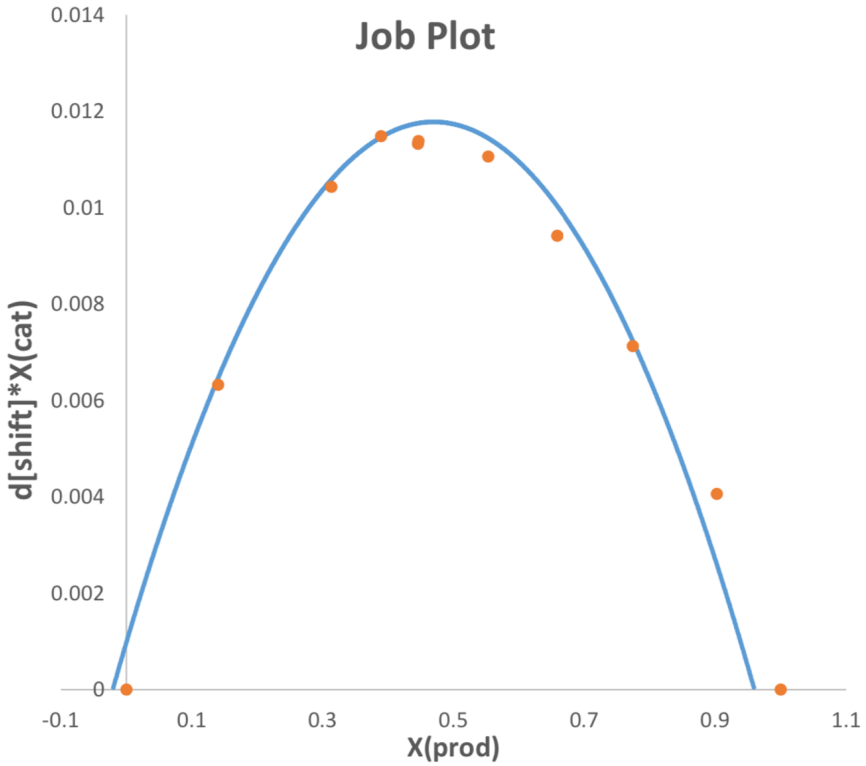

Figure 10. Job plot relationship between BIMP **102** and model product **96** suggesting 1:1 binding coefficient.

Next, product-doping studies were performed to obtain direct evidence for a product-inhibition mechanism. To investigate this effect, the synthesis of aldol adduct **124** was performed under standard conditions in the presence of varying amounts of aldol-adduct **96** (**Figure 11**). The main criteria for the choice of **124** and **96** was minimal overlap of resonances in the ^{1}H NMR spectrum of a mixture of both compounds.

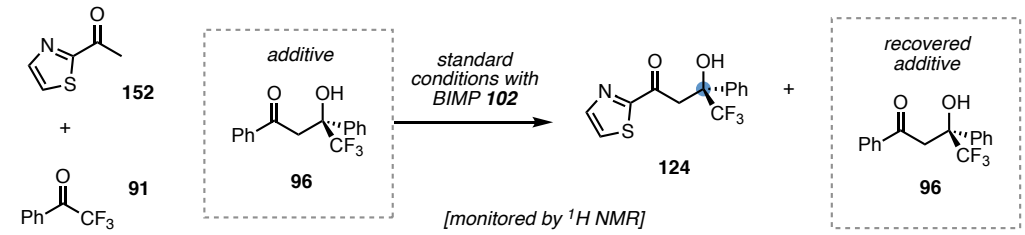

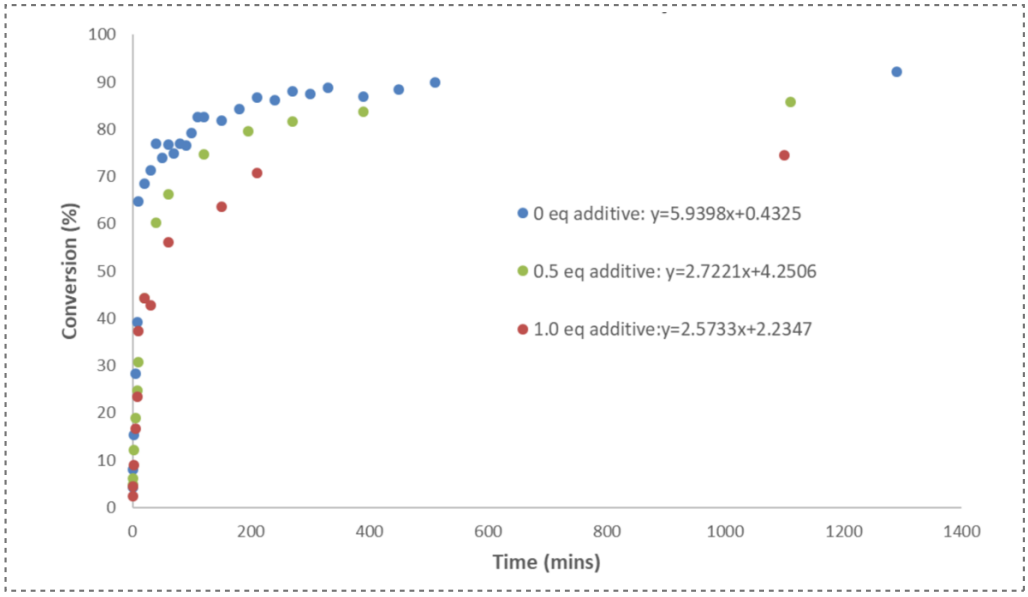

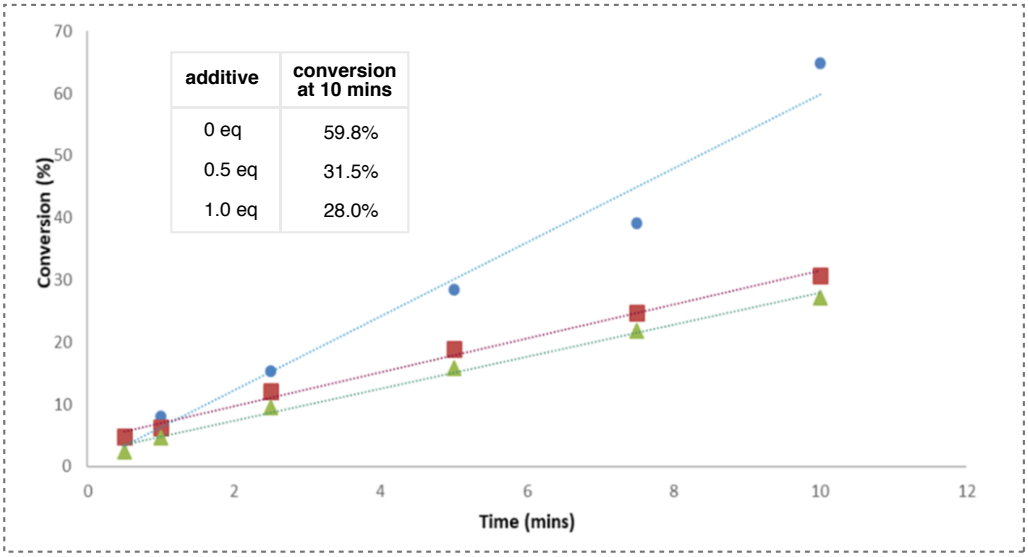

additive	conversion at 10 mins
0 eq	59.8%
0.5 eq	31.5%
1.0 eq	28.0%

Figure 11. Product-doping experiments in the reaction of **152** with **91**

In the presence of 1.0 eq of **96**, the initial reaction rate for the formation of **124** was 2.1 times slower compared to the reaction without any product additive. With only 0.5 eq of additive the results were very similar, with a rate reduction factor of 1.9. After 10 minutes, conversion reached almost 60% in the absence of additive, whereas conversion reached only approximately 30% in the presence of either 0.5 or 1.0 eq of additive. This suggests that 10 mol% of catalyst **102** is effectively inhibited in the presence of at least 0.5 eq additive. Based on these findings and taking the results of the Job plot into account it is likely that catalyst **102** is poisoned to some extent by competitive binding of the β-hydroxy ketone products. However, at 10 mol% catalyst loading, and using the standard reaction conditions, this process has minimal effect on the outcome of reaction over a duration of 18 hours, and good yields can be obtained in much lower timespans.

2.7.5 Catalyst decomposition

Another interesting observation made is linked to catalyst decomposition. It was noted from the NMR spectra of crude reactions that a common impurity was present in almost all the direct aldol additions performed with catalyst **102**. Upon isolation of this impurity, it appeared to be the primary amine **154** (**Scheme 29**). In theory, this impurity could readily arise *via aza*-Wittig reaction of the iminophosphorane catalyst with a trifluoromethyl ketone to afford the corresponding trifluoromethyl imine and *tris*(*para*-methoxyphenyl)phosphine oxide (**153**). Hydrolysis of the imine by trace water present in the reaction mixture would thereafter afford the primary amine **154**. Alternatively, direct hydrolysis of the iminophosphorane by water could also be possible. This finding was easily confirmed by

independent synthesis of **154**; hydrogenation of azide **149** over palladium on carbon afforded amine **154** in 90% yield. The observed decomposition product and the synthesised amine indeed had matching ^{1}H NMR spectra.

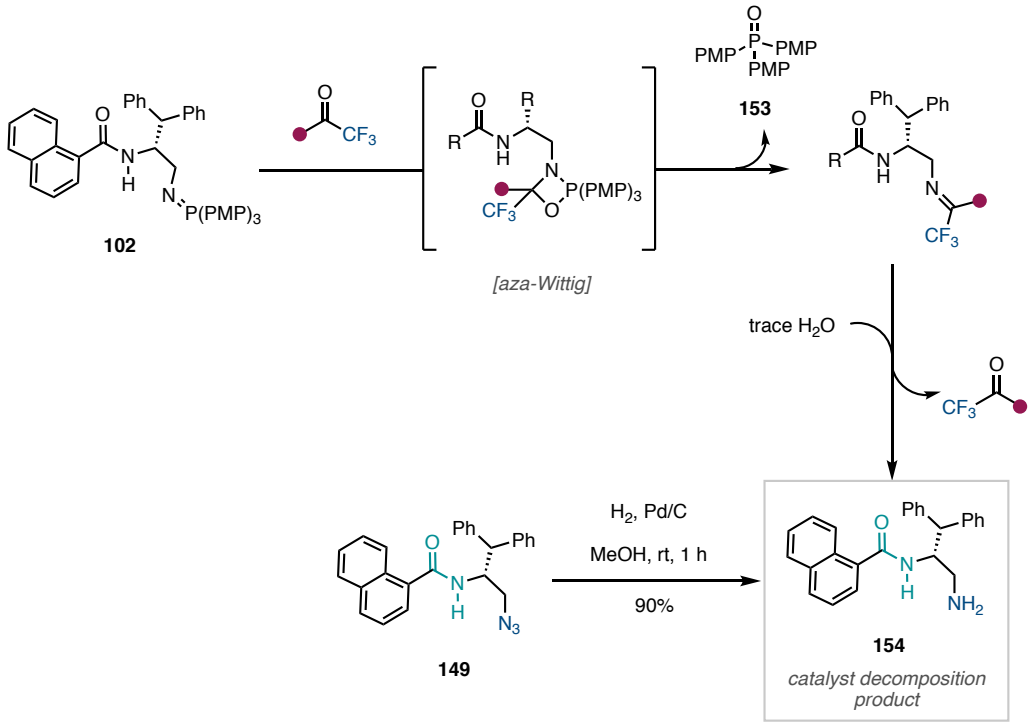

Scheme 29. Trifluoromethyl ketones catalyse the decomposition of iminophosphoranes via an aza-Wittig reaction.

With this knowledge we were able to rationalise the failure of some substrates to afford any product in the studied aldol reaction. Trifluoromethyl ketones bearing highly electron-withdrawing substituents generally failed. This can be explained by the acceleration of the *aza*-Wittig reaction with electron-poor substrates compared to electron-rich trifluoromethyl ketones, and hence the rapid depletion of all active catalyst. In these examples, decomposition of the catalyst is significantly faster than aldol addition. For example, with *bis*(3,5-trifluoromethyl) trifluoromethyl ketone **134**, full decomposition of 10 mol% catalyst

is achieved in less than 10 minutes under the standard reaction conditions. Even with 100 mol% **102**, only traces of the reaction between **95** and **134** is observed; otherwise only clean catalyst decomposition to amine **154** is found. These findings represent the largest drawback of this new methodology. However, this side-reaction can be significantly limited in some examples by slow addition of the trifluoromethyl ketone to the reaction mixture, thereby ensuring a lower concentration of the electrophile relative to catalyst **102** and the methyl ketone substrate. In particular, the slow-addition technique was found to be essential in the preparative scale synthesis of 4-bromo aldol adduct **104** (described in Chapter 2.5), due to the lower catalyst loading of 2 mol%.

Primary amine catalysis is typically employed for aldol addition reactions of alkyl ketone pro-nucleophiles. Hence, for the avoidance of doubt, the role of amine **143** in the model reaction between acetophenone and **91** was examined (**Scheme 30**). As expected, **154** is not catalytically competent in this reaction and did not afford any trace of aldol adduct **96**.

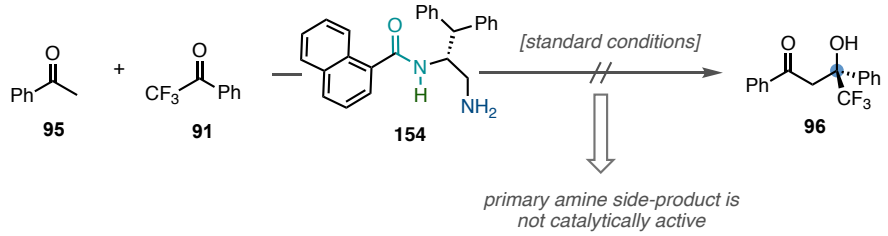

Scheme 30. Testing primary amine **96** for catalytic competency in the aldol addition of **95** to **91**.

2.7.6 Retro-aldol activity

Given the high basicity of catalyst **102**, and the relatively low pK_a of the tertiary-alcohol products compared to the ketone substrates, we expected to observe some level of retro-aldol activity. However, subjecting the enantioenriched model product **96** to BIMP **102** under the standard reaction conditions for 7 days showed no erosion of enantiopurity, or any acetophenone release (**Scheme 31**). This experiment suggests that BIMP **102** does not catalyse this reverse/degradation process. The pK_a of product **96** is expected to be in the range of BIMP basicity (approximately pK_a 24-26 in MeCN). Hence, it is unlikely that the resistance of the aldol products towards degradation under BIMP catalysis can be explained solely on the basis of relative pK_a's, suggesting that steric hindrance may play a role. Catalyst **102** may not be able to efficiently access the alcohol proton due to high steric crowding around this tertiary carbon centre. Furthermore, intramolecular H-bonding may lend some additional stability to the aldol adducts.

Furthermore, exposure of aldol product **96** to a stoichiometric quantity of BIMP **102**, following by quenching with deuterium oxide did not lead to deuterium incorporation at the α-keto position to afford ***d*$_1$-96**. Hence, the given rationalisation for the lack of retro-aldol activity on the basis of steric repulsion may also explain why over-addition is not observed; catalyst **102** also cannot access and enolise the α-keto CH_2 position. Meanwhile, efficient α-deprotonation followed by deuteration of acetophenone (**95**) was observed to occur with BIMP **102** to afford d_1-acetophenone (***d*$_1$-95**), further supporting the hypothesis that steric

hinderance due to the adjacent tertiary centre prevents the formation of over-addition products.

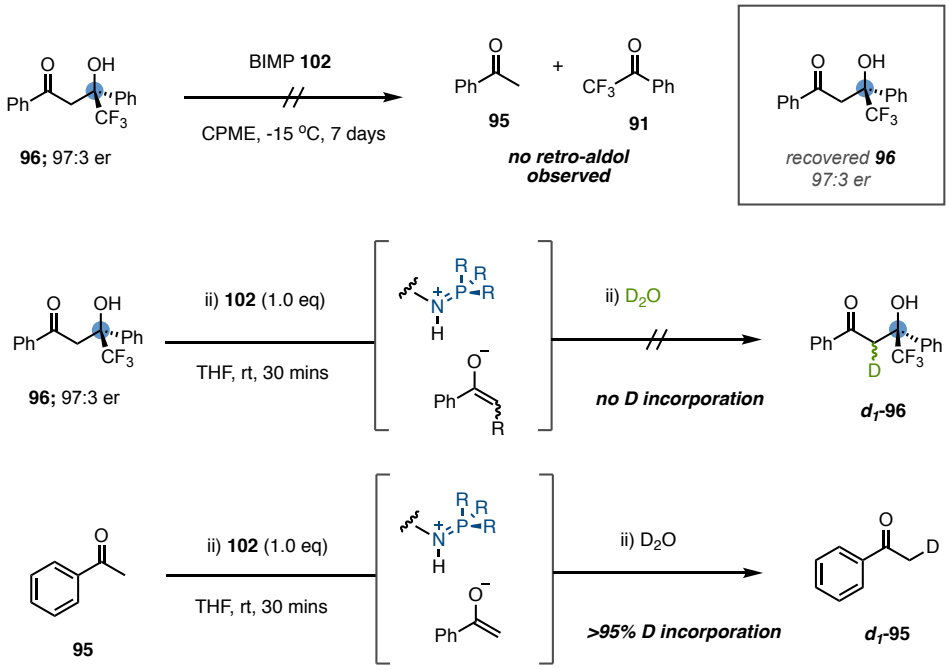

Scheme 31. No retro-aldol activity or deprotonation of the alpha-keto position is observed in **96**.

2.8 Conclusion

In summary, a method for the enantioselective direct aldol addition of (hetero)aryl methyl ketones to α-fluorinated (hetero)aryl ketones has been developed. Reliant on a novel BIMP catalyst, **102** has sufficient superbasicity to rapidly enolise aryl methyl ketones, which are trapped by trifluoromethyl ketones to allow facile access to a library of chiral β-hydroxy ketone scaffolds. The protocol is tolerant of a range of functional groups and affords

enantioenriched products with generally high yield and enantioselectivity. A range of late-stage modifications demonstrated the high synthetic utility of the products with the preparation of enantioenriched building blocks.

NMR studies of the catalytic system revealed several interesting findings. Most notably, the developed method boasts a >1400-fold rate enhancement compared to the previous state-of-the-art catalytic procedure. Evidence for inhibition of the catalyst by the tertiary alcohol products was also found *via* product-doping experiments and the preparation of a Job plot, which suggests a 1:1 binding stoichiometry. The reaction was amenable to preparative scale synthesis; decagrams of product could be isolated without chromatography, and the product can be crystallised to enantiopurity. Recovery of the catalyst was achieved through an operationally simple procedure and recycling was demonstrated without degradation of catalytic activity.

Chapter 3

Catalytic Enantioselective Synthesis of 2-Pyrazolines

3.1 Chapter overview

This chapter describes the concepts relevant to pyrazoline synthesis and the related reactivity of hydrazine-type reagents. Against this backdrop, the development of a catalytic strategy for the enantioselective synthesis of 2-pyrazolines utilizing hydrazines in a simple one-pot approach is detailed. A readily prepared bifunctional *Cinchona*-derived amide is key to a two-stage catalytic aza-Michael addition/condensation strategy. The use of aldehydes to generate hydrazone derivatives *in situ* is central to curtailing background reactivity of the hydrazine reagents and tuning the catalyst-controlled enantioselectivity. The developed method is

easily performed, broad in scope, and tolerates a range of functional groups. Enantioselectivity is generally high and up to >99:1 er was achieved. Significant scalability of this methodology was demonstrated with the synthesis of over 80 grams of a pyrazoline product in a single batch. Furthermore, the catalyst was easily recovered and reused without issue.

3.2 Introduction

Nitrogen-containing heterocycles constitute one of the most important and abundant classes of chemicals, and their ubiquity surpasses that of all other heterocycle varieties.[194–197] Unique reactivities and therapeutic roles have cemented the proliferation of these heterocycles in the pharmaceutical, agrochemical and materials industries. As with the broader field of nitrogen-based chemistry, there is a justified demand for new and increasingly sophisticated synthetic methods to access nitrogen heterocycles due to the massive therapeutic potential that has been realized thus far. Specifically, the development of enantioselective approaches towards optically active heterocycles is needed to further leverage their applications in efficient ways.

Over 200 natural products are known to contain an N-N bond. **Figure 12** illustrates some of the structural diversity found in these naturally occurring compounds.[198] For example, the dimeric indolo-sesquiterpene dixiamycin B (**158**), which was recently synthesized by Baran and co-workers by an electrochemical oxidative N-N coupling, was found to be an order of magnitude more potent that its constituent monomeric indole in antibacterial assays.[199] Furthermore, N-N bonds are commonplace in synthetic therapeutics. Three of the

bestselling drugs of 2019 contained this structural feature; Januvia (**159**), Imbruvica (**160**) and Eliquis (**161**) totaled $24 billion in sales during 2019 alone.[200–204] Likewise, heterocycles featuring 3- or 4-contiguous nitrogen bonds are abundant in agrochemical compounds, for example, the recently approved next-generation fungicides Pavecto (**162**) and Indiflin (**163**).[205,206] The subject of this Chapter – pyrazolines – are also common motifs, particularly

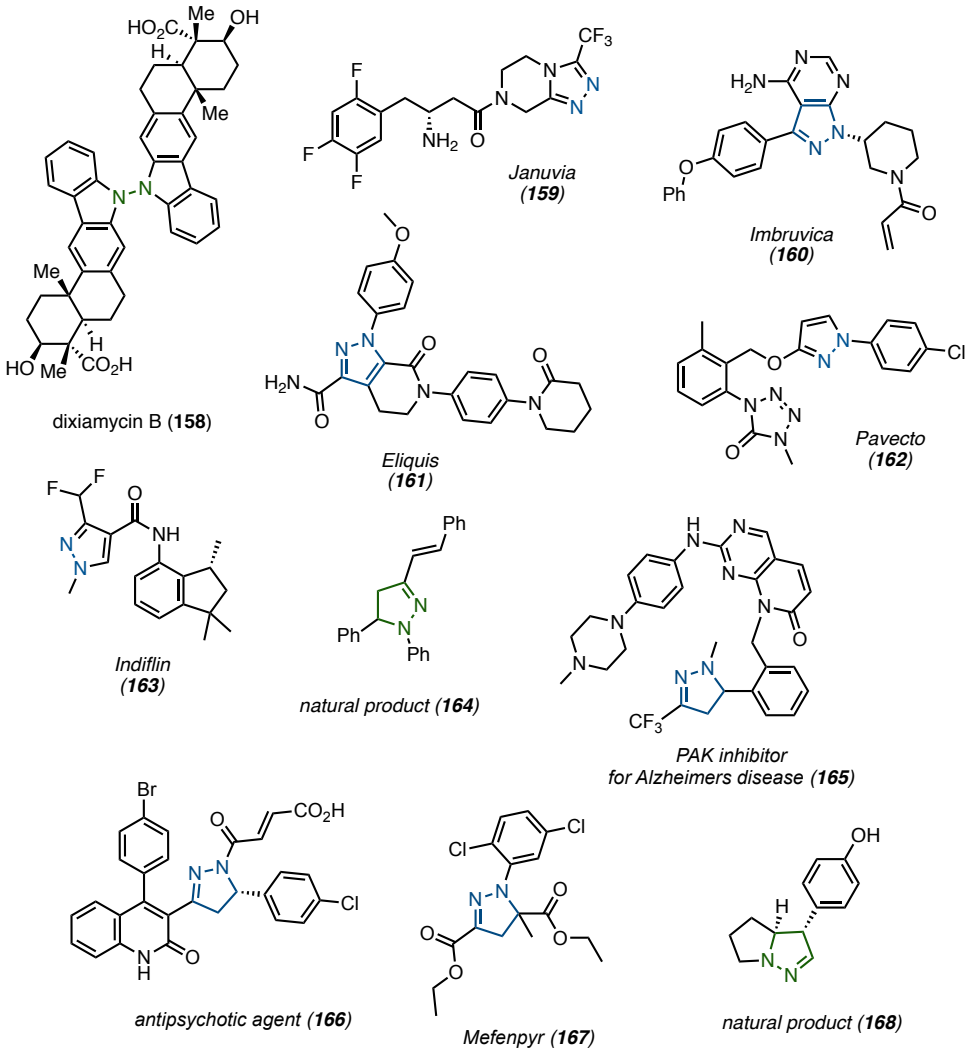

Figure 12. Man-made (blue coloured) and naturally-occurring (green coloured) compounds featuring N-N bond containing heterocycles.

in man-made N-N bond containing heterocyclic compounds (**164**-**168**). The vast array of structural diversity displayed by N-N heterocycles also includes cyclic hydrazines, hydrazones, piperazines, pyradizines, and indazoles.

Pyrazolines represent some of the most therapeutically useful N-N bond containing motifs, finding widespread use in small-molecule drugs and agrochemicals. [207,208] Furthermore, the use of pyrazolines as valuable intermediates in the synthesis of cyclopropanes (through N_2 extrusion) and pyrazoles (by oxidation) is well-documented.[209–216] A wide variety of functional diversity has been reported around these simple 5-membered rings. Specifically, optically active pyrazolines and their derivatives have long been in high demand for their intrinsic biological properties, and significant effort has been invested into the stereoselective preparation of pyrazolines.[217] The remainder of Chapter 3 will focus on methods of preparation for pyrazolines in their racemic and enantioenriched forms.

3.2.1 Preparation of racemic pyrazolines

Most typically, racemic 2-pyrazolines are prepared using hydrazines in a condensation-Michael addition reaction to furnish the unsaturated 5-membered ring (**Scheme 32A**).[218–223] In this context, hydrazines are highly reactive nucleophiles, and simple mono-substituted alkyl hydrazines rapidly react with chalcones to afford 3,5-bis-aryl-2-pyrazolines. Hence, the use of hydrazines in the synthesis of racemic pyrazolines is well established under mild conditions. However, the high reactivity of hydrazines also limits their application in stereoselective synthesis due to elevated background reactivity even at reduced temperatures.

Another well-established method for the manufacture of racemic 2-pyrazolines is the 1,3-dipolar cycloaddition (**Scheme 32B**).[224–226] The *in situ* generation of highly reactive nitrile imines from *C*-halo-hydrazones yields 2-pyrazolines following cycloaddition with an alkene.

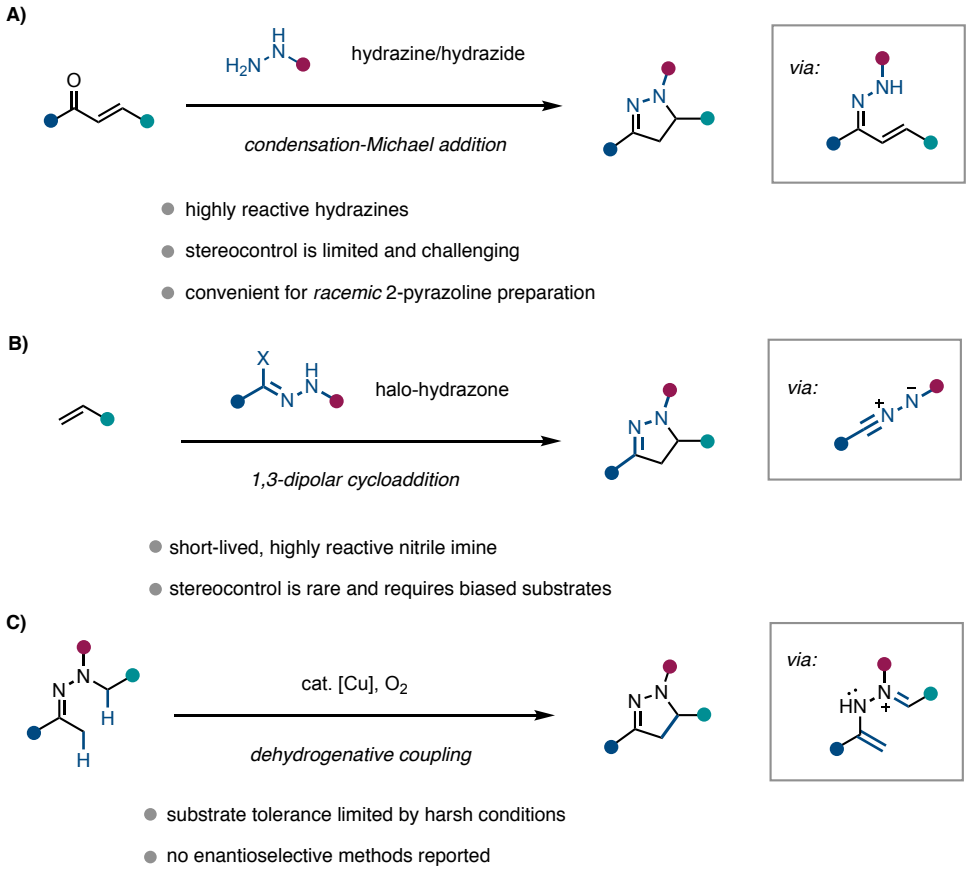

Scheme 32. Strategies towards racemic 2-pyrazoline preparation, including: (A) Michael additons (B) cycloadditions, and (C) dehydrogenative coupling reaction.

Due to the high reactivity and short lifetime of dipolar nitrile imines, enantioselective cycloaddition reactions leading to optically active 2-pyrazolines are relatively rare and limited to highly biased substrates under cryogenic conditions. Finally, 2-pyrazolines have been

prepared by dehydrogenative coupling of alpha-alkyl hydrazones (**Scheme 32C**).[227] However, no enantioselective variants of this reaction have been reported, to the best of our knowledge.

3.2.2 Enantioselective preparation of pyrazolines

Enantioselective, auxiliary-free methods to access 2-pyrazolines remain relatively limited. Kanai reported in 2000 the first enantioselective synthesis of this chemical family through a Lewis acid catalyzed 1,3-dipolar cycloaddition of TMS-diazomethane (**169**) to alkenoyl-oxazolidinones such as **170**.[228] The strategy relied on a cooperative chiral-ligand/achiral-auxiliary approach with a Mg-centered Lewis-acid formed *in situ* from $MgBr_2$ and BOX ligand **171** (**Scheme 33**). Cryogenic temperatures were required to maintain high levels of enantioselectivity but resulted in long reactions of up to 4 days to achieve satisfactory yields. Importantly, **169** was chosen as a non-coordinating dipole to ensure the Lewis-acidic catalyst is not deactivated by dipole association. The authors suggest a trigonal bipyramidal transition state around a central magnesium atom ligated with the dipolarophile and ligand. High enantiofacial discrimination is dictated by efficient chiral shielding by the suitably positioned phenyl groups of the remote oxazolidines.

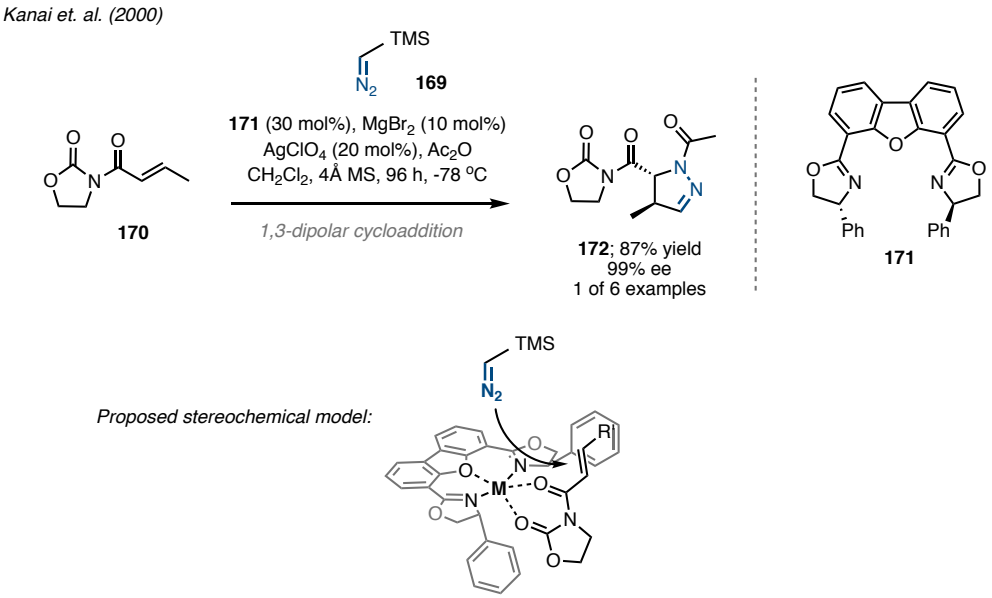

Scheme 33. An enantioselective 1,3-dipolar cycloaddtion of diaozmethanes catalysed by a chiral Lewis acid complex.

Kanai's seminal report was subsequently followed by Sibi and co-workers with a similar preparation *via* the 1,3-dipolar cycloaddition reaction of *in situ* generated nitrile imines (from **173**) and pyrazolidinone-derived dipolarophiles **172** (**Scheme 34**).[229–231] The method uses a cyclopropyl-bridged BOX ligand (**174**) to afford highly enantioenriched 2-pyrazolines – **175** was isolated in 93% yield with 99% ee. While both cycloadditions reported by Kanai and Sibi afford products with high enantioselectivity, they suffer from unattractive reaction conditions and poor efficiency with respect to the low atom-economy of auxiliaries.

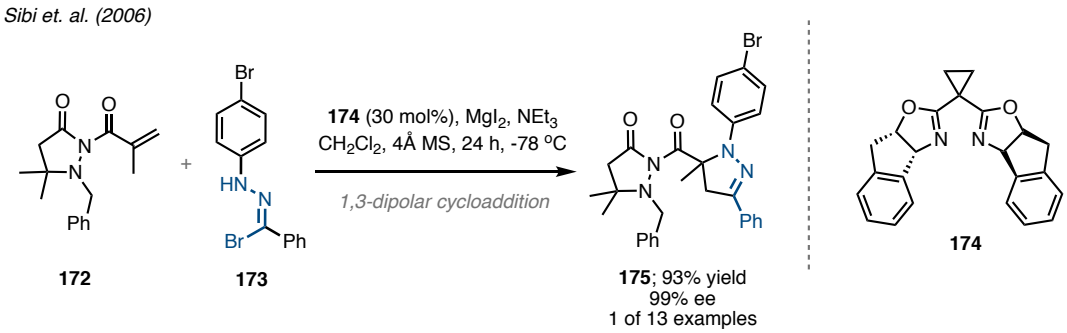

Scheme 34. Enantioselective 1,3-dipolar cycloaddition of nitrile imines reported by Sibi.

In 2009 List and co-workers presented a conceptually novel electrocyclization of α,β-unsaturated hydrazones such as **176**, promoted by the BINOL-derived chiral phosphoric acid **177** (**Scheme 35**). Products were isolated in high yield and with excellent enantioselectivity, for example *N*-phenyl-2-pyrazoline **178** was obtained in 85% yield and with 93:7 er.[232] Although this protocol requires long reaction times of 3-4 days, the mild conditions and easily prepared catalyst make this an attractive method. However, the application of the method was limited to only 5-methyl substituted products. Mechanistically, the authors noted that the conjugated hydrazone substrate would have to undergo two conformational changes to be positioned in a reactive form for the subsequent cyclisation. Specifically, the reactive conformation is *(Z)-s-cis*, requiring C-C single-bond rotation along with C-N double-bond isomerization. Indeed, these isomerization events were observed upon addition of the phosphoric acid **177** and could be followed over time by HPLC analysis. The ensuing 6π-electrocyclization generally afforded 2-pyrazolines with a high degree of enantioselectivity.

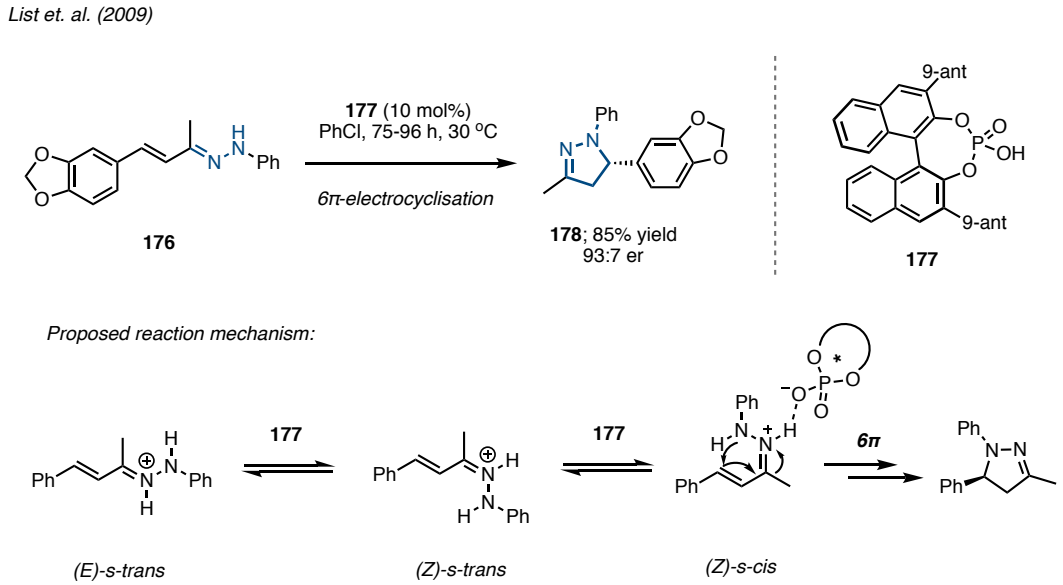

Scheme 35. A conceptually novel enantioselective electrocyclisation of hydrazones from List and co-workers.

More recently, the enantioselective synthesis of 2-pyrazolines under phase-transfer conditions was demonstrated by Briere and co-workers.[233,234] In this elegant method, the addition of carbazates, for example Boc-hydrazine **179**, to chalcones (e.g., **180**) is catalyzed by quaternary *Cinchona* alkaloid salt **181** (**Scheme 36**). The authors propose that the high enantioselectivity of this straightforward method is a result of tight chiral ion pair formation between the ammonium catalyst and carbazate anion. Model product **182** was isolated in 77% yield and 92% ee. While effective, this method is limited to simple substituted chalcones. Deng also reported a similar phase-transfer method using *N*-benzyl-*N'*-Cbz protected hydrazines.[235]

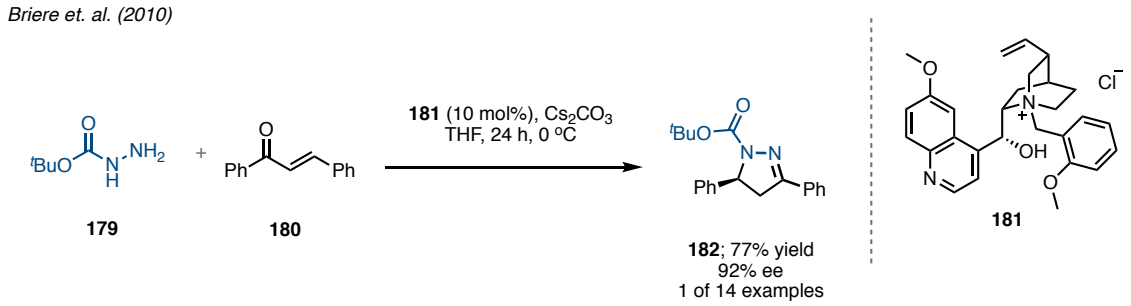

Scheme 36. Enantioselective phase-transfer catalysed synthesis of 2-pyrazolines.

Collectively the methods outlined above represent a valuable toolkit for the synthesis of enantioenriched 2-pyrazolines. However, limitations such as the requirement for auxiliaries and/or pre-formation of hydrazones characterize inadequacies in the available methods. Furthermore, the clear limitations of substrate scope pave the way for new methodologies. Hence, the challenge of developing a broadly applicable platform for the metal-free, expeditious synthesis of enantioenriched 2-pyrazolines remained attractive to us. Opportunities for new catalyst design further bolstered the appeal of this challenge.

3.2.3 Hydrazines and the alpha-effect

In a view to prepare pharmaceutically relevant chiral heterocycles from simple building blocks, we recognized hydrazines as commercially available nitrogen-nitrogen synthons for the preparation of 2-pyrazolines. The lack of enantioselective methods utilizing these reagents in their reaction with enones is most likely due to their high reactivity resulting in challenging stereocontrol. Hydrazines have inherently higher nucleophilicity compared to their corresponding amines. For example, methyl hydrazine is empirically more nucleophilic than methyl amine.[236] This phenomenon is termed the alpha-effect and is purported to arise

in many nucleophiles bearing a heteroatom adjacent to another nucleophilic heteroatom, resulting in anomalously high reactivity.[237–240] Similar effects have also been observed in oxygen-based nucleophiles; for example, the peroxide ion (HOO^-) is significantly more reactive than the hydroxide ion (HO^-), meanwhile hydroxylamine (NH_2OH) is about 100 times more nucleophilic than ammonia (NH_3). Rate accelerations due to the alpha effect of up to 1000-fold have been reported, and enhanced reactivity at electrophilic positions such as phosphorus centres, carbonyls, carbocations, and unsaturated C-C bonds have all been demonstrated.

The so-called supernucleophiles collectively play an important role in synthetic chemistry, yet no consensus has been reached on the physical theory behind the alpha-effect.[241] The original proponents of this phenomenon – Edwards and Pearson in 1962 – hypothesised that the adjacent lone-pair of the additional heteroatom can stabilise partial-positive charge formed during nucleophilic attack.[242] However, recent investigations in solution and gas-phase have failed to produce an overarching theory, and it remains unclear if the alpha-effect arises from physical properties intrinsic to the nucleophile or if a larger solvent-effect is in play.

3.3 Reaction Development

To circumvent the supernucleophilicity of hydrazines we envisaged the use of an aldehyde to generate a hydrazone derivative *in situ*. Hydrazones are typically less reactive, and as such, hydrazines may become amenable to enantioselective chemistry through their temporary

'masking'.[243–246] Furthermore, the aldehyde component would provide an additional handle for tunability during optimization of the reaction through variation of its steric and/or electronic properties. With the use of a chiral, non-racemic catalyst this approach could promote an enantioselective aza-Michael addition of the masked hydrazine to enones (**Scheme 37**). With the stereocenter set, cleavage of the hydrazone would release a primary amine from the masked hydrazine. Subsequent intramolecular condensation would then afford enantioenriched 2-pyrazolines.

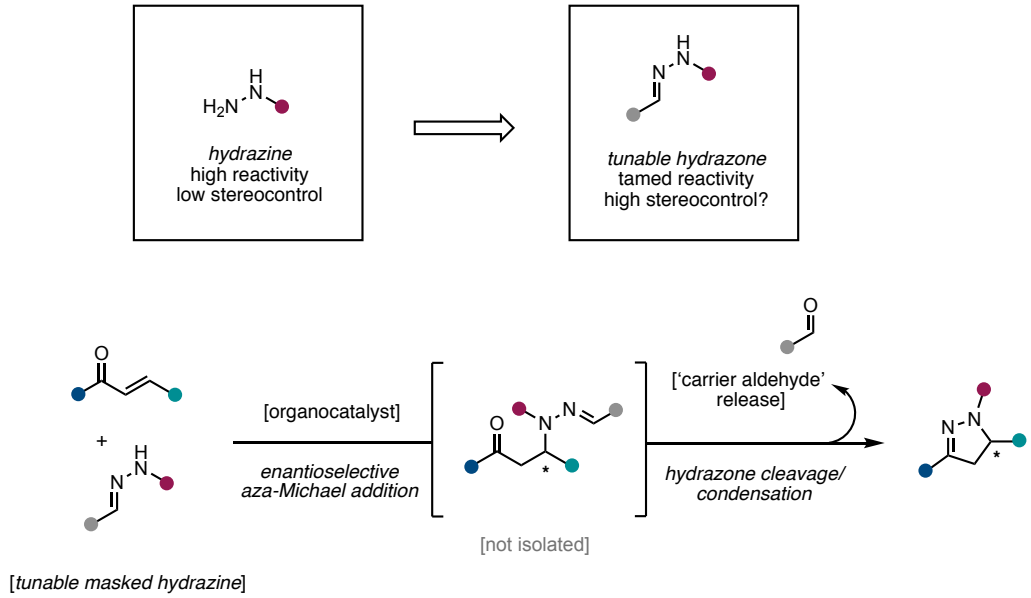

Scheme 37. Concept for the enantioselective synthesis of 2-pyrazolines through a two-step one-pot strategy.

3.3.1 Proof of concept: the enantiodetermining aza-Michael addition

To explore feasibility of the aforementioned reaction system, the key stereoselective step was initially investigated. Firstly, to confirm our expectations for the high reactivity of hydrazines, we treated chalcone **180** with methyl hydrazine in diethyl ether at -15 °C to obtain

a 94% yield of 2-pyrazoline **183** after only 15 minutes (**Table 2**; entry 1). This result illustrates the high background reactivity that is necessary to be overcome to access **183** with satisfactory enantioselectivity. Subsequently, a screen of 1st- and 2nd-generation BIMP catalysts failed to afford any significant level of enantiocontrol in the same reaction (**Table 2**; entries 2-11). Adjustments to reaction temperature, solvent concentration and stoichiometry provided a best-case result of 54% yield and 65:15 er, when using 30 mol% of thiourea BIMP **185** and 2.0 eq of methyl hydrazine in 0.02 M diethyl ether at -15 °C. Furthermore, *Cinchona* derived catalysts **189**-**191** performed very poorly, failing to afford **183** with better than 55:45 er (**Table 2**; entries 12-14).

Given the failure of selected organocatalysts to mediate the hydrazine addition reaction with any acceptable level of enantioselectivity, we continued with our hydrazone plan as outlined earlier. As a model system, methylhydrazine-derived hydrazone **192** was prepared *ex situ* and reacted with chalcone **180** in the presence of various organocatalysts. It was hypothesized that a bifunctional Brønsted base/H-bond-donor catalyst could efficiently affect the desired enantiodetermining aza-Michael addition step. Importantly, the model system of chalcone **180** and hydrazone **192** did not afford any aza-Michael adduct **193** in the absence of a catalyst after 7 days at room temperature in toluene (**Table 3**; entry 1).

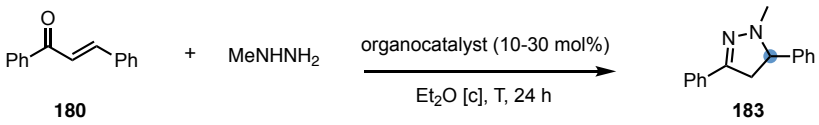

180 **183**

entry	catalyst	eq. $MeNHNH_2$	[c]	T	183 [%][a]	183 er[b]
1[c]	-	4.0	0.5	-15 °C	94%	-
2	**57** [30 mol%]	4.0	0.5	rt	95%	60:10
3	**184** [30 mol%]	4.0	0.5	rt	84%	52.5:47.5
4	**185** [30 mol%]	4.0	0.5	rt	93%	55.5:44.5
5	**186** [10 mol%]	2.0	0.25	rt	81%	54.5:45.5
6	**187** [10 mol%]	2.0	0.25	rt	99%	58:42
7	**188** [10 mol%]	2.0	0.25	rt	86%	50:50
8	**185** [30 mol%]	4.0	0.5	-15 °C	89%	55:45
9	**185** [30 mol%]	4.0	0.5	-78 °C	0%	-
10[d]	**185** [30 mol%]	2.0	0.02	-15 °C	54%	65:15
11	**185** [30 mol%]	2.0	0.02	-15 °C	41%	64.5:15.5
12	**189** [30 mol%]	2.0	0.1	rt	82%	50:50
13	**190** [30 mol%]	2.0	0.1	rt	87%	52:48
14	**191** [30 mol%]	2.0	0.1	rt	81%	55:45

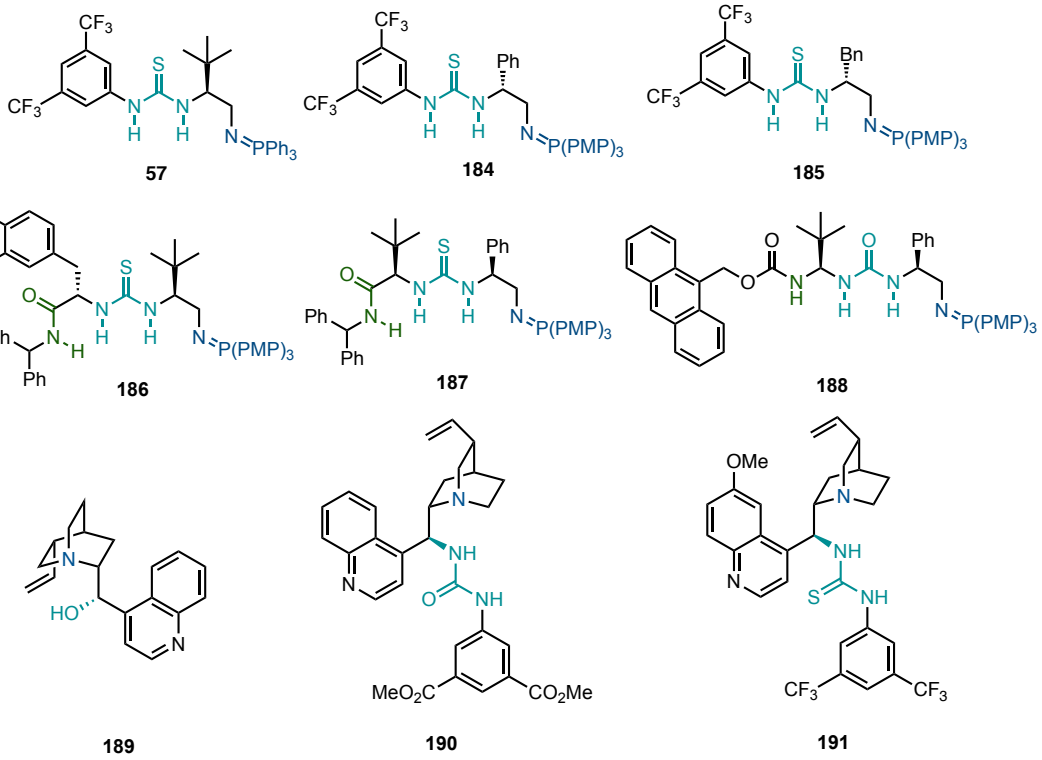

Table 2. Attempted optimization of the aza-Michael addition/condensation of methylhydrazine to chalcone (**180**), and the structures of selected investigated catalysts. [a] isolated yields. [b] er determined by chiral stationary-phase HPLC. [c] 15 minutes reaction time. [d] dropwise addition of methylhydrazine (in Et_2O) over 2 hours.

Primarily we envisaged the use of a bifunctional iminophosphorane superbase such as the catalysts developed by the Dixon group described in Chapter 1.5.5. It was expected that these superbasic catalysts should be competent in the desired aza-Michael addition. Surprisingly however, after 24 hours at room temperature in toluene, with 10 mol% of BIMP catalyst **185** or **98** afforded only 20% and 4% conversion to aza-Michael product **193**, both with unsatisfactory enantioselectivities of 56:44 er and 53:47 er, respectively (**Table 3**; entries 2 and 5). These disappointing results could be due to competition with rapid retro-Michael addition; however, this possibility was not studied. Hence, we were alerted to the possible problem of reversibility and therefore erosion of enantioselectivity under base-catalyzed conditions, and suggested that "taming" of the Brønsted base catalyst would be necessary to achieve an efficient method. Initially we attempted to reduce the basicity of BIMP catalyst **185** by using electron-neutral and electron-poor phosphines in the formation of the iminophosphorane. Substituting the electron-donating *tris*(*para*-methoxy phenyl)phosphine for electron-withdrawing *tris*(3,5-bis-(trifluoromethyl)phenyl)phosphine to give BIMP **195** reduced the conversion to only 12% with negligible enantioselectivity of 52:48 er (**Table 3**; entry 3). As a middle-ground experiment, triphenylphosphine-derived iminophosphorane **196** was tested and found to give 13% conversion to the desired aza-Michael intermediate again with only 52:48 er (**Table 3**; entry 4).

The disappointing results directed us to investigate alternative organocatalyst architectures. Considering the proliferation of *Cinchona* alkaloid derived structures in organocatalysis, our attention naturally turned to these scaffolds. Furthermore, *Cinchona* alkaloids are much less

basic than BIMPs, therefore reducing their ability to catalyse the retro aza-Michael addition of **193.**

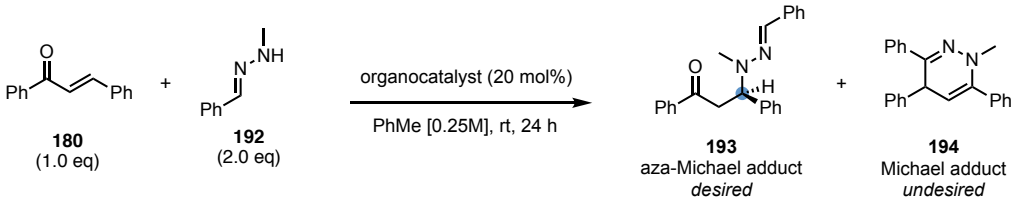

entry	catalyst	193 [%][a]	194 [%][a]	193 er[b,c]
1[d]	-	0	0	-
2	**185**	20	0	56:44
3	**195**	12	0	52:48
4	**196**	13	0	52:48
5	**98**	4	0	53:47
6	**189**	86	0	71:29
7	**197**	74	0	36:64
8	**190**	69	9	80:20
9	**198**	50	29	82:18
10	**199**	58	7	86:14
11	**200**	56	17	87:13

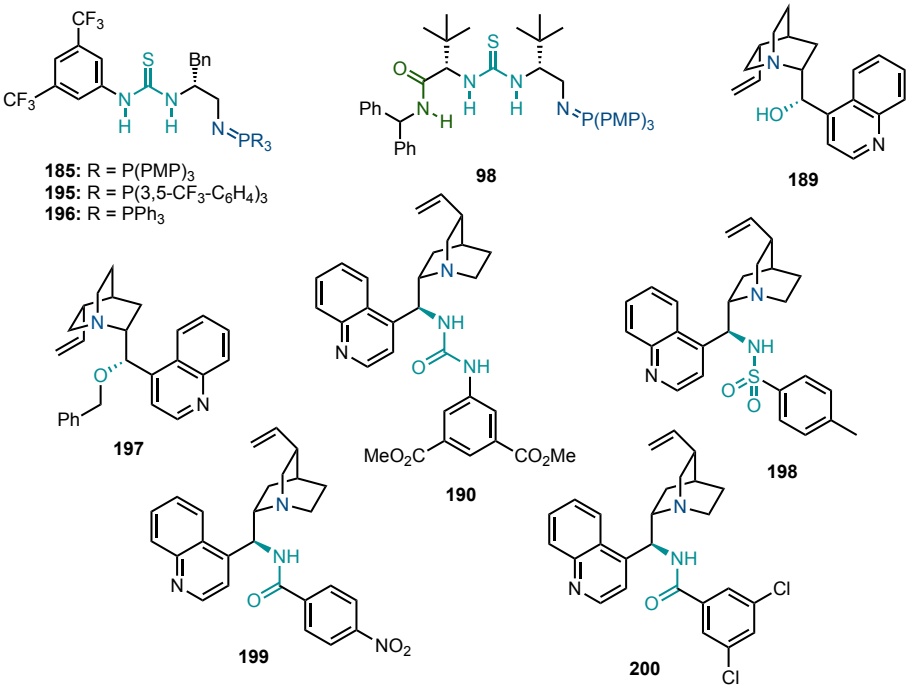

Table 3. Optimization of the enantiodetermining *aza*-Michael addition of hydrazone **192** to chalcone (**180**), and the structures of selected investigated catalysts. [a] determined by ^{1}H NMR analysis of crude reaction mixture. [b] er determined by chiral stationary-phase HPLC. [c] **194** was always obtained as a racemic mixture. [d] performed for 7 days.

We embarked on a screening program of various *Cinchona*-derived organocatalysts. All catalysts were either obtained directly from our in-house database or synthesized from the commercially available alkaloids. Catalysts of this type are prepared in two simple steps from cinchonidine (**201**), namely Mitsunobu deoxy-azidation and subsequent *in situ* Staudinger hydrolysis, followed by amide-bond formation (**Scheme 38**). This investigation yielded some promising results from early on. Utilizing the parent alkaloid cinchonine (**189**) afforded aza-Michael product **193** with 86% conversion and 71:29 er after 24 hours at room temperature (**Table 3**; entry 6). Use of *O*-benzyl cinchonine (**197**) resulted in a selectivity decrease and, interestingly, a reversal of the dominant enantiomer of product to give **193** in 36:64 er (**Table 3**; entry 7). Variation of the H-bond donor to give the cinchonidine-derived bifunctional urea (**190**) resulted in an enhancement to 80:20 er, while the cinchonidine-derived sulfonamide **198** similarly afforded **193** with 82:18 er (**Table 3**; entries 8-9). Pivoting from a sulfonamide to an amide further boosted stereoselectivity. Amides **199** and **200** derived from reacting (4-nitro)benzoyl chloride or (3,5-dichloro)benzoyl chloride with 9-amino-(9-deoxy)-epicinchonidine improved selectivity to 86:14 and 87:13 er, respectively (**Table 3**; entries 10-11). Following this lead, a panel of amides derived from amine **202** were synthesized but failed to improve on the selectivity observed with catalyst **200**. A broad-spectrum screen of aprotic solvents was also conducted. Highly polar solvents such as DMSO and DMF performed very poorly, possibly due to their propensity to interrupt the H-bonding required for organization. Meanwhile ethereal solvents such as diethyl ether and THF afforded moderate enantioselectivities (see Chapter 4.3.1 for full optimization table). Anhydrous toluene ultimately proved to be optimal.

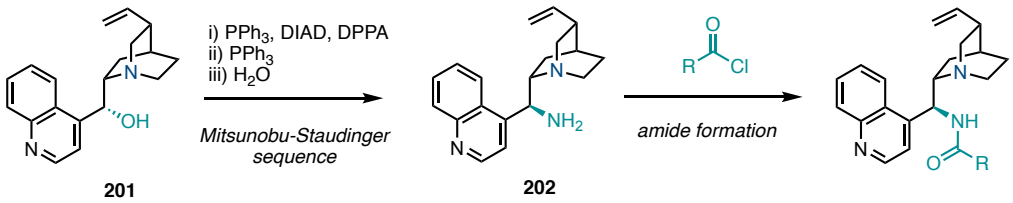

Scheme 38. General stratgey for the synthesis of cinchona-amide catalysts.

3.3.2 Competitive Michael addition

Michael adduct **194** was unexpectedly observed in many cases as a competitive side-product when using *Cinchona*-derived catalysts. The Michael adducts were always racemic, and their formation most likely proceeds through the mechanism illustrated in **Scheme 39**; reversible aza-Michael addition subsequently leads to irreversible Michael addition through the imine

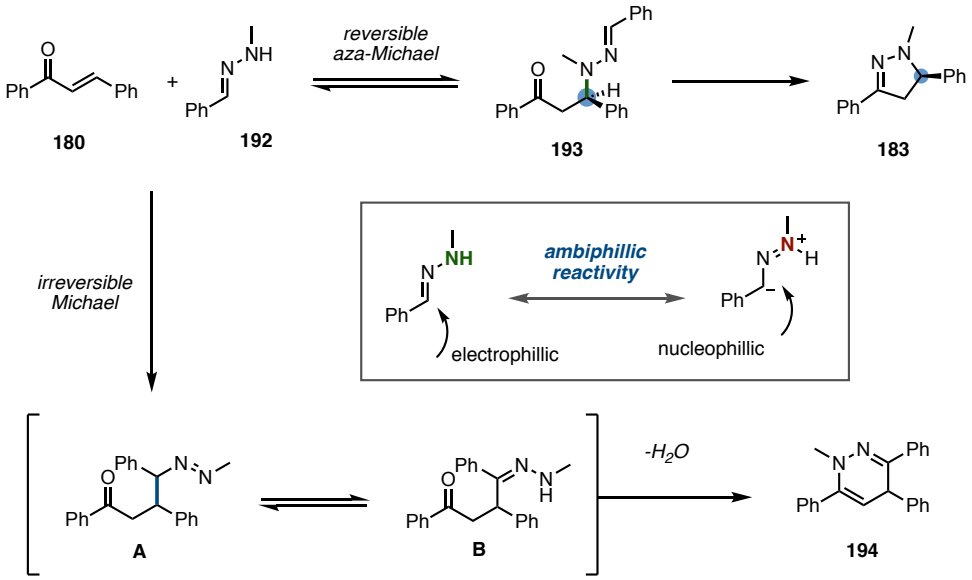

Scheme 39. Proposed mechanism for the formation of undesired Michael adducts, hinging on the ambiphillic properties of hydrazones.

carbon atom of **192** to form a new C-C bond (intermediate **A**), thereby creating a kinetic trap for the undesired side-process. The dihydropyridazine Michael adduct **194** is ultimately formed following tautomerization of azene **A** to hydrazone **B** and subsequent condensation onto the adjacent carbonyl. However, this plausible mechanism was not studied experimentally.

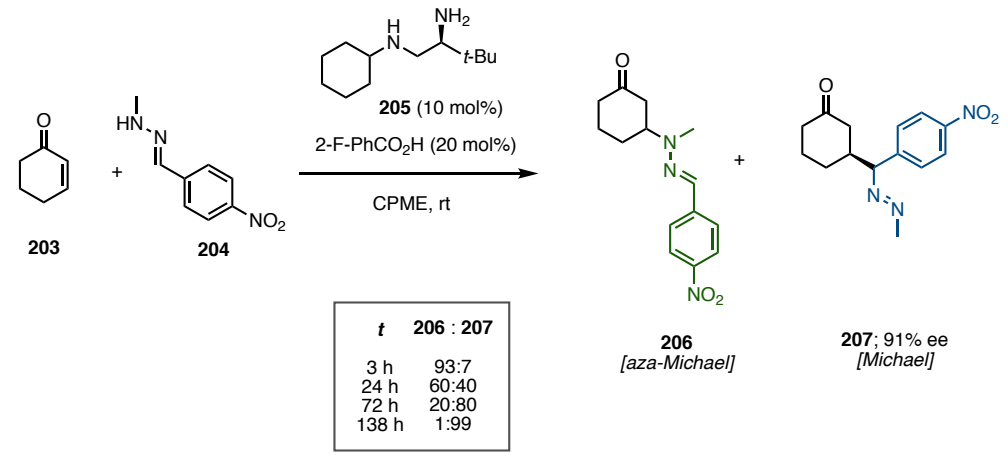

Scheme 40. Precedent for *aza*- vs *carba*-Michael addition competition, from Ye and co-workers.

This mechanistic model is consistent with the well-known ambiphillic nature of hydrazones.[246,247] Indeed, processes of this type have been reported before. For example, Ye and co-workers reported a similar competitive system, wherein the enantioselective aza-Michael (and Michael) additions of hydrazones (e.g., **204**) to *cyclic* enones such as cyclohexanone (**203**) were both catalyzed by a chiral diamine salt formed *in situ* from diamine **205** and (2-fluoro)benzoic acid (**Scheme 40**).[248] In the early stages of the reaction almost all product was that of the aza-Michael addition (**206**), however, the authors observed

concomitant steady decrease in **206** concentration with an increase of Michael addition product **207**.

3.3.3 Optimisation of the hydrazone

Attention next turned to structural variation of the hydrazone and its potential as a further point of optimization. The electronic and steric influence of the arene component of the hydrazone on the stereochemical outcome of the reaction was the focal point of study. With 4-methyl and 2-methyl hydrazones **208** and **209** enantioselectivity was modestly improved to 89:11 and 88:12 er, respectively, compared to 87:13 er with unsubstituted phenyl hydrazone **192** (**Table 4**; entries 2-3). Pleasingly, hydrazone **210** derived from 4-*tert*-butyl benzaldehyde was found to give the most substantial, although small, uplift in enantioselectivity to 90:10 er (**Table 4**; entry 4). Further investigations were fruitless: hydrazones derived from 4-fluorobenzaldehyde (**211**), 4-phenylbenzaldehyde (**212**), 2-naphthylaldehyde, (**213**) and cyclohexylcarboxaldehyde (**214**) did not demonstrate improved enantioselectivity (**Table 4**; entries 5-8).

Further optimization focused on the reaction conditions. Catalyst loading could be reduced to 10 mol% with negligible effect and coupling this change with an extended reaction time of 48 hours, and lowering the reaction temperature to -15 °C, afforded *tert*-butyl *aza*-Michael adduct **215** in 93% isolated yield with 95:5 er (**Table 4**; entries 9-10).

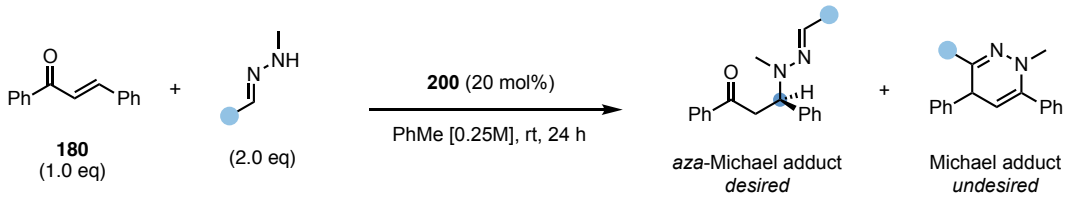

entry	R	aza-Michael (%)[a]	Michael (%)[a]	aza-Michael er[b]
1	Ph (**192**)	56	17	87:13
2	4-tol (**208**)	87	2	89:11
3	2-tol (**209**)	65	11	88:12
4	4-tBu-C_6H_5 (**210**)	90	0	90:10
5	4-F-C_6H_5 (**211**)	52	11	84:16
6	4-Ph-C_6H_5 (**212**)	69	3	88:12
7	2-nap (**213**)	36	5	N.D.
8	cyclohexyl (**214**)	75	13	67:33
9[c]	4-tBu-C_6H_5 (**210**)	68	0	88:12
10[d]	4-tBu-C_6H_5 (**210**)	93	0	95:5

Table 4. Optimization of the hydrazone in the enantiodetermining *aza*-Michael addition to **180** catalysed by **200.** [a] determined by ^{1}H NMR analysis of crude reaction mixture. [b] er determined by chiral stationary-phase HPLC. [c] 10 mol% of catalyst **200**. [d] performed at -15 ^{o}C for 48 hours.

3.3.4 Optimisation of hydrazine release

With a stereoselective aza-Michael addition in hand, we next turned our attention to the *in situ* cleavage of hydrazone intermediate **215**. A range of reagents and conditions were explored to promote release of either aldehyde **217** or oxime **218**, thereby unmasking the primary amine in **215**, which is positioned for cyclo-condensation. Acidic conditions were examined first. Convenient solid-supported media including the strongly acidic Amberlyst-15R® and weakly acidic Amberlite-CG50® resulted in decomposition and no reaction, respectively (**Table 5**; entries 1-2). Aqueous hydrochloric acid, or wet silica gel, were also insufficient to promote cleavage of the hydrazone (**Table 5**; entries 3-5). Conversely,

aqueous sulfuric acid afforded a mixture of the undesired Michael product **216**, along with the desired pyrazoline **183**, which suffered enantiodegradation to 79:21 er (**Table 5**; entry 6).

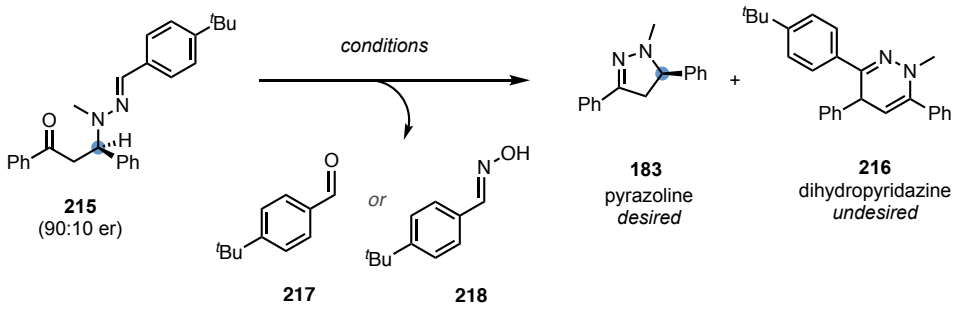

entry	conditions	183 [%][a]	216 [%][a]	183 er[b]
1	Amberlyst-15R®	decomp.	-	-
2	Amberlite-CG50®	N.R.	-	-
3	aq. HCl/dioxane, rt, 6 h (1.5 eq)	N.R	-	-
4	aq. HCl/dioxane, rt, 6 h (10.0 eq)	N.R	-	-
5	silica gel, H_2O	N.R.	-	-
6	aq. H_2SO_4/MeOH, rt, 6 h (0.5 eq)	70	21	71:29
7	30% NH_2OH/MeOH, rt, 2 h (2.0 eq)	>95	0	90:10
8	30% NH_2OH/MeOH, 60 °C, 2 h (2.0 eq)	>95	0	89:11

Table 5. Optimization of the cleavage/cyclocondensation reaction of aza-Michael adduct **215** to afford 2-pyrazoline **183**. [a] determined by ^{1}H NMR analysis of crude reaction mixture. [b] er determined by chiral stationary-phase HPLC.

Ultimately, it was found that quantitative and clean removal of the masked aldehyde could be achieved by addition of 2.0 equivalents of hydroxylamine in methanol at room temperature for 2 hours (**Table 5**; entries 7-8). Under these conditions, oxime **218** is released and easily separated from the desired product by column chromatography. The unmasked primary hydrazine could not be observed by ^{1}H NMR, suggesting that spontaneous condensation occurs immediately to give the 2-pyrazoline **183**. Importantly, no erosion of enantiopurity was observed in this transformation.

3.3.5 A one-pot protocol

Having streamlined the aza-Michael addition and hydrazone cleavage steps, we finally set out to include *in situ* formation of the hydrazone from methylhydrazine and aldehyde **217** in the reaction protocol. We were pleased to find that no significant optimization was necessary. Hydrazone **210** could be formed in the same reaction solvent (toluene) used for subsequent steps, and at the same concentration. The addition of molecular sieves was necessary to prevent a loss of enantioselectivity in the subsequent enantioselective addition step. Hence, a streamlined one-pot strategy to deliver enantioenriched 2-pyrazolines from hydrazines was produced (**Scheme 41**).

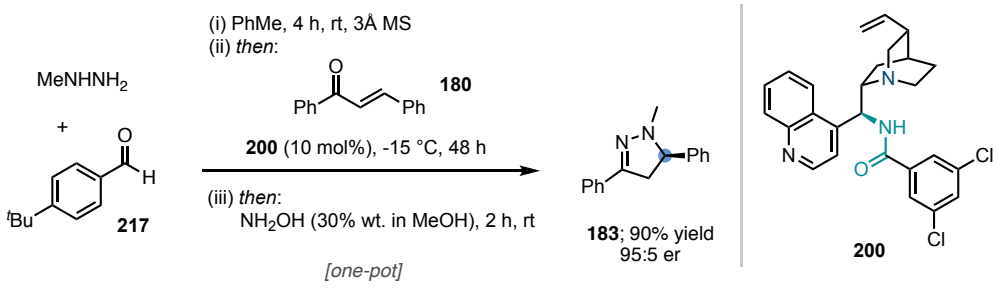

Scheme 41. Streamlined one-pot method for the enantioselective synthesis of model product **183** from chalcone and methylhydrazine.

In summary, hydrazone **210** was prepared from methylhydrazine and 4-*tert*-butylbenzaldehyde (**217**) in toluene at room temperature for 4 hours in the presence of 3Å molecular sieves. The mixture was cooled to -15 °C, followed by addition of catalyst **200** and chalcone (**180**). After 48 hours, hydroxylamine in methanol was added at room temperature, and the reaction worked up and purified by column chromatography after 2 hours, allowing 2-pyrazoline **183** to be isolated in 90% yield and 95:5 er.

3.4 Evaluation of Reaction Scope

3.4.1 Scope with respect to *bis*-aryl enones

With an efficient and practical protocol in hand, assessment of the method with respect to the enone scope was pursued. Pleasingly, minimal variation of enantioselectivity was generally observed across an array of substrates (**Scheme 42**). Chalcones with substitution at the 4-position of either arene ring were well-tolerated; 4-bromo (**219**), chloro (**220**), vinyl (**221**), nitro (**222**), nitrile (**223**) and benzoate (**224**) products were all isolated with at least 95:5 er and high yields. Whereas when the starting chalcone was substituted with a 4-methoxy group, the one-pot method afforded product **225** with only 46% yield and a poorer enantioselectivity of 91:9 er. Addition of the medicinally relevant difluorocyclopropane motif at the 4-position afforded **226** with 91:9 er and 1:1 dr (at the benzylic cyclopropane carbon).[249,250] Substitution at the 3-position of one arene ring was tolerated – 3-methyl derivative **227** was obtained with 94:6 er and 51% yield. Unfortunately, the method showed little tolerance for *ortho*-substituents and only the 2-fluoro product **228** could be prepared, with the fluorine atom only tolerated on the ketone side of the starting chalone. This lack of tolerance for ortho-substitution is possibly due to the interruption of key H-bonds by the placement of additional steric bulk near essential binding sites. Chalcones with *bis*-substitution of relatively neutral or electron-withdrawing groups performed well; indane **229**, 3,5-*bis*-trifluoromethyl **230**, and 3,4-dichloro **231** were all isolated with high enantioselectivity. Meanwhile, less satisfactory enantioselectivities were obtained with *bis*-substituted electron-rich chalcones, including dioxole **232** (82:18 er) and 3,4-dimethoxy (**233**, 81:19 er). Heterocycles were also competent substrates, albeit with disappointing enantioselectivities.

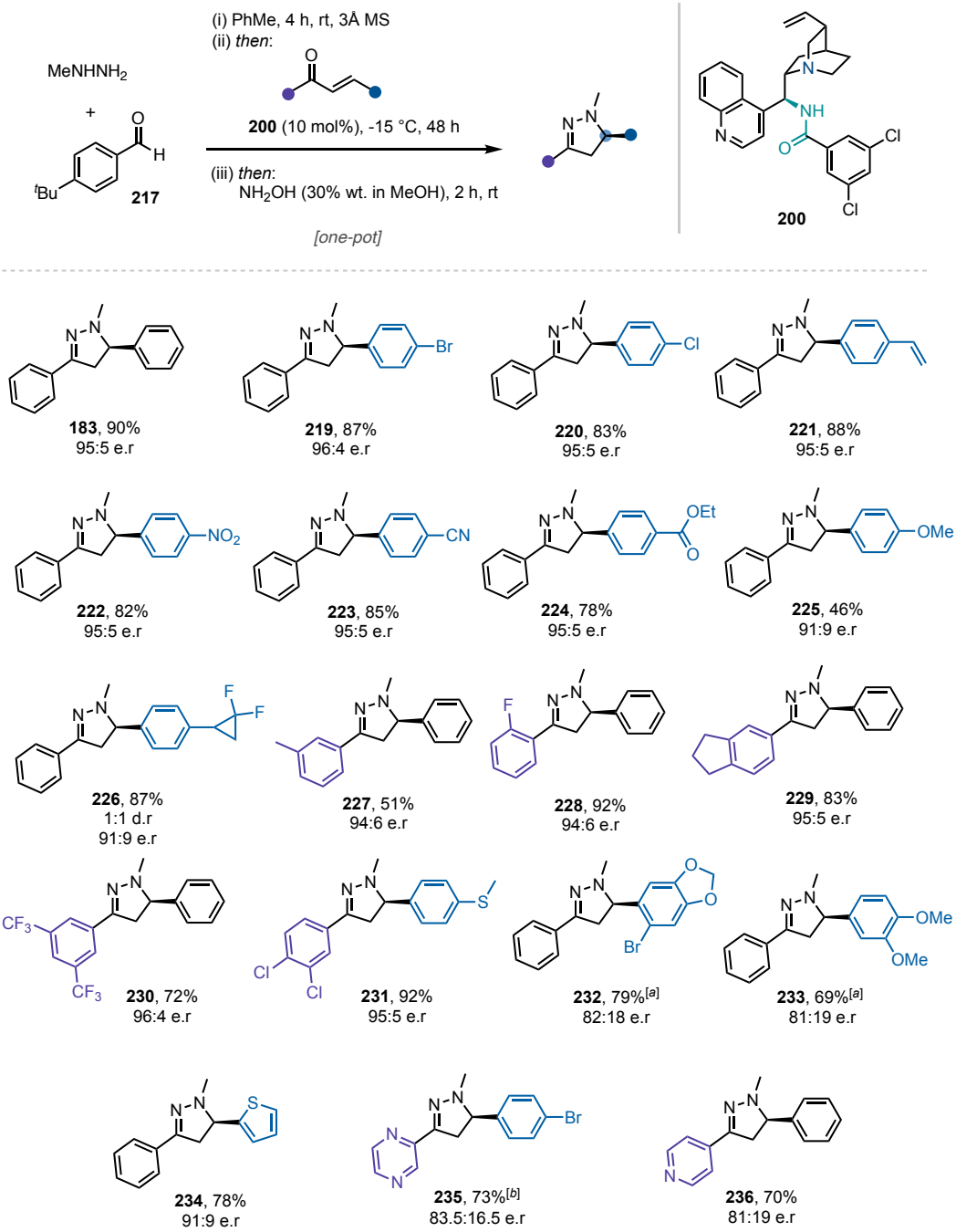

Scheme 42. Scope of the one-pot synthesis of enantioenriched 2-pyrazolines with respect to bis-aryl chalcones. [a] performed in CH_2Cl_2. [b] performed at -40 °C.

Thiophene product **234** was obtained with 78% yield and 91:9 er, while 2-pyrazolines prepared derived from either a pyrazine (**235**) or pyridine (**236**) performed less satisfactorily, affording products with only 83.5:13.5 er and 81:19 er, respectively. The poor selectivity is most likely due to the presence of Lewis-basic nitrogen atoms, which may interfere with the discreet hydrogen-bonding interactions between catalyst **200** and the respective substrates that are essential for high stereocontrol.

3.4.2 Scope with respect to alkyl enones

Chalcones derived from alkyl aldehydes (*via* aldol condensation with the corresponding acetophenone) were remarkably compatible with the newly developed method (**Scheme 43**). Cyclohexyl- and cyclopropyl-pyrazolines **237** and **238** were both furnished with an excellent selectivity of 98:2 er. Furthermore, *n*-hexyl substituted pyrazoline **239** was obtained as a single enantiomer (>99:1 er) in 82% yield when performed at -40 °C for 24 hours. Ynenones also behaved efficiently in the one-pot method to afford the 5- and 3-alkyne substituted 2-pyrazolines **240** and **241** in 95:5 er and 97:3 er, respectively. Alkenyl 2-pyrazoline **242** was prepared from a symmetrical *bis*-enone in 73% yield and 89:11 er. Finally, 3-trifluoromethyl-2-pyrazoline **243** was obtained in 80% yield and 95:5 er following reaction at -40 °C. 2-Pyrazoline structures bearing a 3-CF_3 substituent such as **243** are particularly common in drug molecules, making this an attractive example in the context of pharmaceutical development.[251–253]

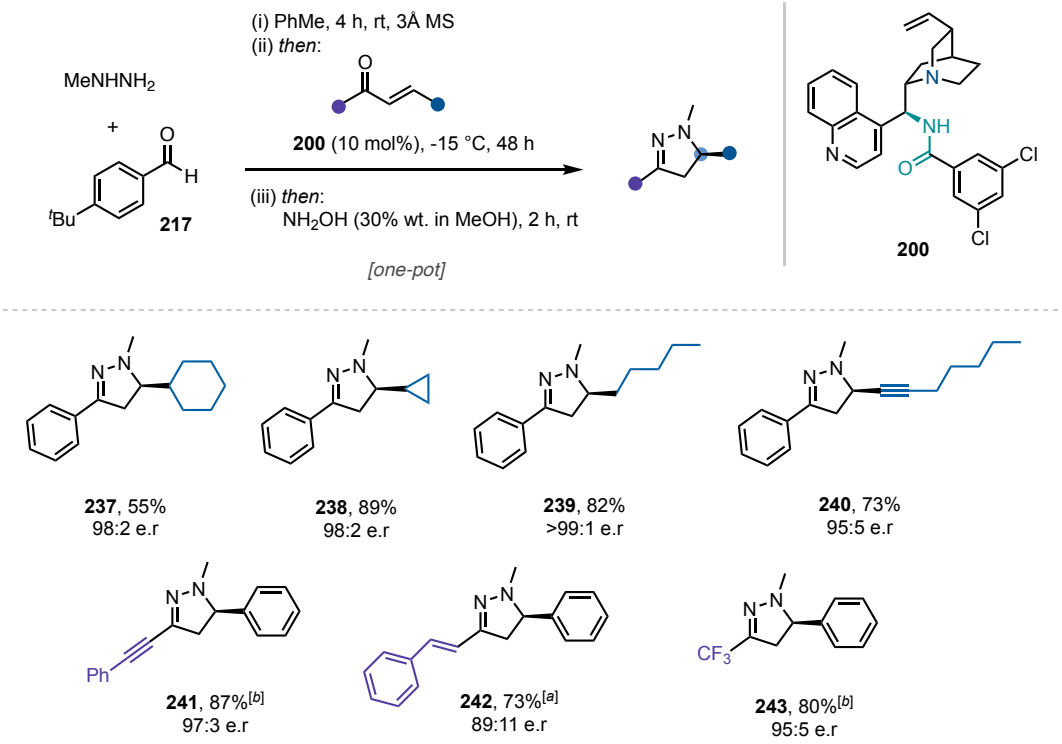

Scheme 43. Scope of the one-pot synthesis of enantioenriched 2-pyrazolines with respect to enones substituted with alkyl, alkene and alkyne groups. [a] performed in CH_2Cl_2. [b] performed at -40 °C.

3.4.3 Scope with respect to the hydrazine

Variation of the hydrazine substrate afforded the *N*-ethyl (**244**), *N*-cyanoethyl (**245**), and *N*-benzyl (**246**)-2-pyrazolines in good yield and enantioselectivity at reaction rates similar to the model methyl hydrazine system (**Scheme 44**). These examples demonstrate the wider applicability of this chemistry towards the synthesis of a broad range of products. Unfortunately, the use of phenyl hydrazine did not afford any product.

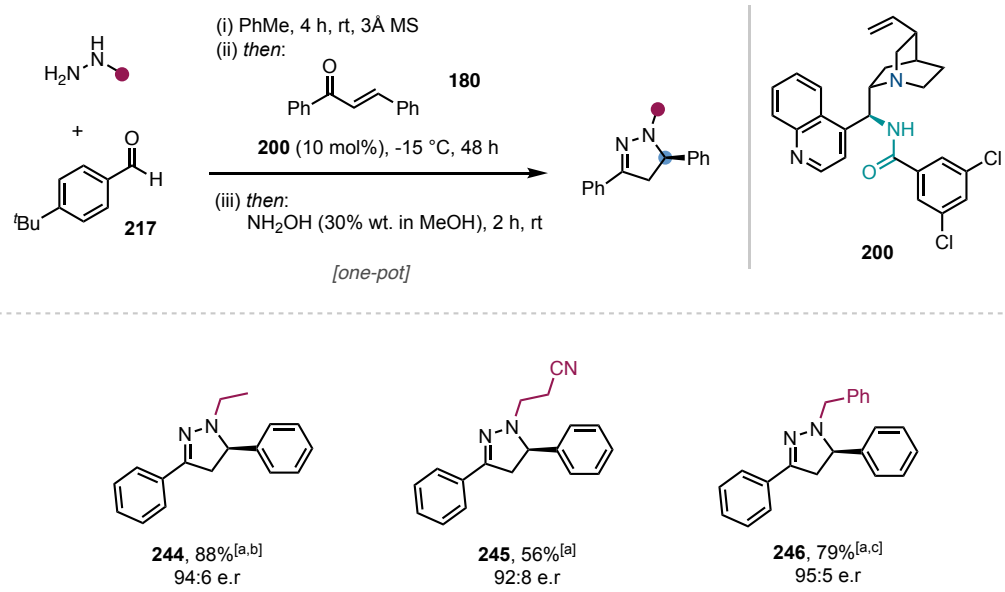

Scheme 44. Scope of the one-pot synthesis of enantioenriched 2-pyrazolines with respect to the hydrazine. [a] performed in CH_2Cl_2. [b] with $EtNHNH_2$-oxalate and 1.95 equiv DIPEA. [c] with $BnNHNH_2$-2HCl and 3.8 equiv DIPEA.

3.5 Large Scale Synthesis and Catalyst Recycling

Considering the importance of reaction scalability to the industrial utility of a synthetic method, we investigated the large-scale preparation of 4-bromo 2-pyrazoline **219**. With affordability in mind, the reaction was performed with benzaldehyde rather than 4-(*tert*-butyl)benzaldehyde due to its significantly lower cost. Likewise, in consideration of practicality, the reaction was performed at room temperature instead of -15 °C. Although it was anticipated that these modifications would result in slightly lower enantioselectivity, we assumed that a purification by recrystallisation would both improve the enantiopurity to >99:1 er and eliminate the need for a costly and time-consuming purification by chromatography. With the eventual goal of performing the reaction using 100 grams of

chalcone **247**, we initially tested the viability of our aim with a 10-gram (of **247**) trial reaction. Hence, using the aforementioned modifications to the reaction conditions, a test run successfully afforded 8.9 grams of desired 2-pyrazoline (**219**) in 81% yield and 99:1 er after a single recrystallisation.

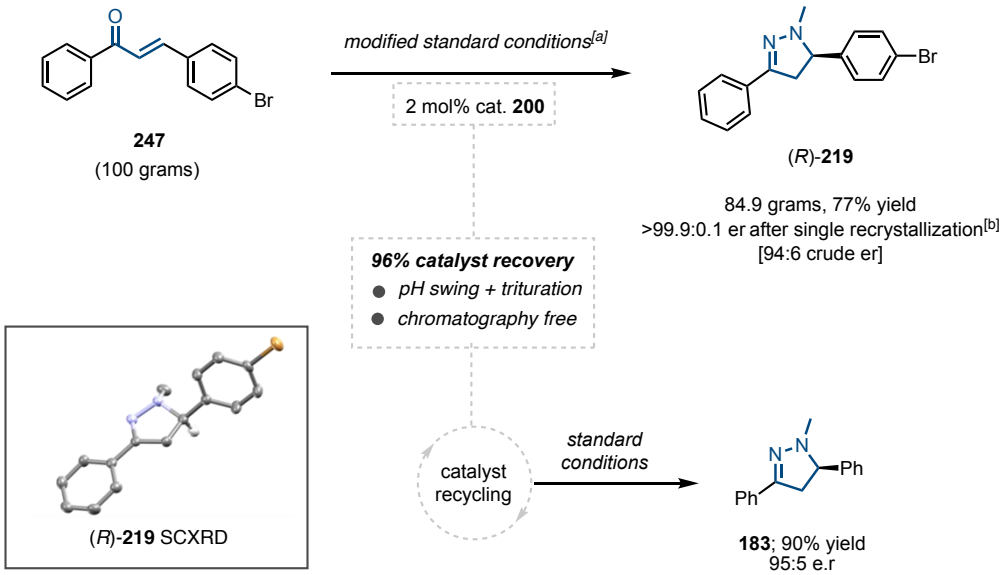

Scheme 45. Preparative scale synthesis of **219**, with demonstration of catalyst recovery and recycling. Stereochemical configuration of **219** was determined by single crystal X-ray diffraction studies.[a] all steps performed at room temperature, benzaldehyde used instead of **217**, [PhMe] = 0.38M.

Following a successful 10-gram scale-up, the reaction was repeated on 10-fold scale (350 mmol, 100 grams) with respect to the enone (**Scheme 45**). Smooth reactivity and a clean reaction profile allowed the isolation of 84.9 grams of the pyrazoline product **219** in 77% yield as colorless needles. The crude product (after work-up) had 94:6 er; only a single recrystallization from ethanol was required to improve this to essentially a single enantiomer (>99.9:0.1 er). Single-crystal X-ray diffraction studies on 4-bromo product **219** revealed (*R*) stereochemical configuration at the benzylic stereocentre.

Catalyst **200** was recovered simply by pouring the concentrated crude residue into chilled diethyl ether. The resulting precipitate was dissolved in ethyl acetate and a subsequent pH-swing afforded pure catalyst **200** in 89% yield after concentration and a final trituration in cold pentane. The recovered catalyst was resubjected to the model reaction under standard conditions. Model product **183** was obtained with no loss of reactivity or selectivity, compared to the reaction performed using fresh catalyst (**Scheme 45**). In addition to the recovered catalyst, the oxime by-product **218** was also easily separated from the desired pyrazoline product. Extractive work-up afforded over 61 grams of pure oxime **218** in 97% yield.

3.6 Synthetic Utility of the 2-Pyrazoline Motif

With the aim of demonstrating synthetic utility of enantioenriched 2-pyrazolines, enantiopure **219** was explored as a scaffold for late-stage derivatization (**Scheme 46**). The 2-pyrazoline motif was first investigated as a novel directing group for C-H activation. Accordingly, **219** was treated with ethyl acrylate, catalytic $[RuCl_2(p\text{-cymene})]_2$, $AgSbF_6$, and super-stoichiometric $Cu(OAc)_2$ under an atmosphere of air.[254,255] Pleasingly, after 18 hours at 90 °C in DME, the *ortho*-alkenylated product **248** was isolated in an unoptimized 48% yield on the first attempt. To the best of our knowledge, this is the first example of C-H functionalization directed by a 2-pyrazoline.

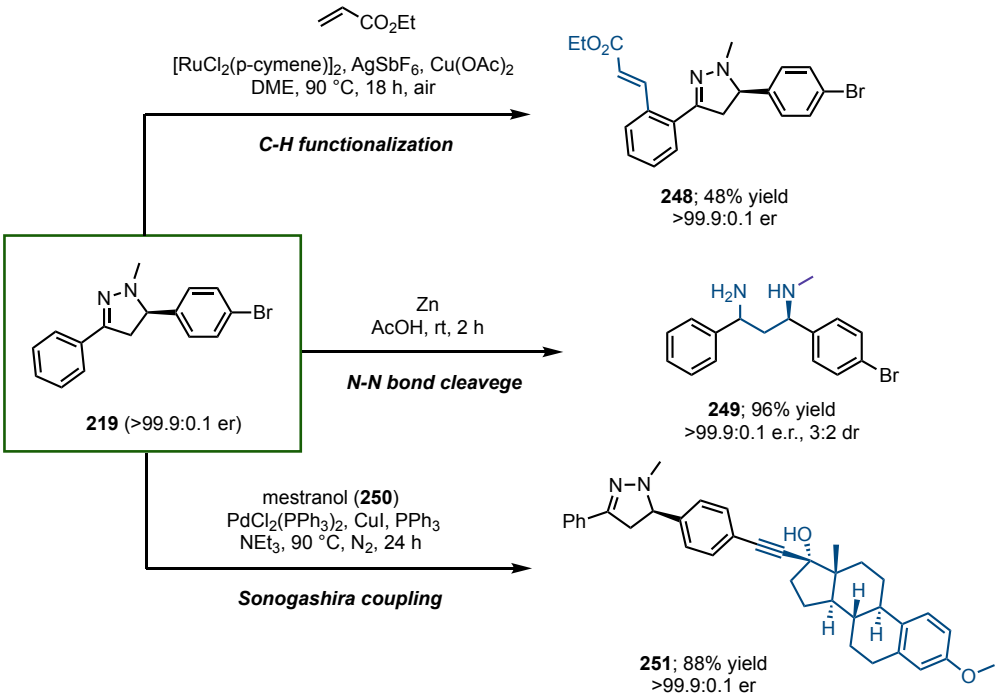

Scheme 46. Late-stage derivatisation of 2-pyrazoline **219**.

Furthermore, the 2-pyrazoline motif was recognized as a potentially convenient source of valuable 1,3-diamines by reductive cleavage of the N-N bond. Methods to access such optically active 1,3-diamines are relatively limited.[256,257] Hence an efficient protocol for N-N bond cleavage could present a simple route to access these compounds. Against this backdrop, we were pleased to find that treatment of **219** with activated zinc powder in neat acetic acid at room temperature furnished a 3:2 diastereomeric mixture of the enantioenriched diamine **249** in 96% yield after 2 hours. This approach is a simple and synthetically powerful method for obtaining enantioenriched 1,3-diamines. Attempts to improve the diastereomeric outcome of the reaction by varying reaction temperature and solvent mixtures failed.

Finally, palladium-catalyzed cross-coupling allowed rapid introduction of a drug-like structural fragment. 2-Pyrazoline **219** tolerated Sonogashira cross-coupling conditions with the hormone drug mestranol (**250**). Enantiopure internal alkyne **251** was readily furnished in 88% yield. It should be noted that in all derivatization reactions described here no oxidation of the substrates or products to the corresponding saturated pyrazole was observed.

3.7 Conclusion

In summary, a simple protocol for the preparation of enantioenriched 2-pyrazoline scaffolds has been developed. The method combines a three-stage strategy into a one-pot procedure to afford pyrazolines from simple hydrazines and enones. Moderating the hydrazine reactivity via *in situ* hydrazone formation was key to achieving high enantiocontrol. The enantiodetermining aza-Michael addition is efficiently facilitated by a bifunctional Brønsted -base/H-bond donor catalyst.

The new synthetic method is compatible with a range of heterocycles and functional groups, and decagram-scale synthesis was demonstrated in a simplified procedure. Moreover, facile catalyst removal and simple purification of the 2-pyrazoline product allowed recovery of the pure catalyst in 89% yield, and the desired product as a single enantiomer in 77% yield. A range of late-stage derivatizations demonstrated the synthetic versatility and utility of the 2-pyrazoline products, including a novel C-H activation directed by the 2-pyrazoline motif. The scalability and simplicity of the method, coupled with the diversity of products and

range of possible late-stage functionalizations presents this aldehyde-mediated method as an attractive synthetic protocol with potential applications in biomedical and agrochemical discovery programs.

Chapter 4

Experimental

4.1 General Experimental Information

Reagents and solvents were purchased as reagent-grade from Acros Organics, Sigma-Aldrich, Alfa Aeser, and Fluorochem and used without further purification unless stated. Solvents for extraction or column chromatography were of technical quality. All water used was purified via a Merck Millipore reverse osmosis purification system prior to use. Anhydrous solvents (tetrahydrofuran, toluene, dichloromethane, and diethyl ether) were dried by filtration through activated alumina (Sigma-Aldrich, 58 Å pore size, powder 150 mesh, basic) columns and stored under N_2 atmosphere

prior to use. CPME was dried by storing over 3Å-molecular sieves for at least 72 hours. Solvents were removed under reduced pressure using Büchi Rotavapor apparatus.

Reactions were performed under N_2 atmosphere unless otherwise stated. Schlenck techniques were adopted for the handling of sensitive reagents and for carrying out air/moisture sensitive experiments. Reaction temperatures refer to external probe temperature of the heating oil bath.

Thin-layer chromatography was performed on SiO_2-60 UV_{254} coated aluminium sheets from Merck (silica gel 60 F254). Visualisation was achieved with a UV lamp at a wavelength of 254 nm, or with a $KMnO_4$ solution.

Flash column chromatography was carried out on silica gel 60 (VWR, 40-63 μm). Solvents for extraction and chromatography were of technical quality. Solvent mixtures are individually reported in parenthesis.

Proton, Carbon, and Fluorine nuclear magnetic resonance (^{1}H, ^{13}C, and ^{19}F NMR) spectra were recorded on a Bruker AVIII HD (400 MHz ^{1}H, 500 MHz ^{1}H, 101 MHz ^{13}C, 151 MHz ^{13}C, and 376 MHz ^{19}F) spectrometer at 25 °C. Chemical shifts (δ) are given in ppm, coupling constants (*J*) in Hz. The residual deuterated solvent was used as internal standard ($CDCl_3$: δ_H = 7.26 ppm). HSQC, COSY and HMBC experiments were used for ^{1}H and ^{13}C NMR signals assignment where required.

Melting points (m.p.) were determined with a Leica Galen III Hot-stage melting point apparatus and microscope and on a Kofler hot block and are reported uncorrected.

Infrared (IR) spectra were recorded on a Bruker Tensor 27 FT-IR spectrometer as a thin film. Selected absorption bands are reported in wave numbers (cm^{-1}) with relative signal intensities described as s (strong), m (medium), or w (weak). When applicable, peak shape is characterised by br (broad).

High-resolution mass spectrometry (HR-MS-ESI) was performed on a Bruker μTOF mass spectrometer. The molecular ion (M^+) is reported in m/z units.

X-Ray Crystallography studies of single-crystals by X-Ray diffraction were performed on an Enraf-Nonius KCCD diffractometer or on an Oxford Diffraction SuperNova diffractometer at 150 K. Crystal structures were solved with SIR92 software and refined with CRYSTALS by Dr Heyao Shi (University of Oxford) with training and guidance from Dr Amber L. Thompson and Dr Kirsten E. Christensen (University of Oxford Chemical Crystallography department).

4.2 Experimental Details for Chapter 2

4.2.1 Optimisation Studies

General Procedure A for optimization of the model reaction:

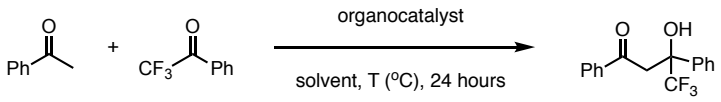

A freshly prepared stock solution of acetophenone (**95**) and 2,2,2,-trifluoroacetophenone (**91**) in the specified solvent was added to the catalyst at RT in a 1.7 mL mass-spec vial. After flushing the vial with N_2 gas, the reaction was stirred at the specified temperature for 24 hours. Conversion was determined by crude ^{1}H NMR. Volatiles were removed by a stream of N_2 gas, followed by filtration through silica gel with 30% CH_2Cl_2 in pentane. The crude product **96** was analysed by chiral HPLC (Chiralpak AD-H, 4.6 x 250 mm; 3% *i*PrOH/hexanes, 1.0 mL/min; t_R (minor) = 15.1 min, t_R (major) = 17.0 min. **Table 6** details the results of this screening program. **Figure 13** illustrates chosen catalysts.

Entry	Catalyst	(mol%)	solvent	T	96 (%)[a]	96 (er)[b]
1	**S1**	10 mol%	Et_2O (0.1 M)	RT	trace	N.D
2	**200**	10 mol%	Et_2O (0.1 M)	RT	trace	N.D
3	**198**	10 mol%	Et_2O (0.1 M)	RT	trace	N.D
4	**S2**	10 mol%	Et_2O (0.1 M)	RT	trace	N.D
5	**199**	10 mol%	Et_2O (0.1 M)	RT	trace	N.D
6	**S3**	10 mol%	Et_2O (0.1 M)	RT	trace	N.D
7	**S4**	10 mol%	Et_2O (0.1 M)	RT	trace	N.D
8	**189**	10 mol%	Et_2O (0.1 M)	RT	trace	N.D
9	**197**	10 mol%	Et_2O (0.1 M)	RT	trace	N.D
10	**S5**	10 mol%	Et_2O (0.1 M)	RT	trace	N.D
11	**98**	10 mol%	Et_2O (0.1 M)	RT	64%	62:38:00
12	**97**	10 mol%	Et_2O (0.1 M)	RT	52%	61:39:00
13	**S6**	10 mol%	Et_2O (0.1 M)	RT	21%	50:50:00
14	**S7**	10 mol%	Et_2O (0.1 M)	RT	88%	74:26:00
17	**S8**	10 mol%	Et_2O (0.1 M)	RT	0%	N.D
18	**99**	10 mol%	Et_2O (0.1 M)	RT	>95	78:22:00
19	**99**	10 mol%	Et_2O (0.5 M)	RT	90	75:25:00
20	**99**	10 mol%	Et_2O (0.02 M)	RT	90	78:22:00
21	**99**	10 mol%	PhMe (0.1 M)	RT	58	80:20:00
22	**99**	10 mol%	THF (0.1 M)	RT	13	75:25:00
23	**99**	10 mol%	CH_2Cl_2 (0.1 M)	RT	3	71:29:00
24	**99**	10 mol%	CPME (0.1 M)	RT	93	82:18:00
25	**99**	10 mol%	MeCN (0.1 M)	RT	8	61:39:00
26	**99**	10 mol%	EtOAc (0.1 M)	RT	11	77:23:00
27	**99**	10 mol%	Et_2O (0.1 M)	4 °C	90	83.5:16.5
28	**99**	10 mol%	Et_2O (0.1 M)	-15 °C	88	84:16:00
29	**100**	10 mol%	Et_2O (0.1 M)	RT	8	N.D.
30	**65**	10 mol%	Et_2O (0.1 M)	RT	63	74.5:25.5
31	**S9**	10 mol%	Et_2O (0.1 M)	RT	trace	N.D.
32	**99**	5 mol%	Et_2O (0.1 M)	RT	54	82:18:00
33	**99**	20 mol%	Et_2O (0.1 M)	RT	72	78:22:00

Entry	Catalyst	(mol%)	solvent	T	96 (%)[a]	96 (er)[b]
34[c]	**99**	10 mol%	Et_2O (0.1 M)	RT	89	79.5:20.5
35[d]	**99**	10 mol%	Et_2O (0.1 M)	RT	85	81.5:18.5
36	**99**	10 mol%	CPME (0.1 M)	-15 °C	>95%	90:10:00
38	**S10**	10 mol%	CPME (0.1 M)	-15 °C	90%	91:09:00
39	**S11**	10 mol%	CPME (0.1 M)	-15 °C	72%	90:10:00
40	**S12**	10 mol%	CPME (0.1 M)	-15 °C	>95%	88.5:11.5
41	**S13**	10 mol%	CPME (0.1 M)	-15 °C	92%	87.5:12.5
42	**S14**	10 mol%	CPME (0.1 M)	-15 °C	>95%	90:10:00
43	**S15**	10 mol%	CPME (0.1 M)	-15 °C	81%	85:15:00
44	**102**	10 mol%	CPME (0.1 M)	-15 °C	>95%	97:03:00
45[e]	**101**	10 mol%	CPME (0.1 M)	-15 °C	>95%	94:06:00
46	**S16**	10 mol%	CPME (0.1 M)	-15 °C	<10%	94:06:00
47	**S17**	10 mol%	CPME (0.1 M)	-15 °C	26%	72:28:00
48	**S18**	10 mol%	CPME (0.1 M)	-15 °C	45%	85:15:00
49	**S19**	10 mol%	CPME (0.1 M)	-15 °C	65%	80.5:19.5
50	**S20**	10 mol%	CPME (0.1 M)	-15 °C	78%	91:09:00
51	**S21**	10 mol%	CPME (0.1 M)	-15 °C	70%	96:04:00
52	**S22**	10 mol%	CPME (0.1 M)	-15 °C	73%	93:07:00

Table 6. Detailed optimization results for the aldol addition of acetophenone (**95**) to trifluoromethylketone **91**. N.D.: not determined. [a]conversion determined by ^{1}H NMR. [b]determined by chiral HPLC. [c]with 2.0 eq acetophenone. [d]with 2.0 eq 2,2,2-trifluoroacetophenone. [e]performed for 18 hours.

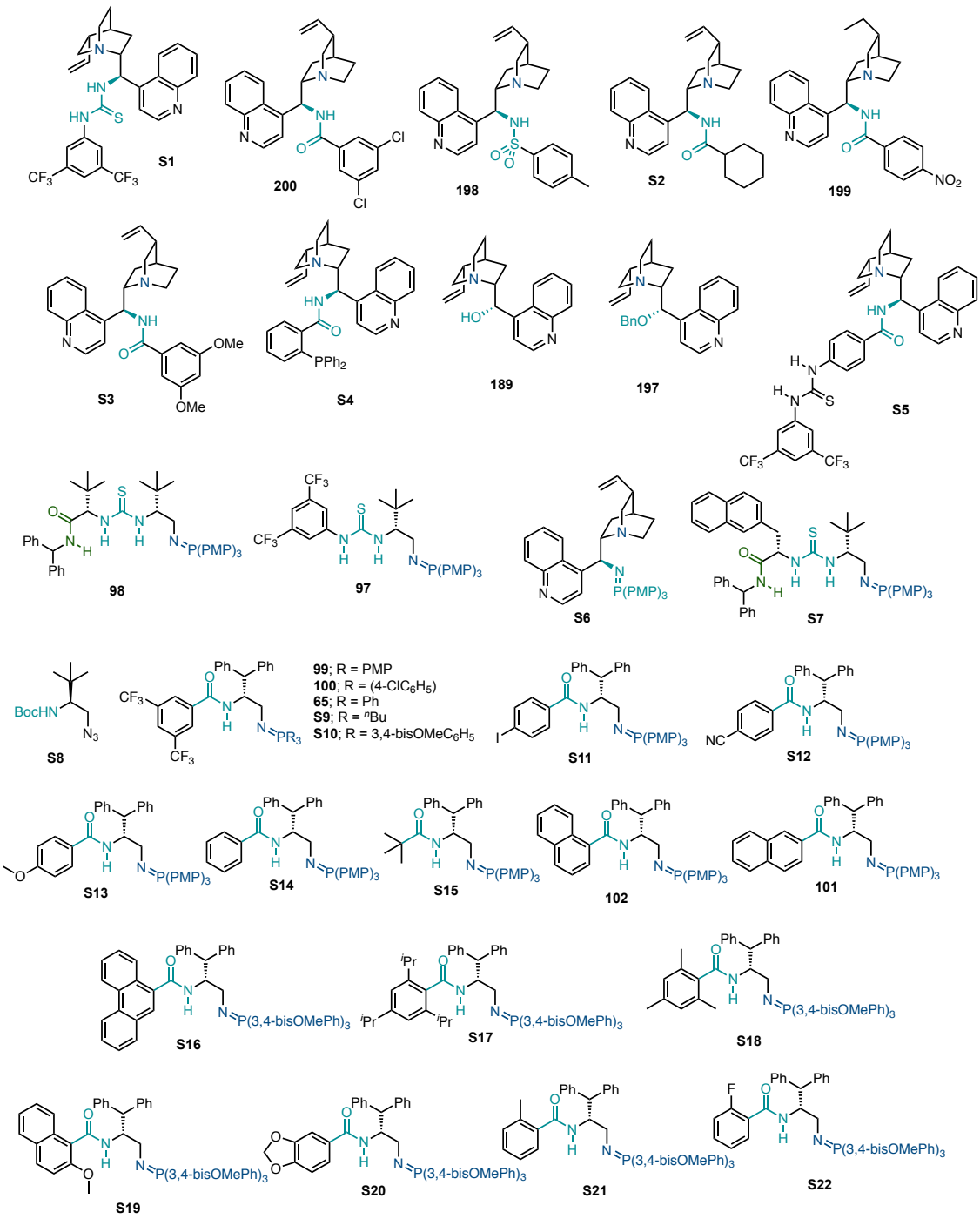

Figure 13. Selected catalysts studied in optimisation of the model reaction between **95** and **91**.

4.2.2 Synthesis of Starting Materials

Starting materials were purchased from commercial suppliers, synthesised as described below, or obtained from the library of Bayer CropScience.

General Procedure B for the synthesis of trifluoromethyl-ketones:

To a solution of aryl bromide (1.0 eq) in THF (0.5 M) at -78 °C was added dropwise *n*-BuLi (1.6 M in hexanes, 1.1 eq). The resulting solution was stirred at -78 °C for 1 hour before dropwise addition of ethyl 2,2,2-trifluoroacetate (1.5 eq). After 1 hours at -78 °C, the reaction mixture was warmed to RT and stirred overnight. The reaction was quenched with sat. aq. NH_4Cl solution, extracted with EtOAc (2 x 100 mL), drying over Na_2SO_4, filtered, and evaporated to dryness *in vacuo* to afford the crude trifluoroketone. Purification by silica gel chromatography (EtOAc in pentane) afforded the pure trifluoroketone products.

General Procedure C for the synthesis of trifluoroketones:

Mg turnings (1.5 eq) were stirred vigorously *in vacuo* for 1 hour before addition of anhydrous THF (8 mL/g Mg) and 1,2-dibromoethane (0.05 mL). A solution of the appropriate aryl bromide in anhydrous THF (1.0 M) was added dropwise to the resulting Mg slurry. After complete addition, the slurry was heated to 50 °C (if a gentle reflux did not occur naturally) for 1 hour to afford a solution of the appropriate Grignard reagent. The Grignard solution was added dropwise to a -78 °C solution of ethyl 2,2,2-trifluoroacetate (1.2 eq) in THF (1.0 M). The resulting solution was stirred at this temperature for 1 hour, then warmed quenched slowly with NH_4Cl saturated aqueous solution followed by 10% aq. HCl solution. The aqueous layer was extracted with diethyl ether (2 x 100 mL), dried over Na_2SO_4, filtered and

evaporated to dryness *in vacuo*. Purification by silica gel chromatography (EtOAc in pentane) or short-path distillation afforded the pure trifluoroketone products.

Methyl 4-acetyl-2-methylbenzoate (S23)

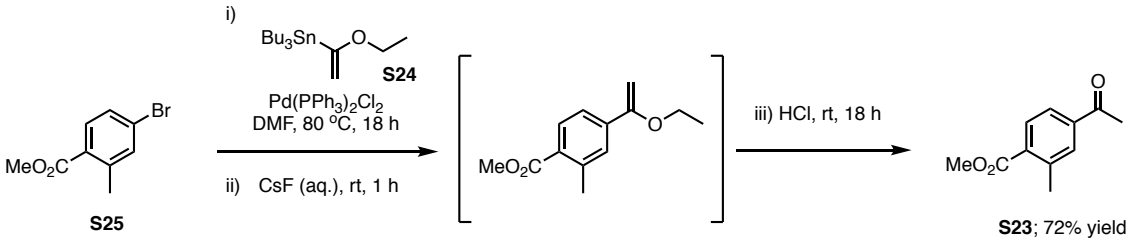

To a solution of ethyl vinyl ether (1.6 mL, 16.69 mmol) in THF (15 mL) at -78 °C was added slowly *tert*-butyllithium (1.7 M in pentane) (solution turns yellow). The solution was warmed to 0 °C over 15 minutes (solution becomes colourless) before immediately re-cooling to -78 °C. A solution of tributyltin chloride (3.77 mL, 13.91 mmol) in THF (3 mL) was added dropwise, the cooling bath was removed, and the mixture stirred at RT for 30 minutes. The resulting yellow solution was quenched with saturated aqueous ammonium chloride (15 mL), extracted with diethyl ether (3 x 25 mL), dried over Na_2SO_4 and evaporated to dryness in vacuo to afford the intermediate stannyl vinyl ether **S24** as a yellow oil which was used in the next step without further purification. **S24** (3.78 g, 10.44 mmol, 1.5 eq) was combined with **S25** (1.58 g, 6.96 mmol, 1.0 eq) and anhydrous DMF (15 mL) followed by $Pd(PPh_3)_2Cl_2$ (366 mg, 0.52 mmol, 0.075 eq) in a dry Schlenck tube under a nitrogen atmosphere. The mixture was stirred at 80 °C for 18 hours before addition of a 10% aqueous CsF solution (15 mL) at RT. After stirring at this temperature for 1 hour, 4M HCl solution in dioxane (15

mL) was added. The mixture was stirred at RT overnight then extracted with EtOAc (2x15 mL), dried over Na_2SO_4, filtered and evaporated under reduced pressure to afford the crude product as a brown oil. Purification by silica gel chromatography (5% acetone in pentane) afforded **S23** as a light-yellow oil (962 mg, 72%). Data is consistent with the published literature.[258]

^{1}H NMR (400 MHz, $CDCl_3$): δ 7.96 (d, *J* = 8.0 Hz, 1H, ArH), 7.86 – 7.72 (m, 2H, ArH), 3.92 (s, 3H, OC*H*$_3$), 2.64 (s, 3H, C*H*$_3$), 2.61 (s, 3H, C*H*$_3$) ppm; **^{13}C NMR (101 MHz, $CDCl_3$)**: δ 196.65 (*C*(O)), 178.17 (CH_3OC(O)), 142.33 (Ar*C*), 138.68 (Ar*C*), 134.63 (Ar*C*), 131.26 (Ar*C*H), 128.36 (Ar*C*H), 123.81 (Ar*C*H), 51.24 (O*C*H$_3$), 26.81 (*C*H$_3$), 20.47 (*C*H$_3$) ppm.

2,2,2-trifluoro-1-phenylethan-1-one (91)

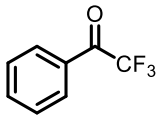

Prepared following General Procedure **C** using bromobenzene (30.6 ml, 287.0 mmol). Purification by short-path distillation (135 °C, 250 mbar) afforded the title compound as a colourless oil (40.2 g, 81%). Data is consistent with the published literature.[258]

^{1}H NMR (400 MHz, $CDCl_3$): δ 8.06 (dt, *J* = 8.2, 1.3 Hz, 2H, Ar*H*), 7.75 – 7.64 (m, 1H, Ar*H*), 7.53 (t, *J* = 7.8 Hz, 2H, Ar*H*) ppm; **^{19}F NMR (376 MHz, $CDCl_3$)**: δ -71.50 (s) ppm.

4-vinylacetophenone (S26)

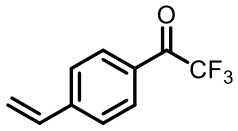

Prepared following General Procedure **C**, using 4-bromostyrene (6.37 g, 35.0 mmol) to afford the title compound as a pale-yellow oil (4.62 g, 66%). Data is consistent with the published literature.[259]

^{1}H NMR (400 MHz, $CDCl_3$): δ 8.17 – 7.89 (m, 2H, Ar*H*), 7.63 – 7.47 (m, 2H, Ar*H*), 6.78 (dd, *J* = 17.6, 10.9 Hz, 1H, ArC*H*$CH_{cis}H_{trans}$), 5.96 (d, *J* = 17.6 Hz, 1H, $ArCHCH_{cis}H_{trans}$), 5.51 (d, *J* = 10.9 Hz, 1H, $ArCHCH_{cis}H_{trans}$) ppm; **^{19}F NMR (376 MHz, $CDCl_3$)**: δ -71.36 (s) ppm.

1-(benzo[d][1,3]dioxol-5-yl)-2,2,2-trifluoroethan-1-one (S27)

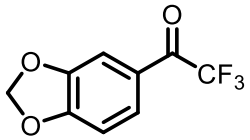

Prepared following General Procedure **B**, using 5-bromobenzo[d][1,3]dioxole (5.0 g, 24.8 mmol) to afford the title compound as colourless crystals (3.67 g, 68%) after silica gel chromatography (2% Et_2O in pentane). Data is consistent with the published literature.[260]

^{1}H NMR (400 MHz, $CDCl_3$): δ 7.71 (ddt, *J* = 8.3, 3.1, 1.3 Hz, 1H, Ar*H*), 7.50 (dt, *J* = 1.6, 0.8 Hz, 1H, Ar*H*), 6.93 (d, *J* = 8.3 Hz, 1H, Ar*H*), 6.11 (s, 2H, CH_2) ppm; **^{19}F NMR (376 MHz, $CDCl_3$)**: δ -70.73 (s) ppm.

2,2,2-trifluoro-1-(6-methoxynaphthalen-2-yl)ethan-1-one (S28)

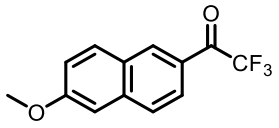

Prepared following General Procedure **B**, using 2-bromo-6-methoxynaphthalene (3.17 g, 12.1 mmol) to afford the title compound as colourless crystals (2.21 g, 72%) after silica gel chromatography and a single recrystallization from EtOH. Data is consistent with the published literature.[261]

^{1}H NMR (400 MHz, $CDCl_3$): δ 8.56 – 8.43 (m, 1H, Ar*H*), 8.02 (ddd, *J* = 8.8, 1.9, 0.9 Hz, 1H, Ar*H*), 7.91 – 7.81 (m, 1H, Ar*H*), 7.81 (s, 1H, Ar*H*), 7.23 (dd, *J* = 9.0, 2.5 Hz, 1H, Ar*H*), 7.14 (d, *J* = 2.5 Hz, 1H, Ar*H*), 3.96 (s, 3H, OCH_3) ppm; **^{13}C NMR (101 MHz, $CDCl_3$)**: δ 180.1 (q, *J* = 34.4 Hz,(*C*(O)), 161.1 (Ar*C*), 138.5 (Ar*C*), 132.9 (q, *J* = 2.3 Hz, Ar*C*), 131.8 (Ar*C*H), 127.7 (Ar*C*H), 127.5 (Ar*C*), 125.1 (Ar*C*), 125.1 (Ar*C*H), 120.4 (Ar*C*H), 117.0 (q, *J* = 291.6 Hz, CF_3), 105.9 (Ar*C*H), 55.5 (OCH_3) ppm; **^{19}F NMR (376 MHz, $CDCl_3$)**: δ -70.56 (s) ppm.

(*R*)-N-(3-azido-1,1-diphenylpropan-2-yl)-1-naphthamide (149)

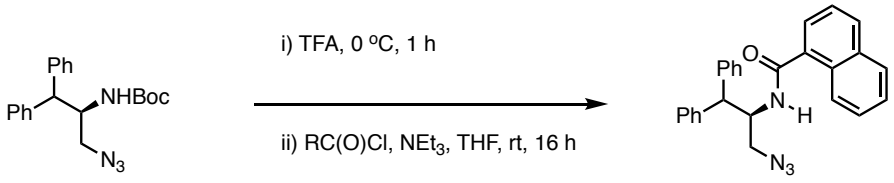

S29 **149**; 90% yield

Intermediate azide **S29** was prepared according to the previously reported method from Dixon and co-workers (31% yield over 10 steps).[90] **S29** (1.20 g, 3.41 mmol, 1.0 eq) was stirred at 0 °C in trifluoroacetic acid (3.4 mL) for 2 hours, before warming to RT. Volatiles were removed under a stream of nitrogen gas behind a blast shield. The resulting residue was dissolved in diethyl ether (10 mL) and basified to pH 14 with a 2M aqueous NaOH. The aqueous layer was extracted with diethyl ether (5 x 10 mL). Combined organic layers were dried over Na_2SO_4 and evaporated to dryness under a stream of nitrogen behind a blast shield. The resulting residue was dissolved in anhydrous THF (13 mL) under a nitrogen atmosphere, before addition of naphthoyl chloride (0.777 g, 4.09 mmol, 1.2 eq) and triethylamine (0.664 mL, 4.77 mmol, 1.4 eq). The resulting suspension was stirred at RT for 2 hours before quenching with water and extraction with diethyl ether (3 x 25 mL). The combined organic layers were dried over Na_2SO_4, filtered, and evaporated *in vacuo* to afford the crude product as a white solid. Trituration with CH_2Cl_2, and subsequent filtration from hot EtOH (minimum volume) afforded **149** a white powder (1.15 g, 83%). This procedure could also be performed on 15-gram scale to afford **149** in 80% yield.

^{1}H NMR (400 MHz, $CDCl_3$): δ 7.88 – 7.64 (m, 3H, Ar*H*), 7.51 – 7.09 (m, 14H, Ar*H*), 5.99 (d, *J* = 8.9 Hz, 1H, N*H*), 5.27 (ddt, *J* = 12.1, 9.0, 3.3 Hz, 1H, C*H*NHC(O)), 4.21 (d, *J* = 11.7 Hz, 1H,

Ph_2CH), 3.75 (dd, J = 12.5, 3.3 Hz, 1H, CH_2N_3), 3.37 (dd, J = 12.4, 3.3 Hz, 1H, CH_2N_3) ppm; **^{13}C NMR (101 MHz, $CDCl_3$)**: δ 169.2 (*C*(O)), 141.1 (Ar*C*), 141.1 (Ar*C*), 134.2 (Ar*C*), 133.5 (Ar*C*), 130.6(Ar*C*H), 129.9 (Ar*C*), 129.2 (Ar*C*H), 129.0 (Ar*C*H), 128.2 (Ar*C*H), 128.0 (Ar*C*H), 127.3 (Ar*C*H), 127.2 (Ar*C*H), 127.1 (Ar*C*H), 126.4 (Ar*C*H), 125.1 (Ar*C*H), 125.0 (Ar*C*H), 124.7 (Ar*C*H), 53.5 (Alk*C*H), 53.2 (Alk*C*H), 51.9 (Alk*C*H) ppm; **FT-IR (thin film)** ν_{max} 3253, 3029, 2083, 1633, 1581, 1548, 1493, 1450, 1341, 1301, 1273 cm^{-1}; **HRMS** (ESI) m/z calcd. for $C_{26}H_{23}ON_4$ ($[M+H]^+$) 407.18664, found 407.18689; **m.p.**: 209-211 °C; **$[\alpha]_D^{25}$** = -41.8 (c = 0.5, $CHCl_3$).

4.2.3 Synthesis of Racemic Products

To a solution of methylketone (0.1 mmol) and trifluoromethylketone (0.1 mmol) in CH_2Cl_2 (0.5 M) at RT, was added DBU (0.2 eq). The resulting solution was stirred at RT for 0.5-18 hours, with the reaction followed by TLC (eluting with pentane/DCM/diethyl ether mixtures). Silica gel chromatography (CH_2Cl_2 in pentane) afforded samples of racemic compounds for HPLC analysis.

4.2.4 Synthesis of enantioenriched products

General Procedure D for the synthesis of β-hydroxyketones**:**

Preparation of catalyst solution: to an oven-dried 3.0 ml screw-cap mass-spec vial was added an oven-dried magnetic stirrer bar. Catalyst precursor azide **149** (0.02 mmol, 0.1 eq), tris(4-methoxyphenyl)phosphine (0.02 mmol, 0.1 eq), and anhydrous CPME (0.4 mL) were added. The vial was flushed with nitrogen gas, capped, and sealed with parafilm. The mixture was stirred at RT for 4 hours, before use of the catalyst solution directly without further purification. Conversion can be confirmed by ^{31}P NMR (phosphine @ -10 ppm; iminophosphorane @ +10 ppm in C_6D_6; phosphine oxide @ +25 ppm). The crude catalyst solution (0.4 ml, as above) was cooled to -15 °C (in a household freezer equipped with stirrer-hotplate) in a vial capped with a suba seal, under a N_2 atmosphere. To this was added a solution of the appropriate trimethylketone (0.2 mmol, 1.0 eq) in anhydrous CPME (1.2 mL). After cooling for 15 minutes, a solution of the appropriate alpha-fluorinated ketone (0.2 mmol, 1.0 eq) in anhydrous CPME (0.4 mL) was added dropwise over at least 10

minutes. The reaction was stirred at -15 °C for the appropriate time. After completion, volatiles were removed under a stream of nitrogen gas. Purification by silica gel chromatography afforded the enantioenriched β-hydroxy ketones.

Slow addition of the α-fluorinated ketone is important for achieving high yields in some reactions and is essential for all reactions using very electron-poor trifluoromethylketones. Slow addition over up to 1 hour is preferred. This modification significantly reduces catalyst decomposition, which is caused by aza-Wittig reaction of the iminophosphorane with an electron-poor trifluoroketone.

(*S*)-4,4,4-trifluoro-3-hydroxy-1,3-diphenylbutan-1-one (96)

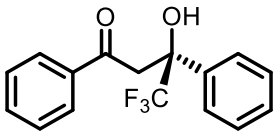

96 was prepared following General Procedure **D**, using acetophenone and 2,2,2-trifluoroacetophenone. Purification by silica gel chromatography (20% CH_2Cl_2 in pentane) afforded the title compound as a colourless solid (56 mg, 96%, 97:3 er). Data is consistent with the published literature.[262]

^{1}H NMR (400 MHz, $CDCl_3$): δ 7.97 – 7.88 (m, 2H, Ar*H*), 7.67 – 7.58 (m, 3H, Ar*H*), 7.52 – 7.45 (m, 2H, Ar*H*), 7.40 – 7.31 (m, 3H, Ar*H*), 5.67 (s, 1H, O*H*), 4.04 (d, *J* = 17.4 Hz, 1H, C*H*$_2$), 3.65 (d, *J* = 17.4 Hz, 1H, C*H*$_2$) ppm; **^{13}C NMR (101 MHz, $CDCl_3$)**: δ 199.1 (*C*(O)), 136.7 (Ar*C*), 135.0 (Ar*C*), 133.9 (Ar*C*H), 128.3 (Ar*C*H), 127.9 (Ar*C*H), 127.2 (Ar*C*H), 127.2 (Ar*C*H), 125.6 (Ar*C*H), 123.3 (q, J = 282.7 Hz, *C*F$_3$), 75.6 (q, J = 29.2 Hz, *C*(CF$_3$)OH), 39.4 (*C*H$_2$) ppm; **^{19}F NMR (376 MHz, $CDCl_3$)**: δ -80.23 (s) ppm; **FT-IR (thin film)** ν_{max} 3345, 2970, 2929, 2160, 2026, 1670, 1597, 1411, 1160, 1128 cm^{-1}; **HRMS** (ESI) m/z calcd. for $C_{16}H_{17}N_2$ ([M+H]$^+$) 237.1386, found 237.1387; **$[\alpha]_D^{25}$** = +47.8 (c = 0.5, $CHCl_3$); **Chiral HPLC**: Chiralpak AD-H, 4.6 x 250 mm; 3% *i*PrOH/hexanes, 1.0 mL/min; t_R (minor) = 15.1 min, t_R (major) = 17.0 min, 97:3 er.

(*S*)-4,4,4-trifluoro-3-(4-fluorophenyl)-3-hydroxy-1-phenylbutan-1-one (103)

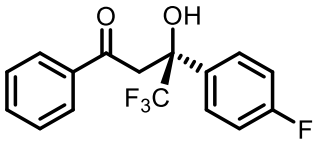

103 was prepared following General Procedure **D**, using acetophenone and 4'-fluoro-2,2,2-trifluoroacetophenone. Purification by silica gel chromatography (20% CH_2Cl_2/20% EtOAc/60% pentane) afforded the title compound as a colourless solid (56 mg, 90%, 95:5 er). Data is consistent with the published literature.[262]

^{1}H NMR (400 MHz, $CDCl_3$): δ 7.90 – 7.78 (m, 2H, Ar*H*), 7.57 (ddt, *J* = 7.9, 7.0, 1.3 Hz, 1H, Ar*H*), 7.54 – 7.47 (m, 2H, Ar*H*), 7.47 – 7.39 (m, 2H, Ar*H*), 7.05 – 6.92 (m, 2H, Ar*H*), 5.76 – 5.42 (m, 1H, O*H*), 3.93 (d, *J* = 17.3 Hz, 1H, CH_2), 3.56 (d, *J* = 17.4 Hz, 1H, CH_2) ppm; **^{13}C NMR (101 MHz, $CDCl_3$)**: δ 198.6 (*C*(O)), 162.1 (d, J = 291.1 Hz, Ar*C*F), 135.8 (Ar*C*), 133.3 (Ar*C*), 132.1 (Ar*C*H), 128.1 (Ar*C*H), 128.4 (Ar*C*H), 127.3 (Ar*C*H), 123.2 (q, J = 281.9 Hz, *C*F_3), 112.4 (d, J = 23.1 Hz, Ar*C*), 75.6 (q, J = 28.0 Hz, *C*(CF_3)OH), 38.9 (*C*H_2) ppm; **^{19}F NMR (376 MHz, $CDCl_3$)**: δ -80.48 (s), -113.39 (s) ppm; **$[\alpha]_D^{25}$** = +219.3 (c = 0.5, $CHCl_3$); **Chiral HPLC**: Chiralpak AS-H, 4.6 x 250 mm; 1% *i*PrOH/hexanes, 1.0 mL/min; t_R (minor) = 26.5 min, t_R (major) = 29.1min, 95:5 er.

(*S*)-1-(4-bromophenyl)-4,4,4-trifluoro-3-hydroxy-3-phenylbutan-1-one (104)

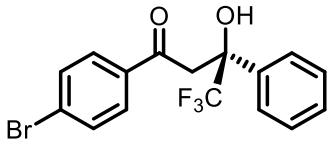

104 was prepared following General Procedure **D**, using 4-bromoacetophenone and 2,2,2-trifluoroacetophenone. Purification by silica gel chromatography (10% EtOAc in pentane) afforded the title compound as a colourless solid (68 mg, 90%, 96:4 er). Data is consistent with the published literature.[262]

^{1}H NMR (400 MHz, $CDCl_3$): δ 7.77 – 7.67 (m, 2H, Ar*H*), 7.60 – 7.54 (m, 2H, Ar*H*), 7.54 – 7.47 (m, 2H, Ar*H*), 7.33 – 7.24 (m, 3H, Ar*H*), 5.44 (s, 1H, O*H*), 3.92 (d, *J* = 17.3 Hz, 1H, CH_2), 3.54 (d, *J* = 17.3 Hz, 1H, CH_2) ppm; **^{13}C NMR (101 MHz, $CDCl_3$)**: δ 198.6 (*C*(O)), 135.6 (Ar*C*), 135.2 (Ar*C*), 133.8 (Ar*C*), 130.4 (Ar*C*H), 128.6 (Ar*C*H), 127.0 (Ar*C*H), 127.4 (Ar*C*H), 123.3 (q, J = 283.0 Hz, *C*F_3), 122.5, 75.1 (q, J = 29.0 Hz, *C*(CF_3)OH), 39.0 (*C*H_2) ppm; **^{19}F NMR (376 MHz, $CDCl_3$)**: δ -80.20 (s) ppm; **FT-IR (thin film)** ν_{max} 3467, 2970, 2160, 1977, 1682, 1587, 1379, 1153 cm^{-1}; **HRMS** (ESI) m/z calcd. for $C_{16}H_{13}O_2{}^{79}BrF_3$ ($[M+H]^+$) 373.00455, found 373.00467; **$[\alpha]_D{}^{25}$** = 295.7 (c = 1.0, $CHCl_3$); **Chiral HPLC**: Chiralpak OD-H, 4.6 x 250 mm; 2% *i*PrOH/hexanes, 1.0 mL/min; t_R (minor) = 22.6 min, t_R (major) = 25.8 min, 96:4 er; **m.p.**: 78 – 80 °C.

(*S*)-4,4,4-trifluoro-3-hydroxy-3-(3-iodophenyl)-1-phenylbutan-1-one (105)

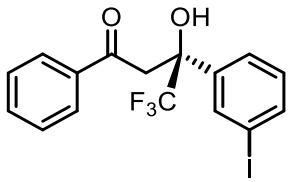

105 was prepared following General Procedure **D**, using acetophenone and 2,2,2-trifluoro-1-(3-iodophenyl)ethan-1-one. Purification by silica gel chromatography (5% acetone in pentane) afforded the title compound as a colourless oil (63 mg, 75%, 95:5 er).

^{1}H NMR (400 MHz, C_6D_6): δ 8.19 (q, *J* = 1.6 Hz, 1H, Ar*H*), 7.46 – 7.38 (m, 2H, Ar*H*), 7.38 – 7.28 (m, 2H, Ar*H*), 7.09 – 7.00 (m, 1H, Ar*H*), 6.94 – 6.86 (m, 2H, Ar*H*), 6.51 (t, *J* = 7.9 Hz, 1H, Ar*H*), 5.97 (s, 1H, O*H*), 3.35 (d, *J* = 17.2 Hz, 1H, C*H*$_2$), 3.18 (d, *J* = 17.2 Hz, 1H, C*H*$_2$) ppm; **^{13}C NMR (101 MHz, C_6D_6)**: δ 199.2 (*C*(O)), 140.5 (Ar*C*), 137.7 (Ar*C*H), 136.1 (Ar*C*), 135.5 (Ar*C*H), 133.8 (Ar*C*H), 129.9 (Ar*C*H), 128.5 (Ar*C*H), 128.0 (Ar*C*H), 125.5 (Ar*C*H), 124.8 (q, *J* = 285.3 Hz, *C*F$_3$), 94.4 (Ar*C*), 76.0 (q, *J* = 29.2 Hz, *C*(CF$_3$)OH), 39.5 (*C*H$_2$) ppm; **^{19}F NMR (376 MHz, C_6D_6)**: δ -80.01 (s) ppm; **FT-IR (thin film)** ν_{max} 3351, 2981, 2930, 2160, 2015, 1672, 1598, 1164, 1130 cm^{-}1; **HRMS** (ESI) m/z calcd. for $C_{16}H_{12}F_3IO_2$ ([M-H]) 418.9761, found 418.9764; **$[\alpha]_D^{25}$** = +52.1 (c = 0.5, $CHCl_3$); **Chiral HPLC**: Chiralpak IB, 4.6 x 250 mm; 1% *i*PrOH/hexanes, 1.0 mL/min; t_R (minor) = 13.4 min, t_R (major) = 25.5 min, 95:5 er; **$[\alpha]_D^{25}$** = +47.8 (c = 0.5, $CHCl_3$).

(*S*)-4,4,4-trifluoro-3-hydroxy-1-(4-nitrophenyl)-3-phenylbutan-1-one (106)

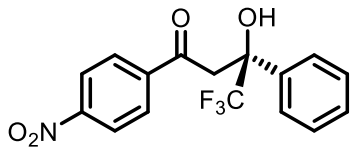

106 was prepared following General Procedure **D**, using 4-nitroacetophenone and 2,2,2-trifluoroacetophenone to afford the title compound as a colourless solid (63 mg, 93%, 90:10 er).

^{1}H NMR (400 MHz, $CDCl_3$): δ 8.32 (ddt, *J* = 9.1, 6.7, 2.3 Hz, 2H, Ar*H*), 8.16 – 8.04 (m, 2H, Ar*H*), 7.63 – 7.53 (m, 2H, Ar*H*), 7.42 – 7.31 (m, 3H, Ar*H*), 5.18 (s, 1H, O*H*), 4.07 (d, *J* = 17.5 Hz, 1H, CH_2), 3.73 (d, *J* = 17.4 Hz, 1H, CH_2) ppm; **^{13}C NMR (101 MHz, $CDCl_3$)**: δ 197. (*C*(O)), 150.98 (Ar*C*), 140.0 (Ar*C*), 137.1 (Ar*C*), 129.3 (Ar*C*H), 129. (Ar*C*H), 128.6 (Ar*C*H), 126.1 (Ar*C*H), 124.4 (q, J = 284.2 Hz, *C*F_3), 124.1 (Ar*C*H), 76.5 (q, J = 29.3 Hz, *C*(CF_3)OH), 41.3 (*C*H_2) ppm; **^{19}F NMR (376 MHz, $CDCl_3$)**: δ -80.15 (s) ppm; **FT-IR (thin film)** ν_{max} 3367, 2160, 1686, 1603, 1530, 1450, 1344, 1319, 1166 cm^{-1}; **HRMS** (ESI) m/z calcd. for $C_{16}H_{12}F_3NO_4$ ([M-H]$^-$) 338.06461, found 338.06454; **$[\alpha]_D^{25}$** = 262.6 (c = 1.0, $CHCl_3$); **Chiral HPLC**: Chiralpak IA, 4.6 x 250 mm; 10% *i*PrOH/hexanes, 1.0 mL/min; t_R (minor) = 23.9 min, t_R (major) = 26.6 min, 90:10 er; **m.p.**: 141 – 143 °C

(*S*)-4,4,4-trifluoro-3-hydroxy-1-phenyl-3-(4-vinylphenyl)butan-1-one (107)

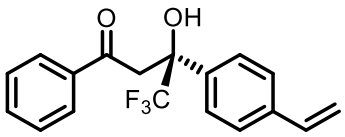

107 was prepared following General Procedure **D**, using acetophenone and **S26**. Purification by silica gel chromatography (5% CH_2Cl_2 and 5% Et_2O in pentane) afforded the title compound as a colourless solid (50 mg, 78%, 97:3 er).

^{1}H NMR (400 MHz, $CDCl_3$): δ 8.01 – 7.89 (m, 2H, Ar*H*), 7.64 (ddt, *J* = 8.7, 6.9, 1.3 Hz, 1H, Ar*H*), 7.60 – 7.53 (m, 2H, Ar*H*), 7.53 – 7.43 (m, 2H, Ar*H*), 7.43 – 7.34 (m, 2H, Ar*H*), 6.68 (dd, *J* = 17.6, 10.9 Hz, 1H, ArC*H*CH$_{cis}$H$_{trans}$), 5.75 (dd, *J* = 17.6, 0.9 Hz, 1H, ArCHCH$_{cis}$*H$_{trans}$*), 5.65 (s, 1H, O*H*), 5.26 (dd, *J* = 10.9, 0.9 Hz, 1H, ArCHC*H$_{cis}$*H$_{trans}$), 4.04 (d, *J* = 17.4 Hz, 1H, C*H*$_2$), 3.63 (d, *J* = 17.4 Hz, 1H, C*H*$_2$) ppm; **^{13}C NMR (101 MHz, $CDCl_3$)**: δ 199.6 (*C*(O)), 138.0 (Ar*C*), 137.0 (Ar*C*), 136.2 (*C*HCH$_2$), 136.0 (Ar*C*H), 134.4 (Ar*C*H), 128.9 (Ar*C*H), 128.2 (Ar*C*H), 126. (Ar*C*H), 126.2(Ar*C*H), 124.5 (q, J = 284.7 Hz, *C*F$_3$), 114.8 (CH*C*H$_2$), 76.4 (q, J = 29.1 Hz, *C*(CF$_3$)OH), 40. (*C*H$_2$) ppm; **^{19}F NMR (376 MHz, $CDCl_3$)**: δ -80.27 (s) ppm; **HRMS** (ESI) m/z calcd. for $C_{18}H_{15}O_2F_3{}^{23}Na$ ([M+Na]$^+$) 343.09164, found 343.09164; **$[\alpha]_D^{25}$** = 118.6 (c = 1.0, $CHCl_3$); **Chiral HPLC**: Chiralpak AD-H, 4.6 x 250 mm; 5% *i*PrOH/hexanes, 1.0 mL/min; t_R (minor) = 19.4 min, t_R (major) = 32.1 min, 97:3 er; **m.p.**: 224-226 °C; **FT-IR (thin film)** ν_{max} 3342, 2970, 1667, 1600, 1386, 1161, 756 cm^{-1}

(*S*)-4-(4,4,4-trifluoro-3-hydroxy-3-phenylbutanoyl)benzonitrile (108)

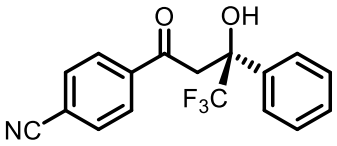

108 was prepared following General Procedure **D**, using 4-acetylbenzonitrile and 2,2,2-trifluoroacetophenone. Purification by silica gel chromatography (5% CH_2Cl_2 and 5% Et_2O in pentane) afforded the title compound as a colourless solid (53 mg, 83%, 90:10 er).

^{1}H NMR (400 MHz, $CDCl_3$): δ 8.07 – 7.92 (m, 2H, Ar*H*), 7.87 – 7.73 (m, 2H, Ar*H*), 7.66 – 7.48 (m, 2H, Ar*H*), 7.45 – 7.29 (m, 3H, Ar*H*), 5.22 (s, 1H, OH), 4.03 (d, *J* = 17.4 Hz, 1H, C*H*$_2$), 3.69 (d, *J* = 17.5 Hz, 1H, C*H*$_2$) ppm; **^{13}C NMR (101 MHz, $CDCl_3$)**: δ 198.1 (*C*(O)), 139.0 (Ar*C*), 137.1 (Ar*C*), 132.7 (Ar*C*H), 128.9 (Ar*C*H), 128.6 (Ar*C*H), 128.5 (Ar*C*H), 126. (Ar*C*H), 124.4 (q, J = 284.7 Hz, *C*F$_3$), 117.6 (*C*N), 117.5 (Ar*C*), 76.4 (q, J = 29.1 Hz, *C*(CF$_3$)OH), 41.07 (*C*H$_2$) ppm; **^{19}F NMR (376 MHz, $CDCl_3$)**: δ -80.17 (s) ppm; **FT-IR (thin film)** ν_{max} 3485, 2919, 2359, 2230, 2161, 1978, 1681, 1604, 1565, 1403, 1166 cm^{-1}; **HRMS** (ESI) m/z calcd. for $C_{17}H_{11}O_2NF_2$ ([M-H]$^-$) 318.07474, found 318.07452; **$[\alpha]_D^{25}$** = 272.6 (c = 1.0, $CHCl_3$); **Chiral HPLC**: Chiralpak IA, 4.6 x 250 mm; 10% *i*PrOH/hexanes, 1.0 mL/min; t_R (minor) = 21.4 min, t_R (major) = 25.9 min, 90:10 er; **m.p.**: 79 – 81 °C.

(*S*)-4,4,4-trifluoro-3-hydroxy-1-(4-(methylthio)phenyl)-3-phenylbutan-1-one (109)

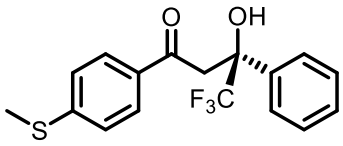

109 was prepared following General Procedure **D**, using 4-thiomethylacetophenone and 2,2,2-trifluoroacetophenone. Purification by silica gel chromatography (5% EtOAc in pentane) afforded the title compound as a colourless solid (55 mg, 81%, 96:4 er).

^{1}H NMR (400 MHz, $CDCl_3$): δ 7.88 – 7.78 (m, 2H, Ar*H*), 7.63 – 7.50 (m, 2H, Ar*H*), 7.39 – 7.30 (m, 3H, Ar*H*), 7.30 – 7.22 (m, 2H, Ar*H*), 5.83 (s, 1H, O*H*), 3.98 (d, *J* = 17.2 Hz, 1H, CH_2), 3.58 (d, *J* = 17.1 Hz, 1H, CH_2), 2.52 (s, 3H, SCH_3) ppm; **^{13}C NMR (101 MHz, $CDCl_3$)**: δ 198.5 (*C*(O)), 148.2 (Ar*C*), 137.7 (Ar*C*), 132.4 (Ar*C*), 128.7 (Ar*C*H), 128.6 (Ar*C*H), 128.4 (Ar*C*H), 126.3 (Ar*C*H), 124.6 (q, J = 284.6 Hz, *C*F_3), 125.0 (Ar*C*H), 76.4 (q, J = 29.0 Hz, *C*(CF_3)OH), 39.8 (*C*H_2), 14.6 (S*C*H_3) ppm; **^{19}F NMR (376 MHz, $CDCl_3$)**: δ -80.20 ppm; **HRMS** (ESI) m/z calcd. for $C_{17}H_{16}O_2F_3{}^{32}S$ ($[M+H]^+$) 341.08176, found 341.08188; **$[\alpha]_D{}^{25}$** = 42.6 (c = 0.5, $CHCl_3$); **Chiral HPLC**: Chiralpak AD-H, 4.6 x 250 mm; 5% *i*PrOH/hexanes, 1.0 mL/min; t_R (minor) = 22.5 min, t_R (major) = 30.2 min, 95:5 er; **FT-IR (thin film)** ν_{max} 2916, 2848, 1665, 1588, 1556, 1165, 1094 cm^{-1}.

(*S*)-1-([1,1'-biphenyl]-4-yl)-4,4,4-trifluoro-3-hydroxy-3-phenylbutan-1-one (110)

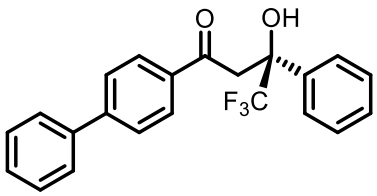

110 was prepared following General Procedure **D**, using 4-acetylbiphenyl and 2,2,2-trifluoroacetophenone. Purification by silica gel chromatography (10% CH_2Cl_2 in pentane) afforded the title compound as a colourless solid (44 mg, 60%, 96:4 er).[262]

^{1}H NMR (400 MHz, $CDCl_3$): δ 8.07 – 7.96 (m, 2H, Ar*H*), 7.76 – 7.67 (m, 2H, Ar*H*), 7.67 – 7.60 (m, 4H, Ar*H*), 7.53 – 7.30 (m, 6H, Ar*H*), 5.74 (s, 1H, O*H*), 4.07 (d, *J* = 17.3 Hz, 1H, CH_2), 3.68 (d, *J* = 17.2 Hz, 1H, CH_2) ppm; **^{13}C NMR (101 MHz, $CDCl_3$)**: δ 199.1 (*C*(O)), 147.1 (Ar*C*), 139.4 (Ar*C*), 137.7 (Ar*C*), 134.9 (Ar*C*), 129.0 (Ar*C*H), 128.8 (Ar*C*H), 128.7 (Ar*C*H), 128.6 (Ar*C*H), 128.4 (Ar*C*H), 127.5 (Ar*C*H), 127.3 (Ar*C*H), 126.3 (Ar*C*H), 124.5 (q, J = 284.7 Hz, *C*F_3), 76.3 (q, J = 29.0 Hz, *C*(CF_3)OH), 40.2 (*C*H_2) ppm; **^{19}F NMR (376 MHz, $CDCl_3$)**: δ -80.19 (s) ppm; **FT-IR (thin film)** ν_{max} 3355, 2971, 1667, 1602, 1466, 1406, 1380, 1342, 1305, 1161, 1128, 949 cm^{-1}; **HRMS** (ESI) m/z calcd. for $C_{22}H_{18}O_2F_3$ ($[M+H]^+$) 371.12534, found 371.12527; **$[\alpha]_D^{25}$** = 94.0 (c = 0.5, $CHCl_3$); **Chiral HPLC**: Chiralpak AD-H, 4.6 x 250 mm; 5% *i*PrOH/hexanes, 1.0 mL/min; t_R (minor) = 25.2 min, t_R (major) = 32.7 min, 96:4 er.

(*S*)-4,4,4-trifluoro-3-hydroxy-3-phenyl-1-(m-tolyl)butan-1-one (111)

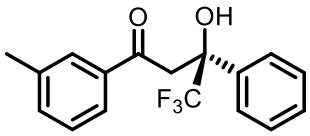

111 was prepared following General Procedure **D**, using 3-methylacetophenone and 2,2,2-trifluoroacetophenone to afford the title compound as a colourless solid (52 mg, 85%, 95:5 er). Data is consistent with the published literature.[168]

^{1}H NMR (400 MHz, $CDCl_3$): δ 7.65 (dd, *J* = 7.6, 1.4 Hz, 2H, Ar*H*), 7.58 – 7.46 (m, 2H, Ar*H*), 7.41 – 7.17 (m, 5H, Ar*H*), 5.65 (s, 1H, O*H*), 3.94 (d, *J* = 17.4 Hz, 1H, CH_2), 3.55 (d, *J* = 17.4 Hz, 1H, CH_2), 2.33 (s, 3H, ArCH_3) ppm; **^{13}C NMR (101 MHz, $CDCl_3$)**: δ 199.8 (*C*(O)), 138.8 (Ar*C*), 137.7 (Ar*C*), 136.3 (Ar*C*), 135.2 (Ar*C*H), 128.8 (Ar*C*H), 128.7 (Ar*C*H), 128.6 (Ar*C*H), 128.4 (Ar*C*H), 126.32 (Ar*C*H), 125.5 (Ar*C*H), 124.1 (q, J = 285.6 Hz, *C*F_3), 76.4 (q, J = 29.1 Hz, *C*(CF_3)OH), 40.2 (*C*H_2), 21.3 (Ar*C*H_3) ppm: **^{19}F NMR (376 MHz, $CDCl_3$)**: δ -80.19 (s) ppm; **HRMS** (ESI) m/z calcd. for $C_{17}H_6O_2F_3$ ([M-H]$^-$) 309.10969, found 309.10977; **$[\alpha]_D^{25}$** = +34.6 (c = 1.0, $CHCl_3$); **Chiral HPLC**: Chiralpak IA, 4.6 x 250 mm; 5% *i*PrOH/hexanes, 1.0 mL/min; t_R (minor) = 8.9 min, t_R (major) = 10.7 min, 95:5 er.

(*S*)-4,4,4-trifluoro-3-hydroxy-1-(3-methoxyphenyl)-3-phenylbutan-1-one (112)

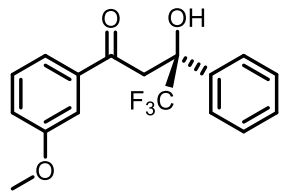

112 was prepared following General Procedure **D**, using 3-methoxyacetophenone and 2,2,2-trifluoroacetophenone to afford the title compound as a colourless oil (42 mg, 65%, 95:5 er).

^{1}H NMR (400 MHz, $CDCl_3$): δ 7.67 – 7.58 (m, 2H, Ar*H*), 7.55 (ddd, *J* = 7.7, 1.7, 1.0 Hz, 1H, Ar*H*), 7.46 – 7.31 (m, 5H, Ar*H*), 7.18 (ddd, *J* = 8.2, 2.6, 0.9 Hz, 1H, Ar*H*), 5.67 (s, 1H, O*H*), 4.04 (d, *J* = 17.3 Hz, 1H, CH_2), 3.83 (s, 3H, OCH_3), 3.65 (d, *J* = 17.4 Hz, 1H, CH_2) ppm; **^{13}C NMR (101 MHz, $CDCl_3$)**: δ 199.5 (*C*(O)), 160.0 (Ar*C*), 137.7 (Ar*C*), 137.6 (Ar*C*), 129.9 (Ar*C*H), 128.7 (Ar*C*H), 128.46 (Ar*C*H), 126.3 (Ar*C*H), 124.6 (q, J = 248.8 Hz, *C*F_3), 120.8 (Ar*C*H), 112.4 (Ar*C*H), 55.4 (O*C*H_3), 40.3 (*C*H_2) ppm; **^{19}F NMR (376 MHz, $CDCl_3$)**: δ -80.18 (s) ppm; **HRMS** (ESI) m/z calcd. for $C_{17}H_{15}O_3F_3{}^{23}Na$ ([M+Na]$^+$) 347.08655, found 347.08649; **$[\alpha]_D{}^{25}$** = 39.0 (c = 0.5, $CHCl_3$); **Chiral HPLC**: Chiralpak IA, 4.6 x 250 mm; 3% *i*PrOH/hexanes, 1.0 mL/min; t_R (minor) = 14.2 min, t_R (major) = 20.5 min, 95:5 er.

(*S*)-4,4,4-trifluoro-1-(2-fluorophenyl)-3-hydroxy-3-phenylbutan-1-one (113)

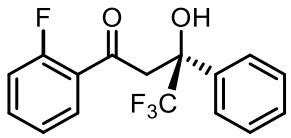

113 was prepared following General Procedure **D**, using 2-fluoroacetophenone and 2,2,2-trifluoroacetophenone. Purification by silica gel chromatography (3% acetone in pentane) afforded the title compound as a colourless oil (55 mg, 88%, 96:4 er). Data is consistent with the published literature.[168]

^{1}H NMR (400 MHz, $CDCl_3$): δ 7.63 (td, *J* = 7.6, 1.9 Hz, 1H, Ar*H*), 7.56 – 7.46 (m, 3H, Ar*H*), 7.32 – 7.22 (m, 3H, Ar*H*), 7.19 – 7.06 (m, 2H, Ar*H*), 5.28 (s, 1H, O*H*), 3.99 (dd, *J* = 18.1, 2.0 Hz, 1H, CH_2), 3.64 (dd, *J* = 18.1, 2.0 Hz, 1H, CH_2) ppm; **^{13}C NMR (101 MHz, $CDCl_3$)**: δ 197.9 (d, *J* = 3.9 Hz, *C*(O)), 162.0 (d, *J* = 255.5 Hz, Ar*C*F), 137.6 (Ar*C*), 135.9 (d, *J* = 9.5 Hz, Ar*C*H), 130.5 (d, *J* = 2.3 Hz, Ar*C*H), 128.7 (Ar*C*H), 128.4 (Ar*C*H), 126.3 (Ar*C*H), 125.1 (d, *J* = 11.3 Hz, Ar*C*), 124.8 (q, *J* = 284.5 Hz, *C*F_3), 124.8 (d, *J* = 3.2 Hz, Ar*C*H), 116.9 (d, *J* = 23.3 Hz, Ar*C*H), 76.7 (q, *J* = 29.0 Hz, *C*(CF_3)OH), 45. (d, *J* = 8.8 Hz, *C*H_2) ppm; **^{19}F NMR (376 MHz, $CDCl_3$)**: δ -80.32 (s, C(OH)*C*F_3), 107.97 – -109.69 (m, ArC*F*) ppm; **$[\alpha]_D^{25}$** = +94 (c = 2.5, $CHCl_3$); **Chiral HPLC**: Chiralpak IA, 4.6 x 250 mm; 5% *i*PrOH/hexanes, 1.0 mL/min; t_R (minor) = 8.3 min, t_R (major) = 9.9 min, 96:4 er.

Methyl (*S*)-2-methyl-4-(4,4,4-trifluoro-3-hydroxy-3-phenylbutanoyl)benzoate (114)

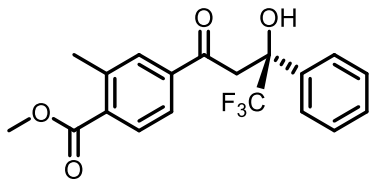

114 was prepared following General Procedure **D**, using methyl 4-acetyl-2-methylbenzoate and 2,2,2-trifluoroacetophenone. Purification by silica gel chromatography (5% acetone in pentane) afforded the title compound as a pale-yellow oil (61 mg, 83%, 95:5 er).

^{1}H NMR (400 MHz, C_6D_6): δ 7.75 (d, *J* = 8.1 Hz, 1H, Ar*H*), 7.62 – 7.54 (m, 2H, Ar*H*), 7.43 (dt, *J* = 2.0, 0.6 Hz, 1H, Ar*H*), 7.26 (ddd, *J* = 8.2, 1.9, 0.7 Hz, 1H, Ar*H*), 7.10 – 7.04 (m, 2H, Ar*H*), 7.04 – 6.98 (m, 1H, Ar*H*), 5.79 (s, 1H, Ar*H*), 3.62 (d, *J* = 17.3 Hz, 1H, CH_2), 3.44 (s, 3H, OCH_3), 3.30 (d, *J* = 17.3 Hz, 1H, CH_2), 2.38 (s, 3H, ArCH_3) ppm; **^{19}F NMR (376 MHz, C_6D_6)**: δ -79.72 (s) ppm; **^{13}C NMR (101 MHz, C_6D_6)**: δ 199.0 (*C*(O)CH$_2$), 166.3 (*C*(O)OCH$_3$), 140.4 (Ar*C*), 138.2 (Ar*C*), 137.9 (Ar*C*), 134.5 (Ar*C*), 130.9 (Ar*C*H), 130.4 (Ar*C*H), 128.5 (Ar*C*H), 128.3 (Ar*C*H), 126.3 (Ar*C*H), 125.18 (Ar*C*H), 125.1 (q, *J* = 284.9 Hz, *C*F$_3$), 76.5 (q, *J* = 28.9 Hz, *C*(CF$_3$)OH), 51.3 (C(O)O*C*H$_3$), 40.3 (*C*H$_2$), 21.1 (Ar*C*H$_3$) ppm; **FT-IR (thin film)** ν_{max} 3490, 2360, 2160, 1722, 1676, 1435, 1260, 1236, 1162, 1085 cm^{-1}; **HRMS** (ESI) m/z calcd. for $C_{19}H_{18}F_3O_4$ ([M+H]$^+$) 367.11517, found 367.11560; **$[\alpha]_D^{25}$** = +64.7 (c = 2.0, $CHCl_3$); **Chiral HPLC**: Chiralpak AD-H, 4.6 x 250 mm; 2% *i*PrOH/hexanes, 1.0 mL/min; t_R (minor) = 20.6 min, t_R (major) = 32.2 min, 95:5 er.

(*S*)-1-(4-bromophenyl)-4,4,4-trifluoro-3-hydroxy-3-(4-methyl-3-(trifluoromethyl)phenyl)butan-1-one (115)

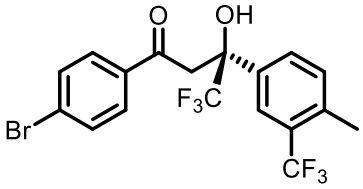

115 was prepared following General Procedure **D**, using 4-bromoacetophenone and 2,2,2-trifluoro-1-(4-methyl-3-(trifluoromethyl)phenyl)ethan-1-one. Purification by silica gel chromatography (5% acetone in pentane) afforded the title compound as a colourless oil (67 mg, 74%, 92:8 er).

^{1}H NMR (400 MHz, C_6D_6): δ 8.10 – 8.00 (m, 1H, Ar*H*), 7.47 (dd, *J* = 8.1, 1.9 Hz, 1H, Ar*H*), 7.05 (d, *J* = 0.8 Hz, 4H, Ar*H*), 6.72 (d, *J* = 8.1 Hz, 1H, Ar*H*), 5.78 (s, 1H, O*H*), 3.35 (d, *J* = 17.3 Hz, 1H, C*H*$_2$), 3.08 (d, *J* = 17.3 Hz, 1H, C*H*$_2$), 2.11 (q, *J* = 1.9 Hz, 3H, ArC*H*$_3$) ppm; **^{13}C NMR (101 MHz, $CDCl_3$)**: δ 198.1 (*C*(O)), 137.4 (Ar*C*), 136.0 (Ar*C*), 134.5 (Ar*C*), 132.2 (Ar*C*H), 131.8 (Ar*C*H), 129.6 (Ar*C*H), 129.4 (Ar*C*), 129.4 (Ar*C*H), 128.9 (q, *J* = 30.2 Hz, Ar*C*CF$_3$), 124.7 (q, *J* = 284.3 Hz, *C*F$_3$), 123.6 (q, *J* = 5.9 Hz, Ar*C*), 76.1 (q, *J* = 29.4 Hz, *C*(CF$_3$)OH), 39.4 (*C*H$_2$), 18.4 (Ar*C*H$_3$) ppm; **^{19}F NMR (376 MHz, C_6D_6)**: δ -79.90 (s, C(OH)C*F*$_3$), -61.55 (s, ArC*F*$_3$) ppm; **FT-IR (thin film)** ν_{max} 3361, 2980, 1672, 1402, 1159 cm^{-1}; **HRMS** (ESI) m/z calcd. for $C_{18}H_{13}F_6O_2Br^{79}$ ([M-H]$^-$) 452.9933, found 452.9933; **$[\alpha]_D^{25}$** = +81.3 (c = 1.0, $CHCl_3$); **Chiral HPLC**: Chiralpak AD, 4.6 x 250 mm; 2% to 30% gradient *i*PrOH/hexanes, 1.0 mL/min; t_R (minor) = 10.5 min, t_R (major) = 12.5 min, 92:8 er.

(*S*)-4,4,4-trifluoro-3-hydroxy-1-(naphthalen-2-yl)-3-phenylbutan-1-one (116)

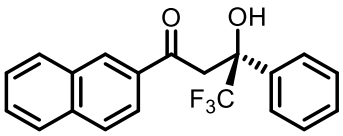

116 was prepared following General Procedure **D**, using 2-acetylnaphthalene and 2,2,2-trifluoroacetophenone. Purification by silica gel chromatography (5% EtOAc in pentane) afforded the title compound as a colourless solid (60 mg, 88%, 93.5:6.5 er). Data is consistent with the published literature.[168]

^{1}H NMR (400 MHz, $CDCl_3$): δ 8.53 – 8.43 (m, 1H, Ar*H*), 8.07 – 7.94 (m, 1H, Ar*H*), 7.94 – 7.81 (m, 3H, Ar*H*), 7.71 – 7.51 (m, 4H, Ar*H*), 7.42 – 7.29 (m, 3H, Ar*H*), 5.76 (s, 1H, O*H*), 4.20 (d, *J* = 17.2 Hz, 1H, CH_2), 3.77 (d, *J* = 17.2 Hz, 1H, CH_2) ppm; **^{13}C NMR (101 MHz, $CDCl_3$)**: δ 199.6 (*C*(O)), 137.7 (Ar*C*), 136.2 (Ar*C*), 133.3 (Ar*C*), 132.2 (Ar*C*), 130.8 (Ar*C*H), 130.0 (Ar*C*H), 129.6 (Ar*C*H), 128.9 (Ar*C*H), 128.8 (Ar*C*H), 128.5 (Ar*C*H), 127.9 (Ar*C*H), 127.25 (Ar*C*H), 126.4 (Ar*C*H), 124.9 (q, J = 283.0 Hz, *C*F_3), 123.2 (Ar*C*), 76.7 (q, J = 28.4 Hz, *C*(CF_3)OH), 40.4 (*C*H_2) ppm; **^{19}F NMR (376 MHz, $CDCl_3$)**: δ -80.15 (s) ppm; **HRMS** (ESI) m/z calcd. for $C_{20}H_{16}O_2F_3$ ([M+H]$^+$) 345.10969, found 345.10965; **$[\alpha]_D^{25}$** = 273.5 (c = 1.0, $CHCl_3$); **Chiral HPLC**: Chiralpak IA, 4.6 x 250 mm; 5% *i*PrOH/hexanes, 1.0 mL/min; t_R (minor) = 13.9 min, t_R (major) = 22.3 min, 93:7 er.

(*S*)-1-(4-bromophenyl)-4,4,4-trifluoro-3-hydroxy-3-(6-methoxynaphthalen-2-yl)butan-1-one (117)

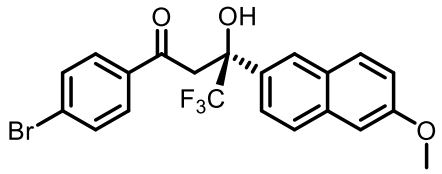

117 was prepared following General Procedure **D**, using 4-bromoacetophenone and **S28.** Purification by silica gel chromatography (5% CH_2Cl_2 and 5% EtOAc in pentane) afforded the title compound as a colourless solid (72 mg, 80%, 96:4 er).

^{1}H NMR (400 MHz, $CDCl_3$): δ 7.93 (d, *J* = 1.9 Hz, 1H, Ar*H*), 7.76 – 7.68 (m, 2H, Ar*H*), 7.65 (dd, *J* = 8.8, 3.3 Hz, 2H, Ar*H*), 7.59 – 7.50 (m, 3H, Ar*H*), 7.08 (dd, *J* = 8.9, 2.5 Hz, 1H, Ar*H*), 7.02 (d, *J* = 2.5 Hz, 1H, Ar*H*), 5.57 (s, 1H, O*H*), 4.01 (d, *J* = 17.3 Hz, 1H, CH_2), 3.83 (s, 3H, OCH_3), 3.60 (d, *J* = 17.3 Hz, 1H, CH_2) ppm; **^{13}C NMR (101 MHz, $CDCl_3$)**: δ 198.6 (*C*(O)), 158. (Ar*C*), 135.02 (Ar*C*), 134.4 (Ar*C*), 132.4 (Ar*C*), 132.3 (Ar*C*H), 129.9 (Ar*C*H), 129.9 (Ar*C*), 129.6 (Ar*C*H), 128.3 (Ar*C*), 127.1 (Ar*C*H), 125.9 (Ar*C*H), 124.2 (q, J = 284.5 Hz, *C*F_3), 123.9 (Ar*C*H), 119.4 (Ar*C*H), 105.4 (Ar*C*H), 76.7, 76.6 (q, J = 28.6 Hz, *C*(CF_3)OH), 55.36 (OCH_3), 40.3 (*C*H_2) ppm; **^{19}F NMR (376 MHz, $CDCl_3$)**: δ -80.02 (s) ppm; **FT-IR (thin film)** ν_{max} 3320, 2963, 2935, 2161, 2031, 1585, 1296, 1121 cm^{-1}; **HRMS** (ESI) m/z calcd. for $C_{21}H_{16}O_3{}^{79}BrF_3{}^{23}Na$ ($[M+Na]^+$) 475.01271, found 475.01282; **$[\alpha]_D{}^{25}$** = 232.6 (c = 1.0, $CHCl_3$); **Chiral HPLC**: Chiralpak IA, 4.6 x 250 mm; 3% *i*PrOH/hexanes, 1.0 mL/min; t_R (minor) = 41.2 min, t_R (major) = 56.2 min, 96:4 er; **m.p.**: 100 – 102 °C.

(S)-3-(benzo[d][1,3]dioxol-5-yl)-4,4,4-trifluoro-3-hydroxy-1-phenylbutan-1-one (118)

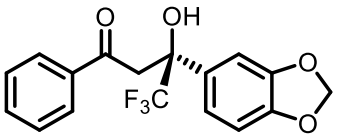

118 was prepared following General Procedure **D**, using acetophenone and **S27** to afford the title compound as a pale yellow oil (43 mg, 64%, 97:3 er).

^{1}H NMR (400 MHz, C_6D_6): δ 7.54 – 7.41 (m, 2H, Ar*H*), 7.26 (d, *J* = 1.9 Hz, 1H, Ar*H*), 7.12 – 7.01 (m, 1H, Ar*H*), 6.93 (m, 3H, Ar*H*), 6.47 (d, *J* = 8.2 Hz, 1H, Ar*H*), 5.91 (s, 1H, O*H*), 5.17 (m, 2H, OCH_2O), 3.59 (d, *J* = 17.3 Hz, 1H, CH_2), 3.20 (d, *J* = 17.3 Hz, 1H, CH_2) ppm; **^{13}C NMR (101 MHz, C_6D_6)**: δ 199.4 (*C*(O)), 148.1 (Ar*C*), 148.0 (Ar*C*), 136.2 (Ar*C*), 133.6 (Ar*C*H), 131.8 (Ar*C*), 128.4 (Ar*C*H), 128.0 (Ar*C*H), 125.0 (q, *J* = 284.7 Hz, *C*F_3), 120.1 (Ar*C*H), 107.8 (Ar*C*H), 107.3 (Ar*C*H), 100.9 (O*C*H_2O), 76.4 (q, *J* = 28.8 Hz, C*C*F_3), 39.8 (*C*H_2) ppm; **^{19}F NMR (376 MHz, C_6D_6)**: δ -80.07 (s) ppm; **HRMS** (ESI) m/z calcd. for $C_{17}H_{14}O_4F_3$ ($[M+H]^+$) 339.08387, found 339.08398; **FT-IR (thin film)** ν_{max} 3446, 2921, 2160, 1976, 1702, 1504, 1449, 1347, 1241, 1162 cm^{-1}; **$[\alpha]_D^{25}$** = +67.7 (c = 1.5, $CHCl_3$); **Chiral HPLC**: Chiralpak OD-H, 4.6 x 250 mm; 3% *i*PrOH/hexanes, 1.0 mL/min; t_R (minor) = 25.0 min, t_R (major) = 27.0 min, 97:3 er.

(3*S*,3'*S*)-1,1'-(1,4-phenylene)bis(4,4,4-trifluoro-3-hydroxy-3-phenylbutan-1-one) (120)

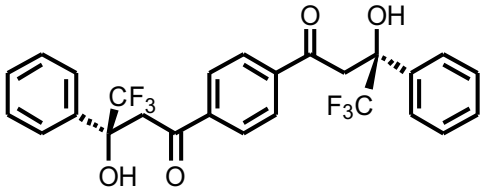

120 was prepared following General Procedure **D**, using 1,4-diacetylbenzene and 2,2,2-trifluoroacetophenone (3.0 eq). Purification by silica gel chromatography (5% acetone to 25% acetone in pentane) afforded the title compound as a colourless powder (87 mg, 80%), crude 20:1 dr, 95:5 er (major diastereomer).

^{1}H NMR (400 MHz, acetone-d_6): δ 8.17 (s, 4H, Ar*H*), 7.75 (dd, *J* = 7.6, 2.0 Hz, 4H, Ar*H*), 7.48 – 7.29 (m, 5H, Ar*H*), 5.79 (s, 2H, O*H*), 4.42 (d, *J* = 17.5 Hz, 2H, CH_2), 3.94 (d, *J* = 17.6 Hz, 2H, CH_2) ppm; **^{13}C NMR (101 MHz, acetone-d_6)**: δ 197.7 (*C*(O)), 140.4 (Ar*C*), 138.0 (Ar*C*), 128.5 (Ar*C*H), 128.3 (Ar*C*H), 128.0 (Ar*C*H), 126. (Ar*C*H), 125.1(q, *J* = 284.8 Hz, *C*F_3), 76.2 (q, *J* = 28.3 Hz, *C*(CF_3)OH), 41.3 (*C*H_2) ppm; **^{19}F NMR (376 MHz, acetone-d_6)**: δ -80.72 (s) ppm; **FT-IR (thin film)** ν_{max} 3514, 1701, 1674, 1401, 1246, 1154, 1134, 1024 cm^{-1}; **HRMS** (ESI) m/z calcd. for $C_{26}H_{19}F_6O_4$ ($[M-H]^-$) 509.11930, found 509.11983; **$[\alpha]_D^{25}$** = +64.8 (c = 1.0, $CHCl_3$); **Chiral HPLC**: Chiralpak IB, 4.6 x 250 mm; gradient 0.5% to 30% *i*PrOH/hexanes over 60 minutes, 1.0 mL/min; t_R (major diastereomer, minor enantiomer) = 39.0 min, t_R (major diastereomer, major enantiomer) = 51.3 min, 95:5 er (major diastereomer).

(*S*)-4,4,4-trifluoro-3-hydroxy-3-phenyl-1-(quinolin-6-yl)butan-1-one (121)

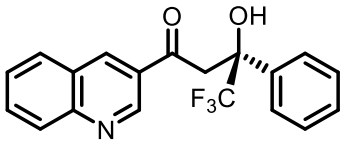

121 was prepared following General Procedure **D**, using 3-acetylquinoline and 2,2,2-trifluoroacetophenone. Purification by silica gel chromatography (5% EtOAc in pentane) afforded the title compound as a colourless solid (61 mg, 89%, 97:3 er).

^{1}H NMR (400 MHz, $CDCl_3$): δ 9.34 (d, *J* = 2.3 Hz, 1H, Ar*H*), 8.71 (d, *J* = 2.2 Hz, 1H, Ar*H*), 8.16 (dd, *J* = 8.5, 1.1 Hz, 1H, Ar*H*), 7.97 (dd, *J* = 8.2, 1.3 Hz, 1H, Ar*H*), 7.88 (ddd, *J* = 8.5, 6.9, 1.5 Hz, 1H, Ar*H*), 7.73 – 7.60 (m, 3H, Ar*H*), 7.42 – 7.29 (m, 3H, Ar*H*), 5.53 (s, 1H, O*H*), 4.16 (d, *J* = 17.1 Hz, 1H, CH_2), 3.78 (d, *J* = 17.1 Hz, 1H, CH_2) ppm; **^{13}C NMR (101 MHz, $CDCl_3$)**: δ 198.3, (*C*(O)), 150.2 (Ar*C*), 148.4 (Ar*C*H), 137.7 (Ar*C*H), 137.3 (Ar*C*), 132.8 (Ar*C*H), 129.6 (Ar*C*), 129.5 (Ar*C*H), 128.8 (Ar*C*H), 128.5 (Ar*C*H), 128.0 (Ar*C*H), 126.5 (Ar*C*), 126.2 (Ar*C*H), 124.6 (q, J = 284.7 Hz, *C*F_3), 76.5 (q, J = 29.4 Hz, *C*(CF_3)OH), 40.8 (*C*H_2) ppm; **^{19}F NMR (376 MHz, $CDCl_3$)**: δ -80.07 (s) ppm; **FT-IR (thin film)** ν_{max} 3062, 2539, 1667, 1602, 1466, 1406, 1380, 1342, 1305, 1161, 1128, 949 cm^{-1}; **HRMS** (ESI) m/z calcd. for $C_{19}H_{14}F_3NO_2$ ($[M+H]^+$) 346.10494, found 346.10491; **$[\alpha]_D^{25}$** = +237.6 (c = 1.0, $CHCl_3$); **Chiral HPLC**: Chiralpak IA, 4.6 x 250 mm; 15% *i*PrOH/hexanes, 1.0 mL/min; t_R (minor) = 17.3 min, t_R (major) = 15.5 min, 93:7 er; **m.p.**: 104 – 106 °C.

(*S*)-4,4,4-trifluoro-3-hydroxy-3-phenyl-1-(pyrazin-2-yl)butan-1-one (122)

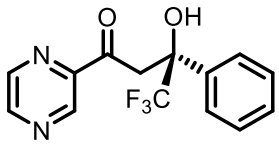

122 was prepared following General Procedure **D**, using acetylpyrazine and 2,2,2-trifluoroacetophenone. Purification by silica gel chromatography (20% EtOAc in pentane) afforded the title compound as a colourless oil (52 mg, 88%, 92:8 er).

^{1}H NMR (400 MHz, $CDCl_3$): δ 9.09 (d, *J* = 1.5 Hz, 1H, Ar*H*), 8.77 (d, *J* = 2.5 Hz, 1H, Ar*H*), 8.63 (dd, *J* = 2.5, 1.5 Hz, 1H, Ar*H*), 7.60 – 7.46 (m, 2H, Ar*H*), 7.35 – 7.21 (m, 3H, Ar*H*), 5.66 (s, 1H, O*H*), 4.28 (d, *J* = 16.8 Hz, 1H, CH_2), 3.73 (d, *J* = 16.8 Hz, 1H, CH_2) ppm; **^{13}C NMR (101 MHz, $CDCl_3$)**: δ 199.4 (*C*(O)), 148.4 (Ar*C*H), 146.4 (Ar*C*), 144.2 (Ar*C*H), 143.2 (Ar*C*H), 137.0 (Ar*C*), 128.8 (Ar*C*H), 128.3 (Ar*C*H), 126.5 (Ar*C*H), 124.5 (q, J = 285.1 Hz, *C*F_3), 76.3 (q, J = 29.1 Hz, *C*(CF_3)OH), 41.5 (*C*H_2); **^{19}F NMR (376 MHz, $CDCl_3$)**: δ -80.39 (s) ppm; **HRMS** (ESI) m/z calcd. for $C_{14}H_{12}O_2N_2F_3$ ([M+H]$^+$) 297.08454, found 297.08447; **FT-IR (thin film)** ν_{max} 3447, 2160, 1697, 1573, 1406, 1241, 1155 cm^{-1}; **$[\alpha]_D^{25}$** = 100.9 (c = 1.0, $CHCl_3$); **Chiral HPLC**: Chiralpak IA, 4.6 x 250 mm; 1% *i*PrOH/hexanes, 1.0 mL/min; t_R (minor) = 18.2 min, t_R (major) = 24.1 min, 92:8 er.

(*S*)-4,4,4-trifluoro-3-hydroxy-1-(6-methoxypyridin-3-yl)-3-phenylbutan-1-one (123)

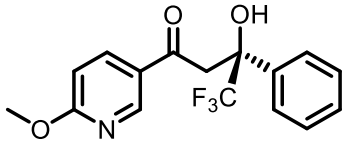

123 was prepared following General Procedure **D**, using 1-(6-methoxypyridin-3-yl)ethan-1-one and 2,2,2-trifluoroacetophenone. Purification by silica gel chromatography (5% acetone in pentane) afforded the title compound as a colourless oil (61 mg, 93%, 96:4 er).

^{1}H NMR (400 MHz, C_6D_6): δ 8.74 (dd, *J* = 2.6, 0.7 Hz, 1H, Ar*H*), 7.98 (dd, *J* = 8.8, 2.5 Hz, 1H, Ar*H*), 7.59 – 7.48 (m, 2H, Ar*H*), 7.37 – 7.20 (m, 3H, Ar*H*), 6.72 (dd, *J* = 8.8, 0.7 Hz, 1H, Ar*H*), 5.59 (s, 1H, O*H*), 3.95 (s, 3H), 3.85 (d, *J* = 17.0 Hz, 1H, CH_2), 3.50 (d, *J* = 17.0 Hz, 1H, CH_2) ppm; **^{13}C NMR (101 MHz, C_6D_6)**: δ 197.1 (*C*(O)), 167.2 (Ar*C*), 149.5 (Ar*C*H), 138.0 (Ar*C*), 137.6 (Ar*C*H), 128.4 (Ar*C*H), 128.2 (Ar*C*H), 126.3 (Ar*C*H), 126.1 (Ar*C*), 125.1 (d, *J* = 285.1 Hz, *C*F_3), 110.9 (Ar*C*H), 76.5 (d, *J* = 29.0 Hz, *C*(CF_3)OH), 53.5 (OCH_3), 39.4 (*C*H_2) ppm; **^{19}F NMR (376 MHz, C_6D_6)**: δ -80.16 (s) ppm; **FT-IR (thin film)** ν_{max} 3420, 2954, 2360, 2160, 1665, 1601, 1561, 1497, 1374, 1163, 1019 cm^{-1}; **HRMS** (ESI) m/z calcd. for $C_{16}H_{15}F_3NO_2$ ($[M+H]^+$) 326.0999, found 326.0998; **$[\alpha]_D^{25}$** = +133.0 (c = 2.0, $CHCl_3$); **Chiral HPLC**: Chiralpak IB, 4.6 x 250 mm; 2% *i*PrOH/hexanes, 1.0 mL/min; t_R (minor) = 14.8 min, t_R (major) = 32.6 min, 96:4 er.

(*S*)-4,4,4-trifluoro-3-hydroxy-3-phenyl-1-(thiazol-2-yl)butan-1-one (124)

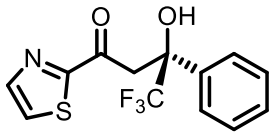

124 was prepared following General Procedure **D**, using 2-acetylthiazole and 2,2,2-trifluoroacetophenone. Purification by silica gel chromatography (5% acetone in pentane) afforded the title compound as a colourless oil (59 mg, 98%, 93:7 er).

^{1}H NMR (400 MHz, C_6D_6): δ 7.78 (ddd, *J* = 8.1, 1.8, 1.0 Hz, 2H, Ar*H*), 7.29 (d, *J* = 3.0 Hz, 1H, Ar*H*), 7.14 – 7.06 (m, 2H, Ar*H*), 7.06 – 6.98 (m, 1H, Ar*H*), 6.57 (s, 1H, O*H*), 6.46 (d, *J* = 3.0 Hz, 1H, Ar*H*), 4.03 (d, *J* = 15.9 Hz, 1H, CH_2), 3.73 (d, *J* = 16.0 Hz, 1H, CH_2) ppm; **^{13}C NMR (101 MHz, C_6D_6)**: δ 190.7 (*C*(O)), 166.5 (Ar*C*H), 144.0 (Ar*C*H), 137.4 (Ar*C*H), 128.6 (Ar*C*H), 128.2 (Ar*C*H), 126.9 (Ar*C*H), 125.3 (d, *J* = 285.4 Hz, *C*F_3), 123.9, 121.1, 76.1 (q, *J* = 29.2 Hz, *C*(CF_3)OH), 43.7 (*C*H_2) ppm; **^{19}F NMR (376 MHz, C_6D_6)**: δ -79.93 (s) ppm; **FT-IR (thin film)** ν_{max} 3118, 2360, 1680, 1450, 1240, 1154 cm^{-1}; **HRMS** (ESI) m/z calcd. for $C_{13}H_{11}F_3O_2NS$ ($[M+H]^+$) 302.0456, found 302.0457; **$[\alpha]_D^{25}$** = +113.8 (c = 2.0, $CHCl_3$); **Chiral HPLC**: Chiralpak IB, 4.6 x 250 mm; 2% *i*PrOH/hexanes, 1.0 mL/min; t_R (minor) = 11.9 min, t_R (major) = 13.2 min, 93:7 er.

(*S*)-4,4,4-trifluoro-3-hydroxy-3-(6-methoxynaphthalen-2-yl)-1-(thiazol-4-yl)butan-1-one (125)

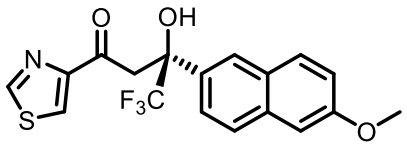

25 was prepared following General Procedure **D**, using 1-(thiazol-4-yl)ethan-1-one and 2,2,2-trifluoro-1-(6-methoxynaphthalen-2-yl)ethan-1-one. Purification by silica gel chromatography (5% acetone in pentane) afforded the title compound as a pale-yellow gum (68 mg, 89%, 93:7 er).

^{1}H NMR (400 MHz, C_6D_6): δ 8.32 (d, *J* = 1.9 Hz, 1H, Ar*H*), 7.92 (ddt, *J* = 8.7, 2.1, 1.1 Hz, 1H, Ar*H*), 7.68 (d, *J* = 2.1 Hz, 1H, Ar*H*), 7.55 – 7.49 (m, 1H, Ar*H*), 7.40 (dd, *J* = 9.0, 0.7 Hz, 1H, Ar*H*), 7.32 (d, *J* = 2.1 Hz, 1H, Ar*H*), 7.06 (dd, *J* = 8.9, 2.5 Hz, 1H, Ar*H*), 6.79 (d, *J* = 2.5 Hz, 1H, Ar*H*), 6.75 (s, 1H, O*H*), 4.23 (d, *J* = 16.1 Hz, 1H, CH_2), 3.85 (d, *J* = 16.1 Hz, 1H, CH_2), 3.31 (s, 3H, OCH_3) ppm; **^{13}C NMR (101 MHz, C_6D_6)**: δ 192.6 (*C*(O)), 158.4 (Ar*C*), 154.5 (Ar*C*), 152.7 (Ar*C*H), 134.7 (Ar*C*), 132.9 (Ar*C*), 130.0 (Ar*C*H), 128.5 (Ar*C*), 126.8 (Ar*C*H), 126.7 (Ar*C*H), 126.3 (Ar*C*H), 125.5 (q, *J* = 285.2 Hz), 124.7 (Ar*C*H), 119.2 (Ar*C*H), 105.3 (Ar*C*H), 76.5 (q, *J* = 29.2 Hz, *C*(CF_3)OH), 54.4 (OCH_3), 44.0 (*C*H_2) ppm; **^{19}F NMR (376 MHz, C_6D_6)**: δ -79.83 (s) ppm; **FT-IR (thin film)** ν_{max} 3113, 1681, 1606, 1482, 1160, 1032 cm^{-1}; **HRMS** (ESI) m/z calcd. for $C_{18}H_{14}F_3O_3NS$ ([M-H]$^-$) 382.0719, found 382.0719; **$[\alpha]_D^{25}$** = +1.5 (c = 2.0, $CHCl_3$); **Chiral HPLC**: Chiralpak AD, 4.6 x 250 mm; 2% to 30% gradient over 60 minutes *i*PrOH/hexanes, 1.0 mL/min; t_R (minor) = 26.9 min, t_R (major) = 36.9 min, 93:7 er.

(*S*)-1-(3-(difluoromethyl)-5-fluoro-1-methyl-1H-pyrazol-4-yl)-4,4,4-trifluoro-3-hydroxy-3-(4-vinylphenyl)butan-1-one (126)

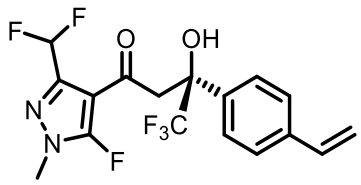

126 was prepared following General Procedure **D**, using 1-(3-(difluoromethyl)-5-fluoro-1-methyl-1H-pyrazol-4-yl)ethan-1-one and 2,2,2-trifluoro-1-(4-vinylphenyl)ethan-1-one. Purification by silica gel chromatography (20% isopropanol in pentane) afforded the title compound as a pale yellow gum (78 mg, 94%, 96:4 er).

^{1}H NMR (400 MHz, C_6D_6): δ 7.64 (d, *J* = 8.2 Hz, 2H, Ar*H*), 7.24 – 7.17 (m, 2H, Ar*H*), 6.70 (t, *J* = 53.6 Hz, 1H, C*H*F_2), 6.46 (dd, *J* = 17.6, 10.9 Hz, 1H, ArC*H*$CH_{trans}H_{cis}$), 5.83 (s, 1H, O*H*), 5.53 (dd, *J* = 17.6, 1.0 Hz, 1H ArCHC*H*$_{trans}H_{cis}$), 5.04 (dd, *J* = 10.9, 0.9 Hz, 1H, ArCHCH_{trans}*H*$_{cis}$), 3.42 – 3.28 (m, 2H, C*H*$_2$), 2.56 (d, *J* = 1.6 Hz, NC*H*$_3$) ppm; **^{13}C NMR (101 MHz, C_6D_6)**: δ 190.3 (d, *J* = 5.2 Hz, *C*(O)), 152.8 (d, *J* = 290.1 Hz, Ar*C*F), 138.1 (Ar*C*), 137.3 (Ar*C*), 135.9 (*C*HCH_2), 126.5 (Ar*C*), 126.4 (Ar*C*H), 126.3 (Ar*C*H), 123.7 (Ar*C*), 114.5 (CH*C*H_2), 109.4 (t, *J* = 237.6 Hz, *C*HF_2), 76.3 (q, *J* = 29.0 Hz, *C*(CF$_3$)OH), 42.5 (d, *J* = 3.9 Hz, *C*H$_2$), 33.0 (NCH_3) ppm. (*C*F$_3$ resonance not found); **^{19}F NMR (376 MHz, C_6D_6)**: δ -79.76 (s, C(OH)C*F*$_3$), -115.33 – -119.43 (m, Ar*F*), -121.25 (s, CH*F*$_2$) ppm; **FT-IR (thin film)** ν_{max} 3390, 2160, 1664, 1546, 1495, 1160 cm^{-1}; **HRMS** (ESI) m/z calcd. for $C_{14}H_{14}F_6N_2NO_2$ ([M+Na]$^+$) 415.0852, found 415.0849; **$[\alpha]_D^{25}$** = +75.6 (c = 0.5, $CHCl_3$); **Chiral HPLC**: Chiralpak IB, 4.6 x 250 mm; 2% *i*PrOH/hexanes, 1.0 mL/min; t_R (minor) = 19.7 min, t_R (major) = 20.3 min, 98:2 er.

(*R*)-1-(4-bromophenyl)-4,4,4-trifluoro-3-hydroxy-3-(thiophen-2-yl)butan-1-one (127)

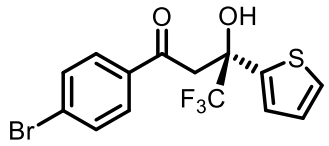

127 was prepared following General Procedure **D**, using 4-bromoacetophenone and 2-(trifluoroacetyl)thiophene. Purification by silica gel chromatography (3% Et_2O and 3% CH_2Cl_2 in pentane) afforded the title compound as a colourless solid (54 mg, 72%, >99:1 er).

^{1}H NMR (400 MHz, $CDCl_3$): δ 7.87 – 7.72 (m, 2H, Ar*H*), 7.71 – 7.57 (m, 2H, Ar*H*), 7.31 (dd, *J* = 5.1, 1.2 Hz, 1H, Ar*H*), 7.11 (ddd, *J* = 3.7, 1.3, 0.6 Hz, 1H, Ar*H*), 6.97 (dd, *J* = 5.1, 3.7 Hz, 1H, Ar*H*), 6.03 (s, 1H, O*H*), 3.91 (d, *J* = 17.1 Hz, 1H, CH_2), 3.55 (d, *J* = 17.1 Hz, 1H, CH_2) ppm; **^{13}C NMR (101 MHz, $CDCl_3$)**: δ 198.5 (*C*(O)), 141.7 (Ar*C*), 134.8 (Ar*C*), 132.3 (Ar*C*H), 130.1 (Ar*C*), 129.7 (Ar*C*H), 127.2 (Ar*C*H), 126.6 (Ar*C*H), 125.9 (Ar*C*H), 123.8 (q, J = 284.6 Hz, CF_3), 75.8 (q, J = 30.4 Hz, *C*(CF_3)OH), 40.9 (*C*H_2) ppm; **^{19}F NMR (376 MHz, $CDCl_3$)**: δ -81.23 (s) ppm; **FT-IR (thin film)** ν_{max} 3450, 1681, 1585, 1398, 1341, 1233, 1156, 1117 cm^{-1}; **HRMS** (ESI) m/z calcd. for $C_{14}H_9F_3O_2Br^{79}S$ ([M-H]$^-$) 378.9443, found 378.9444; **$[\alpha]_D^{25}$** = +25.5 (c = 1.0, $CHCl_3$); **Chiral HPLC**: Chiralpak AD-H, 4.6 x 250 mm; 1% *i*PrOH/hexanes, 1.0 mL/min; t_R (minor) = 10.8 min, t_R (major) = 10.0 min, >99:1 er; **m.p.**: 82 - 84 °C.

(*S*,*E*)-6,6,6-trifluoro-5-hydroxy-1,5-diphenylhex-1-en-3-one (128)

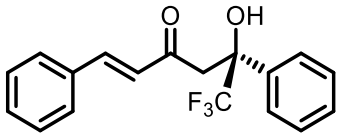

128 was prepared following General Procedure **D**, using benzylideneacetone and 2,2,2-trifluoroacetophenone. Purification by silica gel chromatography (15% CH_2Cl_2 in pentane) afforded the title compound as a colourless solid (58 mg, 91%, 98:2 er). Data is in agreement with that reported in the reported literature.[168]

^{1}H NMR (400 MHz, C_6D_6): δ 7.63–7.60 (m, 3H, Ar*H*), 7.56–7.53(m, 2H, Ar*H*), 7.44–7.34 (m, 6H, Ar*H* and alkene*CH*), 6.72 (d, *J* = 16.3 Hz, 1H, alkene*CH*), 3.65 (d, *J* = 16.8 Hz, 1H, *CH*$_2$), 3.39 (d, *J* = 16.9 Hz, 1H, *CH*$_2$) ppm; **^{19}F NMR (376 MHz, C_6D_6)**: δ -80.18 (s) ppm; **HRMS** (ESI) m/z calcd. for $C_{18}H_{16}F_3O_2$ ($[M+H]^+$) 321.10969, found 321.10966; **$[\alpha]_D^{25}$** = +237.2 (c = 1.6, $CHCl_3$) [literature for (*R*) enantiomer: -228 (c = 0.11, CH_2Cl_2)]; **Chiral HPLC**: Chiralpak AD-H, 4.6 x 250 mm; 5% *i*PrOH/hexanes, 1.0 mL/min; t_R (minor) = 23.5 min, t_R (major) = 26.7 min, 98:2 er.

(*S*)-4,4,5,5,5-pentafluoro-3-(4-fluorophenyl)-3-hydroxy-1-phenylpentan-1-one (129)

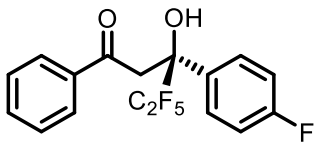

129 was prepared following General Procedure **D**, using acetophenone and 2,2,3,3,3-pentafluoro-1-(4-fluorophenyl)propan-1-one. Purification by silica gel chromatography (5% Et_2O and 5% CH_2Cl_2 in pentane) afforded the title compound as a colourless oil (62 mg, 86%, 97.5:2.5 er).

^{1}H NMR (400 MHz, MeOD): δ 7.86 – 7.76 (m, 2H, Ar*H*), 7.59 – 7.46 (m, 3H, Ar*H*), 7.41 – 7.33 (m, 2H, Ar*H*), 6.98 – 6.89 (m, 2H, Ar*H*), 4.11 (dd, *J* = 17.0, 1.1 Hz, 1H, C*H*$_2$), 3.65 (dd, *J* = 17.0, 0.7 Hz, 1H, C*H*$_2$) ppm. (OH not observed in MeOD); **^{13}C NMR (101 MHz, MeOD)**: δ 198.0 (d, *J* = 8.0 Hz, *C*(O)), 162.6 (d, *J* = 246.0 Hz, Ar*C*F), 137.0 (Ar*C*), 133.8 (q, *J* = 3.3 Hz, C(OH)Ar*C*), 133.4 (Ar*C*H), 128.5 (d, *J* = 8.2 Hz, Ar*C*H), 128.3 (Ar*C*H), 127.9 (Ar*C*H), 119.2 (qt, *J* = 287.7, 36.4 Hz, *C*F$_3$), 114.2 (d, *J* = 21.8 Hz, Ar*C*H), 114.2 (d, *J* = 34.2 Hz), 76.2 (td, *J* = 23.2, 5.0 Hz, *C*(CF$_3$)OH) ppm. *C*H$_2$ resonance obscured by solvent peak; **^{19}F NMR (376 MHz, MeOD)**: δ -78.85 (s, C*F*$_3$), -116.63 (ddd, *J* = 14.7, 9.4, 5.7 Hz, Ar*F*), -120.82 – -123.95 (q, *J* = 275.3 Hz, C*F*$_2$) ppm; **FT-IR (thin film)** ν_{max} 3319, 2961, 2160, 1683, 1601, 1506, 1220, 1149 cm^{-1}; **HRMS** (ESI) m/z calcd. for $C_{17}H_{11}F_6O_2$ ([M-H]$^-$) 361.0669, found 361.0672; **$[\alpha]_D^{25}$** = +72.3 (c = 1.0, $CHCl_3$); **Chiral HPLC**: Chiralpak IB, 4.6 x 250 mm; 3% *i*PrOH/hexanes, 1.0 mL/min; t_R (minor) = 7.4 min, t_R (major) = 9.1 min, 97.5:2.5 er.

(*S*)-1-(4-bromophenyl)-3-(4-chlorophenyl)-4,4,5,5,6,6,7,7,8,8,9,9,10,10,10-pentadecafluoro-3-hydroxydecan-1-one (130)

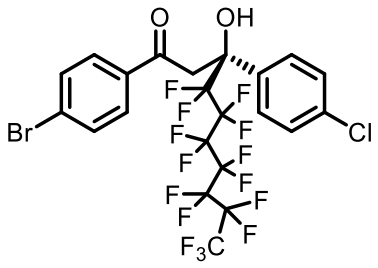

130 was prepared following General Procedure **D**, using 4-bromoacetophenone and 1-(4-chlorophenyl)-2,2,3,3,4,4,5,5,6,6,7,7,8,8,8-pentadecafluorooctan-1-one. Purification by silica gel chromatography (5% acetone in pentane) afforded the title compound as a white solid (117 mg, 83%, 96:4 er).

^{1}H NMR (500 MHz, C_6D_6): δ 7.27 (d, *J* = 8.3 Hz, 2H, Ar*H*), 7.06 (s, 4H, Ar*H*), 7.04 – 6.99 (m, 2H, Ar*H*), 6.05 (s, 1H, O*H*), 3.26 (d, *J* = 17.0 Hz, 1H, CH_2), 3.15 (d, *J* = 17.0 Hz, 1H, CH_2) ppm; **^{13}C NMR (126 MHz, C_6D_6)**: δ 198.6 (*C*(O)), 136.4 (Ar*C*), 134.8 (Ar*C*), 134.6 (Ar*C*), 131.8 (Ar*C*H), 129.5 (Ar*C*), 129.3 (Ar*C*H), 128.4 (Ar*C*H), 117.2^{A} (t, *J* = 30.4 Hz, *C*F_3), 115.9^{B} (*C*F_2), 112.7^{B} (*C*F_2), 111.4^{B} (*C*F_2), 111.1^{B} (*C*F_2), 110.5^{B} (*C*F_2), 108.5^{B} (q, *J* = 28.1 Hz, *C*F_2CF$_3$), 78.2^{C} (t, *J* = 29.0 Hz, *C*(CF_2)OH), 39.9 (*C*H_2) ppm; **^{19}F NMR (471 MHz, C_6D_6)**: δ -120.81 – -121.65 (m, C*F*$_3$), -116.32 (td, *J* = 21.4, 10.4 Hz, C*F*$_2$), -116.89 – -119.43 (m, C*F*$_2$CF$_3$), -120.81 – -121.65 (m, C*F*$_2$), -121.65 – -122.24 (m, C*F*$_2$), -122.41 – -123.09 (m, C*F*$_2$), -125.54 – -127.01 (m, C*F*$_2$) ppm; **FT-IR (thin film)** ν_{max} 3180, 1670, 1587, 1420, 1231, 1089, 1060 cm^{-1}; **HRMS** (ESI) m/z calcd. for $C_{22}H_{11}Br^{79}ClF_{15}O_2$ ([M-H]$^-$) 704.9319, found 704.9315; **$[\alpha]_D^{25}$** = +31.0 (c = 1.0, $CHCl_3$);

Chiral HPLC: Chiralpak AD-H, 4.6 x 250 mm; 2% *i*PrOH/hexanes, 1.0 mL/min; t_R (minor) = 11.0 min, t_R (major) = 12.7 min, 96:4 er; **m.p.**: 97 - 99 °C.

^{13}C NMR notes:

A – only observed in ^{13}C{CF_3 decoupled} NMR experiment

B – only observed in ^{13}C{CF_2 decoupled} NMR experiment

C – triplet only observed in ^{13}C NMR experiment

(*S*)-4-chloro-4,4-difluoro-3-hydroxy-1,3-diphenylbutan-1-one (131)

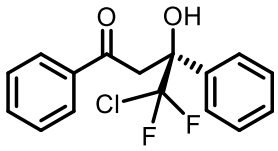

131 was prepared following General Procedure **D**, using acetophenone and 2-chloro-2,2-difluoroacetophenone. Purification by silica gel chromatography (5% CH_2Cl_2 and 5% Et_2O in pentane) afforded the title compound as a colourless solid (53 mg, 85%, 96.5:3.5 er).

^{1}H NMR (400 MHz, $CDCl_3$): δ 7.87 – 7.81 (m, 2H, Ar*H*), 7.65 – 7.60 (m, 3H, Ar*H*), 7.45 – 7.38 (m, 2H, Ar*H*), 7.28 – 7.24 (m, 3H, Ar*H*), 5.74 (d, *J* = 0.9 Hz, 1H, O*H*), 4.06 (d, *J* = 17.2 Hz, 1H, C*H*$_2$), 3.61 (d, *J* = 17.3 Hz, 1H, C*H*$_2$) ppm; **^{13}C NMR (101 MHz, $CDCl_3$)**: δ 199.9 (*C*(O)), 138.2 (Ar*C*), 136.3 (Ar*C*), 134.4 (Ar*C*H), 133.2 (Ar*C*H), 128.8 (q, J = 298.7.0 Hz, *C*F$_3$), 128.7 (Ar*C*H), 128.3 (Ar*C*H), 128.2 (Ar*C*H), 126.7 (Ar*C*H), 79.9 (t, J = 24.6 Hz, *C*(CF_2Cl)OH), 40.7 (*C*H$_2$) ppm; **^{19}F NMR (376 MHz, $CDCl_3$)**: δ -64.08 (d, *J* = 166.4 Hz), -65.05 (d, *J* = 166.5 Hz) ppm; **FT-IR (thin film)** ν_{max} 3231, 1680, 1582, 1419, 1228, 1110 cm^{-1}; **HRMS** (ESI) m/z calcd. for $C_{16}H_{13}ClF_2O_2$ ($[M+H]^+$) 311.06449, found 311.06459; **$[\alpha]_D^{25}$** = 14.0 (c = 0.25, $CHCl_3$); **Chiral HPLC**: Chiralpak AD-H, 4.6 x 250 mm; 5% *i*PrOH/hexanes, 1.0 mL/min; t_R (minor) = 11.5 min, t_R (major) = 12.0 min, 97:3 er; **m.p.**: 100 - 102 °C.

4.2.5 Derivatisation of Compound 104

(*S*)-1,1,1-trifluoro-2,4-diphenylbutan-2-ol (142)

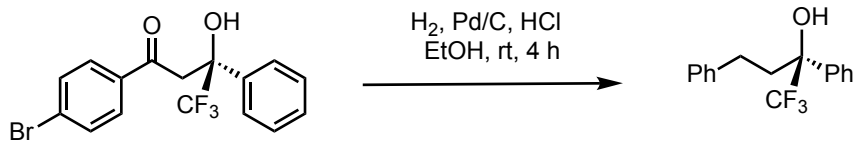

104; >99.5:0.5 er

142; 95% yield
>99.5:0.5 er

To a solution of **104** (100 mg, 0.269 mmol, >99.5:0.5 er) in EtOH (3 ml) was added 10% Pd/C (30 mg, 30% w/w) and conc. HCl (0.5 mL). The mixture was purged with hydrogen gas for 10 minutes then left to stir under a hydrogen atmosphere for 4 hours. The mixture was filtered through celite with CH_2Cl_2 and evaporated to dryness *in vacuo*. Purification by silica gel chromatography (10% EtOAc in pentane) afforded the title compound as a colourless oil (71 mg, 95%).

^{1}H NMR (400 MHz, $CDCl_3$): δ 7.55 – 7.48 (m, 2H, Ar*H*), 7.39 – 7.29 (m, 3H, Ar*H*), 7.14 (s, 2H, Ar*H*), 7.14 – 7.07 (m, 1H, Ar*H*), 7.07 – 6.97 (m, 2H, Ar*H*), 2.64 – 2.52 (m, 1H, $PhCH_2CH_2$), 2.50 – 2.40 (m, 1H, $PhCH_2CH_2$), 2.32 (s, 1H, O*H*), 2.30 – 2.23 (m, 2H, $PhCH_2CH_2$ and $PhCH_2CH_2$) ppm; **^{13}C NMR (101 MHz, $CDCl_3$)**: δ 140.9 (Ar*C*), 136.1 (Ar*C*), 128.6 (Ar*C*H), 128.5 (Ar*C*H), 128.5 (Ar*C*H), 128.2 (Ar*C*H), 126.3 (Ar*C*H), 126.2 (Ar*C*H), 125.5 (q, J = 286.0 Hz, CF_3), 77.3 (q, J = 28.4 Hz, $C(CF_3)OH$), 37.1 ($ArCH_2CH_2$), 28.7 ($ArCH_2CH_2$) ppm; **^{19}F NMR (376 MHz, $CDCl_3$)**: δ -80.09 (s) ppm. 280.1075, found 280.1075; **$[\alpha]_D^{25}$** = +16.3 (c = 2.0, $CHCl_3$); **FT-IR (thin film)** ν_{max} 3548, 3029, 2930, 2160, 1604, 1497, 1451, 1255, 1151 cm^{-1}; **Chiral HPLC**: Chiralpak OD-H, 4.6 x 250 mm; 3% *i*PrOH/hexanes, 1.0 mL/min; t_R (single enantiomer) = 16.9 min, >99.5:0.5 er (minor enantiomer not detected).

(3*S*)-4,4,4-trifluoro-1,3-diphenylbutane-1,3-diol (143)

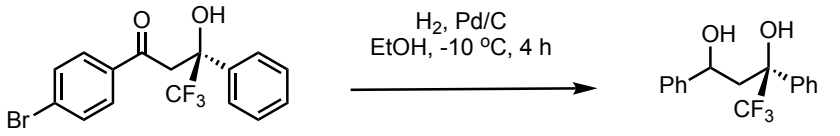

104; >99.5:0.5 er

143; 93% yield
10:1 dr, >99.5:0.5 er

To a solution of **104** (100 mg, 0.269 mmol, >99.5:0.5 er) in EtOH (3 ml) was added 10% Pd/C (5 mg, 5% w/w), then cooled to -10 °C. The mixture was purged with hydrogen gas for 10 minutes then left to stir under a hydrogen atmosphere for 4 hours at this temperature. The mixture was warmed to filtered through celite with CH_2Cl_2 and evaporated to dryness *in vacuo*. Purification by silica gel chromatography (15% EtOAc in pentane) afforded the title compound as a colourless oil (74 mg, 93%, 10:1 dr, configuration of major unknown). Longer reaction times and/or higher temperature led to formation of alcohol **142**.

Characterisation data for major diastereomer: **^{1}H NMR (400 MHz, $CDCl_3$)**: δ 7.64 – 7.55 (m, 2H, Ar*H*), 7.43 – 7.30 (m, 8H, Ar*H*), 5.79 (s, 1H, CF_3O*H*), 5.39 -5.35 (m, 1H, PhC*H*OH), 2.61 – 2.48 (m, 2H, PhCO*H* and CH_2), 2.27 (m, 1H, CH_2) ppm; **^{13}C NMR (101 MHz, $CDCl_3$)**: δ 143.2 (Ar*C*), 139.3 (Ar*C*), 128.8 (Ar*C*H), 128.4 (Ar*C*H), 128.2 (Ar*C*H), 128.2 (Ar*C*H), 126.0 (q, J = 287.7 Hz, CF_3), 125.6 (Ar*C*H), 125.5 (Ar*C*H), 76.8 (q, J = 28.0 Hz), 72.8 (q, J = 1.6 Hz, *C*H(OH)), 44.8 (CH_2) ppm; **^{19}F NMR (376 MHz, $CDCl_3$)**: δ -75.70 (s) ppm; **HRMS** (ESI) m/z calcd. for $C_{16}H_{16}F_3O_2$ ($[M+H]^+$) 297.1102, found 297.1102; **$[\alpha]_D^{25}$** = +53.2 (c = 2.5, $CHCl_3$); **Chiral HPLC**: Chiralpak IA, 4.6 x 250 mm; 7% *i*PrOH/hexanes, 1.0 mL/min; t_R = 12.0 min, >99.5:0.5 er (minor enantiomer not detected).

2,4-diphenyl-2-(trifluoromethyl)oxetane (144)

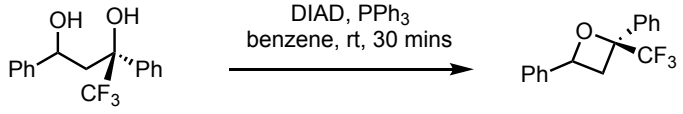

143; >99.5:0.5 er

144; 88% yield
>99.5:0.5 er

To a solution of **143** (10 mg, 0.0338 mmol, >99.5:0.5 er) and PPh_3 (20 g, 0.076 mmol, 2 eq) in benzene (0.4 ml) was added dropwise diisopropyl azodicarboxylate (15 μL, 0.0777 mmol, 2.3 eq) at RT under a nitrogen atmosphere. The resulting colourless solution was stirred at this temperature for 30 minutes, then quenched with brine (5 mL). The mixture was extracted with CH_2Cl_2 (3 x 10 mL), dried over Na_2SO_4, filtered, and evaporated to dryness *in vacuo*. Purification by silica gel chromatography (1% diethyl ether in pentane) afforded the title compound as a colourless oil (8.3 mg, 88%, >20:1 dr).

^{1}H NMR (400 MHz, $CDCl_3$): δ 7.64 – 7.58 (m, 2H, Ar*H*), 7.55 – 7.41 (m, 4H, Ar*H*), 7.40 – 7.27 (m, 4H, Ar*H*), 5.68 (t, *J* = 7.8 Hz, 1H, ArC*H*), 3.36 (dd, *J* = 11.3, 8.2 Hz, 1H, CH_2), 3.11 (ddd, *J* = 11.3, 7.5, 0.8 Hz, 1H, CH_2) ppm; **^{13}C NMR (126 MHz, $CDCl_3$)**: δ 140.5 (Ar*C*), 137.0 (Ar*C*), 128.8 (Ar*C*H), 128.6 (Ar*C*H), 128.4 (Ar*C*H), 128.3 (Ar*C*H), 126.4 (Ar*C*H), 125.6 (Ar*C*H), 123.8 (q, *J* = 282.6 Hz, *C*F_3), 80.5 (q, *J* = 32.3 Hz, *C*CF_3), 77.5 (*C*H), 37.4 (*C*H_2) ppm; **^{19}F NMR (376 MHz, $CDCl_3$)**: δ -80.99 (s) ppm; **HRMS** (ESI) m/z calcd. for $C_{16}H_{14}F_3O$ ($[M+H]^+$) 279.09672, found 279.09348; **$[\alpha]_D^{25}$** = -62.5 (c = 0.4, $CHCl_3$); **Chiral HPLC**: Chiralpak AD-H, 4.6 x 250 mm; 0.5% *i*PrOH/hexanes, 1.0 mL/min; t_R = 8.0 min, **>99.9:0.1 er** (minor enantiomer not detected).

(*S, E*)-4,4,4-trifluoro-3-hydroxy-1,3-diphenylbutan-1-one oxime (145)

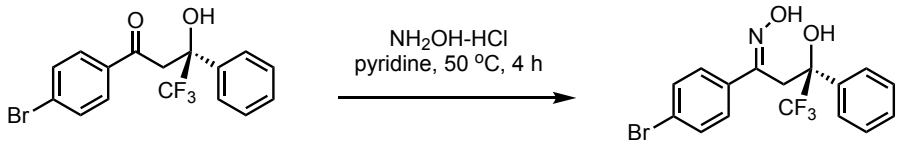

104; >99.5:0.5 er

145; 87% yield
>99.5:0.5 er

To a solution of **104** (500 mg, 1.35 mmol, 1.0 eq, >99.5:0.5 er) in pyridine (10 ml) was added hydroxylamine hydrochloride (233 mg, 3.38 mmol, 2.5 eq). The mixture was heated to 50 °C under a N_2 atmosphere for 4 hours, before removal of pyridine *in vacuo*. The resulting residue was dissolved in CH_2Cl_2 (100 mL) and washed with water (2 x 100 mL) then brine (100 mL). The organic layer was dried over Na_2SO_4, filtered, and evaporated to dryness *in vacuo*. Crude ^{1}H NMR analysis shows a 4:1 mixture of *E*/*Z* isomers. Purification by silica gel chromatography (5% EtOAc in pentane to 20% EtOAc in pentane) afforded the title compound as a single isomer (*S*, *E*) as a colourless oil which slowly crystallised to a white solid on standing (407 mg, 78%, >99.5:0.5 er). NOESY NMR shows correlation of oxime O*H* with CH_2 protons, suggesting *E* configuration of the oxime.

^{1}H NMR (400 MHz, MeOD): δ 7.53 – 7.41 (m, 2H, Ar*H*), 7.28 – 7.21 (m, 2H, Ar*H*), 7.18 – 7.10 (m, 3H, Ar*H*), 7.10 – 7.02 (m, 2H, Ar*H*), 5.02 (s, 1H, O*H*), 3.83 (d, *J* = 13.9 Hz, 1H, CH_2), 3.54 (d, *J* = 13.8 Hz, 1H, CH_2) ppm; **^{13}C NMR (101 MHz, MeOD)**: δ 154.0 (Ar*C*NOH), 137.1 (Ar*C*), 135.9 (Ar*C*H), 130.6 (Ar*C*H), 128.3 (Ar*C*H), 127.8 (Ar*C*H), 127.4 (Ar*C*H), 126.3 (Ar*C*H), 125.7 (q, J = 286.0 Hz, *C*F_3), 122.2 (Ar*C*), 77.5 (q, *J* = 28.0 Hz), 32.7 (*C*H_2) ppm; **^{19}F NMR (376 MHz, MeOD)**: δ -80.04 (s) ppm; **HRMS** (ESI) m/z calcd. for $C_{16}H_{14}O_2NBr^{79}F_3$ ([M+H]$^+$)

390.0134, found 390.0133; **$[\alpha]_D^{25}$** = -54.1 (c = 2.2, $CHCl_3$); **FT-IR (thin film)** ν_{max} 3197, 2919, 2848, 2160, 2027, 1978, 1449, 1266, 1151 cm^{-1}; **Chiral HPLC**: Chiralpak AD-H, 4.6 x 250 mm; 10% *i*PrOH/hexanes, 1.0 mL/min; t_R = 8.4 (minor enantiomer not observed), >99.5:0.5 er; **m.p.**: 88-90 °C.

(2*S*)-4-amino-1,1,1-trifluoro-2,4-diphenylbutan-2-ol (146)

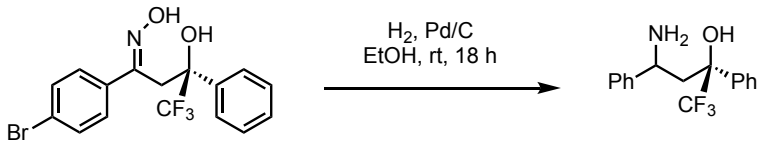

145; >99.5:0.5 er

146; 95% yield
>99.5:0.5 er
7:2 dr

To a solution of **145** (100 mg, 0.258 mmol, >99.9:0.1 er) in EtOH (5 ml) was added 10% Pd/C (30 mg, 30% w/w). The mixture was purged with hydrogen gas for 10 minutes then left to stir under a hydrogen atmosphere for 18 hours. The mixture was filtered through celite with CH_2Cl_2 and evaporated to dryness *in vacuo*. Purification by silica gel chromatography (10% EtOAc in pentane) afforded the title compound as a colourless oil (71 mg, 95%).

Characterised as a ~4:1 mixture of inseparable diastereomers [due to broad NMR peaks, **8** was analysed as HCl salt for ^{1}H and ^{19}F NMR spectroscopy]: **(8.HCl) ^{1}H NMR (400 MHz, D_2O)**: δ 7.58 – 7.39 (m, 5.5H, Ar*H*), 7.39 – 7.28 (m, 4H, Ar*H*), 7.28 – 7.15 (m, 2.5H, Ar*H*), 7.14 – 7.06 (m, 0.5H, Ar*H*), 4.25 (dd, *J* = 8.1, 5.7 Hz, 1H, PhC*H* $_{major}$), 4.14 (dd, *J* = 7.2, 5.6 Hz, 0.26H, PhC*H* $_{minor}$), 3.10 – 3.04 (m, 0.59H, C*H*$_{2\ major}$), 2.91 – 2.75 (m, 2.63H, C*H*$_{2\ major\ and\ minor}$) ppm; **(8.HCl) ^{19}F NMR (376 MHz, D_2O)**: δ -79.15 (s, major diastereomer), -79.75 (s, minor diastereomer) ppm; **^{13}C NMR (101 MHz, $CDCl_3$)**: δ 145.4 (Ar*C* $_{major}$), 145.3 (Ar*C* $_{minor}$), 140.9 (Ar*C* $_{major}$), 138.5 (Ar*C* $_{minor}$), 129.1 (Ar*C*H), 129.1 (Ar*C*H), 128.3 (Ar*C*H), 128.1 (Ar*C*H), 128.0 (Ar*C*H), 127.9 (Ar*C*H), 127.7 (Ar*C*H), 127.7 (Ar*C*H), 127.3 (Ar*C*H), 125.5 (Ar*C*H), 125.3 (Ar*C*H), 125.1 (Ar*C*H), 125.0 (Ar*C*H), 53.6 (q, J = 2.4 Hz, *C*NH$_{2\ major}$), 52.7 (*C*NH$_{2\ minor}$), 42.6 (*C*H$_{2\ major}$), 39.3 (*C*H$_{2\ minor}$) ppm [*C*F$_3$ resonance not observed. *C*CF$_3$ resonance obscured by solvent

peak]; **HRMS** (ESI) m/z calcd. for $C_{16}H_{17}ONF_3$ ($[M+H]^+$) 296.12568, found 296.12567; **FT-IR (thin film)** ν_{max} 3018, 1496, 1453, 1215, 1150, 1074, 748 cm^{-1}; $\mathbf{[\alpha]_D^{25}}$ = +17.8 (c = 2.0, $CHCl_3$); **Chiral HPLC** (major diastereomer): Chiralpak AD-H, 4.6 x 250 mm; 2% *i*PrOH/hexanes, 1.0 mL/min; t_R = 16.9 min (minor enantiomer not observed), >99.5:0.5 er.

***(S)*-3-(4-bromophenyl)-5-phenyl-5-(trifluoromethyl)-4,5-dihydroisoxazole (147)**

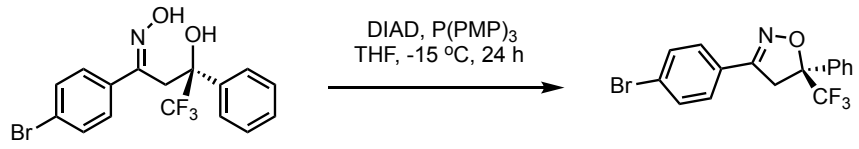

145; >99.5:0.5 er

147; 44% yield
>99.5:0.5 er

To a solution of **145** (60 mg, 0.155 mmol, >99.5:0.5 er) in anhydrous THF (4 ml) was added $P(PMP)_3$ (354 mg, 1.00 mmol, 6.5 eq), followed by dropwise addition of DIAD (172 mg, 0.852 mmol, 5.5 eq) at -15 °C. After 24 hours, the mixture was quenched with water (150 mL) and extracted with DCM (3 x 150 mL). The combined organics were dried over Na_2SO_4, filtered and evaporated to dryness *in vacuo*. Purification by silica gel chromatography (10% EtOAc in pentane) afforded a mixture of the title compound and $P(PMP)_3$. Further purification by silica gel chromatography (3% CH_2Cl_2 in pentane) afforded the title compound a white solid (63 mg, 44%). Data is in agreement with that reported in the literature.[263]

^{1}H NMR (400 MHz, $CDCl_3$): δ 7.64 – 7.51 (m, 6H, Ar*H*), 7.48 – 7.39 (m, 3H, Ar*H*), 4.07 (d, *J* = 17.1 Hz, 1H, C*H*$_2$), 3.74 (dq, *J* = 17.1, 1.0 Hz, 1H, C*H*$_2$) ppm; **^{13}C NMR (101 MHz, $CDCl_3$)**: δ 155.2 (*C*=N), 135.6 (Ar*C*), 132.1 (Ar*C*H), 129.4 (Ar*C*H), 128.7 (Ar*C*H), 128.2 (Ar*C*H), 127.0 (Ar*C*), 126.5 (Ar*C*H), 125.2 (Ar*C*), 124.1 (d, *J* = 284.6 Hz), 87.6 (q, *J* = 29.8 Hz), 43.7 (*C*H$_2$) ppm; **^{19}F NMR (376 MHz, $CDCl_3$)**: δ -79.94 (s) ppm; **HRMS** (ESI) m/z calcd. for $C_{16}H_{12}Br^{81}F_3NO$ ($[M+H]^+$) 372.0030, found 372.0029; **$[\alpha]_D^{25}$** = 67.2 (c = 1.0, $CHCl_3$); **Chiral HPLC**: Chiralpak OD-H, 4.6 x 250 mm; 5% *i*PrOH/hexanes, 1.0 mL/min; t_R = 14.5 min (minor enantiomer not observed), >99.5:0.5 er; **m.p.**: 132-134 °C

(*S*)-N-(4-bromophenyl)-4,4,4-trifluoro-3-hydroxy-3-phenylbutanamide (148)

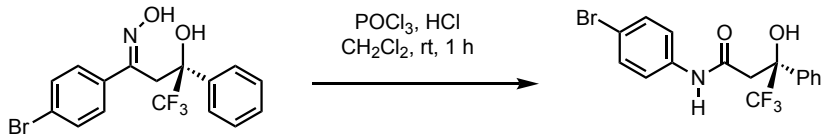

146; >99.5:0.5 er

148; 96% yield
>99.5:0.5 er

To a solution of **145** (100 mg, 0.258 mmol, >99.5:0.5 er) in CH_2Cl_2 (3 mL) at room temperature under a N_2 atmosphere was added $POCl_3$ (0.5 mL) and conc. HCl (0.5 mL). The resulting solution was stirred at room temperature for 1 hour then quenched with water, extracted with CH_2Cl_2 (2 x 25 mL), dried over $N_{a2}SO_4$, filtered and evaporated *in vacuo*. Purification by silica gel chromatography (10% EtOAc in pentane) afforded the title compound as a colourless solid (96 mg, 96%).

^{1}H NMR (400 MHz, DMSO-d_6): δ 10.32 (s, 1H, N*H*), 7.70 – 7.55 (m, 2H, Ar*H*), 7.49 – 7.31 (m, 7H, Ar*H*), 6.85 (s, 1H, O*H*), 3.37 (dd, *J* = 15.2 Hz, 1H, CH_2), 3.20 (d, *J* = 15.2 Hz, 1H, CH_2) ppm; **^{13}C NMR (101 MHz, DMSO-d_6)**: δ 167.9 (*C*(O)), 138.1 (Ar*C*), 137.7 (Ar*C*), 132.0 (Ar*C*H), 128.7 (Ar*C*H), 128.3 (Ar*C*H), 127.0 (Ar*C*H), 125.5 (q, *J* = 264.6 Hz, *C*F_3), 121.6 (Ar*C*H), 115.7 (Ar*C*Br), 75.7 (q, *J* = 28.0 Hz, *C*(CF_3)OH), 40.0 (*C*H_2) ppm; **^{19}F NMR (376 MHz, DMSO-d_6)**: δ -79.18 (s) ppm; **m.p.** 121-123 °C; **HRMS** (ESI) m/z calcd. for $C_{16}H_{14}O_2NBr^{79}F_3$ ($[M+H]^+$) 390.0134, found 390.0133; **FT-IR (thin film)** ν_{max} 3283, 2160, 1651, 1539, 1489, 1399, 1160, 751 cm^{-1}; **$[\alpha]_D^{25}$** = 0.5 (c = 1.0, $CHCl_3$); **Chiral HPLC**: Chiralpak OD, 4.6 x 250 mm; 5% *i*PrOH/hexanes, 1.0 mL/min; t_R (single enantiomer) = 69.2 min, >99.5:0.5 er (minor enantiomer not detected).

4.2.6 Preparative Scale Synthesis of 104

To an oven-dried 100 mL RBF equipped with a suba-seal was added an oven-dried magnetic stirrer bar. Catalyst precursor azide **149** (326 mg, 0.8 mmol, 0.02 eq) and *tris*(4-methoxyphenyl)phosphine (281 mg, 0.8 mmol, 0.02 eq) were added before three cycles of vacuum/N_2 purge. Anhydrous TBME (8.0 mL) was added, and the mixture stirred at RT for 5 hours to give a colourless solution of catalyst **102**. To the crude catalyst solution was added a solution of 4-bromoacetophenone (7.96 g, 40 mmol, 1.0 eq) in anhydrous TMBE (32 mL). The resulting soltuion was cooled with stirring in a -15 °C freezer for 15 minutes. 2,2,2-trifluoroacetophenone (6.96 g, 40 mmol, 1.0 eq) was added dropwise over 6 hours, before stirring at this temperature for a further 30 hours. After this time, ^{1}H NMR showed >90% conversion. The crude reaction mixture was poured into a stirring mixture of water (500 mL) and diethyl ether (250 mL). The resulting white precipitate was filtered to recover catalyst **102**. Extraction with diethyl ether (3 x 250 mL) and washing with brine (750 mL), followed by drying over Na_2SO_4 and evaporation to dryness *in vacuo* gave the crude product as a light-yellow oil which crystallised at RT over several hours.

Analysis of this material by HPLC showed 94.5:5.4 crude er. The crude solid material was dissolved in the minimum volume of CH_2Cl_2 (approx. 15 mL) and then diluted with pentane (500 mL). The mixture was stored in a -15 °C freezer overnight, then filtered to afford the product as a white solid. To afford enantioenriched crystals of product **104**, material was dissolved in the minimum volume of CH_2Cl_2 before carefully layering with pentane in a RBF. The flask was sealed with a suba-seal. A needle was placed in the seal to allow slow

evaporation, which afforded colourless crystals of enantiopure **104** (>99.5:0.5 er, 13.0 g, 87%) after several days.

4.2.7 Single-Crystal X-ray diffraction studies of 104

X-ray diffraction data has been made available in the Cambridge Crystallographic Data Centre as **CCDC 1972194.**

Bond precision	C-C = 0.0021 A
Wavelength	1.54184
Temperature	150 K
Cell	a =7.9216(1) b = 10.3625(1) c = 17.7560(1) alpha=90 beta=90 gamma=90
T Limits	T_{min}= 0.670; T_{max}=0.810
AbsCorr	MULTI-SCAN
Data completeness	1.72/1.00
Theta(max)	76.174
R(reflections)	0.0170(2983)
R2(reflections)	0.0445(3035)
S	1.003
N_{par}	204

	Calculated	**Reported**
Volume	1457.55(2)	1457.55(2)
Space group	P 21 21 21	P 21 21 21

Hall group	P 2ac 2ab	P 2ac 2ab
Moiety formula	C16 H12 Br F3 O2	C16 H12 Br1 F3 O2
Sum formula	C16 H12 Br F3 O2	C16 H12 Br1 F3 O2
Mr	373.16	373.17
Dx,g cm^{-3}	1.701	1.700
Z	4	4
Mu (mm-1)	4.212	4.212
F000	744.0	744.0
F000'	743.65	
h,k,lmax	9,13,22	9,13,22
Nref	3046[1762]	3036
Tmin,Tmax	0.777,0.810	0.670,0.810
Tmin'	0.656	

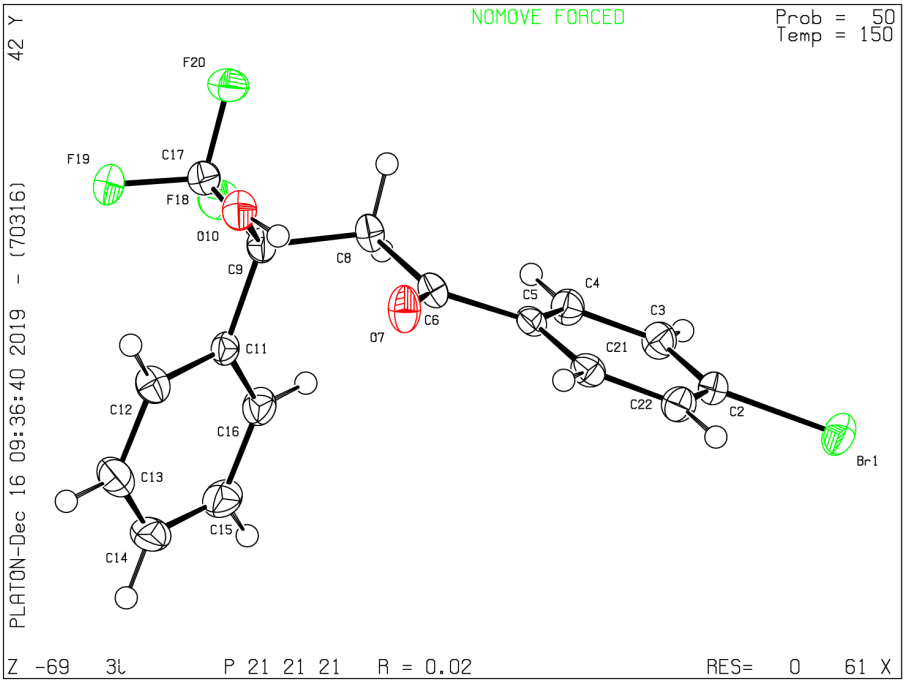

Figure 14. Ball and stick representation of the single crystal X-Ray diffraction data for **104**.

4.2.8 Mechanistic Considerations

4.2.8.1 Reaction rate comparison

The formation of product **96** was conveniently monitored over time by ^{1}H quantitative NMR. Poor reaction performance was observed when the reaction was conducted in an NMR tube in d_8-THF; possibly due to the lack of stirring. This combined with the high cost of deuterated solvents appropriate for the reaction (Et_2O, THF, CPME, dioxane etc.), and the complications with reaction temperature control, we decided to perform a large-scale reaction in a RBF and take aliquots for NMR analysis instead of *in situ* NMR measurements.

Procedure for kinetic experiments followed by NMR spectroscopy:

Both ketone starting materials were combined in CPME (75% of final volume) in a dried RBF under a nitrogen atmosphere. The flask was sealed with a suba seal and tightly wrapped with parafilm and white tape. The flask was equipped with a nitrogen balloon and placed in a -15 °C freezer to cool for 15 minutes, before quick injection of the pre-made BIMP catalyst in CPME (25% of final volume, 0.1 M final concentration) pre-cooled to -15 °C. A timer was started upon complete addition of the catalyst solution. Aliquots (approx. 0.25 mL) were immediately quenched with glacial AcOH (0.1 mL). The aliquots were evaporated under a stream of nitrogen gas, dissolved in $CDCl_3$ (0.65 mL) and taken for immediate NMR analysis (400 MHz or 500 MHz instruments).

Figures 15 - 19 show plots of conversion vs. reaction time. The model reaction conditions found in this study were used to study catalysts **102** and **20** (**Scheme 47**). Meanwhile, the optimized conditions reported by Iketmoto and co-workers were used in the study of

Takemoto's thiourea catalyst **6**. Rate enhancement of the BIMP catalyzed reaction, compared with the use of catalyst **6** under the conditions reported by Iketmoto, was determined from the relative gradients of the initial reaction rate plots:

initial reaction rate BIMP catalyst **102** (initial 10 minutes, 64.8% conv.);

$y = \mathbf{5.9398}x + 0.4325$

initial reaction rate catalyst **6** (initial 1290 minutes, 5.4% conv.);

$y = \mathbf{0.0042}x + 0.0953$

relative rate enhancement = 5.9398/0.0042 = 1414

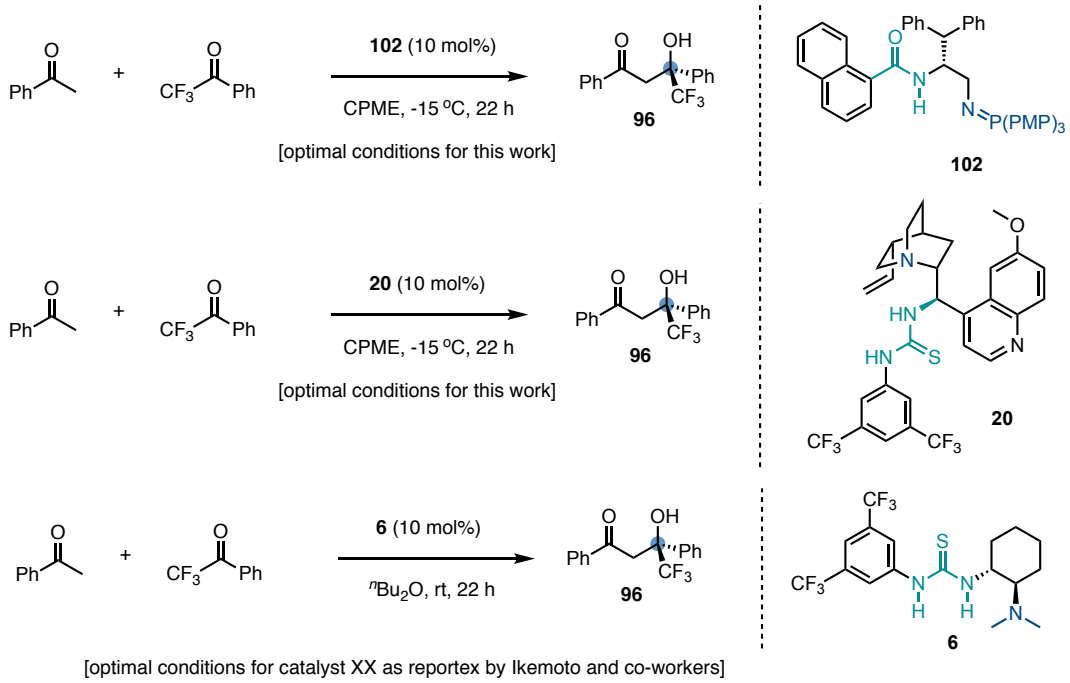

Scheme 47. Given conditions for individual catalysts studied in reaction-rate experiments.

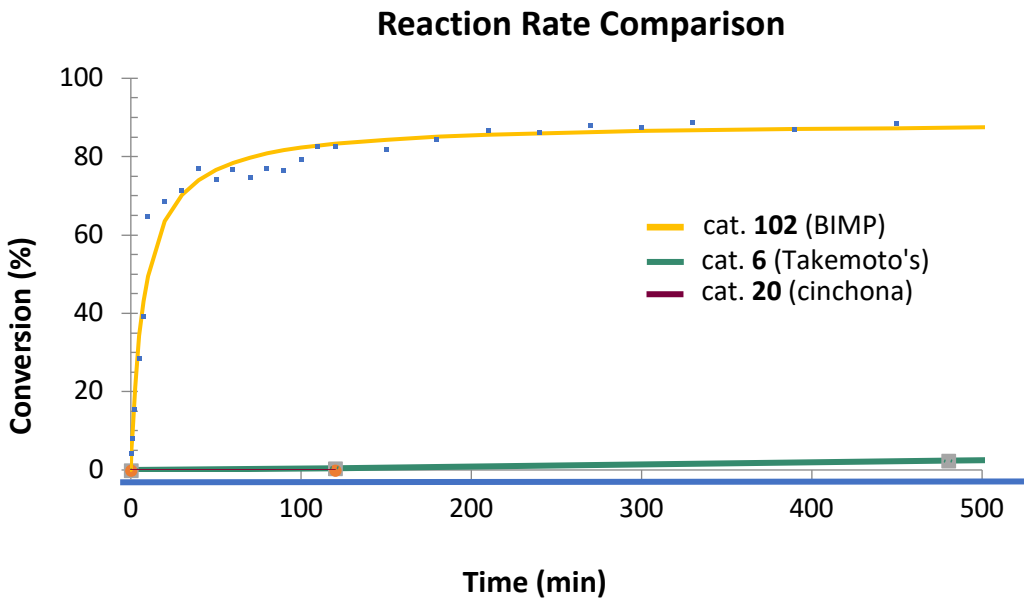

Figure 15. Reaction rate comparison of BIMP, *Cinchona* and thiourea catalysts.

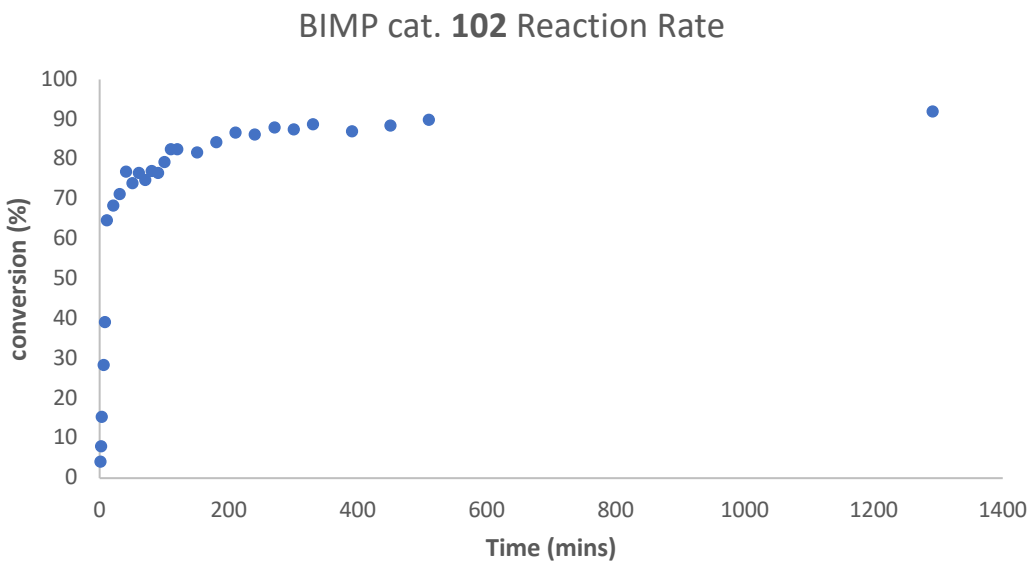

Figure 16. Reaction rate graph for BIMP cat. **102**.

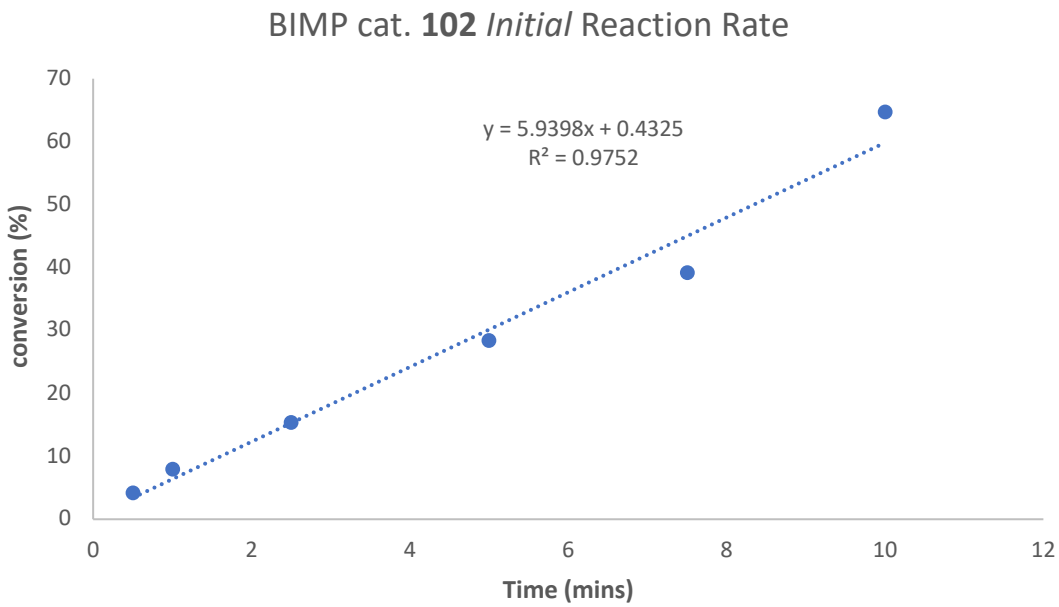

Figure 17. Initial reaction rate graph for BIMP cat. **102** (first 10 minutes of reaction).

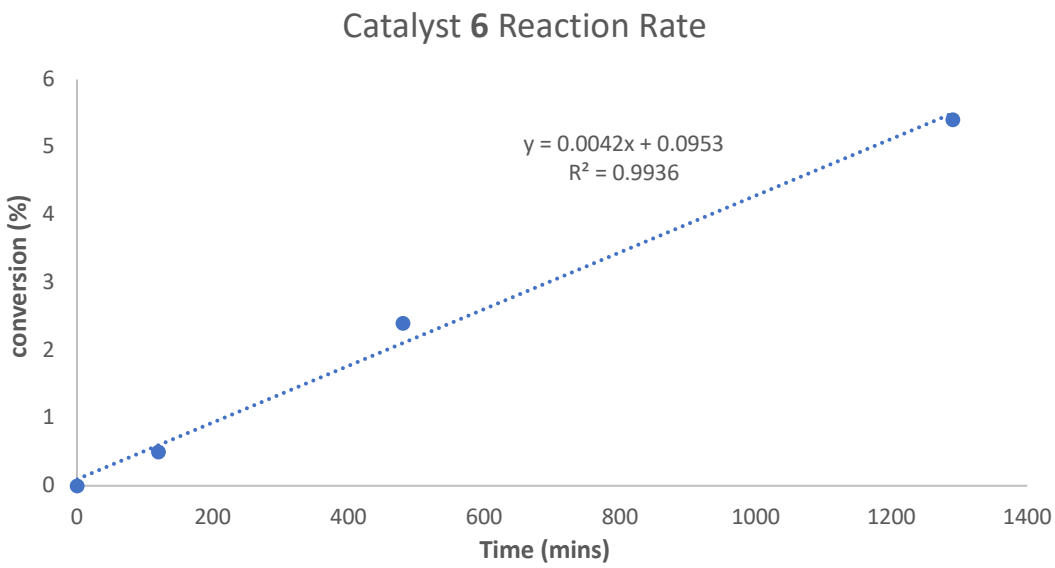

Figure 18. Reaction rate graph for cat. **6**.

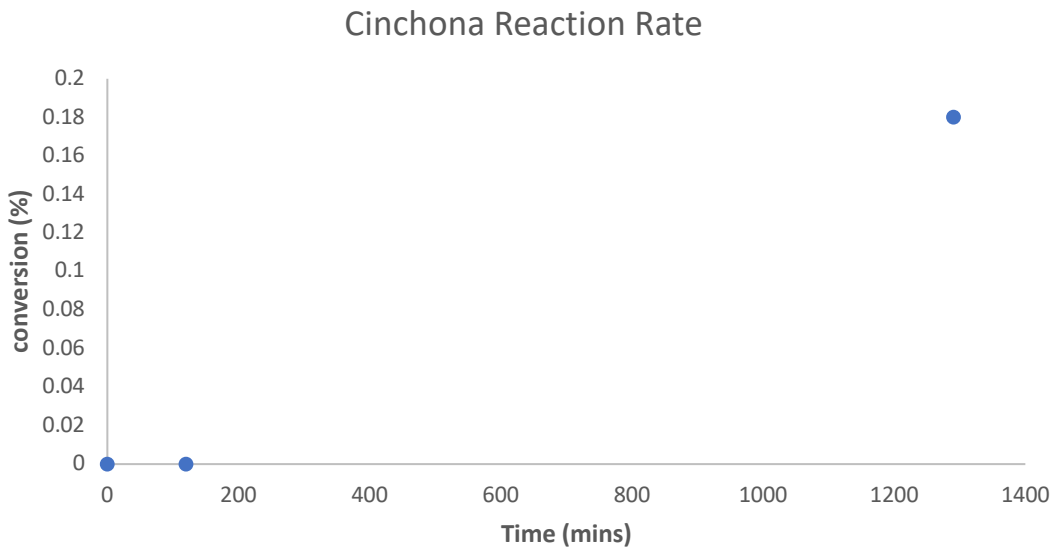

Figure 19. Reaction rate graph for Cinchona alkaloid cat. **20**.

4.2.8.2 Job plot

Catalyst (**102**) to product (**96**, 97:3 er) ratio was varied such that overall mole fraction and overall concentration remained constant throughout the measurements. The experiment began with a high concentration of catalyst **102**. After each measurement, the concentration of catalyst **102** was lowered, and the concentration of product **96** increased by approximately the same amount for the next measurement. After each measurement, the appropriate volume of solution was removed from the NMR tube, in order to reduce catalyst mole fraction. Then, the appropriate volume of stock solution of **96** was added to the NMR tube to adjust the overall concentration to 0.2 M.

Due to experimental error, observed mole fraction (X) values for **96** vary from the theoretical value that was aimed for. Calculations and plots were produced using the observed data, as determined from ^{1}H NMR integrations. Error is most likely due to the very small volumes of solution which were to be removed from the NMR tube in the earliest measurements, and also due to evaporation of solvent over the course of the measurements (several hours).

NMR parameters: THF-d_8, 400 MHz, ^{1}H quantitative (4 scans with 30 seconds relaxation time).

X = mole fraction

d[shift] = difference in NMR shift (in ppm) vs. the starting shift for **96**

Overall concentration was held constant at 0.2 M.

The C<u>H</u>$_3$ resonance of the *p*-OMe group on catalyst **102** was found to be most suitable for determination of d[shift] values, due to the sharpness of the singlet and minimal overlap with other resonances. Several other resonances were also appropriate and showed similar d[shift] across the range of measurements.

NMR #	**theoretical X (102)**	**theoretical X (96)**	**observed X (96)**	**mmol of 102**	**mmol of 96**
1	1	0	0	0.14	0
2	0.9	0.1	0.140	0.126	0.014
3	0.8	0.2	0.313	0.112	0.028
4	0.7	0.3	0.389	0.098	0.042
5	0.6	0.4	0.445	0.084	0.056
6	0.5	0.5	0.445	0.07	0.07
7	0.4	0.6	0.553	0.056	0.084
8	0.3	0.7	0.658	0.042	0.098
9	0.2	0.8	0.774	0.028	0.112
10	0.1	0.9	0.902	0.014	0.126
11	0	1	1	0	0.14

Table 7. Data for determination of binding stoichiometry.

NMR #	d[shift](ppm)	d[shift] x X(102)
1	0	0
2	+0.0045	0.004061694
3	+0.0092	0.007122688
4	+0.0143	0.009412949
5	+0.02	0.011054656
6	+0.0255	0.011378835
7	+0.0254	0.011318616
8	+0.0295	0.011477028
9	+0.0333	0.01042755
10	+0.0451	0.00632098
11	-	-

Table 8. Data points for Job Plot shown in **Figure 20**.

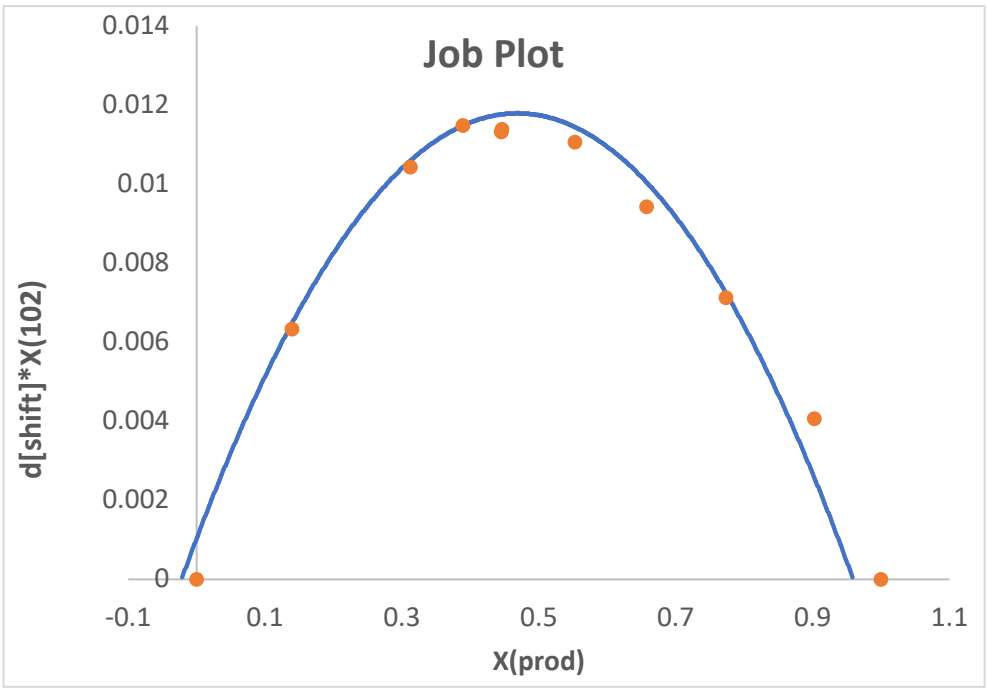

Figure 20. Plot of mole fraction or product [X(prod)] against d[shift]*X(cat).

4.2.8.3 Product inhibition studies

To investigate the effect of product inhibition on reaction rate, the synthesis of aldol product **124** was performed in the presence of 1.0 eq or 0.5 eq of aldol product **96** (**Scheme 48**). These aldol products were chosen so to give useful NMR spectra (i.e. minimal overlap of important resonances).

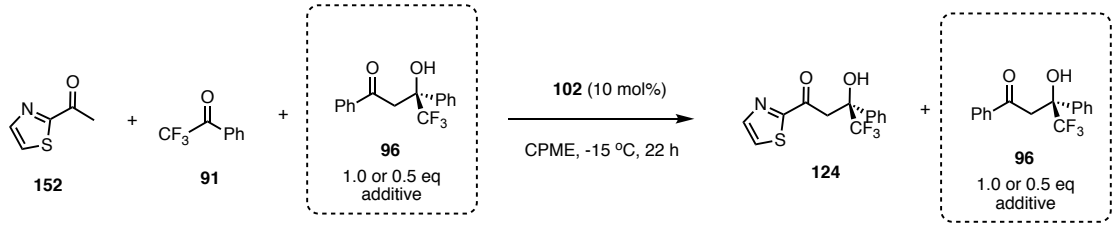

Scheme 48. Reaction details for product inhibition studies.

Addition of 1.0 eq of product **96** resulted in a 2.31 factor reduction of initial reaction rate for the synthesis of **124**, compared to the reaction with 0 eq of product additive **96**. With 0.5 eq of additive, a very small difference of initial reaction rate was observed; 2.18 factor reduction compared to 0 eq of additive. However, over the full reaction time, 1.0 eq of additive resulted in a much lower conversion than with 0.5 eq additive. See **Figures 21-22**.

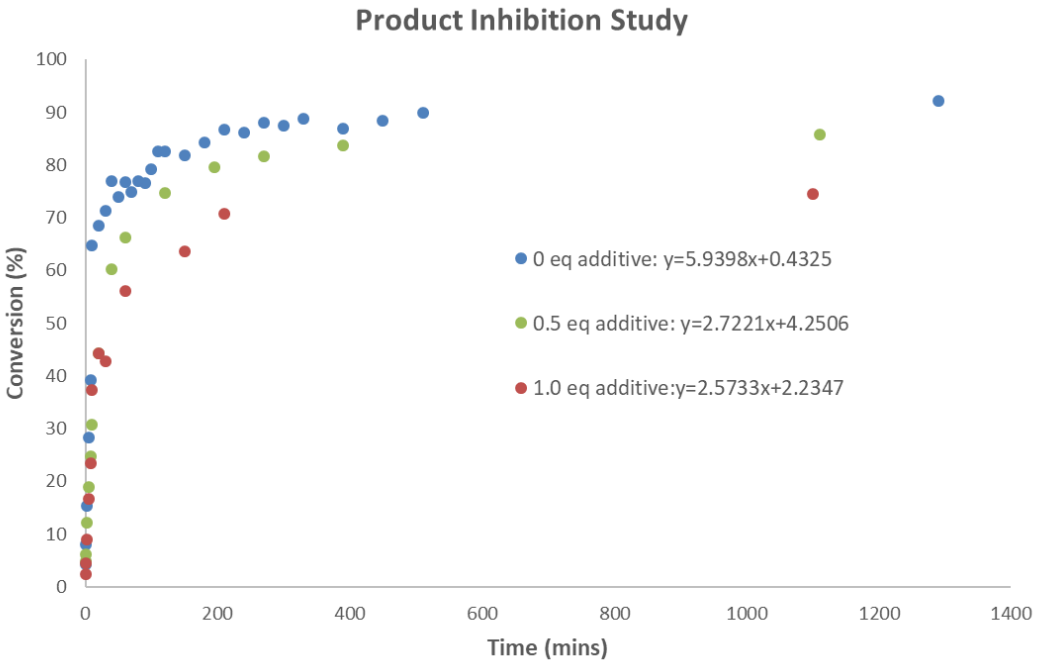

Figure 21. Plot of conversion over time, with varying amount of product additive.

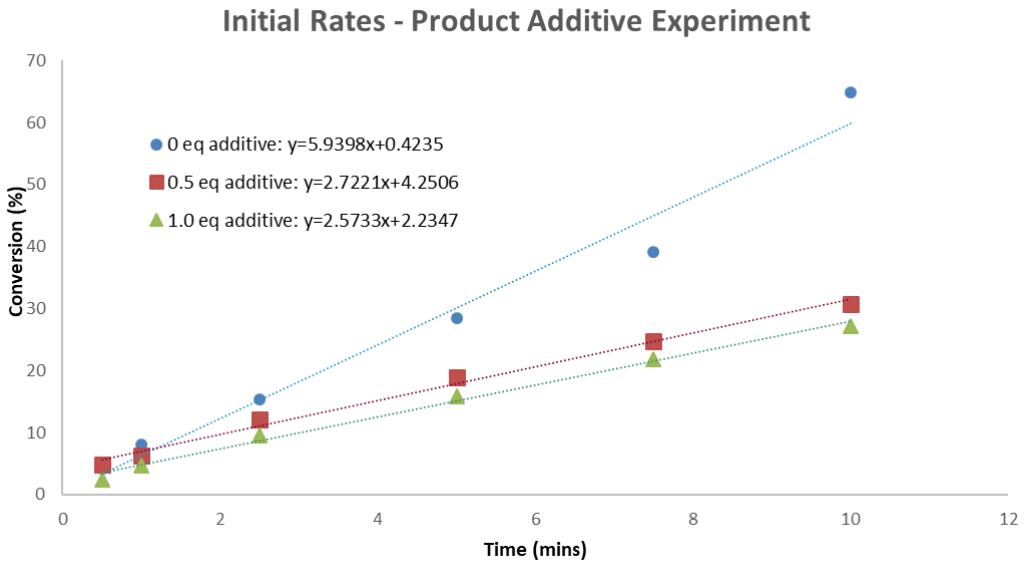

Figure 22. Plot of conversion in first 10 minutes of reaction, with varying amount of product additive.

4.2.8.4 pK_a determination of catalyst 102

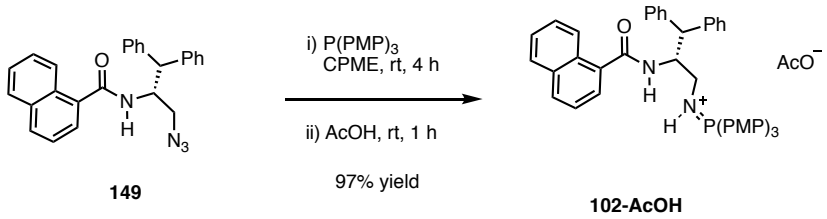

Catalyst **102** (20.0 mg) was prepared *in situ* (CPME, 0.1 M) from azide **149**, as described before. Upon complete conversion to BIMP **102** (determined by ^{31}P NMR) glacial AcOH (excess, 2.0 mL) was added. The mixture was stirred at rt under N_2 for 1 hours, before removal of solvent and excess acid under reduced pressure. The resulting residue was dissolved in the minimal volume of CH_2Cl_2 (approx. 2 mL), then cold pentane was quickly added (approx. 5 mL) to induce precipitation. The mixture was chilled in a freezer overnight, then filtered and dried *in vacuo* to afford catalyst **102-AcOH** salt. **^{1}H NMR (400 MHz, $CDCl_3$):** δ 8.81 (d, *J* = 9.5 Hz, 1H), 7.73 – 7.64 (m, 2H), 7.58 – 7.21 (m, 12H), 7.21 – 7.13 (m, 4H), 7.05 – 6.91 (m, 10H), 5.14 – 4.92 (m, 1H), 4.30 (d, *J* = 11.8 Hz, 1H), 3.81 (s, 9H), 3.35 (ddd, *J* = 13.2, 10.9, 8.1 Hz, 1H), 3.03 – 2.83 (m, 1H), 1.78 (s, 3H) ppm; **^{13}C NMR (101 MHz, $CDCl_3$):** δ 175.1, 170.3 ,164.3, 164.2, 142.3, 142.1, 135.6, 135.5, 134.5, 133.4, 130.2, 129.8, 128.6, 128.4, 127.8, 126.4, 126.3, 126.2, 125.9, 125.6, 125.4, 124.9, 115.4, 115.3, 113.3, 112.2, 55.7, 54.16, 53.2, 52.9, 43.6, 22.0 ppm; **^{31}P NMR (162 MHz, $CDCl_3$):** δ 36.74 (s, 1P) ppm.

This salt was then used without further purification: **102-AcOH** (15.0 mg) was dissolved in CD_3CN (approx. 0.7 mL). Tetramethylguanidine was added. The ^{1}H, ^{13}C and $^{3}1P$ NMR of this mixture was measured. The chemical shifts of CH_2-N=**P**Ph_3 and **C**H_2-N=PPh_3 were used to calculate the equilibrium constant of the reaction, which is subsequently used (together with the known pK_a of TMG) to determine the estimated pK_{BH+} of catalyst **102**. Reference chemical shifts for the pure salt and pure freebase (catalyst **102**) in the same solvent (CD_3CN) were also measured for calculations. See Table 9 for full data.

x1 = [(δ_P N<u>P</u>R_3 (with TMG)) – (δ_P **102**)] / [(δ_P **102**-AcOH) - (δ_P **102**)]

Equations for ^{31}P calculation in **Table 9** below (same applies for ^{13}C calculation using corresponding data):

x1 = [(δ_P <u>NPR_3</u>(with TMG))- δ_P(**102**)]/[δ_P(**102-AcOH**)- δ_P(**102**)]

K_a = $[(1-x1)/(x1)]^2$

^{31}P	**δ_P <u>NPR_3</u> (with TMG)**	**δ_P 102-AcOH**	**δ_P 102**	**pK_a of TMG**	**x1**	**1-x1**	**K_a**	**pK_a 102**
	35.370	36.760	9.156	23.3	0.94965	0.05036	0.00281	25.85
^{13}C	**δ_C <u>C</u>H_2NP (with TMG)**	**δ_C 102-AcOH**	**δ_C 102**	**pK_a of TMG**	**x1**	**1-x1**	**K_a**	**pK_a 102**
	44.847	45.108	47.23	23.3	1.12299	-0.12299	0.01199	25.22
							AVG(pK_a)	**25.5**

Table 9. Calculated pKa value for catalyst 102.

4.2.8.5 Verification of H-bonding

(*R*)-*N*-(3-azido-1,1-diphenylpropan-2-yl)-*N*-methyl-1-naphthamide (150)

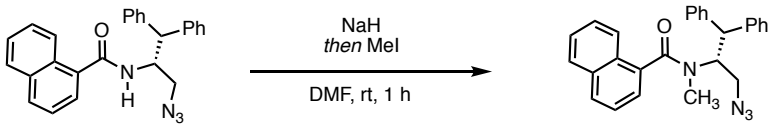

149 **150**

To a solution of azide **149** (203 mg, 0.5 mmol, 1.0 eq) in anhydrous DMF (2.0 ml) at room temperature was added 60% NaH (24 mg, 0.6 mmol, 1.2 eq). After 15 minutes at room temperature, methyl iodide (142 mg, 1.0 mmol, 2.0 eq) was added, and the mixture stirred for a further 1 hour, then poured into brine (100 mL), extracted with EtOAc (2 x 100 mL), dried over sodium sulfate, and concentrated to dryness *in vacuo*. Purification by silica gel chromatography (petroleum ether/EtOAc) afforded **150** as a colourless solid (179 mg, 85% yield).

^{1}H NMR (400 MHz, $CDCl_3$): δ 8.67 – 8.57 (m, 1H), 8.21 – 8.11 (m, 1H), 7.85 – 7.63 (m, 5H), 7.55 – 7.48 (m, 8H), 7.29 – 7.22 (m, 2H), 4.73 (d, *J* = 8.3, 1H), 4.60 – 4.53 (m, *J* = 8.3, 1H), 3.52 (d, *J* = 6.1 Hz, 2H), 2.90 (s, 3H) ppm; **^{13}C NMR (101 MHz, $CDCl_3$)**: δ 170.1, 144.0, 143.4, 135.2, 133.0, 131.2, 129.3, 129.1, 128.9, 128.4, 128.1, 127.9, 127.4, 127.1, 126.7, 125.9, 124.8, 124.4, 52.1, 51.7, 51.2, 32.9 ppm; **HRMS** (ESI) m/z calcd. for $C_{27}H_{24}ON_4$ ($[M+H]^+$) 421.20284, found 421.20289.

4.2.8.6 Catalyst decomposition

(*R*)-*N*-(3-amino-1,1-diphenylpropan-2-yl)-1-naphthamide (154)

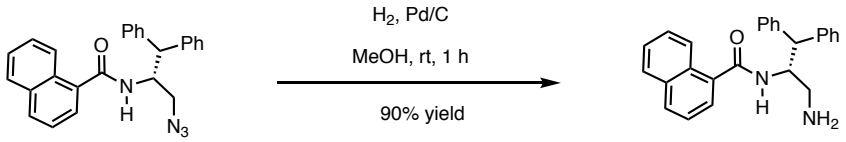

149 **154**

A suspension of azide **149** (203 mg, 0.5 mmol) and 10 wt% Pd/C (20 mg) in anhydrous MeOH (10.0 ml) at room temperature was hydrogenated at balloon pressure for 1 hour, then filtered over celite and concentrated to dryness *in vacuo*. Purification by silica gel chromatography (CH_2Cl_2/EtOAc) afforded **154** as a colourless oil (171 mg, 90% yield).

^{1}H NMR (400 MHz, $CDCl_3$): δ 8.63 – 8.52 (m, 1H), 8.23 – 8.16 (m, 1H), 7.80 – 7.69 (m, 5H), 7.60 – 7.50 (m, 8H), 7.32 – 7.25 (m, 2H), 4.63 – 4.59 (m, 1H), 4.45 – 4.36 (m, 1H), 3.02 – 2.91 (m, 2H) ppm; **^{13}C NMR (101 MHz, $CDCl_3$)**: δ 170.6, 144.5, 143.9, 135.5, 132.1, 130.5, 128.9, 128.7, 128.4, 128.1, 127.6, 127.0, 126.5, 124.3, 123.6, 123.1, 50.1, 47.7, 45.7 ppm; **HRMS** (ESI) m/z calcd. for $C_{26}H_{25}ON_2$ ($[M+H]^+$) 381.19669, found 381.19672.

4.2.8.7 Deuteration study

Acetophenone-d_1 (d_1-95)

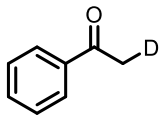

To a solution of catalyst **102** (0.02 mmol, 1.0 eq) in THF (0.1 mL) at room temperature under nitrogen, was added a solution of acetophenone (0.02 mmol, 1.0 eq) in THF (0.1 mL). After stirring at this temperature for 30 minutes, the reaction was quenched with D_2O (0.5 mL) and stirred for a further 5 minutes. The mixture was extracted with diethyl ether (3 x 2 mL), dried over Na_2SO_4, filtered and evaporated to dryness *in vacuo*. The resulting residue was filtered through a pipette of silica (eluting with 30% CH_2Cl_2 in pentane) to remove catalyst. Evaporation of solvent afforded the tittle compound as a colourless oil. ^{1}H NMR analysis shows >95% deuterium incorporation. Spectroscopic data agrees with the reported literature. **^{1}H NMR (400 MHz, $CDCl_3$)**: δ 7.86 (dd, J = 7.2, 1.3 Hz, 2H), 7.54-7.50 (dt, J = 7.6, 1.8 Hz, 1H), 7.51-7.47 (m, 2H), 2.60 (t, J = 2.1 Hz, 2H) ppm.

4.3 Experimental Details for Chapter 3

4.3.1 Optimisation Studies

4.3.1.1 Optimisation of the enantiodetermining aza-Michael addition

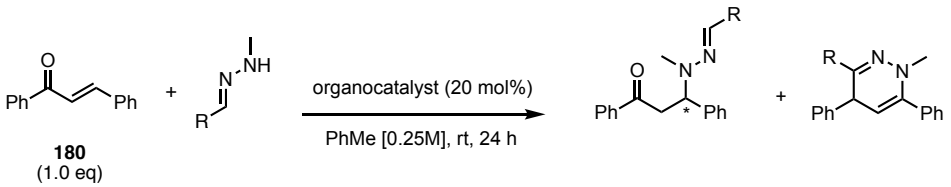

Scheme 49. Optimisation of the aza-Michael addition of hydrazones to chalcone (**180**).

A range of bifunctional H-bond donor catalysts were screened for reactivity and enantioselectivity in the reaction of hydrazones with chalcone **180** (**Scheme 49**), according to the following **General Procedure E** for optimization of aza-Michael addition: To a solution of chalcone (40 mg, 0.19 mmol, 1.0 eq) in PhMe (0.77 mL) at room temperature was added the appropriate hydrazone (0.38 mmol) and catalyst (0.2 eq). Unless otherwise indicated, the mixture was stirred under a N_2 atmosphere at room temperature for 24 hours. Conversion was determined by ^{1}H NMR. Purification by Preparative Thin Layer Chromatography afforded aza-Michael and Michael products, which were analysed by chiral HPLC. Results are given in **Table 10,** with the structures of chosen catalysts illustrated in **Figure 23**.

entry	catalyst	solvent	R	aza-Michael (%)[a]	Michael (%)[a]	aza-Michael er[b]
1	**189**	PhMe	Ph (**192**)	86	0	70.5:29.5
2	**197**	PhMe	Ph (**192**)	74	0	36.5:63.5
3	**190**	PhMe	Ph (**192**)	69	9	80:20
4	**198**	PhMe	Ph (**192**)	50	29	82:18
5	**199**	PhMe	Ph (**192**)	58	7	86.5:13.5
6	**200**	PhMe	Ph (**192**)	56	17	87:13
8	**S32**	PhMe	Ph (**192**)	32	22	85.5:14.5
9	**S3**	PhMe	Ph (**192**)	34	16	55:44
10	**S33**	PhMe	Ph (**192**)	57	13	70:30
11	**S5**	PhMe	Ph (**192**)	21	3	N.D.
12	**S4**	PhMe	Ph (**192**)	36	46	54:66
13	**S2**	PhMe	Ph (**192**)	58	8	70:30
14	**98**	PhMe	Ph (**192**)	4	0	53:47
15	**185**	PhMe	Ph (**192**)	20	0	56:46
16	**S34**	PhMe	Ph (**192**)	45	4	71:29
17	**S35**	PhMe	Ph (**192**)	65	3	78:22
18	**S36**	PhMe	Ph (**192**)	6	65	80:20
19	**6**	PhMe	Ph (**192**)	23	0	47:53
20	**200**	wet PhMe[c]	Ph (**192**)	50	10	78:22
21	**200**	Et_2O	Ph (**192**)	83	17	66:74
22	**200**	DMF	Ph (**192**)	3	5	N.D.
23	**200**	CPME	Ph (**192**)	32	22	62:38
24	**200**	CH_2Cl_2	Ph (**192**)	97	0	82:18
25	**200**	THF	Ph (**192**)	17	34	74:26
26	**200**	PhMe	*p*-Tol (**208**)	87	2	89:11
27	**200**	PhMe	*o*-Tol (**209**)	65	11	88:12

28	**200**	PhMe	Cy (**214**)	75	13	67:33
29	**200**	PhMe	4-*t*BuPh (**210**)	68	0	88:12
30	**200**	PhMe	4-*t*BuPh (**210**)	90	0	90:10
31	**200**	PhMe	4-F-Ph (**211**)	52	11	84:16
32	**200**	PhMe	4-Ph-Ph (**212**)	69	3	N.D.
33	**200**	PhMe	2-nap (**213**)	36	5	67:33
31[d]	**200**	**PhMe**	**4-*t*BuPh** (**210**)	**93** (**3d**)	**0**	**95:5**
32[e]	-	PhMe	Ph (**192**)	trace (**3a**)	0	N.D.

Table 10. Detailed optimization results for the aza-Michael addition of hydrazones to chalcone **180**. N.D.: not determined. [a]determined by ^{1}H NMR. [b]determined by chiral HPLC. [c]with 1% w/w H_2O. [d]performed at -15 ^oC for 48h. [e]no catalyst, performed for 7 days.

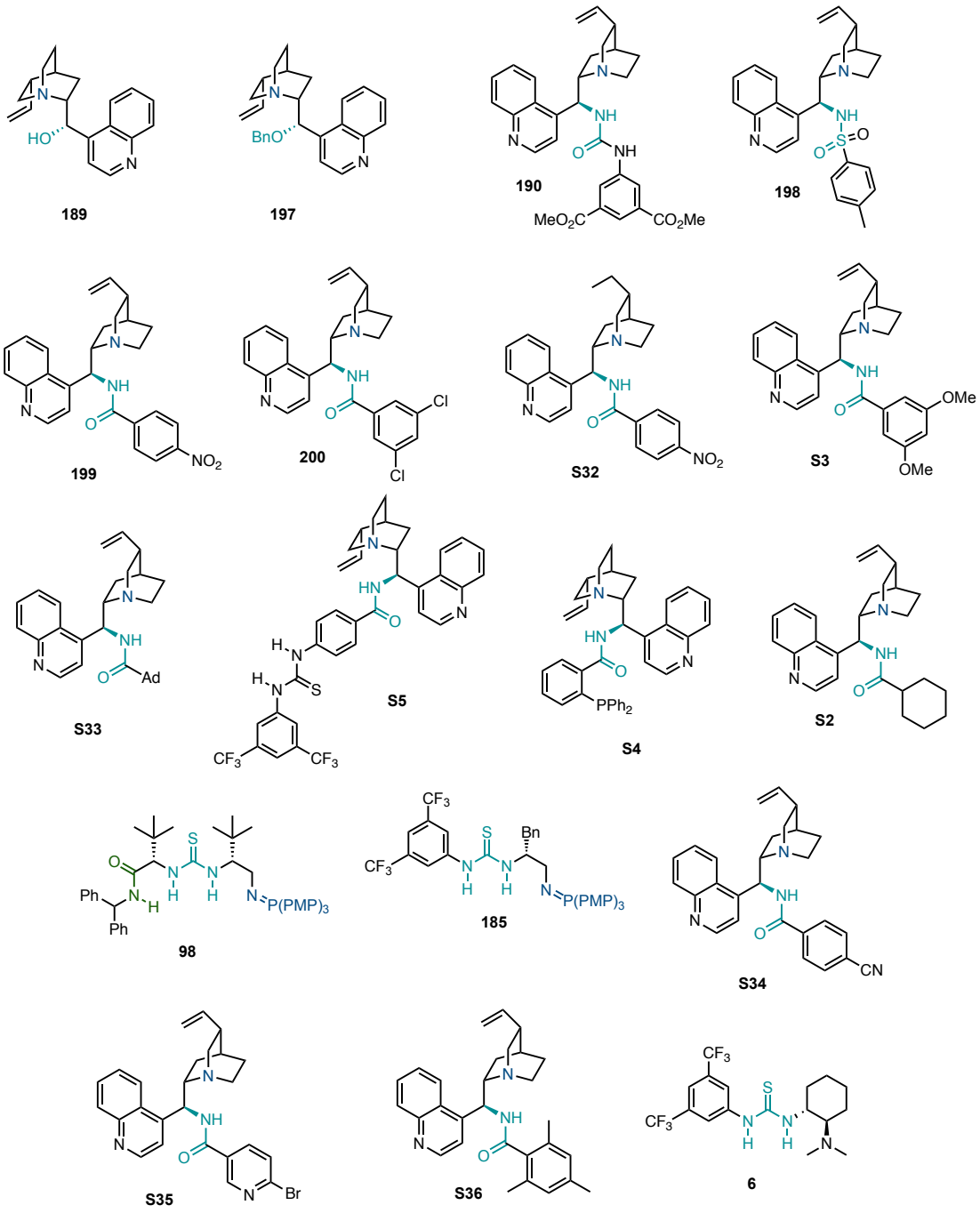

Figure 23. Selected catalysts studied in optimisation of the model reaction.

(*E*)-3-(2-benzylidene-1-methylhydrazineyl)-1,3-diphenylpropan-1-one (215)

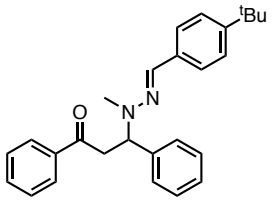

^{1}H NMR (400 MHz, $CDCl_3$): δ 7.99 – 7.86 (m, 2H), 7.80 – 7.72 (m, 2H), 7.64 – 7.51 (m, 1H), 7.49 – 7.42 (m, 5H), 7.36 – 7.24 (m, 5H), 7.23 (s, 1H), 4.59 (dd, *J* = 13.7, 8.6 Hz, 1H), 3.91 (dd, *J* = 15.7, 8.6 Hz, 1H), 3.66 (dd, *J* = 15.7, 13.7 Hz, 1H), 2.80 (s, 3H), 1.32 (s, 9H) ppm; **^{13}C NMR (101 MHz, $CDCl_3$)**: δ 198.1, 134.4, 138.6, 137.9, 134.8, 133.9, 131.6, 130.1, 129.9, 129.6, 128.8, 127.8, 127.8, 126.0, 63.9, 40.7, 39.1, 35.0, 31.6 ppm; **HRMS** (ESI) m/z calcd. for $C_{27}H_{30}N_2O$ ($[M+H]^+$) 399.24364, found 399.24371.

1-methyl-3,4,6-triphenyl-1,4-dihydropyridazine (216)

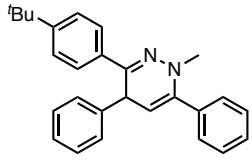

^{1}H NMR (400 MHz, $CDCl_3$): δ 7.98 – 7.89 (m, 2H), 7.62 – 7.55 (m, 2H), 7.40 – 7.33 (m, 3H), 7.29 – 7.24 (m, 21H), 7.20 – 7.12 (m, 5H), 7.10 – 7.02 (m, 1H), 6.03 (d, *J* = 8.4 Hz, 1H), 5.84 (d, *J* = 8.4 Hz, 1H), 3.55 (s, 3H) ppm; **^{13}C NMR (101 MHz, $CDCl_3$)**: δ 151.3, 144.7, 142.8, 139.3, 136.3, 133.6, 131.1, 130.2, 129.7, 129.2, 129.0, 128.4, 127.5, 127.0, 111.4,

44.7, 41.9, 34.3, 31.0 ppm; **HRMS** (ESI) m/z calcd. for $C_{23}H_{21}N_2O$ ($[M+H]^+$) 325.17047, found 325.17052.

4.3.1.2 Optimization of hydrazone cleavage

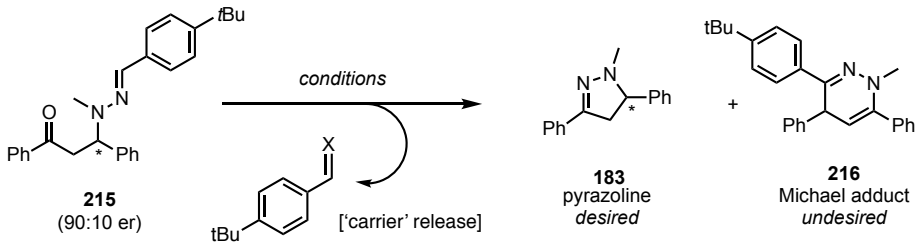

Scheme 50. Cleavage of the chiral hydrazone intermediate **215** to afford 2-pyrazoline **183**.

General Procedure F for optimization of chiral hydrazone cleavage:

To a solution of **215** (20 mg, 0.05 mmol) in PhMe (0.5 mL) was added the appropriate additive. The resulting mixture was stirred under an N_2 atmosphere at room temperature (unless otherwise indicated) for 18 hours. Conversion was determined by ^1H NMR spectroscopy. Results are given in **Table 11**.

Entry	Reagent	Conversion of 215[a]	183 (%)[a] (er)	216 (%)[a]
1	Amberlyst-15R® (100 mg)	100%	decomp. (N.D.)	decomp.
2	Amberlite-CG50® (100 mg)	0%	-	-
3	aq. HCl (1.5 eq.)	0%	0	0
4	aq. HCl (10.0 eq.)	0%	0	0
5	aq. H_2SO_4 (0.5 eq)	100%	76 (N.D.)	24
6	Silica gel (100 mg) and H_2O (0.5 mL)	0%	-	-
7	**30% NH_2OH in MeOH @ RT (2.0 eq)**	**100%**	**100** (90:10)	**0**
8	30% NH_2OH in MeOH @ 65 °C (2.0 eq)	100%	100 (N.D.)	0

Table 11. Reagent screening for the cleavage of 1,3-ketohydrazone intermediate **215**. [a]determined by ^1H NMR.

4.3.2 Synthesis of starting materials

4.3.2.1 Synthesis of enones

General Procedure G for the synthesis of enone starting materials by aldol condensation:

To a solution of the appropriate ketone (1.0 eq, 5.0 mmol) in EtOH (5 ml) at 0 °C was added a 10% aqueous solution of NaOH (5 ml). After 5 minutes, the appropriate aldehyde (1.0 eq, 5.0 mmol) was added in one portion. Typically, the mixture solidified after 5 minutes. The reaction was monitored by TLC. After completion, H_2O (50 ml) was added, and the resulting precipitate filtered. Recrystallization from EtOH afforded the pure enone products. In the cases where precipitation did not occur, the reaction mixture was extracted with EtOAc (2x50 ml). Organic layers were combined, washed with brine, dried over Na_2SO_4, filtered

and evaporated to dryness *in vacuo*. Subsequent purification by flash column chromatography (EtOAc in hexanes) afforded the pure enone products.

General Procedure H for the synthesis of enone starting materials by Wittig olefination:

To a solution of methyltriphenylphosponium bromide (1.5 eq, 17 mmol) in THF (40 ml) and DMF (4 ml) at 0 °C was added NEt_3 (1.5 eq, 17 mmol). After 15 minutes, aldehyde (1.0 eq, 11.3 mmol) was added slowly. The mixture was warmed to RT, then stirred at 80 °C for 20 hours. After completion, the reaction was quenched with saturated aqueous ammonium chloride solution (100 ml) and extracted with EtOAc (2x100ml). Combined organic layers were dried over Na_2SO_4, filtered and evaporated *in vacuo*. Subsequent purification by flash column chromatography (EtOAc in hexanes) afforded the pure enone products.

(*E*)-3-(4-bromophenyl)-1-phenylprop-2-en-1-one (247)

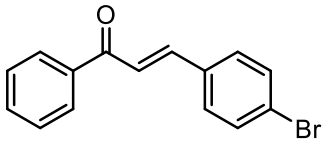

Prepared following **General Procedure G**, using acetophenone and 4-bromobenzaldehyde to afford the title compound as a pale-yellow solid (1.43 g, 97%). Data is consistent with the published literature.[2]

^{1}H NMR (400 MHz, $CDCl_3$): δ 8.06 – 7.96 (m, 2H, Ar*H* and C(O)CHC*H*), 7.75 (d, *J* = 15.7 Hz, 1H, C(O)C*H*CH), 7.62 – 7.53 (m, 3H, Ar*H*), 7.53 – 7.44 (m, 3H, Ar*H*), 7.41 – 7.34 (m, 2H, Ar*H*); **^{13}C NMR (101 MHz, $CDCl_3$)**: δ 190.1 (*C*(O)), 143.2 (C(O)CH*C*H), 138.0 (Ar*C*), 136.4 (Ar*C*), 133.4 (Ar*C*), 132.9 (Ar*C*H), 129.6 (Ar*C*H), 129.2 (Ar*C*H), 128.7 (Ar*C*H), 128.5 (Ar*C*H), 122.5 (C(O)*C*HCH); **m.p.**: 122-123 °C (lit. 121-123 °C).

(*E*)-3-(4-chlorophenyl)-1-phenylprop-2-en-1-one (S37)

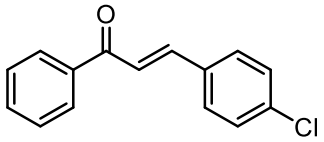

Prepared following **General Procedure G**, using acetophenone and 4-chlorobenzadeldhyde to afford the title compound as a pale-yellow solid (1.14 g, 94%). Data is consistent with the published literature.[3]

^{1}H NMR (400 MHz, $CDCl_3$): δ 8.07-8.01 (m, 2H, Ar*H*), 7.79 (d, *J*=15.7 Hz, 1H, C(O)C*H*CH), 7.64-7.59 (m, 3H, Ar*H* and C(O)CHC*H*), 7.54-7.42 (m, 3H, Ar*H*), 7.40-7.35 (m, 2H, Ar*H*) ppm; **^{13}C NMR (101 MHz, $CDCl_3$)**: δ 192.8 (*C*(O)), 145.9 (C(O)CH*C*H), 140.6 (Ar*C*), 136.0 (Ar*C*), 135.6 (Ar*C*H), 133.7 (Ar*C*), 132.2 (Ar*C*H), 131.9 (Ar*C*H), 131.3 (Ar*C*H), 131.1 (Ar*C*H), 125.1 (C(O)*C*HCH) ppm; **m.p.**: 112-113 °C (lit. 112-113 °C).

(*E*)-3-(naphthalen-2-yl)-1-phenylprop-2-en-1-one (S38)

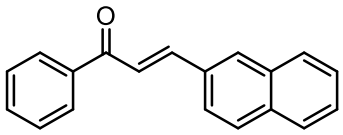

Prepared following **General Procedure G**, using acetophenone and 2-naphthaldehyde to afford the title compound as a pale-yellow solid (1.24 g, 96%). Data is consistent with the published literature.[264]

^{1}H NMR (400 MHz, $CDCl_3$): δ 8.05 (d, *J* = 7.5 Hz, 2 H, Ar*H*), 8.00 (s, 1 H, Ar*H*), 7.94 (d, *J* = 15.4 Hz, 1 H, C(O)CHC*H*), 7.90–7.85 (m, 3 H, Ar*H*), 7.75 (d, *J* = 8.5 Hz, 1 H, Ar*H*), 7.64 (s, 1 H, Ar*H*), 7.62–7.58 (m, 1 H, C(O)C*H*CH), 7.54–7.50 (m, 4 H, Ar*H*) ppm; **^{13}C NMR (101 MHz, $CDCl_3$)**: δ 190.6 (*C*(O)), 144.9 (C(O)CH*C*H), 138.3 (Ar*C*), 134.4 (Ar*C*), 133.3 (Ar*C*), 132.8 (Ar*C*), 132.5 (Ar*C*H), 130.6 (Ar*C*H), 128.7 (Ar*C*H), 128.6 (Ar*C*H), 128.6 (Ar*C*H), 127.8 (Ar*C*H), 127.3 (Ar*C*H), 126.7 (Ar*C*H), 123.6 (Ar*C*H), 123.7 (Ar*C*H), 122.2 (C(O)*C*HCH) ppm; **m.p.**: 157 – 158 °C (lit. 157 – 159 °C).

(*E*)-3-phenyl-1-(m-tolyl)prop-2-en-1-one (S39)

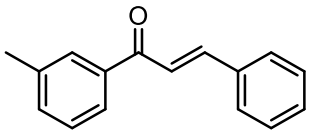

Prepared following **General Procedure G**, using 3-methylacetophenone and benzaldehyde to afford the title compound as a pale-yellow oil (0.988 g, 89%). Data is consistent with the published literature.[265]

^{1}H NMR (400 MHz, $CDCl_3$): δ 7.85 – 7.78 (m, 3H, Ar*H* and C(O)CHC*H*), 7.65 (ddd, *J* = 6.1, 4.5, 2.6 Hz, 2H, Ar*H*), 7.53 (d, *J* = 15.7 Hz, 1H, C(O)C*H*CH), 7.45 – 7.37 (m, 5H, Ar*H*), 2.45 (d, *J* = 0.7 Hz, 3H, ArCH_3) ppm; **^{13}C NMR (101 MHz, $CDCl_3$)**: δ 190.7 (*C*(O)), 144.6 (C(O)CH*C*H), 138.5 (Ar*C*), 138.3 (Ar*C*), 135.0 (Ar*C*), 133.6 (Ar*C*H), 130.5 (Ar*C*H), 129.1 (Ar*C*H), 129.0 (Ar*C*H), 128.5 (Ar*C*H), 128.5 (Ar*C*H), 125.7 (Ar*C*H), 122.3 (C(O)*C*HCH), 21.4 (Ar*C*H_3) ppm; **m.p.**: 61-63 °C (lit. 64 °C).

(*E*)-1-phenyl-3-(4-vinylphenyl)prop-2-en-1-one (S40)

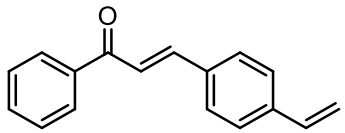

Prepared following **General Procedure G**, using acetophenone and 4-vinylbenzadeldhyde to afford the title compound as a pale-yellow solid (1.12 g, 95%).

^{1}H NMR (400 MHz, $CDCl_3$): δ 8.10 – 8.01 (m, 2H, Ar*H*), 7.82 (d, *J* = 15.7 Hz, 1H, C(O)C*H*CH), 7.66 – 7.58 (m, 3H, Ar*H*), 7.58 – 7.50 (m, 3H, Ar*H* and C(O)CHC*H*), 7.50 – 7.45 (m, 2H, Ar*H*), 6.76 (dd, *J* = 17.6, 10.9 Hz, 1H, ArC*H*$CH_{cis}H_{trans}$), 5.86 (dd, *J* = 17.6, 0.8 Hz, 1H, ArCHC$H_{cis}$$H_{trans}$), 5.36 (dd, *J* = 10.9, 0.7 Hz, 1H, ArCHC$H_{cis}$$H_{trans}$) ppm; **^{13}C NMR (101 MHz, $CDCl_3$)**: δ 190.5 (*C*(O)), 144.4 (C(O)CH*C*H), 139.8 (Ar*C*), 138.3 (Ar*C*), 136.1 (*C*HCH_2), 134.4 (Ar*C*), 132.8 (Ar*C*H), 128.8 (Ar*C*H), 128.6 (Ar*C*H), 128.5 (Ar*C*H), 126.8 (Ar*C*H), 121.8 (C(O)*C*HCH), 115.5 (CH*C*H_2) ppm; **FT-IR (thin film)** ν_{max} 1655, 1577, 1409, 1295, 1037, 1014, 834, 780, 695 cm^{-1}; **HRMS** (ESI) m/z calcd. for $C_{17}H_{15}O$ ($[M+H]^+$) 235.11174, found 235.11169; **m.p.**: 76-78 °C.

(*E*)-3-(4-nitrophenyl)-1-phenylprop-2-en-1-one (S41)

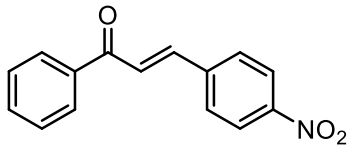

Prepared following **General Procedure G**, using acetophenone and 4-nitrobenzadeldhyde to afford the title compound as an orange solid (1.14 g, 90%). Data is consistent with the published literature.[264]

^{1}H NMR (400 MHz, $CDCl_3$): δ 8.37 – 8.24 (m, 2H, Ar*H*), 8.10 – 8.02 (m, 2H, Ar*H*), 7.87 – 7.76 (m, 3H, Ar*H* and C(O)CHC*H*), 7.65 (d, *J* = 112.6 Hz, 2H, Ar*H* and C(O)C*H*CH), 7.58 – 7.50 (m, 2H, Ar*H*) ppm; **^{13}C NMR (101 MHz, $CDCl_3$)**: δ 189.6 (*C*(O)), 148.5 (Ar*C*), 141.5 (C(O)CH*C*H), 141.0 (Ar*C*), 137.5 (Ar*C*), 133.4 (Ar*C*H), 129.0 (Ar*C*H), 128.8 (Ar*C*H), 128.6 (Ar*C*H), 125.7 (Ar*C*H), 124.2 (C(O)*C*HCH) ppm; **m.p.**: 164-165 °C (lit. 163-164 °C).

(*E*)-4-(3-oxo-3-phenylprop-1-en-1-yl)benzonitrile (S42)

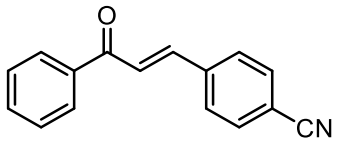

Prepared following **General Procedure G**, using acetophenone and 4-cyanobenzadeldhyde to afford the title compound as a pale-yellow solid (1.07 g, 92%). Data is consistent with the published literature.[266]

^{1}H NMR (400 MHz, $CDCl_3$): δ 7.54−7.52 (m, 2H, Ar*H*), 7.59 (d, *J* = 16.0 Hz, 1H, C(O)CHC*H*), 7.65−7.60 (m, 1H, Ar*H*), 7.75−7.70 (m, 4H, Ar*H*), 7.80 (d, *J* = 16.0 Hz, 1H, C(O)C*H*CH), 8.05−8.01 (m, 2H, Ar*H*) ppm; **^{13}C NMR (101 MHz, $CDCl_3$)**: δ 189.8 (*C*(O)), 142.0 (C(O)CH*C*H), 139.2 (Ar*C*), 137.6 (Ar*C*), 133.3 (Ar*C*H), 132.6 (Ar*C*H), 128.7 (Ar*C*H), 128.7 (Ar*C*H), 128.5 (Ar*C*H), 125.1 (C(O)*C*HCH), 118.3 (*C*N), 113.4 (Ar*C*CN) ppm; **m.p.**: 158-159 °C (lit. 159-160 °C).

(*E*)-3-(4-methoxyphenyl)-1-phenylprop-2-en-1-one (S43)

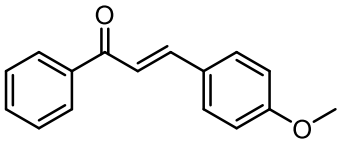

Prepared following **General Procedure G**, using acetophenone and 4-methoxybenzaldehyde to afford the title compound as a pale-yellow solid (1.11 g, 93%). Data is consistent with the published literature.[267]

^{1}H NMR (400 MHz, $CDCl_3$): δ 8.07 – 7.98 (m, 2H, Ar*H*), 7.81 (d, *J* = 15.6 Hz, 1H, C(O)CHC*H*), 7.65 – 7.56 (m, 3H, Ar*H*), 7.51 (ddt, *J* = 8.2, 6.6, 1.3 Hz, 2H), 7.44 (d, *J* = 15.6 Hz, 1H, C(O)C*H*CH), 6.97 – 6.90 (m, 2H, Ar*H*), 3.85 (s, 3H, OCH_3) ppm; **^{13}C NMR (101 MHz, $CDCl_3$)**: δ 190.5 (*C*(O)), 161.7 (Ar*C*), 144.7 (C(O)CH*C*H), 138.5 (Ar*C*), 132.6 (Ar*C*H), 130.3 (Ar*C*H), 128.6 (Ar*C*H), 128.4 (Ar*C*H), 127.6 (Ar*C*), 119.7 (C(O)*C*HCH), 114.4 (Ar*C*H), 55.4 (O*C*H_3) ppm; **m.p.**: 73-74 °C (lit. 73-75 °C).

Ethyl (*E*)-4-(3-oxo-3-phenylprop-1-en-1-yl)benzoate (S44)

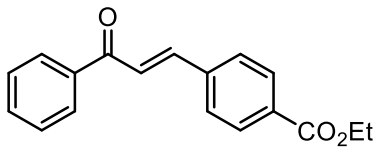

Prepared following **General Procedure G**, using acetophenone and ethyl-4-formylbenzoate to afford the title compound as a pale-yellow solid (1.26 g, 90%). Data is consistent with the published literature.[268]

^{1}H NMR (400 MHz, $CDCl_3$): δ 8.11−8.09 (m, 2H, Ar*H*), 8.06−8.01 (m, 2H, Ar*H*), 7.80 (d, *J* = 15.5 Hz, 1H, C(O)CHC*H*), 7.68 (d, *J* = 8.2 Hz, 2H, Ar*H*), 7.61 (d, *J* = 15.5 Hz, 1H, C(O)CHC*H*), 7.61−7.57 (m, 1H, Ar*H*), 7.54−7.51 (m, 2H, Ar*H*), 4.42 (q, *J* = 6.9 Hz, 2H, C(O)C$H_2$$CH_3$), 1.45 (t, *J* = 7.4 Hz, 3H, C(O)CH_2CH_3); **^{13}C NMR (101 MHz, $CDCl_3$)**: δ 190.2 (*C*(O)), 166.0 (*C*(O)CH_2CH_3), 143.4 (Ar*C*), 139.0 (Ar*C*), 137.9 (C(O)CH*C*H), 133.2 (Ar*C*), 131.9 (Ar*C*H), 130.2 (Ar*C*H), 128.9 (Ar*C*H), 128.6 (Ar*C*H), 128.4 (Ar*C*H), 124.1 (C(O)*C*HCH), 61.4 (C(O)*C*H_2CH_3), 14.4 (C(O)CH_2*C*H_3) ppm; **m.p.**: 81-82 °C (lit. 77-79 °C).

(*E*)-3-(3,4-dimethoxyphenyl)-1-phenylprop-2-en-1-one (S45)

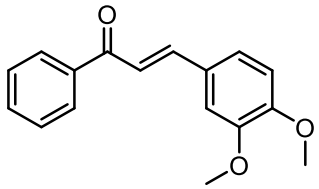

Prepared following **General Procedure G**, using acetophenone and 3,4-(dimethoxy)benzaldehyde to afford the title compound as a pale yellow solid (1.23 g, 92%). Data is consistent with the published literature.[269]

^{1}H NMR (400 MHz, $CDCl_3$): δ 8.02 – 7.95 (m, 2H, Ar*H*), 7.71 (d, *J* = 15.6 Hz, 1H, C(O)CHC*H*), 7.53 – 7.39 (m, 3H, Ar*H*), 7.37 (d, *J* = 15.6 Hz, 1H, C(O)C*H*CH), 7.18 – 7.09 (m, 2H, Ar*H*), 6.81 (d, *J* = 8.3 Hz, 1H, Ar*H*), 3.87 (s, 3H, OCH_3), 3.84 (s, 3H, OCH_3) ppm; **^{13}C NMR (101 MHz, $CDCl_3$)**: δ 190.3 (*C*(O)), 151.4 (Ar*C*), 149.2 (Ar*C*), 144.9 (C(O)CH*C*H), 138.4 (Ar*C*), 132.6 (Ar*C*H), 128.5 (Ar*C*H), 128.4 (Ar*C*H), 127.8 (Ar*C*), 123.2 (Ar*C*H), 119.9 (C(O)*C*HCH), 111.1 (Ar*C*H), 110.1 (Ar*C*H), 55.9 (O*C*H_3) , 55.9 (O*C*H_3) ppm; **m.p.**: 94-95 °C (lit 92-93 °C).

(*E*)-3-(4-(2,2-difluorocyclopropyl)phenyl)-1-phenylprop-2-en-1-one (S46)

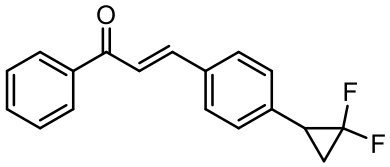

To a solution of **S40** (0.750 g, 3.21 mmol, 1.0 eq) in THF (30 ml) at room temperature under a nitrogen atmosphere was added NaI (1.20 g, 8.01 mmol, 2.50 eq) and trifluoromethyltrimethylsilane (1.14 g, 8.01 mmol, 2.5 eq). The resulting mixture was heated to 50 °C for 20 hours before dilution with EtOAc (50 ml). The mixture was washed with brine (50 ml), dried over Na_2SO_4, filtered and evaporated to dryness *in vacuo*. Purification by flash column chromatography (5% EtOAc in hexanes) afforded the title compound as an orange solid (711 mg, 78 %).

^{1}H NMR (400 MHz, $CDCl_3$): δ 8.00 – 7.90 (m, 2H, Ar*H*), 7.72 (d, *J* = 15.7 Hz, 1H, C(O)C*H*CH), 7.57 – 7.48 (m, 3H, Ar*H*), 7.48 – 7.40 (m, 3H, Ar*H* and C(O)CHC*H*), 7.24 – 7.15 (m, 2H, Ar*H*), 2.80 – 2.62 (m, 1H, ArC*H*), 1.89 - 1.71 (m, 1H, *CH*H), 1.68 – 1.53 (m, 1H, CH*H*) ppm; **^{13}C NMR (101 MHz, $CDCl_3$)**: δ 190.5 (*C*(O)), 144.2 (C(O)CH*C*H), 138.2 (Ar*C*), 136.4 (Ar*C*), 133.9 (Ar*C*), 132.8 (Ar*C*H), 128.6 (Ar*C*H), 128.56 (Ar*C*H), 128.5 (Ar*C*H), 128.5 (Ar*C*H), 122.2 (C(O)*C*HCH), 116.5 – 108.6 (m, *C*FF), 27.8 – 26.7 (m, *C*HCF$_2$), 17.4 (t, *J* = 10.4 Hz, *C*H$_2$) ppm; **^{19}F NMR (377 MHz, $CDCl_3$)** δ -125.56 (ddd, *J* = 154.6, 12.7, 4.0 Hz, C*F*$_A$F$_B$), -142.09 (ddd, *J* = 154.6, 12.8, 5.2 Hz, CF$_A$*F*$_B$) ppm; **FT-IR (thin film)** ν_{max} 1661, 1576, 1518, 1416, 1379, 1084, 902, 696 cm^{-1}; **HRMS** (ESI) m/z calcd. for $C_{18}H_{15}OF_2$ ([M+H]$^+$) 285.10855, found 285.10849; **m.p.**: 81-83 °C.

(*E*)-1-(2,3-dihydro-1H-inden-5-yl)-3-phenylprop-2-en-1-one (S47)

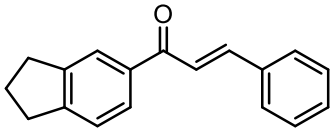

Prepared following **General Procedure G,** using 5-acetylindane and benzaldehyde to afford the title compound as a pale-yellow powder (1.69 g 68%).

^{1}H NMR (400 MHz, $CDCl_3$): δ 7.84 – 7.68 (m, 3H, Ar*H* and C(O)C*H*CH), 7.59 – 7.52 (m, 2H, Ar*H*), 7.46 (d, *J* = 15.7 Hz, 1H, C(O)CHC*H*), 7.36 – 7.30 (m, 2H, Ar*H*), 7.28 – 7.22 (m, 1H, Ar*H*), 2.89 (m, 4H, Ar-C*H*$_2$-CH$_2$-C*H*$_2$-Ar), 2.11 – 1.99 (m, 2H, Ar-CH$_2$-C*H*$_2$-CH$_2$-Ar) ppm; **^{13}C NMR (101 MHz, $CDCl_3$)**: δ 190.4 (*C*(O)), 150.0 (Ar*C*) , 144.9 (Ar*C*), 144.2 (C(O)CH*C*H), 136.7 (Ar*C*), 135.1 (Ar*C*), 130.3 (Ar*C*H) , 128.9 (Ar*C*H), 128.4 (Ar*C*H), 127.1 (Ar*C*H), 124.5 (Ar*C*H), 124.3 (Ar*C*H), 122.5 (C(O)*C*HCH), 33.0 (*C*H$_2$), 32.6 (*C*H$_2$), 25.4 (*C*H$_2$) ppm; **HRMS** (ESI) m/z calcd. for $C_{18}H_{17}O$ ([M+H]$^+$) 249.12739, found 249.12746; **FT-IR (thin film)** ν_{max} 2962, 1678, 1591, 988 cm^{-1}; **m.p.**: 98-100 °C.

(*E*)-1-(2-fluorophenyl)-3-phenylprop-2-en-1-one (S48)

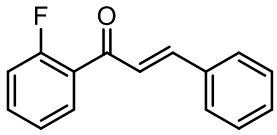

Prepared following **General Procedure G**, using 2'-fluoroacetophenone and benzaldehyde to afford the title compound as a pale-yellow oil (0.972 g, 86%). Data is consistent with the published literature.[270]

^{1}H NMR (400 MHz, $CDCl_3$): δ 7.84 (td, *J* = 7.5, 1.9 Hz, 1H, Ar*H*), 7.77 (dd, *J* = 15.8, 1.8 Hz, 1H, Ar*H,* C(O)CHC*H*), 7.68 – 7.60 (m, 2H, Ar*H*), 7.54 (dddd, *J* = 8.3, 7.1, 5.1, 1.9 Hz, 1H, Ar*H*), 7.47 – 7.38 (m, 4H, Ar*H* and C(O)CHC*H*), 7.28 (td, *J* = 7.5, 1.1 Hz, 1H, Ar*H*), 7.19 (ddd, *J* = 10.8, 8.3, 1.1 Hz, 1H, Ar*H*) ppm; **^{13}C NMR (101 MHz, $CDCl_3$)**: δ 189.0 (d, *J* = 3.0 Hz, (*C*(O))), 161.2 (d, *J* = 252.8 Hz, Ar*C*F), 144.8 (C(O)CH*C*H), 134.7 (Ar*C*), 133.9 (d, *J* = 8.8 Hz, Ar*C*H), 130.9 (d, *J* = 2.5 Hz, Ar*C*H), 130.6 (Ar*C*H), 128.9 (Ar*C*H), 128.6 (Ar*C*H), 127.2 (d, *J* = 13.4 Hz, Ar*C*), 125.6 (d, *J* = 6.4 Hz, (Ar*C*H)), 124.5 (d, *J* = 3.7 Hz, (Ar*C*H)), 116.5 (d, *J* = 23.2 Hz, C(O)*C*HCH) ppm; **^{19}F NMR (376 MHz, $CDCl_3$)**: δ -110.50 – -111.12 (m) ppm.

(*E*)-1-(3,5-bis(trifluoromethyl)phenyl)-3-phenylprop-2-en-1-one (S49)

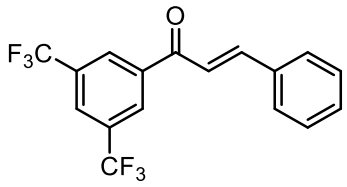

Prepared following **General Procedure G**, using acetophenone and 3,5-(trifluoromethyl)benzaldehyde to afford the title compound as a pale yellow solid (1.36 g, 79%).

^{1}H NMR (400 MHz, $CDCl_3$): δ 8.52 – 8.40 (m, 2H, Ar*H*), 8.16 – 8.07 (m, 1H, Ar*H*), 7.94 (d, *J* = 15.6 Hz, 1H, C(O)C*H*CH), 7.76 – 7.65 (m, 2H, Ar*H*), 7.56 – 7.44 (m, 4H, Ar*H* and C(O)CHC*H*) ppm; **^{13}C NMR (101 MHz, $CDCl_3$)**: δ 187.3 (*C*(O)), 147.3 (C(O)CH*C*H), 139.8 (Ar*C*), 134.1 (Ar*C*), 132.3 (q, *J* = 34.1 Hz, *C*CF_3), 131.3 (Ar*C*H), 129.1 (Ar*C*H), 128.8 (Ar*C*H), 128.4 – 128.3 (m, Ar*C*(H)CCF_3), 126.2 – 125.4 (m, Ar*C*(H)CCF_3), 122.8 (q, *J* = 273.0 Hz, *C*F_3), 120.2 (C(O)*C*HCH) ppm; **^{19}F NMR (377 MHz, $CDCl_3$)** δ -62.90 ppm; **FT-IR (thin film)** ν_{max} 1662, 1575, 1518, 1416, 1288, 957, 654 cm^{-1}; **HRMS** (ESI) m/z calcd. for $C_{17}H_{11}OF_6$ ($[M+H]^+$) 345.07086, found 345.07092; **m.p.**: 84-86 °C.

(*E*)-1-(3,4-dichlorophenyl)-3-(4-(methylthio)phenyl)prop-2-en-1-one (S50)

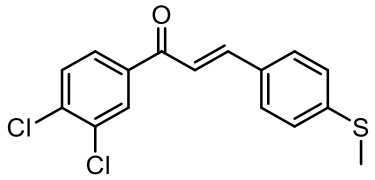

Prepared following **General Procedure G**, using 3,4-dichloroacetophenone and 4-(methylthio)benzadeldhyde to afford the title compound as a bright yellow powder (1.33 g, 83%).

^{1}H NMR (400 MHz, $CDCl_3$): δ 8.01 (d, *J* = 2.1 Hz, 1H, Ar*H*), 7.76 (dd, *J* = 8.3, 2.1 Hz, 1H, Ar*H*), 7.72 (d, *J* = 15.6 Hz, 1H, C(O)CHC*H*), 7.53 – 7.45 (m, 3H, Ar*H*), 7.32 (d, *J* = 15.6 Hz, 1H, C(O)C*H*CH), 7.22 – 7.15 (m, 2H, Ar*H*), 2.45 (s, 3H, SCH_3) ppm; **^{13}C NMR (101 MHz, $CDCl_3$)**: δ 187.8 (*C*(O)), 145.5 (C(O)CH*C*H), 143.1 (Ar*C*), 137.9 (Ar*C*), 137.2 (Ar*C*), 133.2 (Ar*C*), 130.9 (Ar*C*), 130.7 (Ar*C*H), 130.4 (Ar*C*H), 128.9 (Ar*C*H), 127.4 (Ar*C*H), 125.9 (Ar*C*H), 119.77 (C(O)*C*HCH), 15.0 (S*C*H_3) ppm; **HRMS** (ESI) m/z calcd. for $C_{16}H_{13}OCl_2S$ ($[M+H]^+$) 323.00587, found 323.00589; **FT-IR (thin film)** ν_{max} 1655, 585, 1552, 1314, 1216, 1026, 804 cm^{-1}; **m.p.**: 139-141 °C.

(*E*)-3-(6-bromobenzo[*d*][1,3]dioxol-5-yl)-1-phenylprop-2-en-1-one (S51)

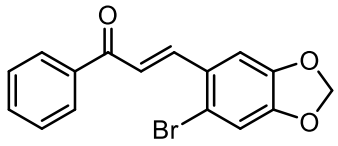

Prepared following **General Procedure G**, using acetophenone and 6-bromobenzo[*d*][1,3]dioxole-5-carbaldehyde to afford the title compound as a pale yellow solid (1.17 g, 71%). Data is consistent with the published literature.[271]

^{1}H NMR (400 MHz, $CDCl_3$): δ 8.06 (d, *J* = 15.7 Hz, C(O)C*H*CH), 8.00 – 7.96 (m, 2 H, Ar*H*), 7.61 – 7.42 (m, 3H, Ar*H*), 7.30 (d, *J* = 15.7, C(O)C*H*CH), 7.22 (s, 1H, Ar*H*), 7.10 (s,1H, Ar*H*), 6.08 (s, 2H, CH_2) ppm; **^{13}C NMR (101 MHz, $CDCl_3$)**: δ 189.6 (*C*(O)), 150.2 (Ar*C*), 147.9 (C(O)CH*C*H), 143.1 (Ar*C*), 138.2 (Ar*C*), 132.7 (Ar*C*H), 128.6 (Ar*C*), 128.4 (Ar*C*H), 126.8 (Ar*C*H), 123.0 (C(O)*C*HCH), 118.8 (Ar*C*H), 113.4 (Ar*C*), 106.5 (Ar*C*H), 102.2 (*C*H_2) ppm; **m.p.**: 143-144 °C (lit. 140-142 °C).

(*E*)-3-(4-bromophenyl)-1-(pyrazin-2-yl)prop-2-en-1-one (S52)

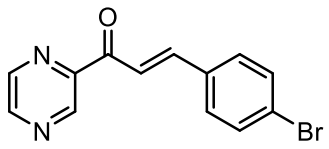

Acetylpyrazine (0.55 g, 4.51 mmol, 1.0 eq), 4-bromobenzaldehyde (0.834 g, 4.51 mmol, 1.0 eq), dimethylamine (0.21 g, 4.51 mmol, 1.0 eq) and pyridine (2.2 mL) were combined and stirred under a N_2 atmosphere at 100 °C for 20 hours. The mixture was quenched with 2M aqueous HCl (100 mL) and extracted with EtOAc (200 mL). The organic layer was dried over Na_2SO_4, filtered and evaporated to a brown solid, which was triturated with pentane. The solid obtained was recrystallized from EtOH to afford the title compound as a bright yellow solid (1.17 g, 71%). Data is consistent with the published literature.12

^{1}H NMR (400 MHz, $CDCl_3$): δ 9.39 (d, *J* = 1.5 Hz, 1H, Ar*H*), 8.80 (d, *J* = 2.5 Hz, 1H, Ar*H*), 8.71 (dd, *J* = 2.5, 1.5 Hz, 1H, Ar*H*), 8.19 (d, *J* = 16.0 Hz, 1H, C(O)C*H*CH), 7.92 (d, *J* = 16.0 Hz, 1H, C(O)C*H*CH), 7.71 – 7.53 (m, 4H, Ar*H*) ppm; **^{13}C NMR (101 MHz, $CDCl_3$)**: δ 188.4 (*C*(O)), 148.3 (Ar*C*), 147.5 (C(O)CH*C*H), 144.9 (Ar*C*H), 144.2 (Ar*C*H), 143.3 (Ar*C*H), 133.6 (Ar*C*), 132.2 (Ar*C*H), 130.2 (Ar*C*H), 125.3 (Ar*C*), 120.6 (C(O)*C*HCH) ppm; **m.p.**: 143-144 °C (lit. 140-142 °C).

(*E*)-1-phenyl-3-(thiophen-2-yl)prop-2-en-1-one (S53)

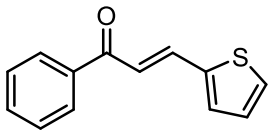

Prepared following **General Procedure G**, using acetophenone and 2-thiophenecarboxaldehyde to afford the title compound as a pale-yellow solid (0.845 g, 79%). Data is consistent with the published literature.[272]

^{1}H NMR (400 MHz, $CDCl_3$): δ 8.07 – 8.00 (m, 2H, Ar*H*), 7.97 (d, *J* = 15.3 Hz, 1H, C(O)CHC*H*), 7.64 – 7.56 (m, 1H, Ar*H*), 7.56 – 7.48 (m, 2H, Ar*H*), 7.46 – 7.31 (m, 3H, Ar*H* and C(O)CHC*H*), 7.11 (dd, *J* = 5.1, 3.6 Hz, 1H, Ar*H*) ppm; **^{13}C NMR (101 MHz, $CDCl_3$)**: δ 189.8 (*C*(O)), 140.4 (Ar*C*), 138.1 (Ar*C*), 137.1 (C(O)CH*C*H), 132.7 (Ar*C*H), 132.0 (Ar*C*H), 128.8 (Ar*C*H), 128.6 (Ar*C*H), 128.4 (C(O)*C*HCH), 128.3 (Ar*C*H), 120.8 (Ar*C*H) ppm; **m.p.**: 58-59 °C (lit. 58-59 °C).

(*E*)-3-phenyl-1-(pyridin-4-yl)prop-2-en-1-one (S54)

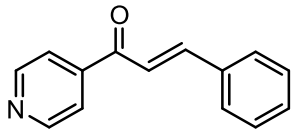

4-acetylpyridine (2.06 g, 17.0 mmol, 1.03 eq) and benzaldehyde (1.75 g, 16.5 mmol, 1.0 eq) were added to 100 mL of water, which was previously cooled to 4 °C. The resulting mixture was shaken vigorously, followed by addition of a 10% aqueous solution of NaOH (10.0 mL) before shaking again. The mixture was allowed to sit (without stirring) at 4 °C for 20 hours. The mixture was periodically shaken during this time. Extraction of the formed solid with EtOAc (3x100 mL) with subsequent drying over Na_2SO_4, filtration and evaporation to dryness in vacuo afforded a dark brown solid. Purification by silica gel chromatography afforded the title compound as a light-yellow powder (2.59 g, 73%). Data is consistent with the published literature.[273]

^{1}H NMR (400 MHz, $CDCl_3$): δ 8.67 (ddd, *J* = 4.7, 1.8, 0.9 Hz, 1H, Ar*H*), 8.23 (d, *J* = 16.0 Hz, 1H, C(O)CHC*H*), 8.12 (dt, *J* = 7.9, 1.1 Hz, 1H, Ar*H*), 7.87 (d, *J* = 16.1 Hz, 1H, C(O)C*H*CH), 7.80 (td, *J* = 7.7, 1.7 Hz, 1H, Ar*H*), 7.71 – 7.60 (m, 2H, Ar*H*), 7.46 – 7.37 (m, 1H, Ar*H,* Ar*H*), 7.36 – 7.30 (m, 3H, Ar*H*) ppm; **^{13}C NMR (101 MHz, $CDCl_3$)**: δ 189.4 (*C*(O)), 154.2 (Ar*C*), 148.8 (Ar*C*H), 144.7 (C(O)CH*C*H), 136.9 (Ar*C*H), 135.1 (Ar*C*), 130.5 (Ar*C*H), 128.8 (Ar*C*H), 126.8 (Ar*C*H), 122.9 (Ar*C*H), 120.9 (C(O)*C*HCH) ppm; **FT-IR (thin film)** ν_{max} 3050, 2161, 1667, 1572, 1665, 1172, 987, 753 cm^{-1}.

(*E*)-3-cyclohexyl-1-phenylprop-2-en-1-one (S55)

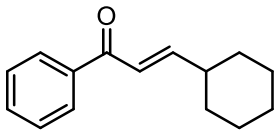

Prepared following **General Procedure H**, using cyclohexanecarboxaldehyde to afford the title compound as a pale-yellow oil (2.06 g, 85%). Data is consistent with the published literature.[274]

^{1}H NMR (400 MHz, $CDCl_3$): δ 7.94 – 7.75 (m, 2H, Ar*H*), 7.50 – 7.42 (m, 1H, Ar*H*), 7.42 – 7.30 (m, 2H, Ar*H*), 6.94 (dd, *J* = 15.6, 6.8 Hz, 1H, C(O)CHC*H*), 6.75 (dd, *J* = 15.5, 1.3 Hz, 1H, C(O)C*H*CH), 2.18 (dddd, *J* = 14.4, 6.8, 3.4, 1.3 Hz, 1H, AlkC*H*), 1.82 – 1.67 (m, 4H, AlkC*H*), 1.62 (dqt, *J* = 10.0, 3.2, 1.6 Hz, 1H, AlkC*H*), 1.34 – 1.02 (m, 5H, AlkC*H*) ppm; **^{13}C NMR (101 MHz, $CDCl_3$)**: δ 191.3 (*C*(O)), 154.8 (C(O)CH*C*H), 138.1 (Ar*C*), 132.5 (Ar*C*H), 128.5 (Ar*C*H), 128.4 (Ar*C*H), 123.4 (C(O)*C*HCH), 41.0 (Alk*C*H), 31.8 (Alk*C*H), 25.9 (Alk*C*H), 25.7 (Alk*C*H) ppm; **FT-IR (thin film)** ν_{max} 3061, 3019, 2935, 2841, 1724, 1663, 1440, 1339, 1009, 981 cm^{-1}.

(*E*)-3-cyclopropyl-1-phenylprop-2-en-1-one (S56)

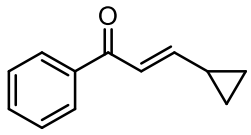

Prepared following **General Procedure H,** using cyclopropanecarboxaldehyde to afford the title compound as a pale-yellow oil (1.71 g, 88%). Data is consistent with the published literature.[274]

^{1}H NMR (400 MHz, $CDCl_3$): δ 8.00 – 7.92 (m, 2H, Ar*H*), 7.60 – 7.52 (m, 1H, Ar*H*), 7.51 – 7.42 (m, 2H, Ar*H*), 7.04 (d, *J* = 15.1 Hz, 1H, C(O)C*H*CH), 6.58 (dd, *J* = 15.1, 10.2 Hz, 1H, C(O)CHC*H*), 1.73 (dddd, *J* = 12.4, 9.1, 6.3, 4.0 Hz, 1H, AlkC*H*), 1.08 – 1.00 (m, 2H, AlkC*H*), 0.79 – 0.72 (m, 2H, AlkC*H*) ppm; **^{13}C NMR (101 MHz, $CDCl_3$)**: δ 189.9 (*C*(O)), 155.1 (C(O)CH*C*H), 138.2 (Ar*C*), 132.4 (Ar*C*H), 128.4 (Ar*C*H), 128.3 (Ar*C*H), 122.8 (C(O)*C*HCH), 15.3 (Alk*C*H), 9.2 (Alk*C*H) ppm; **FT-IR (thin film)** ν_{max} 3070, 2995, 1653, 1450, 1284, 1215, 1175, 929, 891, 700, cm^{-1}.

(*E*)-1-phenyloct-2-en-1-one (S57)

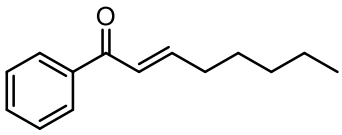

Prepared following **General Procedure G**, using acetophenone and 1-hexanal to afford the title compound as a pale-yellow oil (0.909 g, 90%). Data is consistent with the published literature.[275]

^{1}H NMR (400 MHz, $CDCl_3$): δ 7.96 (d, *J* = 7.2 Hz, 2H, Ar*H*), 7.58 (m, 1H, Ar*H*), 7.46 (m, 2H, Ar*H*), 7.14-7.06 (m, 1H, C(O)C*H*CH), 6.89 (d, *J*= 15.2, 1H, C(O)CHC*H*), 2.29 (dd, *J* = 14.1, 6.4 Hz, 2H, AlkC*H*), 1.49 (m, 2H, AlkC*H*), 1.35 (m, 4H, AlkC*H*), 0.93 (t, *J* = 6.7, 3H, AlkCH_3) ppm; **^{13}C NMR (101 MHz, $CDCl_3$)**: δ 190.9 (*C*(O)), 150.1 (C(O)CH*C*H), 138.0 (Ar*C*), 132.5 (Ar*C*H), 128.2 (Ar*C*H), 128.4 (Ar*C*H), 125.8 (C(O)*C*HCH), 32.8 (Alk*C*H), 31.4 (Alk*C*H), 27.8 (Alk*C*H), 22.4 (Alk*C*H), 13.9 (Alk*C*H_3) ppm; **FT-IR (thin film)** ν_{max} 2972, 2856, 1669, 1619, 1280, 1011, 690 cm^{-1}.

(*E*)-1-phenyldec-2-en-4-yn-1-one (S58)

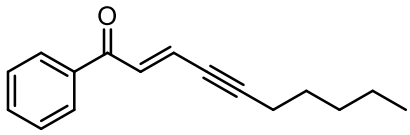

Prepared following **General Procedure A**, using acetophenone and 2-octynal to afford the title compound as a pale-yellow oil (0.915 g, 81%). Data is consistent with the published literature.[276]

^{1}H NMR (400 MHz, $CDCl_3$): δ 8.09 – 7.90 (m, 2H, Ar*H*), 7.64 – 7.53 (m, 1H, Ar*H*), 7.53 – 7.40 (m, 2H, Ar*H*), 7.29 (d, *J* = 15.5 Hz, 2H, C(O)C*H*CH), 6.92 (dt, *J* = 15.5, 2.3 Hz, 1H, C(O)CHC*H*), 2.44 (tdd, *J* = 7.2, 2.4, 0.7 Hz, 2H, AlkC*H*), 1.70 – 1.53 (m, 2H, AlkC*H*), 1.48 – 1.31 (m, 4H, AlkC*H*), 0.95 (t, *J* = 7.1 Hz, 3H, AlkC*H*$_3$) ppm; **^{13}C NMR (101 MHz, $CDCl_3$)**: δ 189.4 (*C*(O)), 137.5 (Ar*C*), 133.2 (C(O)CH*C*H), 133.0 (Ar*C*H), 132.7 (Ar*C*H), 128.8 (Ar*C*H), 126.5 (C(O)CH*C*H), 102.2 (C≡*C*CH$_2$), 79.4 (*C*≡CCH$_2$), 30.6 (Alk*C*H), 28.3 (Alk*C*H), 22.2 (Alk*C*H), 19.8 (Alk*C*H), 13.7 (Alk*C*H) ppm; **FT-IR (thin film)** ν_{max} 2963, 2870, 2859, 2353, 2212, 1585, 1457, 1291, 1199, 1002 cm^{-1}.

(*E*)-1,5-diphenylpent-1-en-4-yn-3-one (S59)

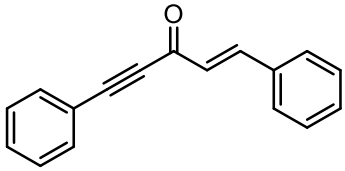

Cinnamoyl chloride (1.35 g, 8.17 mmol, 1.0 eq) was added dropwise to a stirred mixture of phenylacetylene (1.0 g, 9.8 mmol, 1.2 eq), copper iodide (108 mg, 0.57 mmol, 0.07 eq) and $Pd(PPh_3)_2Cl_2$ (172 mg, 0.245 mmol, 0.03 eq) in triethylamine (1.0 mL). The resulting mixture was stirred at room temperature for 90 minutes under an N_2 atmosphere before filtering through celite with EtOAc and evaporating to dryness *in vacuo*. The crude residue was dissolved in CH_2Cl_2 (100 mL), washed with brine, dried over Na_2SO_4, filtered, and evaporated to dryness *in vacuo*. Subsequent purification by flash column chromatography (2% EtOAc in hexanes) afforded the title compound as a yellow powder. Data is consistent with the published literature.[277]

^{1}H NMR (400 MHz, $CDCl_3$): δ 7.93 (d, *J* = 16.1 Hz, 1H, Ar*H*), 7.70 – 7.65 (m, 2H, Ar*H* and C(O)CHC*H*), 7.61 – 7.57 (m, 2H, Ar*H*), 7.50 – 7.37 (m, 6H, Ar*H*), 6.90 (d, *J* = 16.1 Hz, 1H, C(O)C*H*CH) ppm; **^{13}C NMR (101 MHz, $CDCl_3$)**: δ 178.3 (*C*(O)), 148.4 (C(O)CH*C*H), 134.0 (Ar*C*), 132.9 (Ar*C*H), 131.2 (Ar*C*H), 130.6 (Ar*C*H), 129.1 (C(O)*C*HCH), 128.7 (Ar*C*H), 128.7 (Ar*C*H), 128.5 (Ar*C*H), 120.2 (Ar*C*), 91.6 (Ar*C*≡C), 86.6 (ArC≡*C*) ppm; **m.p.**: 71-72 °C (lit. 71-72 °C).

(*E*)-1,1,1-trifluoro-4-phenylbut-3-en-2-one (S60)

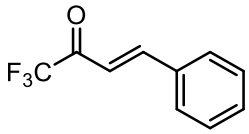

To a solution of benzaldehyde (3.18 g, 30 mmol, 1.0 eq) and 1,1,1-trifluoroacetone (13.44 g, 120 mmol, 4.0 eq) in cyclohexane (45 mL) at room temperature was added piperidine (2.55 g, 30 mmol, 1.0 eq) and acetic acid (2.70 g, 45 mmol, 1.5 eq). The resulting mixture was stirred at room temperature under a N_2 atmosphere for 9 hours. The mixture was quenched with a saturated aqueous solution of $NaHCO_3$ (100 mL), extracted with diethyl ether (200 mL), dried over Na_2SO_4, filtered, and evaporated to dryness. Purification by silica gel chromatography (2% EtOAc in hexanes) afforded the title compound as a bright yellow oil. Data is consistent with the published literature.[278]

^{1}H NMR (400 MHz, $CDCl_3$): δ 7.89 (d, *J* = 15.9 Hz, 1H, C(O)CHC*H*), 7.63 – 7.51 (m, 2H, Ar*H*), 7.46 – 7.33 (m, 3H, Ar*H*), 6.94 (dt, *J* = 16.0, 1.0 Hz, 1H, C(O)C*H*CH) ppm; **^{13}C NMR (101 MHz, $CDCl_3$)**: δ 178.3 (*C*(O)), 148.4 (C(O)CH*C*H), 134.0 (Ar*C*), 132.9 (Ar*C*H), 131.2 (Ar*C*H), 130.6 (Ar*C*H), 129.1 (C(O)*C*HCH), 128.7 (Ar*C*H), 128.7 (Ar*C*H), 128.5 (Ar*C*H), 120.2 (Ar*C*), 91.6 (Ar*C*≡C), 86.6 (ArC≡*C*) ppm; **^{19}F NMR (377 MHz, $CDCl_3$)**: δ -77.6 ppm; **m.p.**: 71-72 °C (lit. 71-72 °C).

4.3.2.2 Synthesis of hydrazones

General Procedure I for the synthesis of hydrazones by condensation:

To a solution of the appropriate aldehyde (1.0 eq) in toluene (0.1M) at room temperature was added 3Å molecular sieves (200 mg), followed by methyl hydrazine (2.0 eq). The reaction was stirred at room temperature for 4 hours, then filtered and concentrated to dryness *in vacuo*. Purification by silica gel chromatography (petroleum ether-EtOAc) afforded the pure hydrazones.

(*E*)-1-benzylidene-2-methylhydrazine (192)

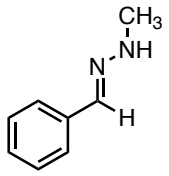

Prepared following General Procedure **I**, using benzaldehyde (1.06 g, 10.0 mmol) to afford the title compound as a colourless solid (1.18 g, 88%). Data is consistent with the published literature.[220]

^{1}H NMR (400 MHz, $CDCl_3$): 7.60 (d, 2H, *J* = 8.0 Hz), 7.56 (s, 1H), 7.42−7.30 (m, 2H), 7.27 (t, 1H, *J* = 7.1 Hz), 2.99 (s, 3H); **^{13}C NMR (101 MHz, $CDCl_3$)**: δ 136.7, 135.9, 128.3, 127.4, 126.1, 35.0 ppm.

(*E*)-1-methyl-2-(4-methylbenzylidene)hydrazine (208)

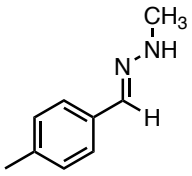

Prepared following General Procedure **I**, using 4-methylbenzaldehyde (1.20 g, 10.0 mmol) to afford the title compound as a colourless solid (1.01 g, 68%). Data is consistent with the published literature.[220]

^{1}H NMR (400 MHz, $CDCl_3$): 7.55 (s, 1H), 7.50 (d, *J* = 8.0 Hz, 2H), 7.12 (d, *J* = 8.0 Hz, 2H), 2.99 (s, 3H), 2.32 (s, 3H) ppm; **^{13}C NMR (101 MHz, $CDCl_3$)**: δ 138.0, 136.4, 133.6, 129.0, 126.0, 34.6, 21.0 ppm.

(*E*)-1-methyl-2-(2-methylbenzylidene)hydrazine (209)

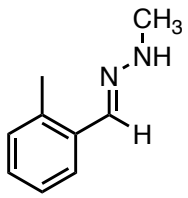

Prepared following General Procedure **I**, using 2-methylbenzaldehyde (1.20g, 10.0 mmol) to afford the title compound as a colourless solid (1.11 g, 75%).

^{1}H NMR (400 MHz, $CDCl_3$): 7.77 – 7.68 (m, 2H), 7.39 – 7.21 (m, 3H), 2.93 (s, 3H), 2.49 (s, 3H) ppm.; **^{13}C NMR (101 MHz, $CDCl_3$)**: δ 140.9, 136.2, 133.0, 131.2, 129.1, 127.8, 127.3, 35.0, 19.8 ppm; **HRMS** (ESI) m/z calcd. for $C_9H_{13}N_2$ ($[M+H]^+$) 148.10787, found 148.10790.

(*E*)-1-(4-(*tert*-butyl)benzylidene)-2-methylhydrazine (210)

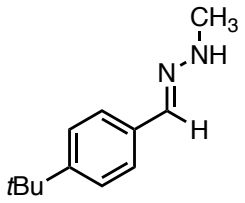

Prepared following General Procedure **I**, using 4-(*tert*-butyl)benzaldehyde (1.62 g, 10.0 mmol) to afford the title compound as a colourless solid (1.56 g, 82%).

^{1}H NMR (400 MHz, $CDCl_3$): 7.50 (s, 1H), 7.46 – 7.40 (m, 2H), 7.16 – 7.09 (m, 2H), 3.00 (s, 3H),1.40 (s, 9H) ppm; **^{13}C NMR (101 MHz, $CDCl_3$)**: δ 137.2, 135.1, 134.0, 128.2, 125.2, 34.9, 32.5 31.0 ppm; **HRMS** (ESI) m/z calcd. for $C_{12}H_{19}N_2$ ($[M+H]^+$) 191.15482, found 191.15478.

(*E*)-1-methyl-2-(4-fluorobenzylidene)hydrazine (211)

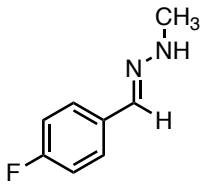

Prepared following General Procedure **I**, using 4-fluorobenzaldehyde (1.24 g, 10.0 mmol) to afford the title compound as a colourless solid (684 mg, 45%).

^{1}H NMR (400 MHz, $CDCl_3$): 7.79 (s, 1H), 7.72 – 7.64 (m, 2H), 7.42 – 7.32 (m, 2H), 2.97 (s, 3H) ppm; **^{13}C NMR (101 MHz, $CDCl_3$)**: δ 161.8 (d, *J* = 248.5 Hz), 142.0, 130.2 (d, *J* = 2.9 Hz), 128.5 (d, *J* = 8.2 Hz), 115.7 (d, *J* = 21.6 Hz), 35.2 ppm; **^{19}F NMR (376 MHz, $CDCl_3$)**: δ -112.9 (s) ppm; **HRMS** (ESI) m/z calcd. for $C_9H_{10}FN_2$ ($[M+H]^+$) 153.08280, found 153.08275.

(*E*)-1-([1,1'-biphenyl]-4-ylmethylene)-2-methylhydrazine (212)

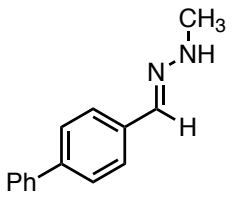

Prepared following General Procedure **I**, using 4-phenylbenzaldehyde (1.82 g, 10.0 mmol) to afford the title compound as a colourless solid (1.07 g, 51%).

^{1}H NMR (400 MHz, $CDCl_3$): 7.56 (s, 1H), 7.50 (d, *J* = 8.0 Hz, 2H), 7.45 – 7.38 (m, 2H), 7.20 – 7.14 (m, 3H), 7.10 (d, *J* = 8.0 Hz, 2H), 2.82 (s, 3H), 2.30 (s, 3H) ppm; **^{13}C NMR (101 MHz, $CDCl_3$)**: δ 138.2, 138.1, 137.1, 136.0, 133.1, 128.2, 125.5, 34.6 ppm; **HRMS** (ESI) m/z calcd. for $C_{14}H_{14}N_2$ ($[M+H]^+$) 211.12352, found 211.12349.

(*E*)-1-methyl-2-(naphthalen-2-ylmethylene)hydrazine (213)

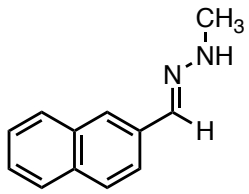

Prepared following General Procedure **I**, using 2-naphthaldehyde (1.56 g, 10.0 mmol) to afford the title compound as a colourless solid (1.09 g, 59%).

^{1}H NMR (400 MHz, $CDCl_3$): 8.21 – 8.15 (m, 1H), 7.90 – 7.83 (m, 3H), 7.80 (s, 1H), 7.60 – 7.53 (m, 2H), 2.88 (s, 3H) ppm.; **^{13}C NMR (101 MHz, $CDCl_3$)**: δ 141.5, 134.0, 132.1, 130.2, 129.3, 128.6, 127.2, 126.9, 124.9, 35.8 ppm; **HRMS** (ESI) m/z calcd. for $C_{12}H_{13}N_2$ ($[M+H]^+$) 185.10787, found 185.10783.

(*E*)-1-(cyclohexylmethylene)-2-methylhydrazine (214)

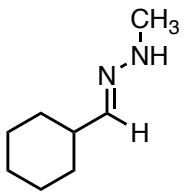

Prepared following General Procedure **I**, using cyclohexylcarboxaldehyde (1.12 g, 10.0 mmol) to afford the title compound as a colourless solid (448 mg, 32%).

^{1}H NMR (400 MHz, $CDCl_3$): 6.91 (s, 1H), 2.84 (s, 3H), 2.47 – 2.38 (m, 1H), 1.90 – 1.61 (m, 4H), 1.55 – 1.35 (m, 6H) ppm; **^{13}C NMR (101 MHz, $CDCl_3$)**: δ 154.3, 39.9, 35.7, 30.1, 29.0, 26.1, 25.6, 24.9 ppm; **HRMS** (ESI) m/z calcd. for $C_8H_{17}N_2$ ($[M+H]^+$) 141.13917, found 141.13921.

4.3.3 Synthesis of catalyst 200

9-amino-9-deoxy-epi-cinchonidine (202)

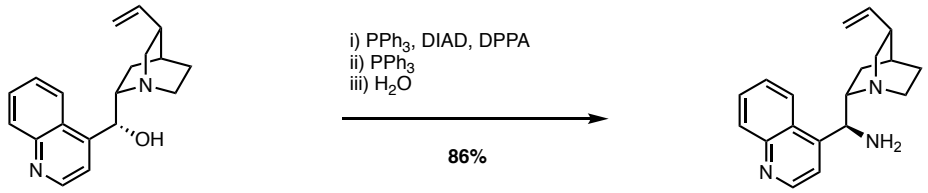

201 202

Prepared according to the literature procedure reported by Melchiorre et. al.[279]

To a solution of PPh_3 (3.48 g, 13.27 mmol, 1.3 eq) and cinchonidine (3.0 g, 10.2 mmol, 1.0 eq) in THF (45 mL) at 0 °C, was added diisopropyl azodicarboxylate (2.69 g, 13.27 mmol, 1.,3 eq) at once. After 15 minutes at 0 °C, diphenyl phosphoryl azide (3.645 g, 13.27 mmol, 1.3 eq) was added dropwise over 15 minutes before warming the mixture to 45 °C. After 24 hours at 45 °C, PPh_3 (3.74 g, 14.28 mmol, 1.4 eq) was added, and the mixture stirred at 45 °C for a further 4 hours before cooling to RT. H_2O (3.0 mL) was added, the mixture stirred atroom temperaturefor 4 hours, then solvents removed *in vacuo*. The resulting yellow oil was dissolved in a 1:1 mixture of CH_2Cl_2:HCl (10% aq. solution) (200 mL). The mixture was stirred vigorously to ensure mixing of the layers. After 15 minutes, the CH_2Cl_2 layer was removed and discarded. The water layer was basified to pH 9-10 with NH_4OH solution, then extracted with EtOAc (3 x 100 mL). Combined organic layers were dried over Na_2SO_4, filtered and evaporated to dryness *in vacuo* to afford the crude product as a yellow oil. Purification by flash column chromatography (50:50:1 EtOAc:MeOH:NH_4OH) afforded the title compound as a yellow oil (2.51 g, 84%). This procedure was repeated on 15.0 g scale

(with respect to cinchonidine) to afford the title compound in identical purity and 86% yield. Data is consistent with the published literature.

^{1}H NMR (400 MHz, $CDCl_3$): δ 8.76 (d, *J* = 4.4, 1H), 8.35 (s, 1H), 8.10 (dd, *J* = 8.4, 1.5, 1H), 7.75 (ddd, *J* = 8.4, 7.0, 1.5, 1H), 7.65-7.60 (m, 1H), 7.57-7.51 (m 1H), 5.81 (ddd, *J* = 17.4, 10.6, 7.5, 1H), 5.06–4.95 (m, 2H), 4.73 (m, 1H), 3.31 (dd, *J* = 13.9, 10.0, 1H), 3.22–3.13 (m, 1H), 3.16–3.04 (m, 1H), 2.86–2.72 (m, 2H), 2.31–2.29 (m, 4H), 1.67–1.60 (m, 1H), 1.49–1.56 (m, 2H), 1.41 (t, *J* =11.4, 1H), 0.76 (ddt, *J* =13.7, 7.4, 2.0, 1H) ppm; **^{13}C NMR (101 MHz, $CDCl_3$)**: δ149.2, 148.2, 141.5, 130.3, 129.1, 127.9, 126.9, 123.8, 119.2, 114.1, 62.7, 56.9, 41.5, 40.0, 30.1, 28.5, 27.9, 25.8 ppm.

3,5-dichloro-N-((*S*)-quinolin-4-yl((1*S*,2*S*,4*S*,5*R*)-5-vinylquinuclidin-2-yl)methyl)benzamide (200)

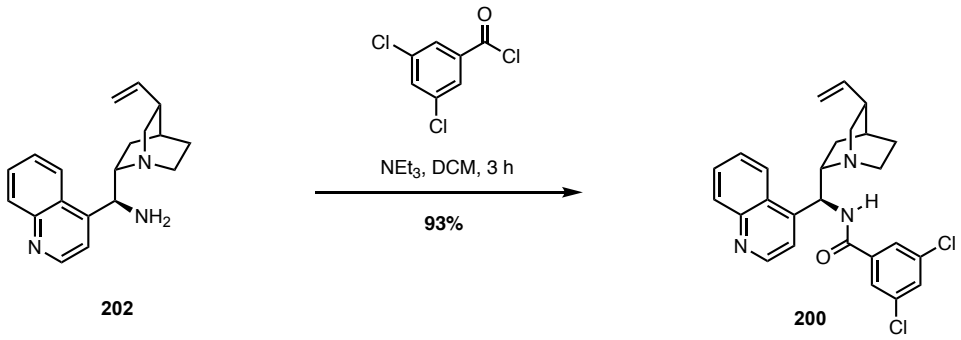

To a solution of 9-amino-9-deoxy-epi-cinchonidine (**202**) (2.66 g, 9.10 mmol, 1.0 eq) in anhydrous CH_2Cl_2 (50 mL) cooled to -15 °C was added NEt_3 (626 mg, 6.20 mmol, 1.37 eq) followed by dropwise addition of a solution of 3,5-dichlorobenzoyl chloride (2.0 g, 9.54 mmol, 1.05 eq) in anhydrous CH_2Cl_2 (5 mL). The reaction mixture was warmed to room temperature and monitored by TLC. After 3 hours, the reaction mixture was washed with brine (100 mL), dried over Na_2SO_4, filtered and evaporated to dryness *in vacuo* to afford the crude amide as a pink powder. Purification by flash column chromatography (20% MeOH in EtOAc) furnished the title compound as a light-yellow powder (3.94 g, 93%). This procedure was repeated on 10.0 g scale (with respect to amine **202**) to afford catalyst **200** in identical purity and 94% yield.

^{1}H NMR (400 MHz, $CDCl_3$): δ 8.90 (d, *J* = 4.5 Hz, 1H, Ar*H*), 8.44 (dd, *J* = 8.6, 1.4 Hz, 1H, Ar*H*), 8.17 (dd, *J* = 8.4, 1.3 Hz, 1H, Ar*H*), 7.86 (s, 1H, N*H*), 7.76 (ddd, *J* = 8.4, 6.8, 1.3 Hz, 1H, Ar*H*), 7.68 – 7.57 (m, 3H, Ar*H*), 7.48-7.43 (m, 2H, Ar*H*), 5.73 (ddd, *J* = 17.4, 10.4, 7.2 Hz, 1H, C*H*CH_2), 5.44 (s, 1H, C*H*NH), 5.04 – 4.96 (m, 2H, CHC*H*$_2$), 3.32 (dd, *J* = 13.9,

10.1 Hz, 1H, AlkCH), 3.25 – 3.14 (m, 2H, AlkCH), 3.14 – 3.03 (m, 1H, AlkCH), 2.79 (tdd, *J* = 14.6, 7.5, 3.8 Hz, 2H, AlkCH), 2.42 – 2.28 (m, 1H, AlkCH), 1.69 (dddd, *J* = 22.8, 13.2, 6.2, 3.0 Hz, 3H, AlkCH), 1.44 (ddt, *J* = 13.2, 9.8, 3.2 Hz, 1H, AlkCH), 1.08 – 0.98 (m, 1H, AlkCH) ppm; **^{13}C NMR (101 MHz, $CDCl_3$)**: δ 164.8 (*C*(O)), 150.1 (Ar*C*H), 148.6 (Ar*C*), 140.3 (*C*HCH$_2$), 136.7 (Ar*C*), 135.3 (Ar*C*H), 134.4 (Ar*C*), 131.4 (Ar*C*H), 130.6 (Ar*C*H), 130.5 (Ar*C*), 129.3 (Ar*C*H), 129.0 (Ar*C*), 127.0 (Ar*C*H), 125.9 (Ar*C*H), 123.0 (Ar*C*H), 115.2 (CH*C*H$_2$), 55.5 (Alk*C*H), 40.8 (Alk*C*H), 39.0 (Alk*C*H), 29.6 (Alk*C*H), 27.4 (Alk*C*H), 27.2 (Alk*C*H), 27.2 (Alk*C*H), 25.6 (Alk*C*H) ppm; **FT-IR (thin film)** ν_{max} 2980, 2161, 2033, 1654, 1527, 1466, 1309, 1236, 1180, 1045, 803, 751, 642 cm^{-1}; **HRMS** (ESI) m/z calcd. for $C_{26}H_{26}ON_3Cl_2$ ($[M+H]^+$) 466.14474, found 466.14450; **m.p.**: 121-123 °C; **$[\alpha]_D^{25}$** = -54.5 (c = 1.0, $CHCl_3$).

4.3.4 Synthesis of 2-pyrazolines

General Procedure J for the synthesis of 2-pyrazolines using methylhydrazine:

To an oven-dried 10 ml screw-cap vial was added ca. 20 molecular sieves (3Å) and a magnetic stirrer bar. Anhydrous PhMe (2.0 mL) was added, followed by the addition of 4-*tert*-butyl-benzaldehyde (162 mg, 1.0 mmol, 2.0 eq) and methylhydrazine (51 μL, 0.975 mmol, 1.95 eq). The mixture was stirred under a nitrogen atmosphere at room temperature. After 4 hours, catalyst **200** (23 mg, 0.05 mmol, 0.1 eq) and the appropriate enone (0.50 mmol, 1.0 eq) were added to the solution of the *in-situ* formed hydrazone. The vial was placed into a freezer and the mixture was stirred at -15 °C for 2 days (unless otherwise indicated) before warming to room temperature and addition of a 30% w/w solution of NH_2OH in methanol (1.0 mL, see page S1 for preparation). The deprotection stage was followed by TLC. After completion (typically two hours), solvents were removed under a stream of nitrogen gas. Purification by silica gel chromatography (EtOAc in hexanes) afforded the enantioenriched 2-pyrazolines.

General Procedure J for the synthesis of 2-pyrazolines using alternative hydrazines:

To an oven-dried 10 ml screw-cap vial was added ca. 20 molecular sieves (3Å) and a magnetic stirrer bar. Anhydrous CH_2Cl_2 (2.0 mL) was added, followed by the addition of 4-*tert*-butyl-benzaldehyde (162 mg, 1.0 mmol, 2.0 eq), the appropriate hydrazine (0.975 mmol, 1.95 eq) and diisopropylethylamine (1.95 eq or 3.8 eq). The mixture was stirred under a nitrogen atmosphere at room temperature. After 4 hours, catalyst **200** (23 mg, 0.05 mmol, 0.1 eq) and

the appropriate enone (0.50 mmol, 1.0 eq) were added to the solution of the *in-situ* formed hydrazone. The vial was placed into a freezer and the mixture was stirred at -15 °C for 2 days (unless otherwise indicated) before warming to room temperature and addition of a 30% w/w solution of NH_2OH in methanol (1.0 mL, see page S1 for preparation). The deprotection stage was followed by TLC. After completion (typically two hours), solvents were removed under a stream of nitrogen gas. Purification by silica gel chromatography (EtOAc in hexanes) afforded the enantioenriched 2-pyrazolines.

(*R*)-1-methyl-3,5-diphenyl-4,5-dihydro-1H-pyrazole (183)

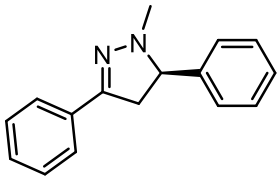

183 was prepared following General Procedure **J**, using chalcone to afford the title compound as a colourless solid (106 mg, 90%, 95:5 er). Data is consistent with the published literature.[280]

^{1}H NMR (400 MHz, $CDCl_3$): δ 7.59 – 7.51 (m, 2H, Ar*H*), 7.39-30 (s, 2H, Ar*H*), 7.28 – 7.15 (m, 6H, Ar*H*), 4.01 (dd, *J* = 14.6, 10.0 Hz, 1H, C*H*NN), 3.35 (dd, *J* = 16.1, 10.0 Hz, 1H, CH_2), 2.92 (dd, *J* = 16.1, 14.6 Hz, 1H, CH_2), 2.83 (s, 3H, NCH_3) ppm; **^{13}C NMR (101 MHz, $CDCl_3$)**: δ 149.6 (*C*(N)), 140.0 (Ar*C*), 132.3 (Ar*C*), 128.4 (Ar*C*H), 128.3 (Ar*C*H), 128.0 (Ar*C*H), 127.7 (Ar*C*H), 127.0 (Ar*C*H), 125.7 (Ar*C*H), 73.4 (*C*NH), 43.4 (*C*H_2), 41.6 (N*C*H_3) ppm; **FT-IR (thin film)** ν_{max} 1531, 1495, 1299, 1269, 983, 803, 788, 692 cm^{-1}; **HRMS** (ESI) m/z calcd. for $C_{16}H_{17}N_2$ ([M+H]$^+$) 237.1386, found 237.1387; **m.p.**: 41-43 °C (lit. 39-41 °C); **$[\alpha]_D^{25}$** = -5.9 (c = 1.0, $CHCl_3$); **Chiral HPLC**: Chiralpak OG, 4.6 x 250 mm; 1% *i*PrOH/hexanes, 1.0 mL/min; t_R (minor) = 8.1 min, t_R (major) = 9.9 min, 95:5 er.

(*R*)-5-(4-bromophenyl)-1-methyl-3-phenyl-4,5-dihydro-1H-pyrazole (219)

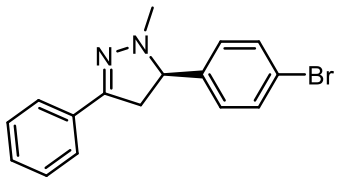

219 was prepared following General Procedure **J**, using (*E*)-1-phenyl-3-(4-bromophenyl)prop-2-en-1-one to afford the title compound as a colourless solid (137 mg, 87%, 96:4 er).

^{1}H NMR (400 MHz, $CDCl_3$): δ 7.71 – 7.62 (m, 2H, Ar*H*), 7.56 – 7.50 (m, 2H, Ar*H*), 7.43 – 7.31 (m, 5H, Ar*H*), 4.11 (dd, *J* = 14.3, 10.0 Hz, 1H, C*H*NN), 3.49 (dd, *J* = 16.1, 10.0 Hz, 1H, CH_2), 2.96 (dd, *J* = 16.1, 14.3 Hz, 1H, CH_2), 2.85 (s, 3H, NCH_3) ppm; **^{13}C NMR (101 MHz, $CDCl_3$)**: δ 149.6 (*C*(N)), 139.5 (Ar*C*), 132.6 (Ar*C*), 131.8 (Ar*C*H), 129.2 (Ar*C*H), 128.7 (Ar*C*H), 128.5 (Ar*C*H), 125.8 (Ar*C*H), 121.6 (Ar*C*), 72.9 (*C*NH), 43.3 (*C*H_2), 41.5 (N*C*H_3) ppm; **HRMS** (ESI) m/z calcd. for $C_{16}H_{16}N_2Br$ ($[M+H]^+$) 315.04914, found 315.04916; **FT-IR (thin film)** ν_{max} 1561, 1445, 1360, 1279, 988, 787, 690 cm^{-1}; **m.p.**: 90-92 °C; **$[\alpha]_D^{25}$** = +26.5 (c = 1.0, $CHCl_3$); **Chiral HPLC**: Chiralpak OD-H, 4.6 x 250 mm; 1% *i*PrOH/hexanes, 1.0 mL/min; t_R (minor) = 16.1 min, t_R (major) = 47.8 min, 96:4 er.

(*R*)-5-(4-chlorophenyl)-1-methyl-3-phenyl-4,5-dihydro-1H-pyrazole (220)

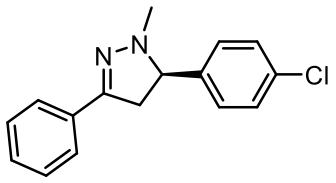

220 was prepared following General Procedure **J**, using (E)-1-phenyl-3-(4-chlorophenyl)prop-2-en-1-one to afford the title compound as a colourless solid (112 mg, 83%, 95:5 er).

^{1}H NMR (400 MHz, $CDCl_3$): δ 7.73 – 7.55 (m, 2H, Ar*H*), 7.47 – 7.30 (m, 7H, Ar*H*), 4.12 (dd, *J* = 14.3, 10.0 Hz, 1H, C*H*NN), 3.49 (dd, *J* = 16.1, 10.0 Hz, 1H, CH_2), 2.97 (dd, *J* = 16.1, 14.3 Hz, 1H, CH_2), 2.85 (s, 3H, NCH_3) ppm; **^{13}C NMR (101 MHz, $CDCl_3$)**: δ 149.7 (*C*(N)), 139.0 (Ar*C*), 133.5 (Ar*C*), 132.7 (Ar*C*), 128.9 (Ar*C*H), 128.8 (Ar*C*H), 128.7 (Ar*C*H), 128.5 (Ar*C*H), 125.8 (Ar*C*H), 72.9 (*C*NH), 43.4 (*C*H_2), 41.5 (N*C*H_3) ppm; **HRMS** (ESI) m/z calcd. for $C_{16}H_{16}N_2Cl$ ($[M+H]^+$) 271.09965, found 271.09952; **FT-IR (thin film)** ν_{max} 1559, 1410, 1272, 986, 731, 646 cm^{-1}; **m.p.**: 97-99 °C; **$[\alpha]_D^{25}$** = +19.5 (c = 1.0, $CHCl_3$); **Chiral HPLC**: Chiralpak AD, 4.6 x 250 mm; 2% *i*PrOH/hexanes, 1.0 mL/min; t_R (minor) = 33.2 min, t_R (major) = 29.6 min, 96:4 er.

(*R*)-1-methyl-3-phenyl-5-(4-vinylphenyl)-4,5-dihydro-1H-pyrazole (221)

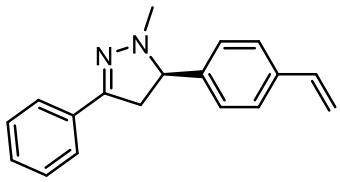

221 was prepared following General Procedure **J**, using (E)-1-phenyl-3-(4-vinylphenyl)prop-2-en-1-one to afford the title compound as a colourless solid (115 mg, 88%, 94.5:5.5 er).

^{1}H NMR (400 MHz, $CDCl_3$): δ 7.72 – 7.65 (m, 2H, Ar*H*), 7.47 (s, 4H, Ar*H*), 7.42 – 7.31 (m, 3H, Ar*H*), 6.77 (dd, *J* = 17.6, 10.9 Hz, 1H, ArC*H*$CH_{cis}H_{trans}$), 5.80 (dd, *J* = 17.6, 0.9 Hz, 1H, ArCHCH_{cis}*H*$_{trans}$), 5.30 (dd, *J* = 10.9, 0.9 Hz, 1H, ArCHC*H*$_{cis}H_{trans}$), 4.14 (dd, *J* = 14.4, 10.0 Hz, 1H, C*H*NN), 3.49 (dd, *J* = 16.1, 10.0 Hz, 1H, CH_2), 3.01 (dd, *J* = 16.1, 14.4 Hz, 1H, CH_2), 2.87 (s, 3H, NCH_3) ppm; **^{13}C NMR (101 MHz, $CDCl_3$)**: δ 149.7 (*C*(N)), 139.9 (Ar*C*), 137.2 (Ar*C*), 136.4 (*C*HCH_2), 132.91 (Ar*C*), 128.6 (Ar*C*H), 128.5 (Ar*C*H), 127.7 (Ar*C*H), 126.5 (Ar*C*H), 125.7 (Ar*C*H), 113.9 (CH*C*H_2), 73.3 (*C*NH), 43.4 (*C*H_2), 41.5 (N*C*H_3) ppm; **HRMS** (ESI) m/z calcd. for $C_{18}H_{19}N_2$ ($[M+H]^+$) 263.15428, found 263.15414; **FT-IR (thin film)** ν_{max} 2969, 1652, 1218, 1407, 989 cm^{-1}; **m.p.**: 57-59 °C; **$[\alpha]_D^{25}$** = -47.3 (c = 1.0, $CHCl_3$); **Chiral HPLC**: Chiralpak AD, 4.6 x 250 mm; 1% *i*PrOH/hexanes, 1.0 mL/min; t_R (minor) = 29.2 min, t_R (major) = 33.1 min, 94.5:5.5 er.

(*R*)-1-methyl-5-(4-nitrophenyl)-3-phenyl-4,5-dihydro-1H-pyrazole (222)

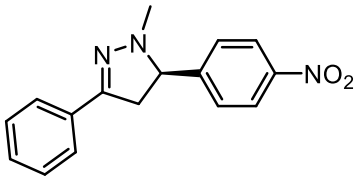

222 was prepared following General Procedure **J**, using (*E*)-3-(4-nitrophenyl)-1-phenylprop-2-en-1-one to afford the title compound as a yellow solid (121 mg, 86%, 95:5 er).

^{1}H NMR (400 MHz, $CDCl_3$): δ 8.36 – 8.09 (m, 2H, Ar*H*), 7.70 – 7.51 (m, 4H, Ar*H*), 7.43 – 7.30 (m, 3H, Ar*H*), 4.26 (dd, *J* = 14.2, 10.2 Hz, 1H, C*H*NN), 3.58 (dd, *J* = 16.2, 10.2 Hz, 1H, CH_2), 2.99 (dd, *J* = 16.1, 14.2 Hz, 1H, CH_2), 2.87 (s, 3H, NCH_3) ppm; **^{13}C NMR (101 MHz, $CDCl_3$)**: δ 149.5 (*C*(N)), 148.3 (Ar*C*), 147.7 (Ar*C*), 132.4 (Ar*C*), 128.9 (Ar*C*H), 128.6 (Ar*C*H), 128.3 (Ar*C*H), 125.8 (Ar*C*H), 124.0 (Ar*C*H), 72.7 (*C*NH), 43.6 (*C*H_2), 41.8 (N*C*H_3) ppm; **HRMS** (ESI) m/z calcd. for $C_{16}H_{19}N_3O_2$ ($[M+H]^+$) 282.12370, found 282.12381; **FT-IR (thin film)** ν_{max} 1525, 1315, 965, 780, 759, 667 cm^{-1}; **m.p.**: 94-96 °C; **$[\alpha]_D^{25}$** = +88.7 (c = 1.0, $CHCl_3$); **Chiral HPLC**: Chiralpak AD, 4.6 x 250 mm; 5% *i*PrOH/hexanes, 1.0 mL/min; t_R (minor) = 24.2 min, t_R (major) = 38.1 min, 95:5 er.

(*R*)-4-(1-methyl-3-phenyl-4,5-dihydro-1H-pyrazol-5-yl)benzonitrile (223)

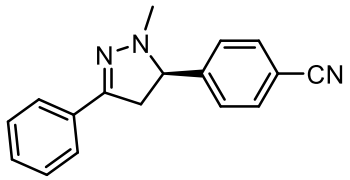

223 was prepared following General Procedure **J**, using (*E*)-4-(3-oxo-3-phenylprop-1-en-1-yl)benzonitrile to afford the title compound as a colourless solid (108 mg, 83%, 95:5 er).

^{1}H NMR (400 MHz, $CDCl_3$): δ 7.70 – 7.54 (m, 6H, Ar*H*), 7.40 – 7.28 (m, 3H, Ar*H*), 4.17 (dd, *J* = 14.2, 10.2 Hz, 1H, C*H*NN), 3.52 (dd, *J* = 16.1, 10.2 Hz, 1H, CH_2), 2.93 (dd, *J* = 16.2, 14.2 Hz, 1H, CH_2), 2.83 (s, 3H, NCH_3) ppm; **^{13}C NMR (101 MHz, $CDCl_3$)**: δ 149.4 (*C*(N)), 146.2 (Ar*C*), 132.5 (Ar*C*H), 132.4 (Ar*C*), 128.9 (Ar*C*H), 128.6 (Ar*C*H), 128.2 (Ar*C*H), 125.8 (Ar*C*H), 118.7 (*C*N), 111.6 (Ar*C*), 72.9 (*C*NH), 43.4 (*C*H_2), 41.7 (N*C*H_3) ppm; **HRMS** (ESI) m/z calcd. for $C_{17}H_{16}N_3$ ($[M+H]^+$) 262.13387, found 262.13382; **FT-IR (thin film)** ν_{max} 2262, 1506, 1476, 1239, 973, 703, 687 cm^{-1}; **m.p.**: 80-82 °C; **$[\alpha]_D^{25}$** = +36.4 (c = 1.0, $CHCl_3$); **Chiral HPLC**: Chiralpak AD, 4.6 x 250 mm; 2% *i*PrOH/hexanes, 1.0 mL/min; t_R (minor) = 33.6 min, t_R (major) = 29.9 min, 95:5 er.

(*R*)-Ethyl 4-(1-methyl-3-phenyl-4,5-dihydro-1H-pyrazol-5-yl)benzoate (224)

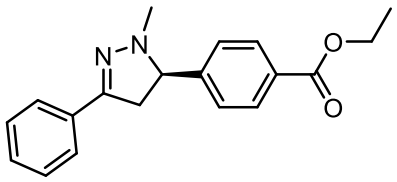

223 was prepared following General Procedure **J**, using ethyl (*E*)-4-(3-oxo-3-phenylprop-1-en-1-yl)benzoate to afford the title compound as a colourless oil (120 mg, 78%, 95:5 er).

^{1}H NMR (400 MHz, $CDCl_3$): δ 8.17 – 8.04 (m, 2H, Ar*H*), 7.72 – 7.62 (m, 2H, Ar*H*), 7.62 – 7.53 (m, 2H, Ar*H*), 7.43 – 7.31 (m, 3H, Ar*H*), 4.42 (q, *J* = 7.1 Hz, 2H, OCH_2CH_3), 4.20 (dd, *J* = 14.3, 10.1 Hz, 1H, C*H*NN), 3.54 (dd, *J* = 16.1, 10.1 Hz, 1H, CH_2), 3.00 (dd, *J* = 16.1, 14.3 Hz, 1H, CH_2), 2.86 (s, 3H, NCH_3), 1.43 (t, *J* = 7.1 Hz, 3H, OCH_2CH_3) ppm; **^{13}C NMR (101 MHz, $CDCl_3$)**: δ 166.3 (*C*(O)OCH_2CH_3), 149.6 (*C*(N)), 145.7 (Ar*C*), 132.7 (Ar*C*), 130.1 (Ar*C*), 130.0 (Ar*C*H), 128.8 (Ar*C*H), 128.5 (Ar*C*H), 127.4 (Ar*C*H), 125.8 (Ar*C*H), 73.7 (*C*NH), 61.0 (C(O)O*C*H_2CH_3), 43.4 (CH_2), 41.7 (NCH_3), 14.4 (C(O)OCH_2CH_3) ppm; **HRMS** (ESI) m/z calcd. for $C_{19}H_{19}O_2N_2$ ($[M+H]^+$) 307.14410, found 307.14417; **FT-IR (thin film)** ν_{max} 1711, 1612, 1272, 1106, 801, 675 cm^{-1}; **$[\alpha]_D^{25}$** = +1.6 (c = 1.0, $CHCl_3$); **Chiral HPLC**: Chiralpak AD, 4.6 x 250 mm; 3% *i*PrOH/hexanes, 1.0 mL/min; t_R (minor) = 51.9 min, t_R (major) = 32.1 min, 95:5 er.

(*R*)-5-(4-methoxyphenyl)-1-methyl-3-phenyl-4,5-dihydro-1H-pyrazole (225)

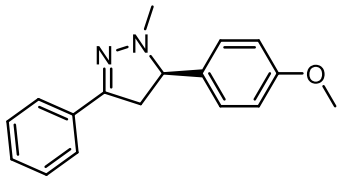

225 was prepared following General Procedure **J**, using (E)-1-phenyl-3-(4-methoxyphenyl)prop-2-en-1-one to afford the title compound as a colourless solid (61 mg, 46%, 91:9 er).

^{1}H NMR (400 MHz, $CDCl_3$): δ 7.58 – 7.49 (m, 2H, Ar*H*), 7.33 – 7.15 (m, 5H, Ar*H*), 6.84 – 6.77 (m, 2H, Ar*H*), 3.94 (dd, *J* = 14.4, 10.0 Hz, 1H, C*H*NN), 3.69 (s, 3H, OCH_3), 3.30 (dd, *J* = 16.1, 9.9 Hz, 1H, CH_2), 2.84 (dd, *J* = 16.1, 14.4 Hz, 1H, CH_2), 2.71 (s, 3H, NCH_3) ppm; **^{13}C NMR (101 MHz, $CDCl_3$)**: δ 159.3 (*C*(N)), 149.7 (Ar*C*), 133.0 (Ar*C*), 132.2 (Ar*C*), 128.6 (Ar*C*H), 128.6 (Ar*C*H), 128.5 (Ar*C*H), 125.8 (Ar*C*H), 114.1 (Ar*C*H), 73.1 (CH*C*H_2), 55.3 (O*C*H_3), 43.2 (*C*H_2), 41.4 (N*C*H_3) ppm; **HRMS** (ESI) m/z calcd. for $C_{17}H_{19}ON_2$ ($[M+H]^+$) 267.14919, found 267.14893; **FT-IR (thin film)** ν_{max} 2996, 2832, 2161, 1977, 1561, 1244, 1078, 763 cm^{-1}; **m.p.**: 52-54 °C; **$[\alpha]_D^{25}$** = -3.3 (c = 1.0, $CHCl_3$); **Chiral HPLC**: Chiralpak AD, 4.6 x 250 mm; 2% *i*PrOH/hexanes, 1.0 mL/min; t_R (minor) = 36.5 min, t_R (major) = 39.9 min, 91:9 er.

(*R*)-5-(4-(2,2-difluorocyclopropyl)phenyl)-1-methyl-3-phenyl-4,5-dihydro-1H-pyrazole (226)

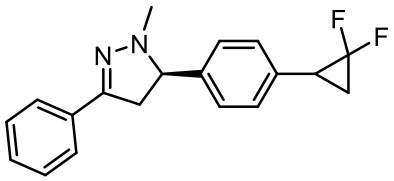

226 was prepared following General Procedure **J**, using (*E*)-3-(4-(2,2-difluorocyclopropyl)phenyl)-1-phenylprop-2-en-1-one to afford the title compound as a colourless oil (136 mg, 87%, 1:1 dr, 91:9 er).

^{1}H NMR (400 MHz, $CDCl_3$): δ 7.69 – 7.62 (m, 2H, Ar*H*), 7.49 – 7.42 (m, 2H, Ar*H*), 7.42 – 7.31 (m, 3H, Ar*H*), 7.30 – 7.23 (m, 2H, Ar*H*), 4.13 (dd, *J* = 14.4, 10.0 Hz, 1H, C*H*NN), 3.55 – 3.44 (dd, *J* = 16.2, 10.0 Hz, 1H, CH_2), 3.00 (dd, *J* = 16.2, 14.4 Hz, 1H, CH_2), 2.85 (s, 3H, NCH_3), 2.79 (m, 1H, ArC*H*), 1.86 (m, 1H, CH_2CF_2), 1.66 (m, 1H, CH_2CF_2) ppm; **^{19}F NMR (377 MHz, $CDCl_3$)**: δ -125.85 (dddd, *J* = 154.2, 13.1, 6.6, 4.1 Hz), -142.30 (dddd, *J* = 154.2, 13.1, 5.4, 2.7 Hz) ppm; [diastereomers could only be observed without resonance overlap by ^{19}F{^{1}H} NMR] **^{19}F{^{1}H} NMR (377 MHz, $CDCl_3$)**: δ -125.83 (d, *J* = 154.1 Hz, diastereomer 1), -125.85 (d, *J* = 154.0 Hz, diastereomer 2), -142.29 (d, *J* = 154.0 Hz, diastereomer 2), -142.30 (d, *J* = 154.1 Hz, diastereomer 1) ppm; **^{13}C NMR (101 MHz, $CDCl_3$)**: δ 149.7 (*C*(N)), 139.4 (Ar*C*), 133.3 (Ar*C*), 132.8 (Ar*C*), 128.7 (Ar*C*H), 128.5 (Ar*C*H), 128.3 (Ar*C*H), 127.6 (Ar*C*H), 125.8 (Ar*C*H), 105.7-100.7 (m, CF_2), 73.2 (*C*NH), 43.3 (C(N)*C*H_2), 41.6 (N*C*H_3), 27.0 (t, *J* = 11.5 Hz, *C*HCF_2), 17.2 (m, *C*H_2CF_2) ppm; **HRMS**

(ESI) m/z calcd. for $C_{19}H_{19}N_2F_2$ ($[M+H]^+$) 313.15108, found 313.15085; **FT-IR (thin film)** ν_{max} 2958, 1467, 1230, 936, 760 cm^{-1}; $\mathbf{[\alpha]_D}^{25}$ = +41.0 (c = 1.0, $CHCl_3$); **Chiral HPLC**: Chiralpak tandem OD-H and OD-H column, 4.6 x 250 mm; 1% *i*PrOH/hexanes, 1.0 mL/min; t_R (minor) = 29.1 and 33.9 mins, t_R (major) = 96.3 and 101.0 mins, 91:9 er.

(*R*)-1-methyl-5-phenyl-3-(m-tolyl)-4,5-dihydro-1H-pyrazole (227)

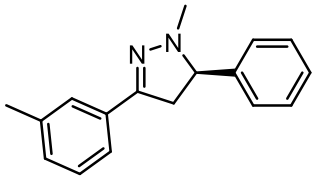

227 was prepared following General Procedure **J**, using (*E*)-3-phenyl-1-(m-tolyl)prop-2-en-1-one to afford the title compound as a colourless oil (64 mg, 51%, 94:6).

^{1}H NMR (400 MHz, $CDCl_3$): δ 7.58 (tt, *J* = 1.7, 0.8 Hz, 1H, Ar*H*), 7.56 – 7.49 (m, 2H, Ar*H*), 7.49 – 7.39 (m, 3H, Ar*H*), 7.39 – 7.33 (m, 1H, Ar*H*), 7.30 (t, *J* = 7.6 Hz, 1H, Ar*H*), 7.18 (ddt, *J* = 7.6, 1.8, 0.9 Hz, 1H, Ar*H*), 4.15 (dd, *J* = 14.4, 10.0 Hz, 1H, C*H*NN), 3.50 (dd, *J* = 16.1, 10.0 Hz, 1H, CH_2), 3.03 (dd, *J* = 16.1, 14.4 Hz, 1H, CH_2), 2.88 (s, 3H, NCH_3), 2.44 – 2.40 (m, 3H, ArCH_3) ppm; **^{13}C NMR (101 MHz, $CDCl_3$)**: δ 149.9 (*C*(N)), 140.4 (Ar*C*), 138.2 (Ar*C*), 132.8 (Ar*C*), 129.5 (Ar*C*H), 128.7 (Ar*C*H), 128.4 (Ar*C*H), 127.8 (Ar*C*H), 127.5 (Ar*C*H), 126.3 (Ar*C*H), 123.1 (Ar*C*H), 73.6 (*C*NH), 43.4 (*C*H_2), 41.6 (N*C*H_3), 21.4 (Ar*C*H_3) ppm; **HRMS** (ESI) m/z calcd. for $C_{17}H_{19}N_2$ ([M+H]$^+$) 251.15428, found 251.15411; **FT-IR (thin film)** ν_{max} 1473, 1363, 1170, 1074, 990, 877, 694 cm^{-1}; **$[\alpha]_D^{25}$** = +16.3 (c = 1.0, $CHCl_3$); **Chiral HPLC**: Chiralpak AD, 4.6 x 250 mm; 2% *i*PrOH/hexanes, 1.0 mL/min; t_R (minor) = 11.2 min, t_R (major) = 14.4 min, 94:6 er.

(*R*)-3-(2-fluorophenyl)-1-methyl-5-phenyl-4,5-dihydro-1H-pyrazole (228)

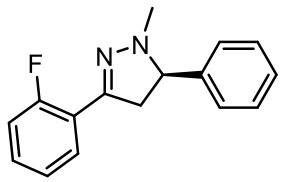

228 was prepared following General Procedure **J**, using (*E*)-1-(2-fluorophenyl)-3-phenylprop-2-en-1-one to afford the title compound as a colourless oil (99 mg, 78%, 94:6 er).

^{1}H NMR (400 MHz, $CDCl_3$): δ 7.90 (td, *J* = 7.8, 1.8 Hz, 1H, Ar*H*), 7.54 – 7.47 (m, 2H, Ar*H*), 7.45 – 7.38 (m, 2H, Ar*H*), 7.38 – 7.25 (m, 2H, Ar*H*), 7.21 – 7.13 (m, 1H, Ar*H*), 7.08 (ddd, *J* = 11.5, 8.3, 1.2 Hz, 1H, Ar*H*), 4.18 (dd, *J* = 14.8, 10.0 Hz, 1H, C*H*NN), 3.61 (m, 1H, CH_2), 3.13 (m, 1H, CH_2), 2.88 (s, 3H, NCH_3) ppm; **^{13}C NMR (101 MHz, $CDCl_3$)**: δ 160.4 (d, *J* = 251.1 Hz, Ar*C*F), 146.1 (d, *J* = 2.4 Hz, *C*(N)), 140.3 (Ar*C*), 130.0 (d, *J* = 8.1 Hz, Ar*C*H), 128.7 (Ar*C*H), 128.5 (d, *J* = 3.6 Hz, Ar*C*H), 127.8 (Ar*C*H), 127.4 (Ar*C*H), 124.1 (d, *J* = 3.2 Hz, Ar*C*H), 121.0 (d, *J* = 11.7 Hz, Ar*C*), 116.20 (d, *J* = 22.3 Hz, Ar*C*H), 73.7 (*C*NH), 45.5 (*C*H_2), 41.3 (N*C*H_3) ppm; **HRMS** (ESI) m/z calcd. for $C_{16}H_{16}N_2F$ ($[M+H]^+$) 255.12920, found 255.12868; **FT-IR (thin film)** ν_{max} 1585, 1487, 1359, 924, 752, 698 cm^{-1}; **$[\alpha]_D^{25}$** = +34.6 (c = 1.0, $CHCl_3$); **Chiral HPLC**: Chiralpak OD-H, 4.6 x 250 mm; 1% *i*PrOH/hexanes, 1.0 mL/min; t_R (minor) = 6.9 min, t_R (major) = 9.9 min, 94:6 er.

(*R*)-3-(2,3-dihydro-1H-inden-5-yl)-1-methyl-5-phenyl-4,5-dihydro-1H-pyrazole (229)

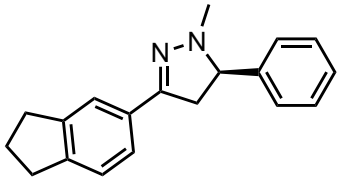

229 was prepared following General Procedure **J**, using (*E*)-1-(2,3-dihydro-1H-inden-5-yl)-3-phenylprop-2-en-1-one to afford the title compound as a colourless solid (128 mg, 93%, 95:5 er).

^{1}H NMR (400 MHz, $CDCl_3$): δ 7.64 – 7.59 (m, 1H, Ar*H*), 7.54 – 7.48 (m, 2H Ar*H*), 7.46 – 7.38 (m, 3H, Ar*H*), 7.38 – 7.32 (m, 1H, Ar*H*), 7.25 (d, *J* = 7.8 Hz, 1H, Ar*H*), 4.12 (dd, *J* = 14.4, 9.9 Hz, 1H, C*H*NN), 3.49 (dd, *J* = 16.1, 9.9 Hz, 1H, CH_2), 3.02 (dd, *J* = 16.1, 14.3 Hz, 1H, CH_2), 2.95 (t, *J* = 7.4 Hz, 4H, ArCH_2CH_2), 2.86 (s, 3H, NCH_3), 2.12 (p, *J* = 7.5 Hz, 2H, ArCH$_2$CH_2) ppm;**^{13}C NMR (101 MHz, $CDCl_3$)**: δ 150.4 (*C*(N)), 145.2 (Ar*C*), 144.7 (Ar*C*), 140.5 (Ar*C*), 131.0 (Ar*C*), 128.67 (Ar*C*H), 127.8 (Ar*C*H), 127.5 (Ar*C*H), 124.3 (Ar*C*H), 124.1 (Ar*C*H), 121.7 (Ar*C*H), 73.6 (*C*NH), 43.6 (*C*H$_2$), 41.7 (N*C*H$_3$), 32.8 (Ar*C*H$_2$CH$_2$), 32.7 (ArCH$_2$CH$_2$), 25.4 (ArCH$_2$*C*H$_2$) ppm; **HRMS** (ESI) m/z calcd. for $C_{19}H_{21}N_2O$ ($[M+H]^+$) 277.16993, found 277.16989; **FT-IR (thin film)** ν_{max} 2980, 1473, 1214, 945, 818, 701 cm^{-1}; **m.p.**: 81-83 °C; **$[\alpha]_D^{25}$** = +26.5 (c = 1.0, $CHCl_3$); **Chiral HPLC**: Chiralpak IA, 4.6 x 250 mm; 2% *i*PrOH/hexanes, 1.0 mL/min; t_R (minor) = 26.6 min, t_R (major) = 27.8 min, 95:5 er.

(*R*)-3-(3,5-bis(trifluoromethyl)phenyl)-1-methyl-5-phenyl-4,5-dihydro-1H-pyrazole (230)

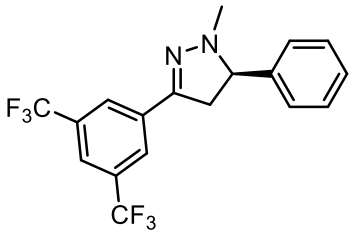

230 was prepared following General Procedure **J**, using (*E*)-1-(3,5-bis(trifluoromethyl)phenyl)-3-phenylprop-2-en-1-one to afford the title compound as a colourless oil (134 mg, 72%, 96:4 er).

^{1}H NMR (400 MHz, $CDCl_3$): δ 7.96 (dd, *J* = 1.8, 0.9 Hz, 2H, Ar*H*), 7.69 (tt, *J* = 1.7, 0.8 Hz, 1H, Ar*H*), 7.43 – 7.21 (m, 5H, Ar*H*), 4.20 (dd, *J* = 14.4, 10.4 Hz, 1H, C*H*NN), 3.43 (dd, *J* = 16.2, 10.4 Hz, 1H, CH_2), 2.95 (dd, *J* = 16.2, 14.4 Hz, 1H, CH_2), 2.82 (s, 3H, NCH_3) ppm; **^{13}C NMR (101 MHz, $CDCl_3$)**: δ 145.8, (*C*(N)), 139.6 (Ar*C*), 135.2 (Ar*C*), 131.9 (q, *J* = 33.1 Hz, *C*CF_3), 128.8 (Ar*C*H), 128.1 (Ar*C*H), 127.3 (Ar*C*H), 125.2 (d, *J* = 4.0 Hz, Ar*C*(H)CCF_3), 123.2 (q, *J* = 272.9 Hz, *C*F_3), 121.5 – 120.8 (m, Ar*C*(H)CCF_3), 73.4 (*C*NH), 42.6 (*C*H_2), 40.9 (N*C*H_3) ppm; **^{19}F NMR (377 MHz, $CDCl_3$)** δ -63.30 ppm; **HRMS** (ESI) m/z calcd. for $C_{18}H_{15}N_2F_6$ ([M+H]$^+$) 373.11339, found 373.11414; **FT-IR (thin film)** ν_{max} 1276, 1170, 1128, 886, 697 cm^{-1}; **$[\alpha]_D^{25}$** = +70.0 (c = 1.0, $CHCl_3$); **Chiral HPLC**: Chiralpak AD-H, 4.6 x 250 mm; 2% *i*PrOH/hexanes, 1.0 mL/min; t_R (minor) = 4.2 min, t_R (major) = 4.5 min, 95:5 er.

(*R*)-3-(3,4-dichlorophenyl)-1-methyl-5-(4-(methylthio)phenyl)-4,5-dihydro-1H-pyrazole (231)

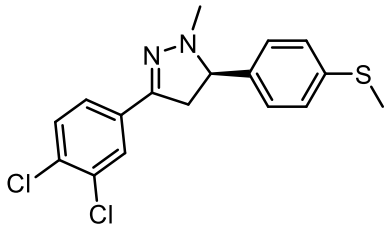

231 was prepared following General Procedure **J**, using (*E*)-1-(3,4-dichlorophenyl)-3-(4-(methylthio)phenyl)prop-2-en-1-one to afford the title compound as a yellow solid (161 mg, 92%, 95.5:4.5 er).

^{1}H NMR (400 MHz, $CDCl_3$): δ 7.63 (d, *J* = 1.8 Hz, 1H, Ar*H*), 7.39 – 7.28 (m, 4H, Ar*H*), 7.22 – 7.18 (m, 2H, Ar*H*), 4.06 (dd, *J* = 14.4, 10.2 Hz, 1H, C*H*NN), 3.31 (dd, *J* = 16.1, 10.2 Hz, 1H, CH_2), 2.84 (dd, *J* = 16.1, 14.4 Hz, 1H, CH_2), 2.75 (s, 3H, NCH_3), 2.43 (s, 3H, SCH_3) ppm; **^{13}C NMR (101 MHz, $CDCl_3$)**: δ 147.0 (*C*(N)), 138.2 (Ar*C*), 136.6 (Ar*C*), 133.0 (Ar*C*), 132.7 (Ar*C*), 132.1 (Ar*C*), 130.4 (Ar*C*H), 127.9 (Ar*C*H), 127.3 (Ar*C*H), 126.8 (Ar*C*H), 124.7 (Ar*C*H), 73.1 (*C*NH), 42.7 (*C*H_2), 41.1 (N*C*H_3), 15.8 (S*C*H_3) ppm; **HRMS** (ESI) m/z calcd. for $C_{17}H_{17}N_2S$ ($[M+H]^+$) 351.04840, found 351.04831; **FT-IR (thin film)** ν_{max} 1574, 1492, 1376, 1130, 948, 819 cm^{-1}; **m.p.**: 99-101 °C; **$[\alpha]_D^{25}$** = +45.7 (c = 1.0, $CHCl_3$); **Chiral HPLC**: Chiralpak AD-H, 4.6 x 250 mm; 1% *i*PrOH/hexanes, 1.0 mL/min; t_R (minor) = 21.6 min, t_R (major) = 42.9 min, 91:9 er.

(*R*)-5-(6-bromobenzo[d][1,3]dioxol-5-yl)-1-methyl-3-phenyl-4,5-dihydro-1H-pyrazole (232)

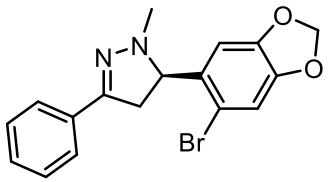

232 was prepared following General Procedure **J**, using (*E*)-3-(6-bromobenzo[d][1,3]dioxol-5-yl)-1-phenylprop-2-en-1-one in CH_2Cl_2 to afford the title compound as a colourless solid (141 mg, 79%, 87:13 er).

^{1}H NMR (400 MHz, $CDCl_3$): δ 7.67 – 7.62 (m, 2H, Ar*H*), 7.40 – 7.29 (m, 3H, Ar*H*), 7.25 (s, 1H, Ar*H*), 7.03 (s, 1H, Ar*H*), 6.02 – 5.94 (m, 2H, OCH_2O), 4.46 (dd, *J* = 13.9, 10.3 Hz, 1H, C*H*NN), 3.68 (dd, *J* = 16.2, 10.3 Hz, 1H, CH_2), 2.87 (s, 3H, NCH_3), 2.71 (dd, *J* = 16.3, 14.0 Hz, 1H, CH_2) ppm; **^{13}C NMR (101 MHz, $CDCl_3$)**: δ 149.3 (*C*(N)), 147.8 (Ar*C*), 147.7 (Ar*C*), 133.4 (Ar*C*), 132.7 (Ar*C*), 128.7 (Ar*C*H), 128.50 (Ar*C*H), 125.8 (Ar*C*H), 113.9 (Ar*C*), 112.6 (Ar*C*H), 107.9 (Ar*C*H), 101.8 (O*C*H_2O), 71.8 (*C*NH), 41.8 (*C*H_2), 41.3 (N*C*H_3) ppm; **HRMS** (ESI) m/z calcd. for $C_{17}H_{16}N_2O_2Br$ ([M+H]$^+$) 359.03897, found 359.03940; **FT-IR (thin film)** ν_{max} 1500, 1240, 1036, 980, 759 cm^{-1}; **m.p.**: 119-121 °C; **$[\alpha]_D^{25}$** = +49.4 (c = 1.0, $CHCl_3$); **Chiral HPLC**: Chiralpak OD-H, 4.6 x 250 mm; 1% *i*PrOH/hexanes, 1.0 mL/min; t_R (minor) = 20.2 min, t_R (major) = 16.8 min, 87:13 er.

(*R*)-5-(3,4-dimethoxyphenyl)-1-methyl-3-phenyl-4,5-dihydro-1H-pyrazole (233)

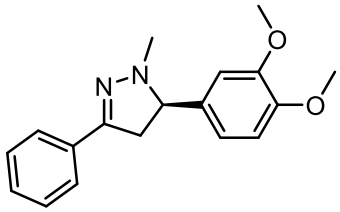

233 was prepared following General Procedure **J**, using (*E*)-3-(3,4-dimethoxyphenyl)-1-phenylprop-2-en-1-one in CH_2Cl_2 to afford the title compound as a colourless solid (104 mg, 70%, 81:19 er).

^{1}H NMR (400 MHz, $CDCl_3$): δ 7.69 – 7.62 (m, 2H, Ar*H*), 7.39 – 7.27 (m, 3H, Ar*H*), 7.07 (d, *J* = 2.0 Hz, 1H, Ar*H*), 6.96 (dd, *J* = 8.2, 2.0 Hz, 1H, Ar*H*), 6.85 (d, *J* = 8.2 Hz, 1H, Ar*H*), 4.05 (dd, *J* = 14.5, 9.9 Hz, 1H, C*H*NN), 3.89 (s, 3H, ArOCH_3), 3.88 (s, 3H, ArOCH_3), 3.43 (dd, *J* = 16.1, 10.0 Hz, 1H, CH_2), 2.97 (dd, *J* = 16.1, 14.5 Hz, 1H, CH_2), 2.83 (s, 3H, NCH_3) ppm; **^{13}C NMR (101 MHz, $CDCl_3$)**: δ 149.8 (*C*(N)), 149.3 (Ar*C*), 148.7 (Ar*C*), 132.9 (Ar*C*), 132.8 (Ar*C*), 128.6 (Ar*C*H), 128.5 (Ar*C*H), 125.7 (Ar*C*H), 120.0 (Ar*C*H), 111.1 (Ar*C*H), 109.9 (Ar*C*H), 73.5 (*C*NH), 55.4 (ArO*C*H_3), 55.9 (ArO*C*H_3), 43.2 (*C*H_2), 41.5 (N*C*H_3) ppm; **HRMS** (ESI) m/z calcd. for $C_{18}H_{21}O_2N_2$ ($[M+H]^+$) 297.15975, found 297.15961; **FT-IR (thin film)** ν_{max} 1653, 1259, 1191, 1070, 692 cm^{-1}; **m.p.**: 97-99 °C; **$[\alpha]_D^{25}$** = +44.6 (c = 1.0, $CHCl_3$); **Chiral HPLC**: Chiralpak AD, 4.6 x 250 mm; 3% *i*PrOH/hexanes, 1.0 mL/min; t_R (minor) = 46.8 min, t_R (major) = 35.0 min, 81:19 er.

(*R*)-1-methyl-3-phenyl-5-(thiophen-2-yl)-4,5-dihydro-1H-pyrazole (234)

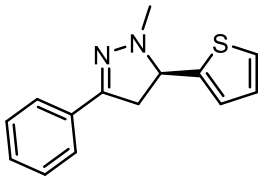

234 was prepared following General Procedure **J**, using (*E*)-1-phenyl-3-(thiophen-2-yl)prop-2-en-1-one to afford the title compound as a colourless oil (94 mg, 78%, 91:9 er).

^{1}H NMR (400 MHz, $CDCl_3$): δ 7.70 – 7.64 (m, 2H, Ar*H*), 7.43 – 7.29 (m, 3H, Ar*H*), 7.10 (ddd, *J* = 3.6, 1.3, 0.6 Hz, 1H, Ar*H*), 7.02 (dd, *J* = 5.1, 3.5 Hz, 1H, Ar*H*), 4.43 (ddt, *J* = 13.8, 9.8, 0.6 Hz, 1H, C*H*NN), 3.54 (dd, *J* = 16.1, 9.8 Hz, 1H, CH_2), 3.11 (dd, *J* = 16.1, 13.8 Hz, 1H, CH_2), 2.92 (s, 3H, NCH_3) ppm; **^{13}C NMR (101 MHz, $CDCl_3$)**: δ 150.2 (*C*(N)), 143.9 (Ar*C*), 132.7 (Ar*C*), 128.7 (Ar*C*H), 128.5 (Ar*C*H), 126.7 (Ar*C*H), 125.84(Ar*C*H), 125.7 (Ar*C*H), 125.0 (Ar*C*H), 68.7 (*C*NH), 43.7 (*C*H_2), 41.4 (N*C*H_3) ppm; **HRMS** (ESI) m/z calcd. for $C_{14}H_{15}N_2S$ ($[M+H]^+$) 243.09505, found 243.09485; **FT-IR (thin film)** ν_{max} 2957, 3834, 1445, 1310, 1128, 934, 759, 693 cm^{-1}; **$[\alpha]_D^{25}$** = +44.9 (c = 1.0, $CHCl_3$); **Chiral HPLC**: Chiralpak AD-H, 4.6 x 250 mm; 1% *i*PrOH/hexanes, 1.0 mL/min; t_R (minor) = 25.3 min, t_R (major) = 46.0 min, 92:8 er.

(*R*)-2-(5-(4-bromophenyl)-1-methyl-4,5-dihydro-1H-pyrazol-3-yl)pyrazine (235)

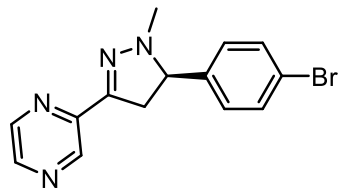

235 was prepared following General Procedure **J**, using (*E*)-3-(4-bromophenyl)-1-(pyrazin-2-yl)prop-2-en-1-one to afford the title compound as a pale yellow solid (115 mg, 73%, 90:10).

^{1}H NMR (400 MHz, $CDCl_3$): δ 9.18 (d, *J* = 1.6 Hz, 1H, Ar*H*), 8.50 – 8.38 (m, 2H, Ar*H*)), 7.59 – 7.40 (m, 2H, Ar*H*)), 7.39 – 7.30 (m, 2H, Ar*H*)), 4.25 (dd, *J* = 14.3, 10.7 Hz, 1H, C*H*NN), 3.68 (dd, *J* = 17.0, 10.7 Hz, 1H, CH_2), 3.01 (dd, *J* = 17.0, 14.3 Hz, 1H, CH_2), 2.91 (s, 3H, NCH_3) ppm; **^{13}C NMR (101 MHz, $CDCl_3$)**: δ 147.7 (*C*(N)), 147.4 (Ar*C*), 143.5 (Ar*C*H), 142.6 (Ar*C*H), 142.67 (Ar*C*H), 139.0 (Ar*C*), 131.9 (Ar*C*H), 129.0 (Ar*C*H), 121.8 (Ar*C*Br), 72.4 (*C*NH), 42.1 (*C*H_2), 40.7 (N*C*H_3) ppm; **HRMS** (ESI) m/z calcd. for $C_{14}H_{14}N_4Br$ ($[M+H]^+$) 317.03964, found 317.03976; **FT-IR (thin film)** ν_{max} 2957, 1560, 1432, 1162, 1101, 942, 822 cm^{-1}; **m.p.**: 114-116 °C; **$[\alpha]_D^{25}$** = +64.1 (c = 1.0, $CHCl_3$); **Chiral HPLC**: Chiralpak AD-H, 4.6 x 250 mm; 3% *i*PrOH/hexanes, 1.0 mL/min; t_R (minor) = 18.2 min, t_R (major) = 22.6 min, 90:10 er.

(*R*)-4-(1-methyl-5-phenyl-4,5-dihydro-1H-pyrazol-3-yl)pyridine (236)

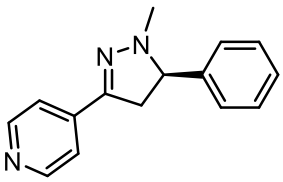

236 was prepared following General Procedure **J**, using (*E*)-3-phenyl-1-(pyridin-4-yl)prop-2-en-1-one to afford the title compound as a colourless oil (83 mg, 70%, 81:19 er).

^{1}H NMR (400 MHz, $CDCl_3$): δ 8.56 (ddd, *J* = 4.9, 1.8, 1.0 Hz, 1H, Ar*H*), 7.93 (dt, *J* = 8.0, 1.1 Hz, 1H, Ar*H*), 7.65 (ddd, *J* = 8.1, 7.5, 1.8 Hz, 1H, Ar*H*), 7.50 – 7.43 (m, 2H, Ar*H*), 7.41 – 7.35 (m, 2H, Ar*H*), 7.35 – 7.27 (m, 1H, Ar*H*), 7.17 (ddd, *J* = 7.5, 4.9, 1.2 Hz, 1H, Ar*H*), 4.22 (dd, *J* = 14.5, 10.4 Hz, 1H, C*H*NN), 3.73 (dd, *J* = 16.9, 10.4 Hz, 1H, CH_2), 3.10 (dd, *J* = 16.8, 14.5 Hz, 1H, CH_2), 2.89 (s, 3H, NCH_3) ppm; **^{13}C NMR (101 MHz, $CDCl_3$)**: δ 152.1 (*C*(N)), 150.3(Ar*C*), 149.1 (Ar*CH*), 140.2 (Ar*C*), 136.0 (Ar*C*H), 128.7 (Ar*C*H), 127.8 (Ar*C*H), 127.5 (Ar*C*H), 122.8 (Ar*C*H), 120.4 (Ar*C*H), 73.6 (*C*NH), 42.6 (*C*H_2), 41.1 (N*C*H_3) ppm; **HRMS** (ESI) m/z calcd. for $C_{15}H_{16}N_3$ ($[M+H]^+$) 238.13387, found 238.13385; **FT-IR (thin film)** ν_{max} 2957, 2918, 1512, 1488, 1360, 989, 756, 698 cm^{-1}; **$[\alpha]_D^{25}$** = +23.1 (c = 1.0, $CHCl_3$); **Chiral HPLC**: Chiralpak OD-H, 4.6 x 250 mm; 2% *i*PrOH/hexanes, 1.0 mL/min; t_R (minor) = 13.9 min, t_R (major) = 15.3 min, 81:19 er.

(*R*)-5-cyclohexyl-1-methyl-3-phenyl-4,5-dihydro-1H-pyrazole (237)

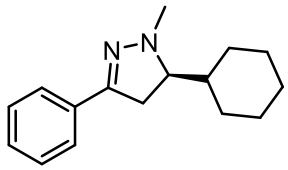

237 was prepared following **General Procedure J,** using (*E*)-3-cyclohexyl-1-phenylprop-2-en-1-one to afford the title compound as a colourless oil (88 mg, 73%, 98:2 er).

^{1}H NMR (400 MHz, $CDCl_3$): δ 7.60 – 7.50 (m, 2H, Ar*H*), 7.30 – 7.19 (m, 3H, Ar*H*), 3.01 – 2.85 (m, 2H, C*H*NN and C(N)CH_2), 2.82 (s, 3H, NCH_3), 2.74 – 2.61 (m, 1H, C(N)CH_2), 1.80 – 1.54 (m, 5H, cyclohexyl-C*H*), 1.29 – 1.05 (m, 4H, cyclohexyl-C*H*), 1.05 – 0.91 (m, 2H, cyclohexyl-C*H*) ppm; **^{13}C NMR (101 MHz, $CDCl_3$)**: δ 149.9 (*C*(N)), 133.3 (Ar*C*), 128.3 (Ar*C*H), 128.2 (Ar*C*H), 125.6 (Ar*C*H), 73.8 (*C*NH), 42.4 (N*C*H_3), 39.5 (CH_2CHCH_2), 35.3 (C(N)*C*H_2), 31.3 (cyclohexyl-*C*H_2), 27.8 (cyclohexyl-*C*H_2), 26.7 (cyclohexyl-*C*H_2), 26.6 (cyclohexyl-*C*H_2), 26.2 (cyclohexyl-*C*H_2) ppm; **HRMS** (ESI) m/z calcd. for $C_{16}H_{23}N_2$ ($[M+H]^+$) 243.18558, found 243.18596; **FT-IR (thin film)** ν_{max} 2925, 2852, 1543, 1447, 1368, 762, 693 cm^{-1}; **$[\alpha]_D^{25}$** = +4.0 (c = 1.0, $CHCl_3$); **Chiral HPLC**: Chiralpak AD, 4.6 x 250 mm; 1% *i*PrOH/hexanes, 1.0 mL/min; t_R (minor) = 21.9 min, t_R (major) = 18.3 min, 98:2 er.

(*R*)-5-cyclopropyl-1-methyl-3-phenyl-4,5-dihydro-1H-pyrazole (238)

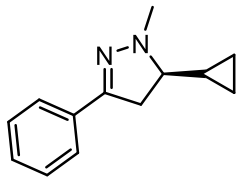

238 was prepared following General Procedure **J**, using (*E*)-3-cyclopropyl-1-phenylprop-2-en-1-one to afford the title compound as a colourless oil (89 mg, 89%, 98:2 er).

^{1}H NMR (400 MHz, $CDCl_3$): δ 7.47 – 7.40 (m, 2H, Ar*H*), 7.21 – 7.06 (m, 3H, Ar*H*), 2.99 (dd, *J* = 16.0, 9.5 Hz, 1H, C*H*NN), 2.80 (s, 3H, NCH_3), 2.67 (dd, *J* = 16.0, 13.0 Hz, 1H, C(N)-CH_2-), 2.32 – 2.17 (m, 1H, C(N)-CH_2-), 0.84 (qt, *J* = 8.3, 5.0 Hz, 1H, NCC*H*), 0.49 (dddd, *J* = 9.0, 7.9, 5.5, 4.5 Hz, 1H, CHCH_2), 0.37 (dddd, *J* = 9.0, 8.3, 5.5, 4.5 Hz, 1H, CHCH_2), 0.15 (ddt, *J* = 9.5, 5.5, 4.5 Hz, 1H, CHCH_2), -0.01 (ddt, *J* = 9.5, 5.5, 4.5 Hz, 1H, CHCH_2) ppm; **^{13}C NMR (101 MHz, $CDCl_3$)**: δ 149.0 (*C*(N)), 132.1 (Ar*C*), 127.3 (Ar*C*H), 1270.2 (Ar*C*H), 124.5 (Ar*C*H), 73.2 (*C*NH), 40.7 (-N-*C*-CH_2-C(N)), 38.4 (-N-C-*C*H_2-C(N)), 11.6 (*C*HCH_2), 3.5 (CH*C*H_2), 0.0 (CH*C*H_2) ppm; **HRMS** (ESI) m/z calcd. for $C_{13}H_{17}N_2$ ($[M+H]^+$) 201.13863, found 201.13855; **FT-IR (thin film)** ν_{max} 1472, 1248, 1177, 755, 690 cm^{-1}; **$[\alpha]_D^{25}$** = +8.5 (c = 1.0, $CHCl_3$); **Chiral HPLC**: Chiralpak AD, 4.6 x 250 mm; 1% *i*PrOH/hexanes, 1.0 mL/min; t_R (minor) = 9.6 min, t_R (major) = 27.5 min, 98:2 er.

(*R*)-1-methyl-5-pentyl-3-phenyl-4,5-dihydro-1H-pyrazole (239)

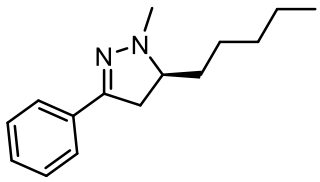

239 was prepared following General Procedure **J**, using (*E*)-1-phenyloct-2-en-1-one to afford the title compound as a colourless oil (94 mg, 82%, >99:1 er).

^{1}H NMR (400 MHz, $CDCl_3$): δ 7.67 – 7.57 (m, 2H, Ar*H*), 7.38 – 7.26 (m, 3H, Ar*H*), 3.19 (dd, *J* = 15.6, 9.4 Hz, 1H, C*H*NN), 3.03 (dtd, *J* = 13.5, 9.4, 3.7 Hz, 1H, CH_2), 2.89 (s, 3H, NCH_3), 2.62 (dd, *J* = 15.6, 13.5 Hz, 1H, CH_2), 1.90 – 1.78 (m, 1H, AlkC*H*), 1.57 (dtd, *J* = 15.2, 9.2, 8.3, 3.9 Hz, 1H, AlkC*H*), 1.47 – 1.29 (m, 6H, AlkC*H*), 0.99 – 0.84 (m, 3H, AlkCH_3) ppm; **^{13}C NMR (101 MHz, $CDCl_3$)**: δ 150.7 (*C*(N)), 133.2 (Ar*C*), 128.4 (Ar*C*H), 128.3 (Ar*C*H), 125.76 (Ar*C*H), 69.5 (*C*NH), 41.7 (*C*H_2), 39.1 (N*C*H_3), 32.7 (Alk*C*H_2), 32.0 (Alk*C*H_2), 26.6 (Alk*C*H_2), 22.6 (Alk*C*H_2), 14.0 (Alk*C*H_3) ppm; **HRMS** (ESI) m/z calcd. for $C_{15}H_{23}N_2$ ([M+H]$^+$) 231.18558, found 231.18535; **FT-IR (thin film)** ν_{max} 2957, 2929, 1445, 758, 692 cm^{-1}; **$[\alpha]_D^{25}$** = +17.8 (c = 1.0, $CHCl_3$); **Chiral HPLC**: Chiralpak AD-H, 4.6 x 250 mm; 1% *i*PrOH/hexanes, 1.0 mL/min; t_R (minor) = 42.4 min, t_R (major) = 20.1 min, 91:9 er.

(*R*)-5-(hept-1-yn-1-yl)-1-methyl-3-phenyl-4,5-dihydro-1H-pyrazole (240)

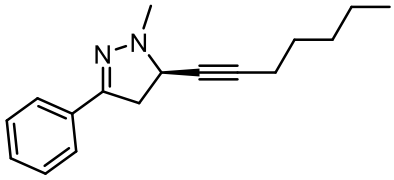

240 was prepared following General Procedure **J**, using (*E*)-1-phenyldec-2-en-4-yn-1-one to afford the title compound as a colourless oil (93 mg, 73%, 95:5 er).

^{1}H NMR (400 MHz, $CDCl_3$): δ 7.68 – 7.59 (m, 2H, Ar*H*), 7.42 – 7.28 (m, 3H, Ar*H*), 3.97 – 3.88 (m, 1H, C*H*NN), 3.29 (dd, *J* = 15.6, 9.6 Hz, 1H, CH_2), 3.09 (dd, *J* = 15.6, 10.9 Hz, 1H, CH_2), 3.02 (s, 3H, NCH_3), 2.24 (td, *J* = 7.1, 2.0 Hz, 2H, C≡CCH_2), 1.43 (m , 6H, CH_2CH_2CH_2CH_3), 0.99 – 0.84 (m, 3H, CH_2CH_3) ppm; **^{13}C NMR (101 MHz, $CDCl_3$)**: δ 150.6 (*C*(N)), 132.7 (Ar*C*), 128.6 (Ar*C*H), 128.4 (Ar*C*H), 125.8 (Ar*C*H), 85.8 (NC-*C*≡C-), 76.8 (NC-C≡*C*-), 58.6 (*C*H_2), 41.0 (*C*H_2), 40.9 (N*C*H_3), 31.0 (*C*H_2), 28.3 (*C*H_2), 22.1 (*C*H_2), 13.9 (*C*H_3) ppm; **HRMS** (ESI) m/z calcd. for $C_{17}H_{23}N_2$ ($[M+H]^+$) 255.18558, found 255.18521; **FT-IR (thin film)** ν_{max} 2241, 1243, 1130, 934, 758, 689 cm^{-1}; **$[\alpha]_D^{25}$** = +23.2 (c = 1.0, $CHCl_3$); **Chiral HPLC**: Chiralpak IA, 4.6 x 250 mm; 2% *i*PrOH/hexanes, 1.0 mL/min; t_R (minor) = 26.6 min, t_R (major) = 27.8 min, 95:5 er.

(*R*)-1-methyl-5-phenyl-3-(phenylethynyl)-4,5-dihydro-1H-pyrazole (241)

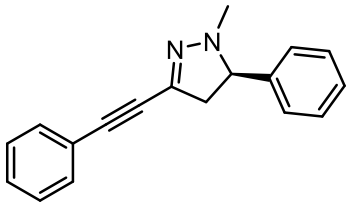

241 was prepared following General Procedure **J**, using (*E*)-1,5-diphenylpent-1-en-4-yn-3-one at -40 °C to afford the title compound as a colourless oil (105 mg, 81%, 97:3).

^{1}H NMR (400 MHz, $CDCl_3$): δ 7.45 – 7.38 (m, 2H, Ar*H*), 7.37 – 7.33 (m, 2H, Ar*H*), 7.32 – 7.27 (m, 2H, Ar*H*), 7.27 – 7.21 (m, 4H, Ar*H*), 4.10 (dd, *J* = 14.8, 10.3 Hz, 1H, C*H*NN), 3.15 (dd, *J* = 16.4, 10.3 Hz, 1H, CH_2), 2.82 (dd, *J* = 16.4, 14.8 Hz, 1H, CH_2), 2.73 (s, 3H, NCH_3) ppm; **^{13}C NMR (101 MHz, $CDCl_3$)**: δ 139.5 (*C*(N)), 133.7 (Ar*C*), 131.6 (Ar*C*H), 128.7 (Ar*C*H), 128.73 (Ar*C*H), 128.3 (Ar*C*H), 128.0 (Ar*C*H), 127.4 (Ar*C*H), 122.4 (Ar*C*), 93.1 (ArC=*C*), 83.0 (Ar*C*=C), 73.4 (*C*NH), 46.3 (CH_2), 40.8 (NCH_3) ppm; **HRMS** (ESI) m/z calcd. for $C_{18}H_{17}N_2$ ([M+H]$^+$) 261.13863, found 261.13865; **FT-IR (thin film)** ν_{max} 1488, 1443, 1360, 1129, 955, 754, 690 cm^{-1}; **$[\alpha]_D^{25}$** = +9.4 (c = 1.0, $CHCl_3$); **Chiral HPLC**: Chiralpak OG, 4.6 x 250 mm; 2% *i*PrOH/hexanes, 1.0 mL/min; t_R (minor) = 8.3 min, t_R (major) = 9.7 min, 97:3 er.

(*R*)-1-methyl-5-phenyl-3-(phenylethynyl)-4,5-dihydro-1H-pyrazole (242)

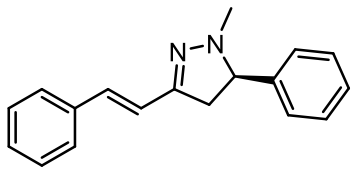

242 was prepared following General Procedure **J**, using (*E*)-1,5-diphenylpent-1-en-4-yn-3-one in CH_2Cl_2 to afford the title compound as a colourless oil (96 mg, 73%, 89:11 er).

^{1}H NMR (400 MHz, $CDCl_3$): δ 7.40 – 7.20 (m, 9H, Ar*H*), 7.15 (ddt, *J* = 7.1, 6.3, 1.3 Hz, 1H, Ar*H*), 6.99 (dd, *J* = 16.3, 0.9 Hz, 1H, ArC*H*CH), 6.47 (d, *J* = 16.3 Hz, 1H, ArCHC*H*), 4.01 (dd, *J* = 14.1, 10.2 Hz, 1H, C*H*NN), 3.25 (dd, *J* = 15.7, 10.2 Hz, 1H, CH_2), 2.77 (ddd, *J* = 15.7, 14.1, 0.9 Hz, 1H, CH_2), 2.72 (s, 3H, NCH_3) ppm; **^{13}C NMR (101 MHz, $CDCl_3$)**: δ 150.8 (*C*(N)), 140.2 (Ar*C*), 136.7 (Ar*C*), 132.5 (ArC=*C*), 128.7 (Ar*C*H), 128.7 (Ar*C*H), 128.0 (Ar*C*H), 127.8 (Ar*C*H), 127.4 (Ar*C*H), 126.6 (Ar*C*H), 122.0 (Ar*C*=C), 73.2 (*C*NH), 42.0 (*C*H_2), 41.1 (N*C*H_3) ppm; **HRMS** (ESI) m/z calcd. for $C_{18}H_{19}N_2$ ($[M+H]^+$) 263.15428, found 263.15414; **FT-IR (thin film)** ν_{max} 3060, 1653, 1541, 1492, 1373, 1283, 948, 691 cm^{-1}; **$[\alpha]_D^{25}$** = +82.6 (c = 1.0, $CHCl_3$); **Chiral HPLC**: Chiralpak AD, 4.6 x 250 mm; 2% *i*PrOH/hexanes, 1.0 mL/min; t_R (minor) = 20.7 min, t_R (major) = 30.5 min, 89:11 er.

(*R*)-1-methyl-5-phenyl-3-(trifluoromethyl)-4,5-dihydro-1H-pyrazole (243)

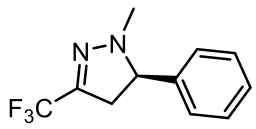

243 was prepared following General Procedure **J**, using (*E*)-1,1,1-trifluoro-4-phenylbut-3-en-2-one at -40 °C to afford the title compound as a colourless oil (91 mg, 80%, 95:5). Data is consistent with the published literature.[281]

^{1}H NMR (400 MHz, $CDCl_3$): δ 7.87 – 7.79 (m, 1H, Ar*H*), 7.48 – 7.27 (m, 4H, Ar*H*), 4.25 (dd, *J* = 15.0, 10.6 Hz, 1H, C*H*NN), 3.15 (dd, *J* = 16.0, 10.6 Hz, 1H, CH_2), 2.84 (dd, *J* = 16.0, 15.0 Hz, 1H, CH_2), 2.76 (s, 3H, NCH_3) ppm; **^{13}C NMR (101 MHz, $CDCl_3$)**: δ 152.3 (q, *J* = 37.5 Hz, *C*(N)), 134.8 (Ar*C*), 128.6 (Ar*C*H), 127.8 (Ar*C*H), 127.3 (Ar*C*H), 120.1 (q, *J* = 274.7 Hz, *C*F_3), 69.7 (*C*NH), 49.1 (*C*H_2), 41.8 (N*C*H_3) ppm; **^{19}F NMR (377 MHz, $CDCl_3$)** δ -66.8 ppm; **HRMS** (ESI) m/z calcd. for $C_{18}H_{17}N_2$ ($[M+H]^+$) 229.09526, found 229.09530; **$[\alpha]_D^{25}$** = +18.5 (c = 1.0, $CHCl_3$); **Chiral HPLC**: Chiralpak OG, 4.6 x 250 mm; 1% *i*PrOH/hexanes, 1.0 mL/min; t_R (minor) = 8.1 min, t_R (major) = 9.9 min, 95:5 er.

(*R*)-1-ethyl-3,5-diphenyl-4,5-dihydro-1H-pyrazole (244)

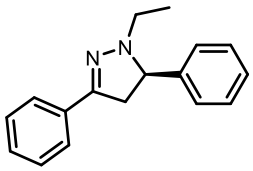

244 was prepared following General Procedure **J**, using chalcone, ethylhydrazine oxalate and diisopropylethylamine (1.95 eq) to afford the title compound as a colourless oil (110 mg, 88%, 94:6 er).

^{1}H NMR (400 MHz, $CDCl_3$): δ 7.73 – 7.67 (m, 2H, Ar*H*), 7.55 – 7.48 (m, 2H, Ar*H*), 7.44 – 7.30 (m, 6H, Ar*H*), 4.33 (dd, *J* = 14.1, 10.2 Hz, 1H, C*H*NN), 3.48 (dd, *J* = 16.1, 10.2 Hz, 1H, C(N)CH_2), 3.17 – 3.07 (m, 1H, CH_2CH_3), 3.06 – 2.93 (m, 1H, C(N)CH_2), 1.28 (t, *J* = 7.1 Hz, 3H, NCH_3) ppm; **^{13}C NMR (101 MHz, $CDCl_3$)**: δ 149.1 (*C*(N)), 141.2 (Ar*C*), 133.2 (Ar*C*), 128.6 (Ar*C*H), 128.4 (Ar*C*H), 128.4 (Ar*C*H), 127.7 (Ar*C*H), 127.6 (Ar*C*H), 125.7 (Ar*C*H), 70.9 (*C*NH), 48.2 (*C*H_2CH$_3$), 43.1 (C(N)*C*H_2), 12.8 (CH$_2$*C*H$_3$) ppm; **FT-IR (thin film)** ν_{max} 1501, 1462, 1300, 994, 776, 691 cm^{-1}; **HRMS** (ESI) m/z calcd. for $C_{17}H_{19}N_2$ ([M+H]$^+$) 251.15428, found 251.15412; **$[\alpha]_D^{25}$** = -7.2 (c = 1.0, $CHCl_3$); **Chiral HPLC**: Chiralpak AS-H, 4.6 x 250 mm; 1% *i*PrOH/hexanes, 1.0 mL/min; t_R (minor) = 4.5 min, t_R (major) = 5.7 min, 94:6 er.

(*R*)-3-(3,5-diphenyl-4,5-dihydro-1H-pyrazol-1-yl)propanenitrile (245)

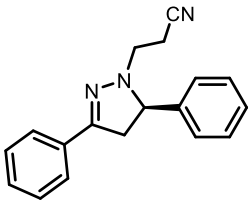

245 was prepared following General Procedure **J**, using chalcone and cyanoethylhydrazine to afford the title compound as a colourless oil (154 mg, 56%, 92:8 er).

^{1}H NMR (400 MHz, $CDCl_3$): δ 7.71 – 7.63 (m, 2H, Ar*H*), 7.54 – 7.47 (m, 2H, Ar*H*), 7.46 – 7.31 (m, 6H, Ar*H*), 4.31 (dd, *J* = 14.0, 9.9 Hz, 1H, C*H*NN), 3.49 (dd, *J* = 16.2, 10.0 Hz, 1H, C(N)CH_2), 3.27 – 3.06 (m, 2H, CH_2CH_2CN), 3.02 (dd, *J* = 16.2, 14.0 Hz, 1H, C(N)CH_2), 2.92 – 2.72 (m, 2H, CH_2CH_2CN) ppm; **^{13}C NMR (101 MHz, $CDCl_3$)**: δ 150.9 (*C*(N)), 139.6 (Ar*C*), 132.4 (Ar*C*), 129.1 (Ar*C*H), 128.9 (Ar*C*H), 128.6 (Ar*C*H), 128.2 (Ar*C*H), 127.5 (Ar*C*H), 125.9 (Ar*C*H), 118.7 (CH_2CN), 71.4 (*C*NH), 49.2 (CH_2CH_2CN), 43.1 (C(N)CH_2), 17.0 (CH_2CH_2CN) ppm; **FT-IR (thin film)** ν_{max} 2221, 1545, 1499, 1252, 813, 783, 692 cm^{-1}; **HRMS** (ESI) m/z calcd. for $C_{18}H_{18}N_3$ ($[M+H]^+$) 276.15007 found 276.15014; **$[\alpha]_D^{25}$** = -36.2 (c = 1.0, $CHCl_3$); **Chiral HPLC**: Chiralpak OG, 4.6 x 250 mm; 2% *i*PrOH/hexanes, 1.0 mL/min; t_R (minor) = 28.7 min, t_R (major) = 36.1 min, 92:8 er.

(*R*)-1-benzyl-3,5-diphenyl-4,5-dihydro-1H-pyrazole (246)

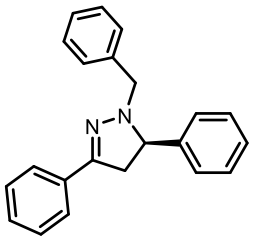

246 was prepared following General Procedure **J**, using chalcone, benzylhydrazine dihydrochloride and diisopropylethylamine (3.8 eq) to afford the title compound as a colourless oil (246 mg, 79%, 95:5 er). Data is consistent with the published literature.[220]

^{1}H NMR (400 MHz, $CDCl_3$): δ 7.65 (dq, *J* = 6.9, 1.3 Hz, 2H, Ar*H*), 7.48 (dd, *J* = 8.1, 1.5 Hz, 2H, Ar*H*), 7.42 – 7.23 (m, 11H, Ar*H*), 4.56 (d, *J* = 14.4 Hz, 1H, PhCH_2), 4.29 (dd, *J* = 14.1, 10.3 Hz, 1H, C*H*NN), 3.99 (d, *J* = 14.4 Hz, 1H, PhCH_2), 3.38 (dd, *J* = 16.0, 10.3 Hz, 1H, CH_2), 2.99 (dd, *J* = 16.0, 14.1 Hz, 1H, CH_2) ppm; **^{13}C NMR (101 MHz, $CDCl_3$)**: δ 148.8 (*C*(N)), 140.6 (Ar*C*), 136.8 (Ar*C*), 133.1 (Ar*C*), 129.6 (Ar*C*H), 128.6 (Ar*C*H), 128.4 (Ar*C*H), 128.3 (Ar*C*H), 128.1 (Ar*C*H), 127.7 (Ar*C*H), 127.7 (Ar*C*H), 127.1 (Ar*C*H), 125.6 (Ar*C*H), 69.0 (*C*NH), 56.6 (*C*H_2), 42.9 (N*C*H_3) ppm; **FT-IR (thin film)** ν_{max} 1527, 1463, 992, 766, 692 cm^{-1}; **HRMS** (ESI) m/z calcd. for $C_{22}H_{21}N_2$ ($[M+H]^+$) 313.16993, found 313.16968; **$[\alpha]_D^{25}$** = -16.4 (c = 1.0, $CHCl_3$); **Chiral HPLC**: Chiralpak IB, 4.6 x 250 mm; 1% *i*PrOH/hexanes, 1.0 mL/min; t_R (minor) = 8.1 min, t_R (major) = 10.3 min, 95:5 er.

4.3.4 Derivatisation of compound 219

Ethyl-(*R*,*E*)-3-(2-(5-(4-bromophenyl)-1-methyl-4,5-dihydro-1H-pyrazol-3-yl)phenyl)-acrylate (248)

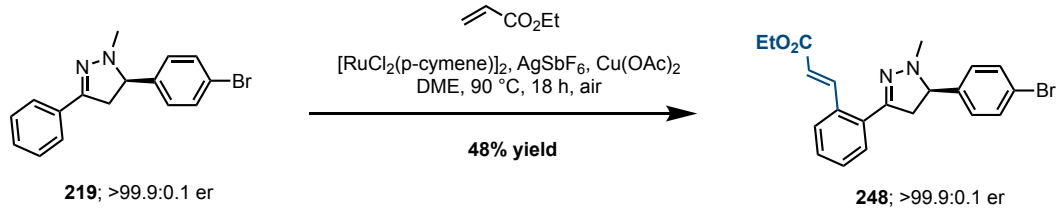

219; >99.9:0.1 er

248; >99.9:0.1 er

To an oven-dried screw-cap vial equipped with a magnetic stirrer bar was added pyrazoline **219** (314 mg, 1.00 mmol, 1.0 eq, >99.9:0.1 er), copper acetate (400 mg, 2.0 mmol, 2.0 eq), silver hexafluoroantimonate (34 mg, 0.1 mmol, 0.1 eq), dichloro(p-cymene)ruthenium(II) dimer (30 mg, 0.05 mmol, 0.05 eq), anhydrous DME (1.0 mL) and then ethyl acrylate (300 mg, 3.0 mmol, 3.0 eq). The reaction mixture was stirred under air at 90 °C for 18 hours. After completion, the reaction mixture was cooled to RT, quenched with water and extracted with EtOAc (3x25 mL). Combined organic layers were dried over Na_2SO_4, filtered and evaporated to afford the crude reaction mixture as a dark brown oily. Purification by silica gel chromatography afforded the title compound as a pale-yellow oil (198 mg, 48%, >99.9:0.1 er).

^{1}H NMR (400 MHz, $CDCl_3$): δ 8.52 (d, *J* = 15.8 Hz, 1H, C(O)CHC*H*), 7.66 – 7.55 (m, 1H, Ar*H*), 7.53 – 7.47 (m, 2H, Ar*H*), 7.42 – 7.27 (m, 5H, Ar*H*), 6.34 (d, *J* = 15.9 Hz, 1H, C(O)C*H*CH), 4.27 (qd, *J* = 7.1, 1.1 Hz, 2H, C(O)OCH_2CH$_3$), 4.12 (dd, *J* = 14.6, 9.9 Hz, 1H, C*H*NN), 3.39 (dd, *J* = 16.0, 9.9 Hz, 1H, C(N)CH_2), 3.04 (dd, *J* = 16.0, 14.6 Hz, 1H,

C(N)CH_2), 2.85 (s, 3H, NCH_3), 1.34 (t, J = 7.1 Hz, 3H, C(O)OCH$_2$CH_3) ppm **^{13}C NMR (101 MHz, CDCl$_3$)**: δ167.0 (C(O)), 148.7 (*C*(N)), 145.0 (C(O)CH*C*H), 139.2 (Ar*C*), 133.7 (Ar*C*), 132.3 (Ar*C*), 131.8 (Ar*C*H), 129.4 (Ar*C*H), 129.1 (Ar*C*H), 121.6 (Ar*C*), 119.3 (C(O)O*C*H$_2$CH$_3$), 72.8 (*C*NH), 60.3 (C(O)O*C*H$_2$CH$_3$), 45.5 (C(N)*C*H$_2$), 41.5 (N*C*H$_3$), 14.4 (C(O)OCH$_2$*C*H$_3$) ppm; **HRMS** (ESI) m/z calcd. for $C_{21}H_{22}O_2N_2{}^{79}Br$ ([M+H]$^+$) 413.08592, found 413.08395; **FT-IR (thin film)** ν_{max} 3017, 2360, 1706, 1630, 1575, 1313, 1173, 1037, 938, 761 cm^{-1}; **[α]$_D$ ^{25}** = +71.8 (c = 1.0, CHCl$_3$); **Chiral HPLC**: Chiralpak AD, 4.6 x 250 mm; 15% *i*PrOH/hexanes, 1.0 mL/min; t_R (single enantiomer) = 39.3 min, >99.9:0.1 er.

(1*R*)-*N*^{1}-methyl-1,3-diphenylpropane-1,3-diamine (249)

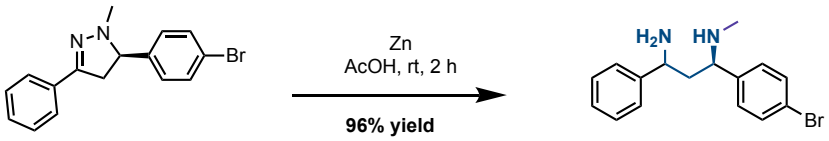

219; >99.9:0.1 er

249; >99.9:0.1 e.r., 3:2 dr

To an oven-dried 10 mL round bottom flask equipped with a magnetic stirred bar was added **219** (314 mg, 1.0 mmol, 1.0 eq) and zinc dust (1.30 g, 20.0 mmol, 20.0 eq). After three cycles of evacuation then nitrogen purge, glacial acetic acid (3.0 mL) was added. The resulting mixture was stirred at room temperature under a N_2 atmosphere for 2 hours. The reaction mixture was poured into a saturated solution of $NaHCO_3$ (200 mL) and extracted with CH_2Cl_2 (2x100 mL). The combined organic layers were dried over Na_2SO_4, filtered and evaporated *in vacuo* to afford a 3:2 diastereomeric mixture the title compound as a colourless oil (306 mg, 96%, >99.9:0.01 er, 3:2 dr).

^{1}H NMR (400 MHz, $CDCl_3$): δ 7.47 – 7.39 (m, 3H, Ar*H*), 7.35 – 7.18 (m, 8H, Ar*H*), 7.17 – 7.06 (m, 3H, Ar*H*), 3.86 – 3.77 (m, 2H, C*H*NN), 3.60 – 3.51 (m, 1H, C*H*NN), 3.36 (t, *J* = 6.9 Hz, 1H, C*H*NN), 2.20 (s, 1H, CH_2), 2.14 (s, 3H, NCH_3), 2.08 – 1.99 (m, 1H), 1.99 – 1.90 (m, 1H, CH_2), 1.84 (ddd, *J* = 13.9, 6.4, 4.7 Hz, 1H) ppm; **^{13}C NMR (101 MHz, $CDCl_3$)**: δ 146.9 (Ar*C*), 145.9 (Ar*C*), 142.9 (Ar*C*), 142.7 (Ar*C*), 131.5 (Ar*C*H), 129.0 (Ar*C*H), 128.8 (Ar*C*H), 128.6 (Ar*C*H), 128.6 (Ar*C*H), 127.1 (Ar*C*H), 127.0 (Ar*C*H), 126.3 (Ar*C*H), 125.9 (Ar*C*H), 63.4 (*C*HNH$_2$), 62.0 (*C*HNH$_2$), 54.5 (*C*HNH$_2$), 53.4 (*C*HNH$_2$), 47.4 (*C*H$_2$), 46.9 (*C*H$_2$), 34.3 (N*C*H$_3$), 34.2 (N*C*H$_3$) ppm; **HRMS** (ESI) m/z calcd. for $C_{16}H_{20}N_2{}^{79}Br$ ([M+H]$^+$)

319.08044, found 319.08047; **FT-IR (thin film)** ν_{max} 3336, 2971, 2159, 2030, 1379, 1160, 1128, 949, 815 cm^{-1}; $[\alpha]_D^{25}$ = -14.0 (c = 1.0, $CHCl_3$).

(8*R*,9*S*,13*S*,14*S*,17*R*)-3-methoxy-13-methyl-17-((4-((*R*)-1-methyl-3-phenyl-4,5-dihydro-1H-pyrazol-5-yl)phenyl)ethynyl)-7,8,9,11,12,13,14,15,16,17-decahydro-6H-cyclopenta[a]phenanthren-17-ol (251)

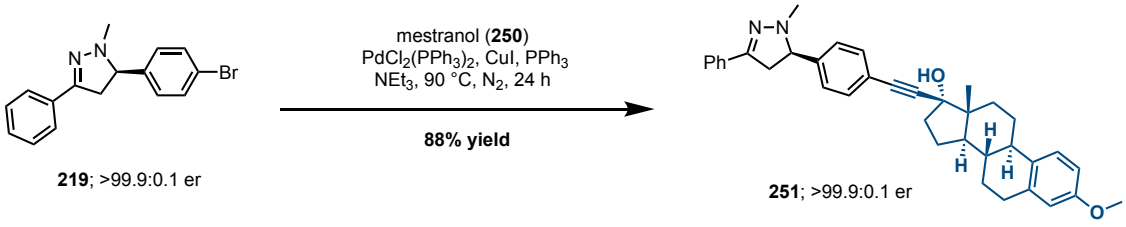

219; >99.9:0.1 er

251; >99.9:0.1 er

To an oven-dried screw-cap vial equipped with a magnetic stirrer bar was added pyrazoline **219** (282 mg, 0.60 mmol, 1.0 eq, >99.9:0.1 er), **250** (200 mg, 0.60 mmol, 1.0 eq), copper iodide (22 mg, 0.12 mmol, 0.2 eq), bis(triphenylphosphine), palladium dichloride (42 mg, 0.06 mmol, 0.1 eq), triphenylphosphine (78 mg, 0.30 mmol, 0.5 eq) and anhydrous triethylamine (2.0 mL). The vial was closed, evacuated and backfilled with nitrogen before heating to 90 °C for 18 hours. After completion, the reaction mixture was cooled to RT, quenched with water and extracted with EtOAc (3x25 mL). Combined organic layers were dried over Na_2SO_4, filtered and evaporated to afford the crude reaction mixture as a yellow oil. Purification by silica gel chromatography afforded the title compound as a pale-yellow powder (287 mg, 88%, >99.9:0.1 er).

^{1}H NMR (400 MHz, $CDCl_3$): δ 7.58 – 7.50 (m, 2H, Ar*H*), 7.36 (q, *J* = 8.3 Hz, 4H, Ar*H*), 7.31 – 7.20 (m, 3H, Ar*H*), 7.16 – 7.08 (m, 1H, Ar*H*), 6.63 (dd, *J* = 8.6, 2.9 Hz, 1H, Ar*H*), 6.55 (d, *J* = 2.9 Hz, 1H, Ar*H*), 4.01 (dd, *J* = 14.4, 10.1 Hz, 1H, C*H*NN), 3.68 (s, 3H, OCH_3),

3.37 (dd, *J* = 16.1, 10.0 Hz, 1H, C(N)C*H*$_2$), 2.85 (dd, *J* = 16.1, 14.4 Hz, 1H, C(N)C*H*$_2$), 2.77 (dq, *J* = 7.1, 4.3, 2.5 Hz, 2H, AlkC*H*), 2.73 (s, 3H, NC*H*$_3$), 2.32 (dddd, *J* = 22.6, 14.7, 10.1, 6.6 Hz, 2H, AlkC*H*), 2.16 – 1.54 (m, 7H, AlkC*H*), 1.53 – 1.13 (m, 4H, AlkC*H*), 0.85 (s, 3H, AlkC*H*$_3$) ppm; **^{13}C NMR (101 MHz, CDCl$_3$)**: δ 157.4 (Ar*C*OCH$_3$), 149.6 (*C*(N)), 140.7 (Ar*C*), 137.9 (Ar*C*), 132.7 (Ar*C*), 132.5 (Ar*C*),132.0 (Ar*C*H), 128.7 (Ar*C*H), 128.5 (Ar*C*H), 127.4 (Ar*C*H), 126.3 (Ar*C*H), 125.8 (Ar*C*H), 122.5 (Ar*C*), 113.8 (Ar*C*H), 111.5 (Ar*C*H), 93.1 (Ar*C*CCOH), 85.6 (ArC*C*COH), 80.3 (ArCC*C*OH), 73.2 (*C*NH), 55.2 (ArO*C*H$_3$), 49.8 (Alk*C*H), 47.7 (Alk*C*CH$_3$), 43.7 (Alk*C*H), 43.3 (C(N)*C*H$_2$), 41.5 (N*C*H$_3$), 39.5 (Alk*C*H), 39.1 (Alk*C*H$_2$), 33.1 (Alk*C*H$_2$), 29.8 (Alk*C*H$_2$), 27.3 (Alk*C*H$_2$), 26.5 (Alk*C*H$_2$), 23.0 (Alk*C*H$_2$), 12.9 (Alk*C*H$_3$) ppm; **HRMS** (ESI) m/z calcd. for $C_{37}H_{41}O_2N_2$ ($[M+H]^+$) 545.31626, found 545.31628; **FT-IR (thin film)** ν_{max} 3491, 2930, 2833, 2360, 1608, 1499, 1446, 1358, 1253, 1132, 1037, 908, 731, 692 cm^{-1}; **m.p.**: 79-81 °C; **$[\alpha]_D^{25}$** = -18.7 (c = 1.0, $CHCl_3$); **Chiral HPLC**: Chiralpak AD, 4.6 x 250 mm; 15% *i*PrOH/hexanes, 1.0 mL/min; t_R (single enantiomer) = 28.2 min, >99.9:0.1 er.

4.3.6 Preparative scale synthesis of 219

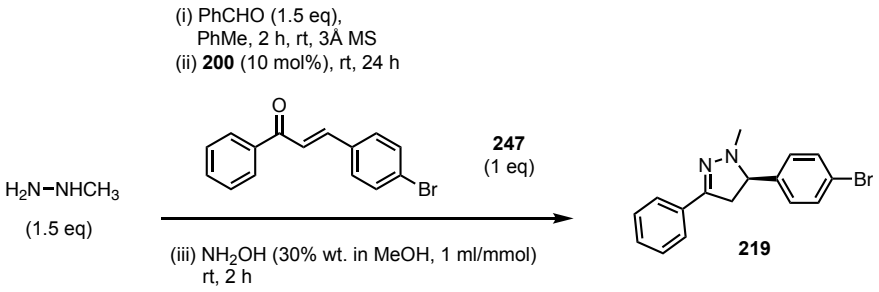

Scheme 51. Large scale synthesis of 4-bromo derivative **219**.

In a similar manner to the 0.5 mmol scale synthesis of pyrazoline **219**, the reaction was repeated on 100-gram (351 mmol) scale, as follows:

100-gram scale; according to **General Procedure C** the reaction was performed using enone **247** (100 g, 350.9 mmol, 1.0 eq), benzaldehyde (55.79 g, 526.4 mmol, 1.5 eq), methyl hydrazine (24.21 g, 526.35 mmol, 1.5 eq), anhydrous toluene (1400 mL), and 3Å molecular sieves (50 g) in a 2000 mL round-bottom flask equipped with a large magnetic stirring bar and a nitrogen balloon. The reaction was stirred at RT, under an atmosphere of nitrogen, for 24 hours. Over this period the reaction turned from a yellow solution to a light brown suspension (due to particulates of molecular sieves). Completion of the aza-Michael addition stage of the reaction was confirmed by TLC and NMR analysis. To the reaction was added a 30% w/w solution of NH_2OH in MeOH (351 ml). Again, completion of this stage of the reaction was confirmed by TLC and NMR analysis. After 2 hours, the reaction was filtered through cotton wool to remove molecular sieves residue. The resulting clear, light-yellow solution was evaporated to dryness *in vacuo* to afford a viscous yellow oil.

Recovery of catalyst **200**: to a 2000 mL round-bottom flask was added a large magnetic stirrer bar and 1500 mL of diethyl ether which was previously cooled to -15 °C. With vigorous stirring, the crude yellow oil obtained above was slowly poured into the cold diethyl ether (gentle heating of the oil beforehand aided in pouring of the oil). Upon addition to the cold diethyl ether, a white precipitate formed. Once addition was complete, the solid catalyst **200** was collected by vacuum filtration (with the aid of cold diethyl ether to wash glassware) before drying *in vacuo* for 12 hours and further purification as described below. The mother liquor from this stage is collected and purified as described below to isolate the pyrazoline product **219** and benzaldehyde oxime (**S61**).

To further purify the recovered catalyst **200**: he recovered white solid (obtained as described above, from diethyl ether) was dissolved in EtOAc (200 mL) and washed with water (200 mL). The organic layer was washed with 6M aqueous HCl (100 mL), then discarded, before basifying the aqueous layer to approximately pH 9.0 with a saturated aqueous solution of potassium carbonate. The aqueous layer was extracted with CH_2Cl_2 (3x50 mL), before drying combined organic layers over Na_2SO_4, filtering and evaporating *in vacuo* to afford a light brown oil. The oil was poured slowly into rapidly stirring pentane (500 mL, previously cooled to -15 °C). After 30 minutes of stirring at room temperature, the resulting solids were collected by filtration to afford analytically pure catalyst **200** as an off-white powder (14.53 g, 31.25 mmol, 89% recovery).

Isolation of pyrazoline product **219**: The diethyl ether mother liquor obtained (as described above) was evaporated to dryness *in vacuo* to give a crude mixture of product and benzaldehyde oxime (**S61**) as a yellow oil. The oil was dissolved in pentane and washed with 5M aqueous KOH solution (3x750 mL). The aqueous layers were retained for isolation of the oxime by-product, as described below. The pentane layer (which contains the desired pyrazoline product) was dried over Na_2SO_4, filtered and evaporated to dryness *in vacuo*. The thus obtained yellow solid was purified by recrystallization from EtOH to afford the pure pyrazoline **219** as colourless needles (84.92 g, 77%, >99.9:0.1 er)

Isolation of oxime by-product **S61**: the aqueous layers obtained from the KOH wash described above were combined and washed with CH_2Cl_2 (3x200 mL). Combined organic layers were dried over Na_2SO_4, filtered and evaporated to dryness in vacuo to afford the oxime **S61** as a colourless oil (61.78 g, 510.56 mmol, 97% recovery).

Chiral HPLC Analysis of Crude Product: Chiralpak OD-H, 4.6 x 250 mm; 1% *i*PrOH/hexanes, 1.0 mL/min; t_R (minor) = 16.9 min, t_R (major) = 47.2 min, **94:6 er**.

Chiral HPLC Analysis of Recrystallized Product: Chiralpak OD-H, 4.6 x 250 mm; 1% *i*PrOH/hexanes, 1.0 mL/min; t_R (single enantiomer) = 46.9 min, **>99.9:0.1 er**.

4.3.7 Recycling of catalyst 200

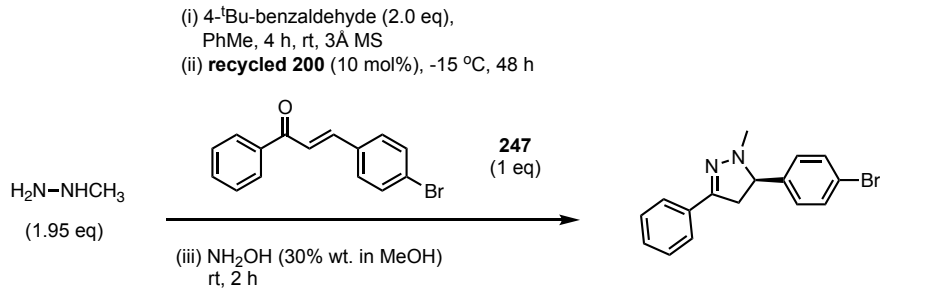

Scheme 52. Synthesis of **219** with recycled catalyst **200**.

Following General Procedure **C**, the reaction of **247** was repeated on 0.5 mmol scale using catalyst **200** recovered from the large-scale synthesis of **219** (**Scheme 52**). Compound **219** was obtained in 88% yield and 96:4 er (compared with 87% yield and 96:4 er in the original synthesis using catalyst **200** which had not previously been used).

4.3.8 Single-Crystal X-ray diffraction studies of 219

X-ray diffraction data has been made available in the Cambridge Crystallographic Data Centre as **CCDC 1871038.**

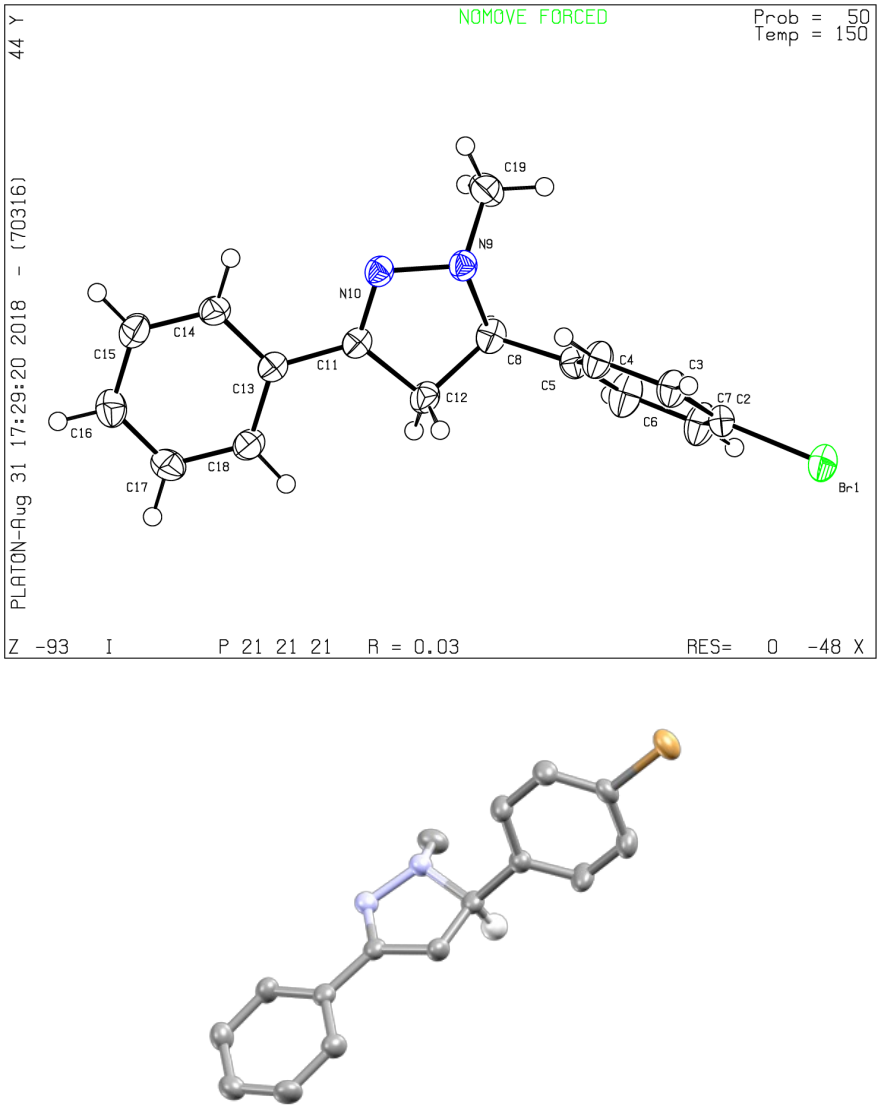

Figure 24. Ball and stick representations of the single crystal X-Ray diffraction data for **219**.

Chemical formula	$C_{16}H_{15}BrN_2$
M_r	315.21
Crystal system, space group	Orthorhombic, $P2_12_12_1$
Temperature (K)	150
***a*, *b*, *c* (Å)**	5.5700 (2), 8.0191 (3), 32.2609 (11)
***V* (Å^3)**	1440.98 (9)
Z	4
Radiation type	Cu $K\alpha$
μ (mm^{-1})	3.77
Crystal size (mm)	0.15 × 0.10 × 0.10
Diffractometer	Oxford Diffraction SuperNova
Absorption correction	Multi-scan *CrysAlis PRO* (Rigaku Oxford Diffraction, 2017)
T_{min}, T_{max}	0.48, 0.69
No. of measured, independent and observed [$I > 2.0\sigma(I)$] reflections	5619, 2956, 2919
R_{int}	0.020
(sin θ/λ)$_{max}$ (Å^{-1})	0.630
$R[F^2 > 2\sigma(F^2)]$, $wR(F^2)$, S	0.026, 0.068, 1.00
No. of reflections	2956
No. of parameters	173
H-atom treatment	H-atom parameters constrained
$\Delta\varrho_{max}$, $\Delta\varrho_{min}$ (e Å^{-3})	0.43, −0.52
Absolute structure	Parsons, Flack & Wagner (2013), 1181 Friedel Pairs
Absolute Structure Parameter	-0.026 (7)

Structure Parameter Data:

Br1—C2	1.908 (2)	N9—C12	1.451 (3)
C2—C3	1.376 (4)	N10—C11	1.280 (3)
C2—C7	1.373 (4)	C11—C12	1.503 (3)
C3—C4	1.394 (3)	C11—C13	1.470 (3)
C4—C5	1.385 (3)	C13—C14	1.395 (3)
C5—C6	1.376 (3)	C13—C18	1.394 (3)
C5—C8	1.513 (3)	C14—C15	1.381 (3)
C6—C7	1.390 (4)	C15—C16	1.393 (4)
C8—N9	1.481 (3)	C16—C17	1.378 (4)
C8—C12	1.533 (3)	C17—C18	1.391 (3)
Br1—C2—C3	119.18 (18)	N10—N9—C19	111.38 (18)
Br1—C2—C7	118.65 (19)	N9—N10—C11	109.58 (19)
C3—C2—C7	122.2 (2)	N10—C11—C12	113.3 (2)
C2—C3—C4	118.4 (2)	N10—C11—C13	121.3 (2)
C3—C4—C5	121.0 (2)	C12—C11—C13	125.4 (2)
C4—C5—C6	118.6 (2)	C8—C12—C11	100.62 (19)
C4—C5—C8	120.9 (2)	C11—C13—C14	120.4 (2)
C6—C5—C8	120.4 (2)	C11—C13—C18	120.9 (2)
C5—C6—C7	121.8 (2)	C14—C13—C18	118.6 (2)
C6—C7—C2	118.1 (2)	C13—C14—C15	120.9 (2)
C5—C8—N9	112.68 (19)	C14—C15—C16	120.1 (2)
C5—C8—C12	114.6 (2)	C15—C16—C17	119.6 (2)
N9—C8—C12	102.38 (19)	C16—C17—C18	120.4 (2)
C8—N9—N10	107.87 (18)	C13—C18—C17	120.4 (2)
C8—N9—C19	114.1 (2)		

References

(1) Chen, X.; Zhang, D.; Deng, J.; Fu, X. Determination of Optical Impurity of Pregabalin by HPLC with Pre-Column Chiral Derivatization. *J. Chromatogr. Sci.* **2008**, *46* (1), 42–44.

(2) Ariens, E. . Ariens, E.J (1989). Chiral Separations by HPLC. Chichester: Ellis Horwwod, Chichester. Pp. 31–68. In *Chiral Separations by HPLC*; 1989; pp 31–68.

(3) Melchert, M.; List, A. The Thalidomide Saga. *Int. J. Biochem. Cell Biol.* **2007**, *39* (7), 1489–1499.

(4) Caner, H.; Groner, E.; Levy, L.; Agranat, I. Trends in the Development of Chiral Drugs. *Drug Discov. Today* **2004**, *9* (3), 105–110.

(5) Porter, W. H. Resolution of Chiral Drugs. *Pure Appl. Chem.* **1991**, *63*, 1119–1122.

(6) Blaser, H. U. The Chiral Pool as a Source of Enantioselective Catalysts and Auxiliaries. *Chem. Rev.* **1992**, *92* (5), 935–952.

(7) Brill, Z. G.; Condakes, M. L.; Ting, C. P.; Maimone, T. J. Navigating the Chiral Pool in the Total Synthesis of Complex Terpene Natural Products. *Chem. Rev.* **2017**, *117* (18), 11753–11795.

(8) Roos, G. Compendium of Chiral Auxiliary Applications. In *Compendium of Chiral Auxiliary Applications*; Academic Press: New York, 2002.

(9) Saha, D. Catalytic Enantioselective Radical Transformations Enabled by Visible Light. *Chem. - An Asian J.* **2020**, *15* (14), 2129–2152.

(10) Editors, T.; Editors, T. Introduction : Enantioselective Catalysis. *Chem. Rev.* **2003**, *103* (8), 2761–2762.

(11) Trost, B. M. Atom Economy—A Challenge for Organic Synthesis: Homogeneous Catalysis Leads the Way. *Angew. Chemie Int. Ed. English* **1995**, *34* (3), 259–281.

(12) Toste, F. D.; You, S. L. Asymmetric Synthesis Enabled by Organometallic Complexes. *Organometallics* **2019**, *38* (20), 3899–3901.

(13) Noyori, R. Asymmetric Catalysis: Science and Opportunities (Nobel Lecture 2001). *Adv. Synth. Catal.* **2003**, *345* (1–2), 15–32.

(14) Winkler, C. K.; Schrittwieser, J. H.; Kroutil, W. Power of Biocatalysis for Organic Synthesis. *ACS Cent. Sci.* **2021**, *7* (1), 55–71.

(15) Arnold, F. H. Innovation by Evolution: Bringing New Chemistry to Life (Nobel Lecture). *Angew. Chemie - Int. Ed.* **2019**, *58* (41), 14420–14426.

(16) MacMillan, D. W. C. The Advent and Development of Organocatalysis. *Nature* **2008**, *455* (7211), 304–308.

(17) Ahrendt, K. A.; Borths, C. J.; MacMillan, D. W. C. New Strategies for Organic Catalysis: The First Enantioselective Organocatalytic 1,3-Dipolar Cycloaddition. *J. Am. Chem. Soc.* **2000**, *122* (17), 4243–4244.

(18) Zoltán G., H.; Parrish, D. R. Asymmetric Bicyclic. *J.Org. Chem* **1974**, *39* (12), 1615–1621.

(19) Eder, U.; Sauer, G.; Wiechert, R. New Type of Asymmetric Cyclization to Optically Active Steroid CD Partial Structures. *Angew. Chemie Int. Ed. English* **1971**, *10* (7), 496–497.

(20) Tanaka, K.; Mori, A.; Inoue, S. The Cyclic Dipeptide Cyclo[(S)-Phenylalanyl-(S)-Histidyl] as a Catalyst for Asymmetric Addition of Hydrogen Cyanide to Aldehydes. *J. Org. Chem.* **1990**, *55* (1), 181–185.

(21) Oku, J. I.; Inoue, S. Asymmetric Cyanohydrin Synthesis Catalysed by a Synthetic Cyclic Dipeptide. *J. Chem. Soc. Chem. Commun.* **1981**, No. 5, 229–230.

(22) Bertelsen, S.; Jørgensen, K. A. Organocatalysis–after the Gold Rush. *Chem. Soc. Rev.* **2009**, *38* (8), 2178–2189.

(23) Dondoni, A.; Massi, A. Asymmetric Organocatalysis: From Infancy to Adolescence. *Angew. Chemie - Int. Ed.* **2008**, *47* (25), 4638–4660.

(24) Matthews, W. S.; Bares, J. E.; Bartmess, J. E.; Cornforth, F. J.; Drucker, G. E.; McCallum, R. J.; McCollum, G. J.; Vanier, N. R.; Bordwell, F. G.; Margolin, Z. Equilibrium Acidities of Carbon Acids. VI. Establishment of an Absolute Scale of Acidities in Dimethyl Sulfoxide Solution. *J. Am. Chem. Soc.* **1975**, *97* (24), 7006–7014.

(25) Palomo, C.; Oiarbide, M.; López, R. Asymmetric Organocatalysis by Chiral Brønsted Bases: Implications and Applications. *Chem. Soc. Rev.* **2009**, *38* (2), 632–653.

(26) Odagi, M.; Nagasawa, K. Recent Advances in Natural Products Synthesis Using Bifunctional Organocatalysts Bearing a Hydrogen-Bonding Donor Moiety. *Asian J. Org. Chem.* **2019**, *8* (10), 1766–1774.

(27) Siau, W. Y.; Wang, J. Asymmetric Organocatalytic Reactions by Bifunctional Amine-Thioureas. *Catal. Sci. Technol.* **2011**, *1* (8), 1298–1310.

(28) Fang, X.; Wang, C. J. Recent Advances in Asymmetric Organocatalysis Mediated by

Bifunctional Amine-Thioureas Bearing Multiple Hydrogen-Bonding Donors. *Chem. Commun.* **2015**, *51* (7), 1185–1197.

(29) Okino, T.; Hoashi, Y.; Takemoto, Y. Enantioselective Michael Reaction of Malonates to Nitroolefins Catalyzed by Bifunctional Organocatalysts. *J. Am. Chem. Soc.* **2003**, *125* (42), 12672–12673.

(30) Hamza, A.; Schubert, G.; Soós, T.; Pápai, I. Theoretical Studies on the Bifunctionality of Chiral Thiourea-Based Organocatalysts: Competing Routes to C-C Bond Formation. *J. Am. Chem. Soc.* **2006**, *128* (40), 13151–13160.

(31) Jiang, L.; Chen, Y. C. Recent Advances in Asymmetric Catalysis with Cinchona Alkaloid-Based Primary Amines. *Catal. Sci. Technol.* **2011**, *1* (3), 354–365.

(32) Marcelli, T.; Hiemstra, H. Cinchona Alkaloids in Asymmetric Organocatalysis. *Synthesis (Stuttg).* **2010**, No. 8, 1229–1279.

(33) Connon, S. J. Asymmetric Catalysis with Bifunctional Cinchona Alkaloid-Based Urea and Thiourea Organocatalysts. *Chem. Commun.* **2008**, No. 22, 2499–2510.

(34) Grayson, M. N.; Houk, K. N. Cinchona Urea-Catalyzed Asymmetric Sulfa-Michael Reactions: The Brønsted Acid-Hydrogen Bonding Model. *J. Am. Chem. Soc.* **2016**, *138* (29), 9041–9044.

(35) Tian, S. K.; Chen, Y.; Hang, J.; Tang, L.; McDaid, P.; Deng, L. Asymmetric Organic Catalysis with Modified Cinchona Alkaloids. *Acc. Chem. Res.* **2004**, *37* (8), 621–631.

(36) Vakulya, B.; Varga, S.; Csámpai, A.; Soós, T. Highly Enantioselective Conjugate Addition of Nitromethane to Chalcones Using Bifunctional Cinchona Organocatalysts. *Org. Lett.* **2005**, *7* (10), 1967–1969.

(37) Li, B. J.; Jiang, L.; Liu, M.; Chen, Y. C.; Ding, L. S.; Wu, Y. Asymmetric Michael Addition of Arylthiols to α,β-Unsaturated Carbonyl Compounds Catalyzed by Bifunctional Organocatalysts. *Synlett* **2005**, No. 4, 603–606.

(38) Ye, J.; Dixon, D. J.; Hynes, P. S. Enantioselective Organocatalytic Michael Addition of Malonate Esters to Nitro Olefins Using Bifunctional Cinchonine Derivatives. *Chem. Commun.* **2005**, No. 35, 4481–4483.

(39) McCooey, S. H.; Connon, S. J. Urea- and Thiourea-Substituted Cinchona Alkaloid Derivatives as Highly Efficient Bifunctional Organocatalysts for the Asymmetric Addition of Malonate to Nitroalkenes: Inversion of Configuration at C9 Dramatically Improves Catalyst Performance. *Angew. Chemie - Int. Ed.* **2005**, *44* (39), 6367–6370.

(40) Marcelli, T.; Van Der Haas, R. N. S.; Van Maarseveen, J. H.; Hiemstra, H.

Asymmetric Organocatalytic Henry Reaction. *Angew. Chemie - Int. Ed.* **2006**, *45* (6), 929–931.

(41) Malerich, J. P.; Hagihara, K.; Rawal, V. H. Chiral Squaramide Derivatives Are Excellent Hydrogen Bond Donor Catalysts. *J. Am. Chem. Soc.* **2008**, *130* (44), 14416–14417.

(42) Bae, H. Y.; Song, C. E. Unprecedented Hydrophobic Amplification in Noncovalent Organocatalysis "on Water": Hydrophobic Chiral Squaramide Catalyzed Michael Addition of Malonates to Nitroalkenes. *ACS Catal.* **2015**, *5* (6), 3613–3619.

(43) Liu, K.; Khan, I.; Cheng, J.; Hsueh, Y. J.; Zhang, Y. J. Asymmetric Decarboxylative Cycloaddition of Vinylethylene Carbonates with β-Nitroolefins by Cooperative Catalysis of Palladium Complex and Squaramide. *ACS Catal.* **2018**, *8* (12), 11600–11604.

(44) Sopeña, S.; Martin, E.; Escudero-Adán, E. C.; Kleij, A. W. Pushing the Limits with Squaramide-Based Organocatalysts in Cyclic Carbonate Synthesis. *ACS Catal.* **2017**, *7* (5), 3532–3539.

(45) Ni, X.; Li, X.; Wang, Z.; Cheng, J. P. Squaramide Equilibrium Acidities in DMSO. *Org. Lett.* **2014**, *16* (6), 1786–1789.

(46) Zhang, Y.; Wang, W. Recent Advances in Organocatalytic Asymmetric Michael Reactions. *Catal. Sci. Technol.* **2012**, *2* (1), 42–53.

(47) Malkar, R. S.; Jadhav, A. L.; Yadav, G. D. Innovative Catalysis in Michael Addition Reactions for C-X Bond Formation. *Mol. Catal.* **2020**, *485* (January), 110814.

(48) Das, T.; Mohapatra, S.; Mishra, N. P.; Nayak, S.; Raiguru, B. P. Recent Advances in Organocatalytic Asymmetric Michael Addition Reactions to α, β-Unsaturated Nitroolefins. *ChemistrySelect* **2021**, *6* (15), 3745–3781.

(49) Bagheri, I.; Mohammadi, L.; Zadsirjan, V.; Heravi, M. M. Organocatalyzed Asymmetric Mannich Reaction: An Update. *ChemistrySelect* **2021**, *6* (5), 1008–1066.

(50) Wang, J.; Liu, X.; Feng, X. Asymmetric Strecker Reactions. *Chem. Rev.* **2011**, *111* (11), 6947–6983.

(51) Yan, H.; Suk Oh, J.; Lee, J. W.; Eui Song, C. Scalable Organocatalytic Asymmetric Strecker Reactions Catalysed by a Chiral Cyanide Generator. *Nat. Commun.* **2012**, *3*, 1–7.

(52) Merino, P.; Marqués-López, E.; Tejero, T.; Herrera, R. P. Enantioselective Organocatalytic Diels-Alder Reactions. *Synthesis (Stuttg).* **2010**, No. 1, 1–26.

(53) Alvarez-Casao, Y.; Marques-Lopez, E.; Herrera, R. P. Organocatalytic Enantioselective Henry Reactions. *Symmetry (Basel).* **2011**, *3* (2), 220–245.

(54) Dong, L.; Chen, F. E. Asymmetric Catalysis in Direct Nitromethane-Free Henry Reactions. *RSC Adv.* **2020**, *10* (4), 2313–2326.

(55) Huang, X.; David, E.; Jubault, P.; Besset, T.; Couve-Bonnaire, S. Organocatalyzed Sulfa-Michael Addition of Thiophenols on Trisubstituted α-Fluoroacrylates, a Straightforward Access to Chiral Fluorinated Compounds. *J. Org. Chem.* **2020**, *85* (21), 14055–14067.

(56) Xu, C.; Bartley, J. K.; Enache, D. I.; Knight, D. W.; Hutchings, G. J. High Surface Area MgO as a Highly Effective Heterogeneous Base Catalyst for Michael Addition and Knoevenagel Condensation Reactions. *Synthesis (Stuttg).* **2005**, No. 19, 3468–3476.

(57) Li, J. N.; Liu, L.; Fu, Y.; Guo, Q. X. What Are the PKa Values of Organophosphorus Compounds? *Tetrahedron* **2006**, *62* (18), 4453–4462.

(58) Shang, M.; Wang, X.; Koo, S. M.; Youn, J.; Chan, J. Z.; Yao, W.; Hastings, B. T.; Wasa, M. Frustrated Lewis Acid/Brønsted Base Catalysts for Direct Enantioselective α-Amination of Carbonyl Compounds. *J. Am. Chem. Soc.* **2017**, *139* (1), 95–98.

(59) Rigby, C. L.; Dixon, D. J. Enantioselective Organocatalytic Michael Additions to Acrylic Acid Derivatives: Generation of All-Carbon Quaternary Stereocentres. *Chem. Commun.* **2008**, No. 32, 3798–3800.

(60) Fang, X.; Dong, X. Q.; Liu, Y. Y.; Wang, C. J. Organocatalytic Asymmetric Sulfa-Michael Addition of Thiols to Trans-3,3,3-Trifluoropropenyl Phenyl Sulfone. *Tetrahedron Lett.* **2013**, *54* (34), 4509–4511.

(61) Dong, X. Q.; Fang, X.; Tao, H. Y.; Zhou, X.; Wang, C. J. Highly Efficient Catalytic Asymmetric Sulfa-Michael Addition of Thiols to Trans-4,4,4-Trifluorocrotonoylpyrazole. *Adv. Synth. Catal.* **2012**, *354* (6), 1141–1147.

(62) Ortín, I.; Dixon, D. J. Direct Catalytic Enantio- and Diastereoselective Mannich Reaction of Isocyanoacetates and Ketimines. *Angew. Chemie - Int. Ed.* **2014**, *53* (13), 3462–3465.

(63) Ishikawa, T. *Superbases for Organic Synthesis: Guanidines, Amidines, Phosphazenes and Related Organocatalysts*; John Wiley & Sons, Ltd.: Chichester, UK, 2009.

(64) Formica, M.; Rozsar, D.; Su, G.; Farley, A. J. M.; Dixon, D. J. Bifunctional Iminophosphorane Superbase Catalysis: Applications in Organic Synthesis. *Acc. Chem. Res.* **2020**, *53* (10), 2235–2247.

(65) Krawczyk, H.; Dzięgielewski, M.; Deredas, D.; Albrecht, A.; Albrecht, Ł. Chiral Iminophosphoranes - An Emerging Class of Superbase Organocatalysts. *Chem. - A Eur. J.* **2015**, *21* (29), 10268–10277.

(66) Ishikawa, T.; Harwood, L. M. Organic Superbases: The Concept at a Glance. *Synlett* **2013**, *24* (19), 2507–2509.

(67) Caubère, P. Unimetal Super Bases. *Chem. Rev.* **1993**, *93* (6), 2317–2334.

(68) Rossini, E.; Bochevarov, A. D.; Knapp, E. W. Empirical Conversion of pKa Values between Different Solvents and Interpretation of the Parameters: Application to Water, Acetonitrile, Dimethyl Sulfoxide, and Methanol. *ACS Omega* **2018**, *3* (2), 1653–1662.

(69) Leow, D.; Tan, C. H. Chiral Guanidine Catalyzed Enantioselective Reactions. *Chem. - An Asian J.* **2009**, *4* (4), 488–507.

(70) Chou, H. C.; Leow, D.; Tan, C. H. Recent Advances in Chiral Guanidine-Catalyzed Enantioselective Reactions. *Chem. - An Asian J.* **2019**, *14* (21), 3803–3822.

(71) Corey, E. J.; Grogan, M. J. Enantioselective Synthesis of α-Amino Nitriles from N-Benzhydryl Imines and HCN with a Chiral Bicyclic Guanidine as Catalyst. *Org. Lett.* **1999**, *1* (1), 157–160.

(72) Fu, X.; Tan, C. H. Mechanistic Considerations of Guanidine-Catalyzed Reactions. *Chem. Commun.* **2011**, *47* (29), 8210–8222.

(73) Fu, X.; Jiang, Z.; Tan, C. H. Bicyclic Guanidine-Catalyzed Enantioselective Phospha-Michael Reaction: Synthesis of Chiral β-Aminophosphine Oxides and β-Aminophosphines. *Chem. Commun.* **2007**, *47*, 5058–5060.

(74) Wang, Y. H.; Cao, Z. Y.; Li, Q. H.; Lin, G. Q.; Zhou, J.; Tian, P. Activating Pronucleophiles with High PKa Values: Chiral Organo-Superbases. *Angew. Chemie - Int. Ed.* **2020**, *59* (21), 8004–8014.

(75) Teng, B.; Lim, W. C.; Tan, C. H. Recent Advances in Enantioselective Bronsted Base Organocatalytic Reactions. *Synlett* **2017**, *28* (11), 1272–1277.

(76) Kondoh, A.; Terada, M. Development of Molecular Transformations on the Basis of Catalytic Generation of Anionic Species by Organosuperbase. *Bull. Chem. Soc. Jpn.* **2021**, *94* (1), 339–356.

(77) Bandar, J. S.; Lambert, T. H. Enantioselective Brønsted Base Catalysis with Chiral Cyclopropenimines. *J. Am. Chem. Soc.* **2012**, *134* (12), 5552–5555.

(78) Bandar, J. S.; Barthelme, A.; Mazori, A. Y.; Lambert, T. H. Structure-Activity

Relationship Studies of Cyclopropenimines as Enantioselective Brønsted Base Catalysts. *Chem. Sci.* **2015**, *6* (2), 1537–1547.

(79) Bandar, J. S.; Sauer, G. S.; Wulff, W. D.; Lambert, T. H.; Vetticatt, M. J. Transition State Analysis of Enantioselective Brønsted Base Catalysis by Chiral Cyclopropenimines. *J. Am. Chem. Soc.* **2014**, *136* (30), 10700–10707.

(80) Nacsa, E. D.; Lambert, T. H. Higher-Order Cyclopropenimine Superbases: Direct Neutral Brønsted Base Catalyzed Michael Reactions with α-Aryl Esters. *J. Am. Chem. Soc.* **2015**, *137* (32), 10246–10253.

(81) Bowman, P. S.; Winterman, D. R.; Goode, N. C.; Miller, N.; Dye, J. L.; Cheney, J.; Alder, R. W.; Casson, A.; Zirnstein, M. A.; Staab, H. A.; Schwesinger, R.; Gornpper, R.; Kramer, U.; Schmid, H.; Guggisberg, A.; Hesse, M.; Schwesinger, R. Peralkylated Polyaminophosphazenes - Extremely Strong, Neutral Nitrogen Bases. *Angew. Chemie (International Ed. English)* **1987**, *26* (11), 1167–1169.

(82) Ullrich, S.; Kovačević, B.; Xie, X.; Sundermeyer, J. Phosphazenyl Phosphines: The Most Electron-Rich Uncharged Phosphorus Brønsted and Lewis Bases. *Angew. Chemie - Int. Ed.* **2019**, *58* (30), 10335–10339.

(83) Schwesinger, R. Extremely Strong, Non-Ionic Bases: Synthesis and Applications. *Chimia (Aarau).* **1985**, *39*, 269–272.

(84) Uraguchi, D.; Sakaki, S.; Ooi, T. Chiral Tetraaminophosphonium Salt-Mediated Asymmetric Direct Henry Reaction. *J. Am. Chem. Soc.* **2007**, *129* (41), 12392–12393.

(85) Simón, L.; Paton, R. S. Phosphazene Catalyzed Addition to Electron-Deficient Alkynes: The Importance of Nonlinear Allenyl Intermediates upon Stereoselectivity. *J. Org. Chem.* **2017**, *82* (7), 3855–3863.

(86) Takeda, T.; Terada, M. Development of a Chiral Bis(Guanidino)Iminophosphorane as an Uncharged Organosuperbase for the Enantioselective Amination of Ketones. *J. Am. Chem. Soc.* **2013**, *135* (41), 15306–15309.

(87) Staudinger, H.; Meyer, J. Uber Neue Organische Phosphorverbindungen III. *Helv. Chim. Acta* **1919**, *2* (1), 635–646.

(88) Palacios, F.; Alonso, C.; Aparicio, D.; Rubiales, G.; de los Santos, J. M. The Aza-Wittig Reaction: An Efficient Tool for the Construction of Carbon-Nitrogen Double Bonds. *Tetrahedron* **2007**, *63* (3), 523–575.

(89) Farley, A. J. M.; Dixon, D. J. 1-[3,5-Bis(Trifluoromethyl)Phenyl]-3-{(2 S)-3,3-Dimethyl-1- [(Triphenylphosphoranylidene)Amino]Butan-2-Yl}thiourea. In *Encyclopedia of Reagents for Organic Synthesis*; John Wiley & Sons, Ltd: Chichester, UK,

2016; pp 1–4.

(90) Núñez, M. G.; Farley, A. J. M.; Dixon, D. J. Bifunctional Iminophosphorane Organocatalysts for Enantioselective Synthesis: Application to the Ketimine Nitro-Mannich Reaction. *J. Am. Chem. Soc.* **2013**, *135* (44), 16348–16351.

(91) Horwitz, M. A.; Zavesky, B. P.; Martinez-Alvarado, J. I.; Johnson, J. S. Asymmetric Organocatalytic Reductive Coupling Reactions between Benzylidene Pyruvates and Aldehydes. *Org. Lett.* **2016**, *18* (1), 36–39.

(92) Fulton, J. L.; Horwitz, M. A.; Bruske, E. L.; Johnson, J. S. Asymmetric Organocatalytic Sulfa-Michael Addition to Enone Diesters. *J. Org. Chem.* **2018**, *83* (6), 3385–3391.

(93) Horwitz, M. A.; Fulton, J. L.; Johnson, J. S. Enantio- and Diastereoselective Organocatalytic Conjugate Additions of Nitroalkanes to Enone Diesters. *Org. Lett.* **2017**, *19* (21), 5783–5785.

(94) Shi, H.; Michaelides, I. N.; Darses, B.; Jakubec, P.; Nguyen, Q. N. N.; Paton, R. S.; Dixon, D. J. Total Synthesis of (-)-Himalensine A. *J. Am. Chem. Soc.* **2017**, *139* (49), 17755–17758.

(95) Yuan, R.; Xu, G.; Lv, C.; Zhou, L.; Yang, R.; Wang, Q. Bifunctional Phosphazene-Thiourea/Urea Catalyzed Ring-Opening Polymerization of Cyclic Esters. *Mater. Today Commun.* **2020**, *22* (November 2019), 100747.

(96) Lv, C.; Zhou, L.; Yuan, R.; Mahmood, Q.; Xu, G.; Wang, Q. Isoselective Ring-Opening Polymerization and Asymmetric Kinetic Resolution Polymerization of: Rac -Lactide Catalyzed by Bifunctional Iminophosphorane-Thiourea/Urea Catalysts. *New J. Chem.* **2020**, *44* (4), 1648–1655.

(97) Goldys, A. M.; Dixon, D. J. Organocatalytic Ring-Opening Polymerization of Cyclic Esters Mediated by Highly Active Bifunctional Iminophosphorane Catalysts. *Macromolecules* **2014**, *47* (4), 1277–1284.

(98) Goldys, A. M.; Núñez, M. G.; Dixon, D. J. Creation through Immobilization: A New Family of High Performance Heterogeneous Bifunctional Iminophosphorane (BIMP) Superbase Organocatalysts. *Org. Lett.* **2014**, *16* (24), 6294–6297.

(99) Robertson, G. P.; Farley, A. J. M.; Dixon, D. J. Bifunctional Iminophosphorane Catalyzed Enantioselective Ketimine Phospha-Mannich Reaction. *Synlett* **2016**, *27* (1), 21–24.

(100) Farley, A. J. M.; Jakubec, P.; Goldys, A. M.; Dixon, D. J. Bifunctional Iminophosphorane Superbases: Potent Organocatalysts for Enantio- and

Diastereoselective Michael Addition Reactions. *Tetrahedron* **2018**, *74* (38), 5206–5212.

(101) Farley, A. J. M.; Sandford, C.; Dixon, D. J. Bifunctional Iminophosphorane Catalyzed Enantioselective Sulfa-Michael Addition to Unactivated α-Substituted Acrylate Esters. *J. Am. Chem. Soc.* **2015**, *137* (51), 15992–15995.

(102) Golec, J. C.; Carter, E. M.; Ward, J. W.; Whittingham, W. G.; Simón, L.; Paton, R. S.; Dixon, D. J. BIMP-Catalyzed 1,3-Prototropic Shift for the Highly Enantioselective Synthesis of Conjugated Cyclohexenones. *Angew. Chemie - Int. Ed.* **2020**, *59* (40), 17417–17422.

(103) Formica, M.; Sorin, G.; Farley, A. J. M.; Díaz, J.; Paton, R. S.; Dixon, D. J. Bifunctional Iminophosphorane Catalysed Enantioselective Sulfa-Michael Addition of Alkyl Thiols to Alkenyl Benzimidazoles. *Chem. Sci.* **2018**, *9* (34), 6969–6974.

(104) Formica, M.; Rogova, T.; Shi, H.; Sahara, N.; Farley, A. J. M.; Christensen, K. E.; Duarte, F.; Dixon, D. J. Enantioselective Nucleophilic Desymmetrisation of Phosphonate Esters. *Chem Rxiv* **2021**.

(105) Su, G.; Thomson, C. J.; Yamazaki, K.; Rozsar, D.; Christensen, K. E.; Hamlin, T. A.; Dixon, D. J. A Bifunctional Iminophosphorane Squaramide Catalyzed Enantioselective Synthesis of Hydroquinazolines: Via Intramolecular Aza-Michael Reaction to α,β-Unsaturated Esters. *Chem. Sci.* **2021**, *12* (17), 6064–6072.

(106) Rozsar, D.; Formica, M.; Yamazaki, K.; Hamlin, T.; Dixon, D. J. Bifunctional Iminophosphorane Catalyzed Enantioselective Sulfa-Michael Addition to Unactivated α,β-Unsaturated Amides. *Chem Rxiv* **2021**.

(107) Yamashita, Y.; Yasukawa, T.; Yoo, W. J.; Kitanosono, T.; Kobayashi, S. Catalytic Enantioselective Aldol Reactions. *Chem. Soc. Rev.* **2018**, *47* (12), 4388–4480.

(108) Chen, L.; Yin, X.-P.; Wang, C.-W.; Zhou, J. Catalytic Functionalization of Tertiary Alcohols to Fully Substituted Carbon Centres. *Org. Biomol. Chem.* **2014**, *12*, 6033–6048.

(109) Liu, Y. L.; Lin, X. T. Recent Advances in Catalytic Asymmetric Synthesis of Tertiary Alcohols via Nucleophilic Addition to Ketones. *Adv. Synth. Catal.* **2019**, *361* (5), 876–918.

(110) Mandal, S.; Mandal, S.; Ghosh, S. K.; Ghosh, A.; Saha, R.; Banerjee, S.; Saha, B. Review of the Aldol Reaction. *Synth. Commun.* **2016**, *46* (16), 1327–1342.

(111) Mestres, R. A Green Look at the Aldol Reaction. *Green Chem.* **2004**, *6* (12), 583–603.

(112) Matsuo, J. I.; Murakami, M. The Mukaiyama Aldol Reaction: 40years of Continuous Development. *Angew. Chemie - Int. Ed.* **2013**, *52* (35), 9109–9118.

(113) Mukaiyama, T.; Narasaka, K.; Banno, K. New Aldol Type Reaction. *Chem. Lett.* **1973**, 1011–1014.

(114) Kan, S. B. J.; Ng, K. K. H.; Paterson, I. The Impact of the Mukaiyama Aldol Reaction in Total Synthesis. *Angew. Chemie - Int. Ed.* **2013**, *52* (35), 9097–9108.

(115) Knocher, P.; Gary, M. Comprehensive Organic Synthesis. Elsevier Science 2014.

(116) Fujimura, O. Platinum-Catalyzed Enantioselective Aldol Addition of Ketene Silyl Acetals to Aldehydes. *J. Am. Chem. Soc.* **1998**, *120* (39), 10032–10039.

(117) Evans, D. A.; Murry, J. A.; Kozlowski, M. C. C2-Symmetric Copper(II) Complexes as Chiral Lewis Acids. Catalytic Enantioselective Aldol Additions of Silylketene Acetals to (Benzyloxy)Acetaldehyde. *J. Am. Chem. Soc.* **1996**, *118* (24), 5814–5815.

(118) Oehme, G. Catalytic Asymmetric Synthesis. *Zeitschrift für Phys. Chemie* **1995**, *191* (1), 141–142.

(119) Mukaiyama, T.; Kobayashi, S.; Uchiro, H.; Shiina, I. Catalytic Asymmetric Aldol Reaction of Silyl Enol Ethers with Aldehydes by the Use of Chiral Diamine Coordinated Tin(II) Triflate. *Chemistry Letters*. 1990, pp 129–132.

(120) Mukaiyama, T.; Inubushi, A.; Suda, S.; Hara, R.; Kobayashi, S. [1,1'-Bi-2-Naphthalenediolato(2−)-O,O']Oxotitanium. An Efficient Chiral Catalyst for the Asymmetric Aldol Reaction of Silyl Enol Ethers with Aldehydes. *Chemistry Letters*. 1990, pp 1015–1018.

(121) Isoda, T.; Akiyama, R.; Oyamada, H.; Kobayashi, S. A 100 Gram-Scale Production of a Key Building Block of Antibacterial Vancomycin: The Use of an Air-Stable Chiral Zirconium Catalyst and Complete Recovery of a Silicon Source in Catalytic Asymmetric Mukaiyama Aldol Reaction. *Adv. Synth. Catal.* **2006**, *348* (14), 1813–1817.

(122) Langner, M.; Bolm, C. C1-Symmetric Sulfoximines as Ligands in Copper-Catalyzed Asymmetric Mukaiyama-Type Aldol Reactions. *Angew. Chemie - Int. Ed.* **2004**, *43* (44), 5984–5987.

(123) Mukaiyama, T.; Matsuo, J.-I. Boron and Silicon Enolates in Crossed Aldol Reaction. In *Modern Aldol Reactions*; Wiley, 2004; pp 127–160.

(124) Schreyer, L.; Kaib, P. S. J.; Wakchaure, V. N.; Obradors, C.; Properzi, R.; Lee, S.; List, B. Confined Acids Catalyze Asymmetric Single Aldolizations of Acetaldehyde Enolates. *Science (80-.).* **2018**, *362*, 216–219.

(125) List, B.; Lerner, R. A.; Barbas III, C. F. Proline-Catalyzed Direct Asymmetric Aldol Reactions. *J. Am. Chem. Soc.* **2000**, *122* (13), 2395–2396.

(126) Danishefsky, S. J.; Masters, J. J.; Young, W. B.; Link, J. T.; Snyder, L. B.; Magee, T. V.; Jung, D. K.; Isaacs, R. C. A.; Bornmann, W. G.; Alaimo, C. A.; Coburn, C. A.; Di Grandi, M. J. Total Synthesis of Baccatin III and Taxol. *J. Am. Chem. Soc.* **1996**, *118* (12), 2843–2859.

(127) Evans, D. A.; Fitch, D. M.; Smith, T. E.; Cee, V. J. Application of Complex Aldol Reactions to the Total Synthesis of Phorboxazole B. *J. Am. Chem. Soc.* **2000**, *122* (41), 10033–10046.

(128) Alagiri, K.; Lin, S.; Kumagai, N.; Shibasaki, M. Iterative Direct Aldol Strategy for Polypropionates: Enantioselective Total Synthesis of (-)-Membrenone a and B. *Org. Lett.* **2014**, *16* (20), 5301–5303.

(129) Matsuzawa, A.; Opie, C. R.; Kumagai, N.; Shibasaki, M. Direct Aldol Strategy in Enantioselective Total Synthesis of Thuggacin B. *Chem. - A Eur. J.* **2014**, *20* (1), 68–71.

(130) Zhao, Y. C.; Zhou, D.; Chen, Q.; Zhang, X. J.; Bian, N.; Qi, A. Di; Han, B. H. Thionyl Chloride-Catalyzed Preparation of Microporous Organic Polymers through Aldol Condensation. *Macromolecules* **2011**, *44* (16), 6382–6388.

(131) Mangion, I. K.; Northrup, A. B.; MacMillan, D. W. C. The Importance of Iminium Geometry Control in Enamine Catalysis. *Angew. Chemie* **2004**, *116* (48), 6890–6892.

(132) Schreyer, L.; Kaib, P. S. J.; Wakchaure, V. N.; Obradors, C.; Properzi, R.; Lee, S.; List, B. Confined Acids Catalyze Asymmetric Single Aldolizations of Acetaldehyde Enolates. *Science.* **2018**, *219*, 216–219.

(133) Northrup, A. B.; Macmillan, D. W. C. Two-Step Synthesis of Carbohydrates by Selective Aldol Reactions. *Science.* **2004**, *305*, 1752–1756.

(134) Yamada, Y. M. A.; Yoshikawa, N.; Sasai, H.; Shibasaki, M. Direct Catalytic Asymmetric Aldol Reactions of Aldehydes with Unmodified Ketones. *Angew. Chemie (International Ed. English)* **1997**, *36* (17), 1871–1873.

(135) Liu, Z.; Takeuchi, T.; Pluta, R.; Arteaga Arteaga, F.; Kumagai, N.; Shibasaki, M. Direct Catalytic Asymmetric Aldol Reaction of α-Alkylamides. *Org. Lett.* **2017**, *19* (3), 710–713.

(136) Shibasaki, M.; Yoshikawa, N. Lanthanide Complexes in Multifunctional Asymmetric Catalysis. *Chem. Rev.* **2002**, *102* (6), 2187–2209.

(137) Kano, T.; Takai, J.; Tokuda, O.; Maruoka, K. Design of an Axially Chiral Amino Acid with a Binaphthyl Backbone as an Organocatalyst for a Direct Asymmetric Aldol Reaction. *Angew. Chemie - Int. Ed.* **2005**, *44* (20), 3055–3057.

(138) Kano, T.; Sugimoto, H.; Maruoka, K. Efficient Organocatalytic Cross-Aldol Reaction between Aliphatic Aldehydes through Their Functional Differentiation. *J. Am. Chem. Soc.* **2011**, *133* (45), 18130–18133.

(139) Ooi, T.; Kameda, M.; Taniguchi, M.; Maruoka, K. Development of Highly Diastereo- and Enantioselective Direct Asymmetric Aldol Reaction of a Glycinate Schiff Base with Aldehydes Catalyzed by Chiral Quaternary Ammonium Salts. *J. Am. Chem. Soc.* **2004**, *126* (31), 9685–9694.

(140) Ooi, T.; Taniguchi, M.; Kameda, M.; Maruoka, K. Direct Asymmetric Aldol Reactions of Glycine Schiff Base with Aldehydes Catalyzed by Chiral Quaternary Ammonium Salts. *Angew. Chemie - Int. Ed.* **2002**, *41* (23), 4542–4544.

(141) Saadi, J.; Wennemers, H. Enantioselective Aldol Reactions with Masked Fluoroacetates. *Nat. Chem.* **2016**, *8* (3), 276–280.

(142) Sakamoto, S.; Kazumi, N.; Kobayashi, Y.; Tsukano, C.; Takemoto, Y. Asymmetric Synthesis of Trisubstituted Oxazolidinones by the Thiourea-Catalyzed Aldol Reaction of 2-Isocyanatomalonate Diester. *Org. Lett.* **2014**, *16* (18), 4758–4761.

(143) Torii, H.; Nakadai, M.; Ishihara, K.; Saito, S.; Yamamoto, H. Asymmetric Direct Aldol Reaction Assisted by Water and a Proline-Derived Tetrazole Catalyst. *Angew. Chemie - Int. Ed.* **2004**, *43* (15), 1983–1986.

(144) Knudsen, K. R.; Risgaard, T.; Nishiwaki, N.; Gothelf, K. V.; Jørgensen, K. A. The First Catalytic Asymmetric Aza-Henry Reaction of Nitronates with Imines: A Novel Approach to Optically Active β-Nitro-α-Amino Acid- and α,β-Diamino Acid Derivatives [1]. *J. Am. Chem. Soc.* **2001**, *123* (24), 5843–5844.

(145) Trost, B. M.; Yeh, V. S. C. A Dinuclear Zn Catalyst for the Asymmetric Nitroaldol (Henry) Reaction. *Angew. Chemie - Int. Ed.* **2002**, *41* (5), 861–863.

(146) Palomo, C.; Oiarbide, M.; Laso, A. Enantioselective Henry Reactions under Dual Lewis Acid/Amine Catalysis Using Chiral Amino Alcohol Ligands. *Angew. Chemie - Int. Ed.* **2005**, *44* (25), 3881–3884.

(147) Evans, D. A.; Seidel, D.; Rueping, M.; Lam, H. W.; Shaw, J. T.; Downey, C. W. A New Copper Acetate-Bis(Oxazoline)-Catalyzed, Enantioselective Henry Reaction. *J. Am. Chem. Soc.* **2003**, *125* (42), 12692–12693.

(148) Li, H.; Wang, B.; Deng, L. Enantioselective Nitroaldol Reaction of α-Ketoesters Catalyzed by Cinchona Alkaloids. *J. Am. Chem. Soc.* **2006**, *128* (3), 732–733.

(149) Li, P.; Zhao, J.; Li, F.; Chan, A. S. C.; Kwong, F. Y. Highly Enantioselective and Efficient Organocatalytic Aldol Reaction of Acetone and β ,γ-Unsaturated α-Keto

Ester. *Org. Lett.* **2010**, *12* (24), 5616–5619.

(150) Wei, A. J.; Nie, J.; Zheng, Y.; Ma, J. A. Ni-Catalyzed Highly Chemo-, Regio-, and Enantioselective Decarboxylative Aldol Reaction of β,γ-Unsaturated α-Ketoesters with β-Ketoacids. *J. Org. Chem.* **2015**, *80* (8), 3766–3776.

(151) Yu, J.; Zhao, X.; Miao, Z.; Chen, R. Highly Diastereoselective Vinylogous Mukaiyama Aldol Reaction of α-Keto Phosphonates with 2-(Trimethylsilyloxy)Furan Catalyzed by Cu(OTf) 2. *Org. Biomol. Chem.* **2011**, *9* (19), 6721–6726.

(152) Samanta, S.; Zhao, C. G. Organocatalytic Enantioselective Synthesis of α-Hydroxy Phosphonates. *J. Am. Chem. Soc.* **2006**, *128* (23), 7442–7443.

(153) Matsuzawa, A.; Noda, H.; Kumagai, N.; Shibasaki, M. Direct Catalytic Asymmetric Aldol Addition of an α-CF3 Amide to Arylglyoxal Hydrates. *J. Org. Chem.* **2017**, *82* (15), 8304–8308.

(154) Hayashi, Y.; Kojima, M. Asymmetric Aldol Reaction of Glyoxal Catalyzed by Diarylprolinol. *ChemCatChem* **2013**, *5* (10), 2883–2885.

(155) Gao, H.; Luo, Z.; Ge, P.; He, J.; Zhou, F.; Zheng, P.; Jiang, J. Direct Catalytic Asymmetric Synthesis of β-Hydroxy Acids from Malonic Acid. *Org. Lett.* **2015**, *17* (24), 5962–5965.

(156) Luppi, G.; Cozzi, P. G.; Monari, M.; Kaptein, B.; Broxterman, Q. B.; Tomasini, C.; Ciamician, C. G.; Mater, A.; Excesses, T. A. E. Dipeptide-Catalyzed Asymmetric Aldol Condensation of Acetone with (N-Alkylated) Isatins. *J. Org. Chem.* **2005**, *70*, 7418–7421.

(157) Guo, Q.; Bhanushali, M.; Zhao, C. G. Quinidine Thiourea-Catalyzed Aldol Reaction of Unactivated Ketones: Highly Enantioselective Synthesis of 3-Alkyl-3-Hydroxyindolin-2-Ones. *Angew. Chemie - Int. Ed.* **2010**, *49* (49), 9460–9464.

(158) Moles, F. J. N.; Guillena, G.; Nájera, C. Aqueous Organocatalyzed Aldol Reaction of Glyoxylic Acid for the Enantioselective Synthesis of α-Hydroxy-γ-Keto Acids. *RSC Adv.* **2014**, *4* (20), 9963–9966.

(159) Xu, X. Y.; Tang, Z.; Wang, Y. Z.; Luo, S. W.; Cun, L. F.; Gong, L. Z. Asymmetric Organocatalytic Direct Aldol Reactions of Ketones with α-Keto Acids and Their Application to the Synthesis of 2-Hydroxy-γ-Butyrolactones. *J. Org. Chem.* **2007**, *72* (26), 9905–9913.

(160) List, B. Amine-Catalyzed Aldol Reactions. In *Modern Aldol Reactions*; Wiley: Weinheim, 2004; pp 161–200.

(161) Dalko, P. I. Enamine Catalysis: Aldol and Mannich-Type Reactions. In *Enantioselective Organocatalysis: Reactions and Experimental Procedures*; Wiley: Weinheim, 2007; Vol. 2007, pp 19–93.

(162) Bahmanyar, S.; Houk, K. N. Transition States of Amine-Catalyzed Aldol Reactions Involving Enamine Intermediates- Theoretical Studies of Mechanism, Reactivity, and Stereoselectivity. *J. Am. Chem. Soc.* **2001**, *123* (45), 11273–11283.

(163) Mukherjee, S.; Yang, J. W.; Hoffmann, S.; List, B. Asymmetric Enamine Catalysis. *Chem. Rev.* **2007**, *107* (12), 5471–5569.

(164) Notz, W.; Tanaka, F.; Barbas, C. F. Enamine-Based Organocatalysis with Proline and Diamines: The Development of Direct Catalytic Asymmetric Aldol, Mannich, Michael, and Diels-Alder Reactions. *Acc. Chem. Res.* **2004**, *37* (8), 580–591.

(165) Dalko, P. I.; Moisan, L. In the Golden Age of Organocatalysis. *Angew. Chemie - Int. Ed.* **2004**, *43* (39), 5138–5175.

(166) List, B. Enamine Catalysis Is a Powerful Strategy for the Catalytic Generation and Use of Carbanion Equivalents. *Acc. Chem. Res.* **2004**, *37* (8), 548–557.

(167) Pluta, R.; Kumagai, N.; Shibasaki, M. Direct Catalytic Asymmetric Aldol Reaction of α-Alkoxyamides to α-Fluorinated Ketones. *Angew. Chemie - Int. Ed.* **2019**, *58* (8), 2459–2463.

(168) Zheng, Y.; Xiong, H. Y.; Nie, J.; Hua, M. Q.; Ma, J. A. Biomimetic Catalytic Enantioselective Decarboxylative Aldol Reaction of β-Ketoacids with Trifluoromethyl Ketones. *Chem. Commun.* **2012**, *48* (36), 4308–4310.

(169) Crotti, S.; Belletti, G.; Di Iorio, N.; Marotta, E.; Mazzanti, A.; Righi, P.; Bencivenni, G. Asymmetric Vinylogous Aldol Addition of Alkylidene Oxindoles on Trifluoromethyl-α,β-Unsaturated Ketones. *RSC Adv.* **2018**, *8* (58), 33451–33458.

(170) Zhu, Y.; Han, J.; Wang, J.; Shibata, N.; Sodeoka, M.; Soloshonok, V. A.; Coelho, J. A. S.; Toste, F. D. Modern Approaches for Asymmetric Construction of Carbon-Fluorine Quaternary Stereogenic Centers: Synthetic Challenges and Pharmaceutical Needs. *Chem. Rev.* **2018**, *118* (7), 3887–3964.

(171) Purser, S.; Moore, P. R.; Swallow, S.; Gouverneur, V. Fluorine in Medicinal Chemistry. *Chem. Soc. Rev.* **2008**, *37* (2), 320–330.

(172) O'hagan, D. Understanding Organofluorine Chemistry. An Introduction to the C–F Bond. *Chem. Soc. Rev.* **2008**, *37* (2), 308–319.

(173) Duangdee, N.; Harnying, W.; Rulli, G.; Neudörfl, J. M.; Gröger, H.; Berkessel, A.

Highly Enantioselective Organocatalytic Trifluoromethyl Carbinol Synthesis-a Caveat on Reaction Times and Product Isolation. *J. Am. Chem. Soc.* **2012**, *134* (27), 11196–11205.

(174) Hara, N.; Tamura, R.; Funahashi, Y.; Nakamura, S. N-(Heteroarenesulfonyl)Prolinamides-Catalyzed Aldol Reaction between Acetone and Aryl Trihalomethyl Ketones. *Org. Lett.* **2011**, *13* (7), 1662–1665.

(175) Yang, W.; Cui, Y. M.; Zhou, W.; Li, L.; Yang, K. F.; Zheng, Z. J.; Lu, Y.; Xu, L. W. Enantioselective Primary Amine Catalyzed Aldol-Type Construction of Trifluoromethylated Tertiary Alcohols. *Synlett* **2014**, *25* (10), 1461–1465.

(176) Wang, Y. J.; Shen, Z. X.; Li, B.; Zhang, Y. W. Proline Catalyzed Asymmetric Aldol Reaction between Methyl Ketones and α-Ketoesters. *Chinese J. Chem.* **2006**, *24* (9), 1196–1199.

(177) Kokotos, C. G. Construction of Tertiary Alcohols Bearing Perfluoroalkyl Chains Catalyzed by Prolinamide-Thioureas. *J. Org. Chem.* **2012**, *77* (2), 1131–1135.

(178) Wang, P.; Li, H. F.; Zhao, J. Z.; Du, Z. H.; Da, C. S. Organocatalytic Enantioselective Cross-Aldol Reaction of o-Hydroxyarylketones and Trifluoromethyl Ketones. *Org. Lett.* **2017**, *19* (10), 2634–2637.

(179) Lutete, L. M.; Miyamoto, T.; Ikemoto, T. Tertiary Amino Thiourea-Catalyzed Asymmetric Cross Aldol Reaction of Aryl Methyl Ketones with Aryl Trifluoromethyl Ketones. *Tetrahedron Lett.* **2016**, *57* (11), 1220–1223.

(180) Sasaki, S.; Kikuchi, K.; Yamauchi, T.; Higashiyama, K. Direct Aldol Reaction of Trifluoromethyl Ketones with Ketones Catalyzed by Diethylzinc and Secondary Amines. *Synlett* **2011**, No. 10, 1431–1434.

(181) Ahmad, A.; Ahmad, A.; Sudhakar, R.; Varshney, H.; Subbarao, N.; Ansari, S.; Rauf, A.; Khan, A. U. Designing, Synthesis, and Antimicrobial Action of Oxazoline and Thiazoline Derivatives of Fatty Acid Esters. *J. Biomol. Struct. Dyn.* **2017**, *35* (15), 3412–3431.

(182) Frump, J. A. Oxazolines: Their Preparation, Reactions, and Applications. *Chem. Rev.* **1971**, *71* (5), 483–505.

(183) Gift, A. D.; Stewart, S. M.; Kwete Bokashanga, P. Experimental Determination of PKa Values by Use of NMR Chemical Shifts. *J. Chem. Educ.* **2012**, *89* (11), 1458–1460.

(184) Gift, A. D.; Stewart, S. M.; Bokashanga, P. K. Experimental Determination of PKa. **2012**, No. 2, 1458–1460.

(185) Bandar, J. S.; Coscia, R. W.; Lambert, T. H. Demonstration of the Facile Reversibility of Fulvene Formation. *Tetrahedron* **2011**, *67* (24), 4364–4370.

(186) Foschi, F.; Tagliabue, A.; Mihali, V.; Pilati, T.; Pecnikaj, I.; Penso, M. Memory of Chirality Approach to the Enantiodivergent Synthesis of Chiral Benzo[d]Sultams. *Org. Lett.* **2013**, *15* (14), 3686–3689.

(187) Kaljurand, I.; Kütt, A.; Sooväli, L.; Rodima, T.; Mäemets, V.; Leito, I.; Koppel, I. A. Extension of the Self-Consistent Spectrophotometric Basicity Scale in Acetonitrile to a Full Span of 28 PKa Units: Unification of Different Basicity Scales. *J. Org. Chem.* **2005**, *70* (3), 1019–1028.

(188) Huang, C. Y. [27] Determination of Binding Stoichiometry by the Continuous Variation Method: The Job Plot. *Methods Enzymol.* **1982**, *87* (C), 509–525.

(189) Olson, E. J.; Bühlmann, P. Getting More out of a Job Plot: Determination of Reactant to Product Stoichiometry in Cases of Displacement Reactions and n: N Complex Formation. *J. Org. Chem.* **2011**, *76* (20), 8406–8412.

(190) Hill, Z. D.; MacCarthy, P. Novel Approach to Job's Method: An Undergraduate Experiment. *J. Chem. Educ.* **1986**, *63* (2), 162–167.

(191) Job, P. Formation and Stability of Inorganic Complexes in Solution. *Ann. Chemie* **1928**, *10* (9), 113–203.

(192) Brynn Hibbert, D.; Thordarson, P. The Death of the Job Plot, Transparency, Open Science and Online Tools, Uncertainty Estimation Methods and Other Developments in Supramolecular Chemistry Data Analysis. *Chem. Commun.* **2016**, *52* (87), 12792–12805.

(193) Ulatowski, F.; Dabrowa, K.; Bałakier, T.; Jurczak, J. Recognizing the Limited Applicability of Job Plots in Studying Host-Guest Interactions in Supramolecular Chemistry. *J. Org. Chem.* **2016**, *81* (5), 1746–1756.

(194) Kumar, V.; Kaur, K.; Gupta, G. K.; Sharma, A. K. Pyrazole Containing Natural Products: Synthetic Preview and Biological Significance. *Eur. J. Med. Chem.* **2013**, *69*, 735–753.

(195) Du, Y. L.; He, H. Y.; Higgins, M. A.; Ryan, K. S. A Heme-Dependent Enzyme Forms the Nitrogen-Nitrogen Bond in Piperazate. *Nat. Chem. Biol.* **2017**, *13* (8), 836–838.

(196) Le Goff, G.; Ouazzani, J. Natural Hydrazine-Containing Compounds: Biosynthesis, Isolation, Biological Activities and Synthesis. *Bioorganic Med. Chem.* **2014**, *22* (23), 6529–6544.

(197) L. C. Behr, R. Fusco, C. H. J. Pyrazoles, Pyrazolines, Pyrazolidines, Indazoles and Condensed Rings. In *The Chemistry of Heterocyclic Compounds*; Interscience Publishers: New York, 1967.

(198) Blair, L. M.; Sperry, J. Natural Products Containing a Nitrogen-Nitrogen Bond. *J. Nat. Prod.* **2013**, *76*, 794–812.

(199) Rosen, B. R.; Werner, E. W.; O'Brien, A. G.; Baran, P. S. Total Synthesis of Dixiamycin B by Electrochemical Oxidation. *J. Am. Chem. Soc.* **2014**, *136* (15), 5571–5574.

(200) De Rooij, M. F. M.; Kuil, A.; Geest, C. R.; Eldering, E.; Chang, B. Y.; Buggy, J. J.; Pals, S. T.; Spaargaren, M. The Clinically Active BTK Inhibitor PCI-32765 Targets B-Cell Receptor- and Chemokine-Controlled Adhesion and Migration in Chronic Lymphocytic Leukemia. *Blood* **2012**, *119* (11), 2590–2594.

(201) Herman, G. A.; Bergman, A.; Liu, F.; Stevens, C.; Wang, A. Q.; Zeng, W.; Chen, L.; Snyder, K.; Hilliard, D.; Tanen, M.; Tanaka, W.; Meehan, A. G.; Lasseter, K.; Dilzer, S.; Blum, R.; Wagner, J. A. Pharmacokinetics and Pharmacodynamic Effects of the Oral DPP-4 Inhibitor Sitagliptin in Middle-Aged Obese Subjects. *J. Clin. Pharmacol.* **2006**, *46* (8), 876–886.

(202) McGrath, N. A.; Brichacek, M.; Njardarson, J. T. A Graphical Journey of Innovative Organic Architectures That Have Improved Our Lives. *J. Chem. Educ.* **2010**, *87* (12), 1348–1349.

(203) Frost, C.; Wang, J.; Nepal, S.; Schuster, A.; Barrett, Y. C.; Mosqueda-Garcia, R.; Reeves, R. A.; Lacreta, F. Apixaban, an Oral, Direct Factor Xa Inhibitor: Single Dose Safety, Pharmacokinetics, Pharmacodynamics and Food Effect in Healthy Subjects. *Br. J. Clin. Pharmacol.* **2013**, *75* (2), 476–487.

(204) Njardarson, J. Top 200 Brand Name Drugs by Retail Sales in 2019 https://njardarson.lab.arizona.edu/content/top-pharmaceuticals-poster (accessed Sep 26, 2021).

(205) Umetsu, N.; Shirai, Y. Development of Novel Pesticides in the 21st Century. *J. Pestic. Sci.* **2020**, *45* (2), 54–74.

(206) Matsuzaki, Y.; Yoshimoto, Y.; Arimori, S.; Kiguchi, S.; Harada, T.; Iwahashi, F. Discovery of Metyltetraprole: Identification of Tetrazolinone Pharmacophore to Overcome QoI Resistance. *Bioorganic Med. Chem.* **2020**, *28* (1), 115211.

(207) Ardiansah, B. Pharmaceutical Importance of Pyrazoline Derivatives: A Mini Review. *J. Pharm. Sci. Res.* **2017**, *9* (10), 1958–1960.

(208) Varghese, B.; Al-Busafi, S. N.; Suliman, F. O.; Al-Kindy, S. M. Z. Unveiling a Versatile Heterocycle: Pyrazoline-a Review. *RSC Adv.* **2017**, *7* (74), 46999–47016.

(209) Gürsoy, A.; Demirayak, Ş.; Çapan, G.; Erol, K.; Vural, K. Synthesis and Preliminary Evaluation of New 5-Pyrazolinone Derivatives as Analgesic Agents. *Eur. J. Med. Chem.* **2000**, *35* (3), 359–364.

(210) Fu, H. B.; Yao, J. N. Size Effects on the Optical Properties of Organic Nanoparticles. *J. Am. Chem. Soc.* **2001**, *123* (7), 1434–1439.

(211) Camacho, M. E.; León, J.; Entrena, A.; Velasco, G.; Carrión, M. D.; Escames, G.; Vivó, A.; Acuña-Castroviejo, D.; Gallo, M. A.; Espinosa, A. 4,5-Dihydro-1H-Pyrazole Derivatives with Inhibitory NNOS Activity in Rat Brain: Synthesis and Structure - Activity Relationships. *J. Med. Chem.* **2004**, *47* (23), 5641–5650.

(212) Zhang, X.; Li, X.; Allan, G. F.; Sbriscia, T.; Linton, O.; Lundeen, S. G.; Sui, Z. Design, Synthesis, and in Vivo SAR of a Novel Series of Pyrazolines as Potent Selective Androgen Receptor Modulators. *J. Med. Chem.* **2007**, *50* (16), 3857–3869.

(213) Girgis, A. S.; Basta, A. H.; El-Saied, H.; Mohamed, M. A.; Bedair, A. H.; Salim, A. S. Synthesis, Quantitative Structure–Property Relationship Study of Novel Fluorescence Active 2-Pyrazolines and Application. *R. Soc. Open Sci.* **2018**, *5* (3).

(214) Lee, D. H.; Jung, B. S.; Jung, S.; Song, J.; Seung, W. H. Mechanism of Action of Base-Catalyzed Oxygenation of Phenol Derivatives. *Tetrahedron Lett.* **2005**, *46* (45), 7721–7723.

(215) Banerjee, D.; Kayal, U.; Karmakar, R.; Maiti, G. 3,4-Dihydro-2H-Pyran Promoted Aerobic Oxidative Aromatization of 1,3,5-Trisubstituted Pyrazolines and Hantzsch 1,4-Dihydropyridines. *Tetrahedron Lett.* **2014**, *55* (38), 5333–5337.

(216) Havryllyuk, D.; Roman, O.; Lesyk, R. Synthetic approaches, structure activity relationshop and biological applications for pharmacologically attractive pyrazole/pyrazoline-thiazolidine-based hybrids. *Eur. J. Med. Chem.* **2016**, *113*, 145-166.

(217) Akranth, M.; Rahmat, A.; Alam, T.; Rikta, S.; Omprakash, T.; Mymoona, A.; Shaquiquzzaman, M.; Pyrazolines: A Biological Review. *Mini Rev. Med. Chem.* **2013**, *13* (6), 921–931.

(218) Descacq, P.; Nuhrich, A.; Varache-Beranger, M.; Capdepuy, M.; Devaux, G.; Arylpyrazolines nitrofuraniques: synthese et proprietes antibacteriennes, *Eur. J. Med. Chem.* **1990**, *25*, 285–290.

(219) Sosnovskikh, V. Y.; Barabanov, M. A.; Usachev, B. I. A Novel Redox Reaction between 8-Aza-5,7-Dimethyl-2-Trifluoromethylchromone and Alkyl

Mercaptoacetates. Facile Synthesis of CF3-Containing 2-Pyridone Derivatives. *J. Org. Chem.* **2004**, *69* (24), 8297–8304.

(220) Wu, X. F.; Neumann, H.; Beller, M. A Straightforward Synthesis of Pyrazolines and Pyrazoles: Palladium-Catalyzed Carbonylative Vinylation-Cyclocondensation Reactions of Aryl Halides. *European J. Org. Chem.* **2011**, *25*, 4919–4924.

(221) Ciupa, A.; Mahon, M. F.; De Bank, P. A.; Caggiano, L. Simple Pyrazoline and Pyrazole "Turn on" Fluorescent Sensors Selective for Cd2+ and Zn2+ in MeCN. *Org. Biomol. Chem.* **2012**, *10* (44), 8753–8757.

(222) El Dine, A. N.; Khalaf, A.; Grée, D.; Tasseau, O.; Fares, F.; Jaber, N.; Lesot, P.; Hachem, A.; Grée, R. Synthesis of Enones, Pyrazolines and Pyrrolines with Gem-Difluoroalkyl Side Chains. *Beilstein J. Org. Chem.* **2013**, *9*, 1943–1948.

(223) Dawood, D. H.; Nossier, E. S.; Ali, M. M.; Mahmoud, A. E. Synthesis and Molecular Docking Study of New Pyrazole Derivatives as Potent Anti-Breast Cancer Agents Targeting VEGFR-2 Kinase. *Bioorg. Chem.* **2020**, *101*, 103916.

(224) Su, Y.; Zhao, Y.; Chang, B.; Zhao, X.; Zhang, R.; Liu, X.; Huang, D.; Wang, K. H.; Huo, C.; Hu, Y. Cycloaddition of Para-Quinone Methides with Nitrile Imines: Approach to Spiro-Pyrazoline-Cyclohexadienones. *J. Org. Chem.* **2019**, *84* (11), 6719–6728.

(225) Tu, L.; Gao, L.; Wang, X.; Shi, R.; Ma, R.; Li, J.; Lan, X.; Zheng, Y.; Liu, J. Cycloaddition of Nitrile Imines with Enamides: An Approach to Functionalized Pyrazolines and Pyrazoles. *J. Org. Chem.* **2021**, *86* (1), 559–573.

(226) Liu, H.; Jia, H.; Wang, B.; Xiao, Y.; Guo, H. Synthesis of Spirobidihydropyrazole through Double 1,3-Dipolar Cycloaddition of Nitrilimines with Allenoates. *Org. Lett.* **2017**, *19* (18), 4714–4717.

(227) Wu, X.; Wang, M.; Zhang, G.; Zhao, Y.; Wang, J.; Ge, H. Copper-Catalyzed Diastereoselective Aerobic Intramolecular Dehydrogenative Coupling of Hydrazones via Sp3 C-H Functionalization. *Chem. Sci.* **2015**, *6* (10), 5882–5890.

(228) Kanemasa, S.; Kanai, T. Lewis Acid-Catalyzed Enantioselective 1,3-Dipolar Cycloadditions of Diazoalkane: Chiral Ligand/Achiral Auxiliary Cooperative Chirality Control [4]. *J. Am. Chem. Soc.* **2000**, *122* (43), 10710–10711.

(229) Sibi, M. P.; Stanley, L. M.; Soeta, T. Enantioselective 1,3-Dipolar Cycloaddition of Nitrile Imines to α-Substituted and α,β-Disubstituted α,β-Unsaturated Carbonyl Substrates: A Method for Synthesizing Dihydropyrazoles Bearing a Chiral Quaternary Center. *Adv. Synth. Catal.* **2006**, *348* (16–17), 2371–2375.

(230) Sibi, M. P.; Stanley, L. M.; Jasperse, C. P. An Entry to a Chiral Dihydropyrazole Scaffold: Enantioselective [3 + 2] Cycloaddition of Nitrile Imines. *J. Am. Chem. Soc.* **2005**, *127* (23), 8276–8277.

(231) Sibi, M. P.; Stanley, L. M.; Soeta, T. Enantioselective 1,3-Dipolar Cycloadditions of Diazoacetates with Electron-Deficient Olefins. *Org. Lett.* **2007**, *9* (8), 1553–1556.

(232) Müller, S.; List, B. A Catalytic Asymmetric 6 π Electrocyclization: Enantioselective Synthesis of 2-Pyrazolines. *Angew. Chemie* **2009**, *121* (52), 10160–10163.

(233) Maké, O.; Dez, I.; Levacher, V.; Briére, J. F. Enantioselective Phase-Transfer Catalysis: Synthesis of Pyrazolines. *Angew. Chemie - Int. Ed.* **2010**, *49* (39), 7072–7075.

(234) Mahé, O.; Dez, I.; Levacher, V.; Brière, J. F. Enantioselective Synthesis of Bio-Relevant 3,5-Diaryl Pyrazolines. *Org. Biomol. Chem.* **2012**, *10* (19), 3946–3954.

(235) Campbell, N. R.; Sun, B.; Singh, R. P.; Deng, L. Cinchona Alkaloid-Catalyzed Enantioselective Amination of α,β-Unsaturated Ketones: An Asymmetric Approach to Δ2-Pyrazolines. *Adv. Synth. Catal.* **2011**, *353* (17), 3123–3128.

(236) Nigst, T. A.; Antipova, A.; Mayr, H. Nucleophilic Reactivities of Hydrazines and Amines: The Futile Search for the α-Effect in Hydrazine Reactivities. *J. Org. Chem.* **2012**, *77* (18), 8142–8155.

(237) Hansen, T.; Vermeeren, P.; Bickelhaupt, F. M.; Hamlin, T. A. Origin of the α-Effect in SN2 Reactions. *Angew. Chemie - Int. Ed.* **2021**, *60* (38), 20840–20848.

(238) Buncel, E.; Um, I. H. The α-Effect and Its Modulation by Solvent. *Tetrahedron* **2004**, *60* (36), 7801–7825.

(239) Ren, Y.; Yamataka, H. The α-Effect in Gas-Phase SN2 Reactions: Existence and the Origin of the Effect. *J. Org. Chem.* **2007**, *72* (15), 5660–5667.

(240) Jencks, W. P.; Carriuolo, J. Reactivity of Nucleophilic Reagents toward Esters. *J. Am. Chem. Soc.* **1960**, *82* (7), 1778–1786.

(241) Klopman, G.; Evans, R. C. Supernucleophiles—II. *Tetrahedron* **1978**, *34* (3), 269–273.

(242) Edwards, J. O.; Pearson, R. G. The Factors Determining Nucleophilic Reactivities. *J. Am. Chem. Soc.* **1962**, *84* (1), 16–24.

(243) Li, E.; Xie, P.; Yang, L.; Liang, L.; Huang, Y. Tuning Catalysts to Tune the Products: Phosphine-Catalyzed Aza-Michael Addition Reaction of Hydrazones with Allenoates. *Chem. - An Asian J.* **2013**, *8* (3), 603–610.

(244) Wang, Y.; Wang, Q.; Zhu, J. Organocatalytic Nucleophilic Addition of Hydrazones

to Imines: Synthesis of Enantioenriched Vicinal Diamines. *Angew. Chemie - Int. Ed.* **2017**, *56* (20), 5612–5615.

(245) Perdicchia, D.; Jørgensen, K. A. Asymmetric Aza-Michael Reactions Catalyzed by Cinchona Alkaloids. *J. Org* **2007**, *72*, 3565–3568.

(246) de Gracia Retamosa, M.; Matador, E.; Monge, D.; Lassaletta, J. M.; Fernández, R. Hydrazones as Singular Reagents in Asymmetric Organocatalysis. *Chem. - A Eur. J.* **2016**, *22* (38), 13430–13445.

(247) Matsuzaki, H.; Takeda, N.; Yasui, M.; Ito, Y.; Konishi, K.; Ueda, M. Synthesis of Pyrazoles Utilizing the Ambiphilic Reactivity of Hydrazones. *Org. Lett.* **2020**, *22* (23), 9249–9252.

(248) Wu, W.; Yuan, X.; Hu, J.; Wu, X.; Wei, Y.; Liu, Z.; Lu, J.; Ye, J. Catalytic Asymmetric Construction of Chiral Hydropyridazines via Conjugate Addition of N-Monosubstituted Hydrazones to Enones. *Org. Lett.* **2013**, *15* (17), 4524–4527.

(249) Wang, F.; Luo, T.; Hu, J.; Wang, Y.; Krishnan, H. S.; Jog, P. V.; Ganesh, S. K.; Prakash, G. K. S.; Olah, G. A. Synthesis of Gem-Difluorinated Cyclopropanes and Cyclopropenes: Trifluoromethyltrimethylsilane as a Difluorocarbene Source. *Angew. Chemie - Int. Ed.* **2011**, *50* (31), 7153–7157.

(250) Thomson, C. J.; Zhang, Q.; Al-Maharik, N.; Bühl, M.; Cordes, D. B.; Slawin, A. M. Z.; O'Hagan, D. Fluorinated Cyclopropanes: Synthesis and Chemistry of the Aryl α,β,β-Trifluorocyclopropane Motif. *Chem. Commun.* **2018**, *54* (60), 8415–8418.

(251) Ndungu, J. M.; Krumm, S. A.; Yan, D.; Arrendale, R. F.; Reddy, G. P.; Evers, T.; Howard, R.; Natchus, M. G.; Saindane, M. T.; Liotta, D. C.; Plemper, R. K.; Snyder, J. P.; Sun, A. Non-Nucleoside Inhibitors of the Measles Virus RNA-Dependent RNA Polymerase: Synthesis, Structure-Activity Relationships, and Pharmacokinetics. *J. Med. Chem.* **2012**, *55* (9), 4220–4230.

(252) Lichter, J.; Vollrath, B.; Campbell, D.; Duron, S. G. Methods for Treating Alzheimer's Disease Corss Reference. WO 2011/044537, 2011.

(253) Reddy, M. V. R.; Billa, V. K.; Pallela, V. R.; Mallireddigari, M. R.; Boominathan, R.; Gabriel, J. L.; Reddy, E. P. Design, Synthesis, and Biological Evaluation of 1-(4-Sulfamylphenyl)-3-Trifluoromethyl-5-Indolyl Pyrazolines as Cyclooxygenase-2 (COX-2) and Lipoxygenase (LOX) Inhibitors. *Bioorganic Med. Chem.* **2008**, *16* (7), 3907–3916.

(254) Leitch, J. A.; Wilson, P. B.; McMullin, C. L.; Mahon, M. F.; Bhonoah, Y.; Williams, I. H.; Frost, C. G. Ruthenium(II)-Catalyzed C-H Functionalization Using the Oxazolidinone Heterocycle as a Weakly Coordinating Directing Group:

Experimental and Computational Insights. *ACS Catal.* **2016**, *6* (8), 5520–5529.

(255) Li, J.; Kornhass, C.; Ackermann, L. Ruthenium-Catalyzed Oxidative C–H Alkenylation of Aryl Carbamates. *Chem. Commun.* **2021**, *48*, 11343–11345.

(256) Rossolini, T.; Leitch, J. A.; Grainger, R.; Dixon, D. J. Photocatalytic Three-Component Umpolung Synthesis of 1,3-Diamines. *Org. Lett.* **2018**, *20* (21), 6794–6798.

(257) Ji, X.; Huang, H. Synthetic Methods for 1,3-Diamines. *Org. Biomol. Chem.* **2016**, *14* (45), 10557–10566.

(258) Albrecht, B. K.; Audia, J. E.; Cook, A.; Gagnon, A.; Harmange, J.-C.; Naveschuck, C. G.; Modulators of methyl modifying enzymes, compositions and uses thereof. US Patent Office WO 2013/075083 A1, 23 May 2013.

(259) Scheidt, F.; Schäfer, M.; Sarie, J. C.; Daniliuc, C. G.; Molloy, J. J.; Gilmour, R. Enantioselective, Catalytic Vicinal Difluorination of Alkenes. *Angew. Chemie - Int. Ed.* **2018**, *57* (50), 16431–16435.

(260) Trost, B. M.; Debien, L. Palladium-Catalyzed Trimethylenemethane Cycloaddition of Olefins Activated by the δ-Electron-Withdrawing Trifluoromethyl Group. *J. Am. Chem. Soc.* **2015**, *137* (36), 11606–11609.

(261) Liu, X.; Liu, L.; Huang, T.; Zhang, J.; Tang, Z.; Li, C.; Chen, T. Trifluoromethylation of Benzoic Acids: An Access to Aryl Trifluoromethyl Ketones. *Org. Lett.* **2021**, *23* (12), 4930–4934.

(262) Li, C.; Shu, X.; Li, L.; Zhang, G.; Jin, R.; Cheng, T.; Liu, G. A Cinchona Alkaloid-Functionalized Mesostructured Silica for Construction of Enriched Chiral β-Trifluoromethyl-β-Hydroxy Ketones over An Epoxidation-Relay Reduction Process. *Chem. - An Asian J.* **2016**, *11* (14), 2072–2077.

(263) Matoba, K.; Kawai, H.; Furukawa, T.; Kusuda, A.; Tokunaga, E.; Nakamura, S.; Shiro, M.; Shibata, N. Enantioselective Synthesis of Trifluoromethyl-Substituted 2-Isoxazolines: Asymmetric Hydroxylamine/Enone Cascade Reaction. *Angew. Chemie - Int. Ed.* **2010**, *49* (33), 5762–5766.

(264) Ding, W.; Hu, J.; Jin, H.; Yu, X.; Wang, S. One-Pot Synthesis of α,β-Unsaturated Esters, Ketones, and Nitriles from Alcohols and Phosphonium Salts. *Synth.* **2018**, *50* (1), 107–118.

(265) Varga, S.; Jakab, G.; Drahos, L.; Holczbauer, T.; Czugler, M.; Soós, T. Double Diastereocontrol in Bifunctional Thiourea Organocatalysis: Iterative Michael-Michael-Henry Sequence Regulated by the Configuration of Chiral Catalysts. *Org. Lett.*

2011, *13* (20), 5416–5419.

(266) Braun, R. U.; Ansorge, M.; Müller, T. J. J. Coupling-Isomerization Synthesis of Chalcones. *Chem. - A Eur. J.* **2006**, *12* (35), 9081–9094.

(267) Kellogg, R. M.; et al., et al. Dutch Resolution: Separation of Enantiomers with Families of Resolving Agents. A Status Report. *ChemInform* **2003**, *34* (40), 1626–1638.

(268) Unoh, Y.; Hirano, K.; Satoh, T.; Miura, M. Palladium-Catalyzed Decarboxylative Arylation of Benzoylacrylic Acids toward the Synthesis of Chalcones. *J. Org. Chem.* **2013**, *78* (10), 5096–5102.

(269) Alam, M. S.; Rahman, S. M. M.; Lee, D. U. Synthesis, Biological Evaluation, Quantitative-SAR and Docking Studies of Novel Chalcone Derivatives as Antibacterial and Antioxidant Agents. *Chem. Pap.* **2015**, *69* (8), 1118–1129.

(270) Verma, M.; Chaudhry, A. F.; Fahrni, C. J. Predicting the Photoinduced Electron Transfer Thermodynamics in Polyfluorinated 1,3,5-Triarylpyrazolines Based on Multiple Linear Free Energy Relationships. *Org. Biomol. Chem.* **2009**, *7* (8), 1536–1546.

(271) Suman, P.; Nageswara Rao, R.; China Raju, B. Microwave-Assisted Convenient Synthesis of α,β-Unsaturated Esters and Ketones via Aldol-Adduct Elimination. *Helv. Chim. Acta* **2013**, *96* (8), 1548–1559.

(272) Mlostoń, G.; Grzelak, P.; Heimgartner, H. Hetero-Diels–Alder Reactions of Hetaryl Thiochalcones with Acetylenic Dienophiles. *J. Sulfur Chem.* **2017**, *38* (1), 1–10.

(273) Sheshenev, A. E.; Boltukhina, E. V.; White, A. J. P.; Hii, K. K. Methylene-Bridged Bis(Imidazoline)-Derived 2-Oxopyrimidinium Salts as Catalysts for Asymmetric Michael Reactions. *Angew. Chemie - Int. Ed.* **2013**, *52* (27), 6988–6991.

(274) Concellón, J. M.; Rodríguez-Solla, H.; Méjica, C. An Efficient Synthesis of (E)-α,β-Unsaturated Ketones and Esters with Total Stereoselectivity by Using Chromium Dichloride. *Tetrahedron* **2006**, *62* (14), 3292–3300.

(275) Provencher, B. A.; Bartelson, K. J.; Liu, Y.; Foxman, B. M.; Deng, L. Structural Study-Guided Development of Versatile Phase-Transfer Catalysts for Asymmetric Conjugate Additions of Cyanide. *Angew. Chemie - Int. Ed.* **2011**, *50* (45), 10565–10569.

(276) Wilson, J. E.; Fu, G. C. Synthesis of Functionalized Cyclopentenes through Catalytic Asymmetric [3+2] Cycloadditions of Allenes with Enones. *Angew. Chemie - Int. Ed.* **2006**, *45* (9), 1426–1429.

(277) Gao, F.; Huang, Y. A Sulfur Ylides-Mediated Domino Benzannulation Strategy to Construct Biaryls, Alkenylated and Alkynylated Benzene Derivatives. *Adv. Synth.*

Catal. **2014**, *356* (11–12), 2422–2428.

(278) Cui, B.; Sun, H.; Xu, Y.; Duan, L.; Li, Y. M. MgCl2-Catalyzed Trifluoromethylation of Carbonyl Compounds Using (Trifluoromethyl)Trimethylsilane as the Trifluoromethylating Agent. *Tetrahedron* **2017**, *73* (48), 6754–6762.

(279) Cassani, C.; Martín-Rapún, R.; Arceo, E.; Bravo, F.; Melchiorre, P. Synthesis of 9-Amino(9-Deoxy)Epi Cinchona Alkaloids, General Chiral Organocatalysts for the Stereoselective Functionalization of Carbonyl Compounds. *Nat. Protoc.* **2013**, *8* (2), 325–344.

(280) Zielinska-Błajet, M.; Kowalczyk, R.; Skarzewski, J. Ring-Closure Reactions through Intramolecular Substitution of Thiophenoxide by Oxygen and Nitrogen Nucleophiles: Simple Stereospecific Synthesis of 4,5-Dihydroisoxazoles and 4,5-Dihydropyrazoles. *Tetrahedron* **2005**, *61* (22), 5235–5240.

(281) Lim, Y. J.; Kim, D. Y. Enantioselective Direct α-Amination of Aromatic Ketones Catalyzed by Binaphthyl-Modified Primary Amine. *Bull. Korean Chem. Soc.* **2013**, *34* (7), 1955–1956.